



Henderson, Livia (2014) *Cellular stress responses in equine tendon fibroblast monolayers*. PhD thesis.

<http://theses.gla.ac.uk/6725/>

Copyright and moral rights for this work are retained by the author

A copy can be downloaded for personal non-commercial research or study, without prior permission or charge

This work cannot be reproduced or quoted extensively from without first obtaining permission in writing from the author

The content must not be changed in any way or sold commercially in any format or medium without the formal permission of the author

When referring to this work, full bibliographic details including the author, title, awarding institution and date of the thesis must be given

Enlighten:Theses
<http://theses.gla.ac.uk/>
theses@gla.ac.uk



University
of Glasgow

Cellular stress responses in equine tendon fibroblast monolayers

By

Livia Henderson

BVSc MRCVS

Submitted in fulfilment of the requirements for the degree of Doctor
of Philosophy

Institute of Infection, Immunology & Inflammation
College of Medicine, Veterinary and Life Sciences
University Of Glasgow

Abstract

The superficial digital flexor tendon (SDFT) is one of the most frequently injured tendons in Thoroughbred racehorses. Exercise associated factors including hyperthermia are thought to lead to cellular dysfunction and cell death of the resident tendon fibroblasts, the cells responsible for the repair of the tendon lesions.

The main aim of this thesis was to investigate the sensitivity of SDFT fibroblasts to hyperthermia and to compare this with the deep digital flexor tendon (DDFT), a non-injury prone tendon. Understanding the physiological mechanisms of the heat shock response in these cells e.g. the use of protein markers will allow preventative strategies to be devised to protect these cells from damage. I determined whether thermotolerance associated with the induction of heat shock proteins (a survival mechanism that allows cells to withstand a subsequent lethal shock) could be induced with both heat and cold shock in these cells.

Firstly, the basal DNA damage levels were quantified in both SDFT and DDFT fibroblasts as the cell culture environment is known to damage cells. My research showed both SDFT and DDFT fibroblasts were susceptible to replication induced DNA damage in vitro. The SDFT in particular had high levels of DNA damage when cultured on a fibronectin matrix in ambient oxygen.

SDFT and DDFT fibroblasts were shown to be susceptible to a lethal heat shock (52°C). When a preconditioned sub-lethal heat shock was given to both tendons, induction of thermotolerance occurred and these cells survived a lethal heat shock. Thermotolerance was induced in preconditioned cold shocked SDFT fibroblasts but not in DDFT fibroblasts.

Finally, a useful protein marker, DAXX (that is involved in cellular stress pathways as a transcriptional repressor and in apoptosis) was shown to disperse into the nucleoplasm during a mild heat shock in SDFT fibroblasts. One of the limitations of this thesis is that sample size was small and as a result, larger numbers of animals will be required for future experiments to determine whether my results are of biological significance.

Table of Contents

Abstract	2
Table of Contents	3
List of Figures	7
List of Tables.....	9
Errata.....	10
Acknowledgements.....	13
Author's declaration	15
Abbreviations	16
Chapter 1) Introduction	23
1.1 Function of the SDFT.....	23
1.1.1 Function of the DDFT	24
1.1.2 Hierarchical structure of the SDFT.....	26
1.1.3 Blood supply of the SDFT	29
1.1.4 Cell populations within the equine SDFT.....	29
1.1.5 Tenocytes (tendon fibroblasts)	30
1.2 SDFT injury	33
1.2.1 Epidemiology	33
1.2.2 The concept of microdamage and degeneration of the SDFT with age and exercise.....	33
1.2.3 Influence of exercise-associated factors in the injury of SDFT tendon.....	35
1.2.4 Does inflammation play a role in tendinopathy?.....	37
1.2.5 Clinical rupture: the problem with regeneration	38
1.3 Cellular injury and cell death pathways	39
1.3.1 DNA damage response	41
1.3.2 Heat shock response	42
1.3.3 Promyelocytic leukaemia (PML) sensing systems	44
1.3.4 Cell death pathways.....	47
1.3.4.1 Apoptosis.....	47
1.3.4.2 Intrinsic apoptotic pathway	48
1.3.4.3 Extrinsic apoptotic pathway	49
1.3.4.4 Necrosis	51
1.3.5 Pro-survival pathways.....	51
1.4 The effects of cooling and the up-regulation of key cold shock proteins	55
1.4.1 The use of cryotherapy	55
1.4.2 The cold shock protein RBM3 and its roles.....	56
1.4.3 Hsp-72 and cold shock	57
1.5 Aims of this work	57
Chapter 2) Materials and Methods	59
2.1 Collection of tendon samples.....	59
2.2 Preparation of tendon specimens for cell culture	60
2.2.1 Tendon specimens.....	60
2.2.2 Extraction and culture of tendon fibroblasts by enzymatic digestion	61
2.2.3 Extraction and culture of tendon fibroblasts by tendon explant ...	62

2.2.4	Cell culture: “normoxic” oxygen (2% oxygen).....	63
2.3	Immunocytochemistry	65
2.3.1	Immunocytochemistry methods for Chapter 3.....	66
2.3.2	Immunocytochemistry methods for Chapter 4.....	68
2.3.3	Immunocytochemistry methods for Chapter 5.....	68
2.4	Senescence staining	71
2.5	Comet assay	72
2.5.1	Quantification of oxidatively damaged cells via comet assay	73
2.6	Choice of heat rig equipment.....	74
2.6.1	Calibration of the Cell MicroControls heating rig	80
2.7	Measurement of Hsp-72 expression in SDFT and DDFT fibroblasts with heating and cooling	83
2.7.1	Heat shock protocol	83
2.7.2	Cold shock protocol	83
2.8	Western blotting.....	84
2.9	Thermotolerance in tendon fibroblasts associated with heating and cooling	90
2.9.1	Protocol for heating and cooling SDFT and DDFT fibroblasts	90
2.9.2	Quantification of cell death	91
2.10	Protein sequence alignments.....	91
2.11	Immunohistochemistry	94
2.12	Statistical analysis	95
2.12.1	Chapter 3	95
2.12.2	Chapter 4	95
2.12.3	Chapter 5	96
Chapter 3)	The influence of the cell culture environment on tenocytes from two tendons with different injury susceptibilities	99
3.2.1	Tendon specific susceptibility to DNA damage.....	104
3.2.2	DNA damage is enriched in the proliferative fraction.....	106
3.2.3	Evidence of aberrant cytokinesis in SDFT fibroblasts	111
3.2.4	Increased lysosomal enzyme activity in tendon cells	117
3.2.5	SDFT and DDFT fibroblasts showed comparable repair capacities following exogenous oxidative DNA damage.....	119
3.3.1	SDFT fibroblasts are sensitive to replication-induced stress in certain culture conditions	123
3.3.2	Binucleation was influenced by oxygen tension in SDFT fibroblasts only	125
3.3.3	Increase in lysosomal enzyme activity in adult SDFT fibroblasts ..	126
3.3.4	The SDFT and DDFT had similar rates of repair	127
Chapter 4)	Heat Shock Protein-72 and thermotolerance in tenocytes	130
4.1	Introduction	130
4.2	Results	134
4.2.1	The tendon of origin and the Hsp-72 expression pattern associated with heating	134
4.2.2	The tendon of origin and the Hsp-72 expression pattern associated with cooling	140

4.2.3	The expression of the cold-shock protein, RBM3 in heated and chilled equine tendon fibroblasts	150
4.2.4	Choosing a lethal temperature for SDFT and DDFT fibroblasts	153
4.2.5	“Thermotolerance” associated with the heat shock response in SDFT and DDFT fibroblasts.	159
4.3	Discussion	163
4.3.1	Calibration of the heating rig is an important criterion when choosing a suitable apparatus for heating cells.	163
4.3.2	The induction of Hsp-72 protein with heat shock in SDFT and DDFT fibroblasts.....	164
4.3.3	The induction of Hsp-72 protein with cold shock in SDFT and DDFT fibroblasts.....	165
4.3.4	Tendon-dependent difference in thermotolerance in response to heat shock.....	167
4.3.5	Thermotolerance only occurred for the first 24hrs post heating in preconditioned cold shocked SDFT fibroblasts.....	168
4.3.6	The expression of RBM3 occurred with both heat and cold shock in SDFT fibroblasts.	169
4.3.7	Restoration of normal cellular morphology is a useful predictor of cell fate following heat shock.....	170
Chapter 5)	Markers of injury sensing in equine tendinopathy	173
5.1	Introduction	173
5.2	Results	177
5.2.1	Validation of DAXX and Caspase-2 in Foetal Equine Palate fibroblasts	177
5.2.2	DAXX immuno-localisation during heat shock	180
5.2.3	Re-shocking SDFT fibroblasts did not prevent DAXX dispersal	183
5.2.4	DAXX puncta size increased during the early hypothermic period, with dispersal during the rewarming period only.	185
5.2.5	Different batches of p62 antibodies displayed different in vitro cellular distributions	188
5.2.6	Bortezomib, a proteasomal inhibitor induced the translocation of p62 from the nucleus into the cytoplasm.....	192
5.2.7	p62 expression is increased in chronic SDFT lesions.....	194
5.2.8	The addition of an exogenous anti-oxidant (N-acetyl cysteine) did not alter the expression or localisation of NRF- 2 in SDFT cells	196
5.2.9	Co-localisation of NRF-2 and Cx43 was seen at gap junctions and other intracellular sites.....	199
5.3	Discussion	201
5.3.1	DAXX re-localisation into the nucleoplasm occurred rapidly during heat shock in SDFT fibroblasts.....	201
5.3.2	DAXX puncta size increased with cold shock in SDFT fibroblasts ..	203
5.3.3	p62 in injured tendons may be associated with the healing response	204
5.3.4	Validation of p62/SQSTM1 antibody	205
5.3.5	The localisation of NRF-2 in the nucleus in SDFT fibroblasts was indicative of oxidative stress in vitro.....	206
5.3.6	NRF-2 co-localisation with Cx43 protein in SDFT fibroblasts.....	207
Chapter 6)	Limitations of the research in this thesis	208

Chapter 7) Conclusions and Future work.....	211
Chapter 8) References.....	217

List of Figures

Figure 1-1	Anatomy of the equine distal forelimb	25
Figure 1-2	The difference in biomechanics between tendons	25
Figure 1-3	The hierarchical structure of the tendon	28
Figure 1-4	Tendon fibroblast phenotypes	32
Figure 1-5	PML NB and its response to cell stress.....	46
Figure 1-6	The intrinsic and extrinsic apoptotic pathways	50
Figure 1-7	p62 transports ubiquitinated protein to the autophagosome	53
Figure 2-1	“Normoxic” oxygen (2%) incubators	64
Figure 2-2	Difference in cell morphology across the cell culture dish.....	77
Figure 2-3	The tendon thermocycler heating apparatus.....	78
Figure 2-4	Resistive heating rig from Cell MicroControls	79
Figure 2-5	A snapshot of the RealTerm software program	81
Figure 2-6	Calibration curves for the Cell MicroControls heating rig.....	82
Figure 2-7	Post translational modification of alpha Tubulin with cooling.....	87
Figure 3-1	Measurement of DNA damage and replication in SDFT and DDFT fibroblasts	109
Figure 3-2	Dual stain for both γ H2AX and TPX2 demonstrates the significant association between replication and DNA damage.	110
Figure 3-3	Binucleate SDFT fibroblasts	113
Figure 3-4	Binucleate cells were detected in all culture environments	114
Figure 3-5	Binucleate cell with bleb containing damaged DNA.....	115
Figure 3-6	p21 expression in SDFT fibroblasts.....	116
Figure 3-7	Senescence-associated beta galactosidase stain was strongest in adult SDFT	118
Figure 3-8	Comet assay in SDFT and DDFT fibroblasts	121
Figure 3-9	Quantification of DNA damage associated with the comet assay ..	122
Figure 4-1.	The expression of Hsp-72 protein in DDFT fibroblasts heated to 43°C.	136
Figure 4-2.	The expression of Hsp-72 in SDFT fibroblasts heated to 43°C	137
Figure 4-4.	The expression of Hsp-72 protein in DDFT fibroblasts exposed to 47°C	139
Figure 4-5.	The expression of Hsp-72 protein in SDFT fibroblasts cooled at 26°C continuously for 72hrs.	142
Figure 4-6.	The expression of Hsp-72 in DDFT fibroblasts cooled continuously at 26°C for 72hrs.	143
Figure 4-7.	The expression of Hsp-72 protein in SDFT fibroblasts given 1hr of cold shock at 26°C followed by 72hrs of recovery at 37°C	144
Figure 4-8.	The expression of Hsp-72 protein in SDFT fibroblasts cold shocked at 26°C for 4hrs followed by recovery at 37°C	145
Figure 4-9.	The expression of Hsp-72 protein in DDFT fibroblasts exposed to 1hr of cold shock at 26°C followed by recovery at 37°C.....	146
Figure 4-10.	The expression of Hsp-72 protein in DDFT fibroblasts exposed to 4hrs of cold shock at 26°C then recovered at 37°C for 72hrs	147
Figure 4-11.	The expression of Hsp-72 protein in SDFT fibroblasts following an overnight cold shock at 26°C followed by recovery at 37°C	148
Figure 4-12.	The expression of Hsp-72 protein in DDFT fibroblasts exposed to 26°C overnight then recovered at 37°C.	149
Figure 4-13.	The pattern of RBM3 expression with heating and cooling in SDFT fibroblasts	152

Figure 4-14.	Two anti-Caspase-3 antibodies from Cell Signalling and R and D Systems did not detect cleaved equine Caspase-3	156
Figure 4-15.	Protein sequence similarity between equine and human Caspase-3	157
Figure 4-16.	Differences in cellular morphology in SDFT fibroblasts according to temperature	158
Figure 4-17.	The percentage of attached SDFT and DDFT fibroblasts when exposed to pre-conditioned heat and cold shock.	162
Figure 5-1	Caspase-2 distribution with heating in equine palate (Eq PalF) cells.. ..	178
Figure 5-2	DAXX disperses with heating in Eq PalF cells	179
Figure 5-3	DAXX dispersal was very rapid in SDFT tendon fibroblasts	181
Figure 5-4	DAXX returned to the PML NBs very rapidly post heating.....	182
Figure 5-5	Reshocking SDFT fibroblasts did not prevent DAXX dispersal	184
Figure 5-6	DAXX dispersal did not occur with cooling.....	186
Figure 5-7	DAXX puncta size changed with temperature	187
Figure 5-8	The distribution of p62 in SDFT fibroblasts stained with anti-p62 antibody is dependent on batch.....	190
Figure 5-9	A similar banding pattern of p62 protein in a western blot when two anti-p62 antibody batches were used	191
Figure 5-10	The administration of bortezomib provokes p62 expression in the cytoplasm at the expense of the nuclear fraction.	193
Figure 5-11	The expression of p62 in a chronic SDFT lesion	195
Figure 5-12	The addition of NAC does not alter the distribution of NRF-2....	197
Figure 5-13	Measurement of NRF-2 expression in SDFT fibroblasts	198
Figure 5-14	Co-localisation of NRF-2 at gap junction plaques and Cx43 foci .	200

List of Tables

Table 1:	List of the horses (and foal) used in my thesis	60
Table 2:	The NCBI reference sequence codes for the proteins used in multiple sequence alignment work	93
Table 3:	Antibodies used for immunocytochemistry	98
Table 4:	Antibodies used for western blot.....	98

Errata

Introduction

1) On page 22, the reference for Figure 1.1 was stated with permission from Smith and Goodship et al, 2004. This should be corrected to Smith et al, 2002.

2) The following references were omitted from these figures in Chapter 1. These references have been inserted in the References Chapter. They are as listed:

- **Figure 1-3:**

RICHARDSON, L., DUDHIA, J., CLEGG, P. & SMITH, R. 2007. Stem cells in veterinary medicine - attempts at regenerating equine tendon after injury. *Trends in biotechnology*, 25, 409 - 416.

- **Figure 1-5:**

ZHONG, S., SALOMONI, P. & PANDOLFI, P. P. 2000a. The transcriptional role of PML and the nuclear body. *Nat Cell Biol*, 2, E85-E90.

- **Figure 1-6:**

MAIURI, M. C., ZALCKVAR, E., KIMCHI, A. & KROEMER, G. 2007. Self-eating and self-killing: crosstalk between autophagy and apoptosis. *Nat Rev Mol Cell Biol*, 8, 741-752.

- **Figure 1-7:**

TYEDMERS, J., MOGK, A. & BUKAU, B. 2010. Cellular strategies for controlling protein aggregation. *Nat Rev Mol Cell Biol*, 11, 777-788.

Chapter 4

The following corrections have been made to these Figures in Chapter 4.

Figure 4.3

- The Amido Black blot from Hsp-72 replicate no. 3 has been switched with the blot from replicate no.1.

Figure 4.8

- The Hsp-72 blots in the original version of the thesis had been taken from an earlier experiment and placed with the wrong Amido Black controls. The amended version contains the correct Hsp-72 blots with their associated Amido Black controls.

Figure 4-9

- The Amido Black blot from Hsp-72 replicate no.2 has been switched with the blot from replicate no.1.

Figure 4-10

- The Amido Black blot from Hsp-72 replicate no. 2 has been switched with the blot from replicate no.3.

Figure 4-11

- The third Hsp-72 blot and the Amido Black control were both too smudged for use and it has been omitted.

Figure 4-12

- The Amido Black blot from Hsp-72 replicate no. 3 has been moved to replicate no. 1. The correct Amido Black blot for replicate no.3 has been duplicated twice in replicate no.1

and no.2. One of these duplicates has been moved to replicate no.3. The Amido Black blot for replicate no.2 has been added to the Figure.

Acknowledgements

Firstly I would like to thank my supervisors, Dr Tina Rich and Professor Janet Patterson-Kane for their supervision and guidance throughout my PhD. I would also like to thank my external supervisor, Dr David Becker and his lab at the University College, London for their support and training especially on the confocal microscope. I would specifically like to thank Dr Daniel Ciantar from Dr Beckers' lab for teaching me how to use the confocal microscope, Image J and for answering all my questions.

I would particularly like to say a special thanks to Professor Sandy Love for all his support, guidance and encouragement throughout my thesis. From the start of my thesis, Professor Love and all the equine clinicians and interns from Weipers' Centre, at the University of Glasgow were fantastic in helping me source equine tendons for sample collection. Other people I would like to thank for their help in sourcing equine tendons include Dr Alistair Foote from Rossdales and Val Turner for allowing me to take horse tendons from the Red Lion Abbatoir from Cheshire. Dr Debbie Guest very kindly allowed me to use her laboratory facilities at the Animal Health Trust in Newmarket for a couple of weeks whilst in the process of extracting tendon cells.

I would like to say a special thank you to Lynn Stevenson, who works in the pathology laboratory at Garscube, at the University of Glasgow. I could not have completed any of the immunohistochemistry staining without her help. An extra special thanks to Margaret Petrie for helping me to edit all my figures. A massive thank you to Dr Hannah Cornell, a member of my lab group, whose help, support, guidance and encouragement was instrumental in getting me finished. My lab buddies, Dr Robert Dean, Elaine Gauson, Adam Bell and Elspeth Waugh, thank you for all the fun lunches and chats in the office.

Finally, I could not have finished this thesis without the love and support of my parents and boyfriend. I would like to dedicate this thesis to the three of you, the most important people in my life.

***Acer et ad plamae per se cursurus honores,
Si tamen hortaris fortius ibit equus.***

- Ovid (Epistulae ex Ponto II.11.21)

Author's declaration

I declare that, except where explicit reference is made to the contribution of others, that this dissertation is the result of my own work and has not been submitted for any other degree at the University of Glasgow or any other institution.

.....

Livia Henderson

Abbreviations

3-MA	3-Methyladenine
3T3 cell line	3-day transfer, inoculum 3 x10 ⁵ cell line
A549	Adenocarcinomic human alveolar basal epithelial cell line
ADAMTS-2	A Disintegrin And Metalloproteinase with a Thrombospondin type 1 motif, member 2
AKT/PKB	Protein kinase B
APAF-1	Apoptotic protease activating factor-1
aPKC	Atypical protein kinase C
ASK-1	Apoptosis signal-regulating kinase-1
AFT6	Activating transcription factor 6
ATG	Autophagy-related gene
ATM	Ataxia telangiectasia mutated
ATP	Adenosine tri-phosphate
ATR	ATM- and Rad3- related
BCL-2	B cell lymphoma-2
BiP	Binding immunoglobulin protein
BMA-1	Bone marrow stromal cells
BMP1	Bone Morphogenetic Protein 1
BN	Binucleate
BRCA1	Breast cancer 1, early onset
BrdU	Bromodeoxyuridine
BSA	Bovine Serum Albumin
Ca ²⁺	Calcium 2+
cAMP	cyclic adenosine monophosphate
CARD	Caspase Activation and Recruitment Domain
CDET	Common digital extensor tendon

CDK2	Cyclin-dependent kinase 2
CDK4	Cyclin-dependent kinase 4
cGMP	cyclic Guanosine Monophosphate
CHIP	Carboxyl-terminus of HSP-70 interacting protein
CHIP	Carboxyl terminus of Hsc/Hsp-70 Interacting Protein
CHO-K1	Chinese Hamster Ovary cells
CHOP	C/EBP homologous protein
CIRP	Cold-inducible RNA binding protein
CK2	Casein Kinase 2
CRM1	Chromosome region maintenance protein homolog
Cx43	Connexin-43
DAB	3,3'-Diaminobenzidine
DAPI	4',6-diamidino-2-phenylindole (nucleic acid dye)
DAXX	Death-associated protein 6
DDFT	Deep digital flexor tendon
DDR	DNA damage response
DISC	Death-inducing Signalling Complex
DMEM	Dulbecco's Modified Eagle's Medium
DNA	Deoxyribonucleic acid
DPX	A mixture of distyrene, a plasticiser and xylene
DSB	Double strand break
ECM	Extracellular matrix
EDTA	Ethylenediaminetetraacetic Acid
Eq PalF	Equine foetal Palate Fibroblasts
ER	Endoplasmic Reticulum
ERAD	ER-associated degradation
ERp57	Also known as PDIA3 (protein disulphide isomerase family A, member 3)
FADD	FAS-associated protein with death domain

FASTA	Fast All
FBS	Foetal Bovine Serum
FITC	Fluorescein isothiocyanate
FRAP	Fluorescence recovery after photobleaching
G1	Gap 1 phase of the cell cycle
G2	Gap 2 phase of the cell cycle
GAG	Glycosaminoglycans
GD25	Derived from murine embryonic stem cell line
GRP-75	Also known as HSPA9, a HSP-70 family member
GRP98	78kDa Glucose-regulated protein
GSH	Glutathione
GTP	Guanosine Triphosphate
H2AX	Histone 2A (member X)
H ₂ O ₂	Hydrogen peroxide
HBSS	Hanks' Balanced Salt Solution
HDAC	Histone deacetylases
HeLa	Henrietta Lacks cell line
HEp-2	Human Epithelial laryngeal carcinoma cell line contaminated with HeLa Cells
HIKP2	Homeodomain-interacting protein kinase 2
HRP	Horseradish peroxidase
HSF-1	Heat shock factor 1
HSP	Heat shock protein
IL-1	Interleukin-1
IMR-90	Foetal human lung fibroblasts
IP3	Inositol triphosphate
IRES	Internal ribosome entry site
IRE1	Inositol-requiring kinase
ITO	Indium tin oxide

JNK	c-Jun N-terminal kinase
KEAP	Kelch-like ECH-associated protein
Ki-67	Clone of TPX2
Ki-S2	Antigen KiS2 also known as TPX2 (Targeting protein for XkIP2)
Ki-S2	Clone of TPX2 - Ki denotes its derivation from the University of Kiel Germany
L540 cells	Human Hodgkin lymphoma cell line
LC3	Light chain 3
LC3B-II	LC3-phosphatidylethanolamine conjugate II
LC3-II	Light chain 3-II
LIR	LC3-interacting region
LSD	Lithium dodecyl sulphate
MALP-2	Macrophage-activating lipopeptide
MCP	Metacarpophalangeal joint
MDM2	Mouse double minute 2 homolog
MEF	Mouse embryonic fibroblast
miRNA	Micro ribonucleic acid
MMP	Matrix Metalloproteinase
MPG	Mercaptopropionyl Glycine
mRNA	messenger Ribonucleic Acid
mTCII	Micro temperature controller
NAC	N-acetyl-cysteine
NC65 cells	Human renal carcinoma cell line
NEMO	NF-kappa-B essential modulator
NES	Nuclear Export Signal
NF- κ B	Nuclear Factor kappa-light- chain-enhancer of activated B cells
NLS	Nuclear localisation signal
NRF-2	Nuclear E2 Related Factor
NRK cells	Normal rat kidney epithelial cell line

P/S	Penicillin/Streptomycin
P1	Passage 1
P2	Passage 2
p21/WAF	Cyclin-dependent kinase inhibitor 1
p27/KIP1	Cyclin-dependent kinase inhibitor 1B
P3	Passage 3
p38	p38 Mitogen activated protein kinases
p53	protein 53 or tumour protein 53
PALF	Foetal equine soft palate cells
PB1	Phox and Bem1 domain
PBS	Phosphate Buffered Saline
PERK	Pancreatic ER elf kinase
PH	Post Heating
PI	Propidium iodide
PIDD	Induced Protein with a Death Domain
PIKK	Phosphatidyl Inositol 3'Kinase-related Kinases
PIP	Proximal Interphalangeal joint
PML	Promyelocytic Leukaemia
PML NBs	Promyelocytic Leukemic Nuclear Bodies
RAD50/51	DNA repair protein RAD50/51
RAIDD	RIP Associated Ich-1/CED homologous Protein with Death Domain
RAW 264.7	Mouse leukaemic monocytic macrophage cell line
RBM3	RNA Binding Motif Protein 3
REAP	Rapid, Efficient And Practical
RING	Really Interesting New Gene
RIP-1	Receptor-Interacting Protein-1
RIPA	Radioimmunoprecipitation Assay buffer
RNA	Ribonucleic Acid

RNF4	RING Finger Protein 4
ROS	Reactive Oxygen Species
RT	Room Temperature
RVC	The Royal Veterinary College
SA-B gal	Senescence-associated beta galactosidase
SDFT	Superficial Digital Flexor Tendon
SDS-PAGE	Sodium Docedyl Sulphate - Polyacrylamide Gel Electrophoresis
SEN-1	Sentrin-specific protease-1
ser46	Serine 46
SIM	SUMO-interacting motif
SiRNA	Small interfering ribonucleic acid
S-phase	Synthesis phase of the cell cycle
SQSTM1/p62	Sequestosome 1
SUMO	Small ubiquitin like modifier
TAMA-26	Mouse Sertoli cell line
TB	Thoroughbred
TEMED	Tetramethylethylenediamine
TGF- β 1	Transforming Growth Factor beta 1
TLR	Toll-like Receptors
TNF	Tumour Necrosis Factor
TORC1	Target of rapamycin complex 1
TPX2	Targeting protein for XKLP2
TRAF-6	TNF receptor associated factor-6
Tris-HCl	Also known as THAM (tris(hydroxymethyl)aminomethane) - Hydrochloric Acid
U373MG	An astrocytoma cell line
U937	Histiocytic lymphoma cell line
UBA	Ubiquitin-associated domain
UPR	Unfolded protein response

UV	Ultraviolet light
VHL	Von-Hippel-Lindau tumour-supressor
WCL	Whole cell lysate
XBP1	X-box binding protein 1
XBP1s	X-box binding protein 1 (spliced)
γ H2AX	Phosphorylated Histone H2A, member X

Chapter 1) Introduction

Large running mammals expend considerable energy to maintain speed over distances. As the weight of the animal increases, the muscle mass must increase to support the energy demands of the limbs (Goff and Stubbs, 2007), (Alexander, 2002). To compensate for this, the horse has adapted by increasing the length of the limb and by concentrating the bulk of the muscular mass on the proximal forelimb. Long tendons replace muscles in the distal forelimb to minimise the weight placed on the forelimb. This allows more economic muscle force generation during exercise. Certain tendons of the forelimb e.g. the superficial digital flexor tendon (SDFT) store elastic energy to minimise muscular energy expenditure, (Alexander, 2002), (Biewener, 1998), (Wilson and Lichtwark, 2011). The SDFT is the most frequently injured tendon in racing Thoroughbreds (Ely et al., 2009). The exact cause for the high prevalence of injuries in this tendon has yet to be fully elucidated.

A number of exercise associated factors including mechanical strain, hyperthermia and ischemia are thought to be involved (Birch et al., 1997a), (Hosaka et al., 2005), (Lavagnino et al., 2006), (Longo et al., 2008). In the adult horse SDFT, the number of tendon fibroblasts is small with fewer than 300/mm² (Stanley et al., 2007). The main functions of tendon fibroblasts are the synthesis, remodelling and repair of the collagenous matrix and any loss of cells through cell death or cellular dysfunction will therefore have a significant impact on tendon healing.

The principal aim of this thesis was to understand how equine tendon fibroblasts respond to various types of stress (particularly hyperthermia), thus allowing preventative protective strategies to be devised.

1.1 Function of the SDFT

During normal weight bearing, the superficial digital flexor tendon (SDFT) supports the metacarpophalangeal (MCP) and proximal interphalangeal joints (PIP) during hyperextension in the stance phase of locomotion (Figure 1-1). It also aids in the flexion of the digit during the swing phase (Denoix, 1994). The SDFT acts as an energy storing tendon by converting both potential and kinetic

energy into elastic energy during weight-bearing associated deformation of the tendon. This reduces the need for muscular energy expenditure and increases the efficiency of locomotion (Alexander, 2002). As such, it has been described as a 'biological spring' but has to undergo large strains (percentage elongation) to ensure appropriate elastic energy storage. Values of strain have been recorded as high as 16.6% in the SDFT of galloping racehorses (Stephens et al., 1989). In vitro measurements of tendon strain indicate that failure limits for this tendon are between 12 and 20% (Riemersma and Schamhardt, 1985), (Wilson and Goodship, 1991) suggesting that there is a low mechanical safety margin for this tendon with consequent increased predisposition to injury when operating at galloping speeds.

1.1.1 Function of the DDFT

The deep digital flexor tendon (DDFT) is another flexor tendon situated under the SDFT in the metacarpal region of the distal forelimb (Figure 1-1). It is also involved in the support of the MCP joint during exercise functioning to limit over-extension. The DDFT is also responsible for flexing the digit in the late swing phase of locomotion which is thought to decelerate the foot and allow the hoof to contact the ground at the appropriate angle (Denoix, 1994), (Butcher et al., 2009). Unlike the SDFT, the DDFT is not an energy storing tendon. The DDF muscle actively contracts to power the stride cycle at high speeds (Butcher et al., 2009). The DDFT therefore does not undergo the same strain values as the SDFT during the walk, trot or canter, the values being approximately a fifth of those of the SDFT. This tendon clearly has different biomechanical properties and the difference in strain values between the two tendons and the suspensory ligament is clearly depicted in Figure 1-2 (Platt et al., 1994), (Butcher et al., 2009).

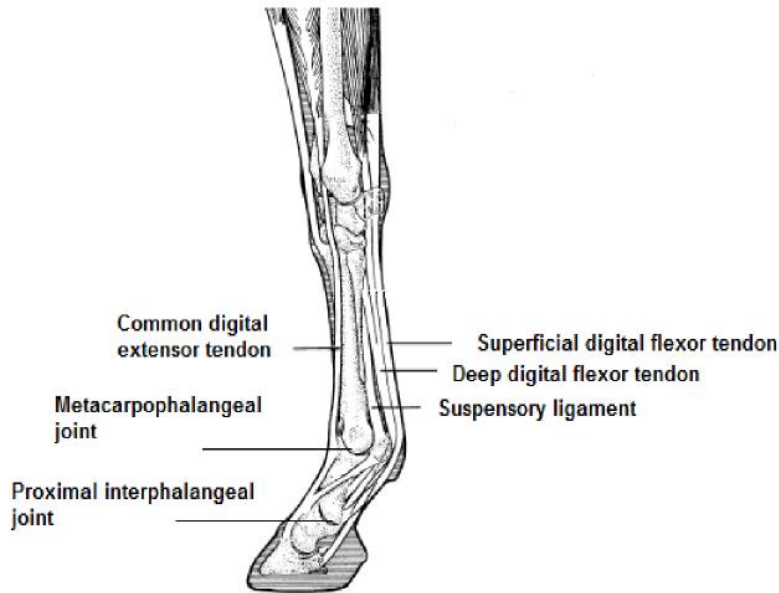


Figure 1-1 Anatomy of the equine distal forelimb

This figure shows the location of the superficial and digital flexor tendons in the equine distal forelimb. Image modified, with permission, from (Smith et al., 2002).

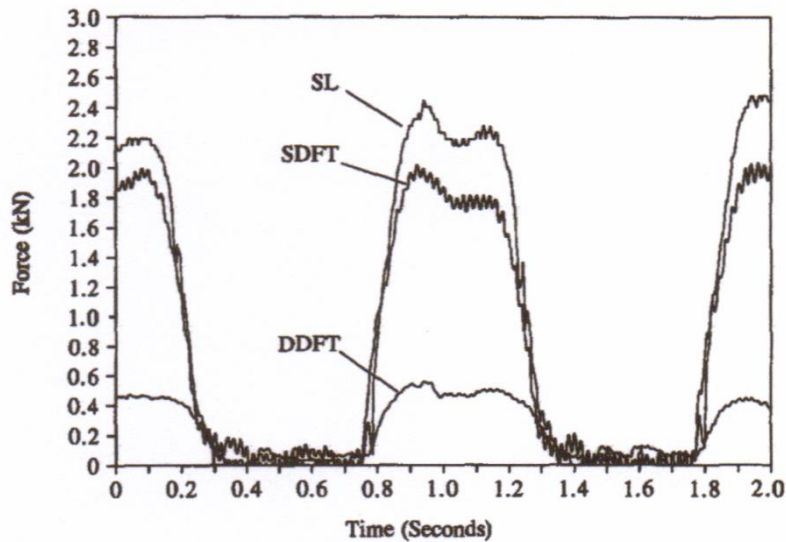


Figure 1-2 The difference in biomechanics between tendons

Force (kNs) experienced by the SDFT, DDFT and the suspensory ligament (SL) in a pony at a walk. Measurement of tensile force was facilitated by the implantation of a force transducer in the body of the tendon(s). Elongation of the collagen fibrils during the walk led to deformation of a deflector leaf in the transducer apparatus allowing force to be measured. The sudden force increase at 0.8 seconds corresponds to collagen fibril elongation when the foot is placed on the ground during the start of the walk stance. At 1.4 seconds, when the foot is being raised at the end of the walk, there is loss of force associated with collagen fibril shortening. As shown in the figure, the SDFT experiences 4/5th more force than the DDFT. Graph reproduced with permission from (Platt et al., 1994).

1.1.2 Hierarchical structure of the SDFT

The SDFT is an organised, hierarchical structure composed of longitudinally arranged fascicle bundles (Figure 1-3). Surrounding the outside of the fascicle bundles is a thin, loose connective tissue sheath, the endotenon, containing the blood vessels, lymphatics and nerves (Kannus, 2000), (Kastelic et al., 1978). Above the endotenon, the entire tendon is covered by the epitenon, a dense, fibrillar network composed of collagen fibrils oriented randomly in various directions including obliquely, transversely and longitudinally. The epitenon in turn is surrounded by the paratenon, a loose areolar connective tissue that acts as an elastic sleeve allowing the tendon to slide against neighbouring tissues (Kannus, 2000), (Jozsa et al., 1991).

The space between the fascicles and the endotenon is composed of an inter-fascicular matrix, a loose connective tissue containing both collagen type III and proteoglycans. A recent study demonstrated that there was a 10% difference in the failure strain between the SDFT (as a whole structure) and its fascicles (Thorpe et al., 2012). It has been suggested that in order for the SDFT to withstand strains of up to 16% during locomotion without rupture of the tendon, the inter-fascicular matrix must undergo load-induced deformation. The lower force experienced by the fascicles in comparison to the whole SDFT would enable the fascicles within the interfascicular matrix to slide and thus make the whole tendon more extensible (Thorpe et al., 2012).

The fascicles are composed of many longitudinally oriented collagen fibrils, the major subunit of tensile strength in the tendon. When viewed longitudinally with a polarised light source, the fibrils are shown to have a characteristic planar, zig-zag waveform (the crimp). This feature allows the fibrils to elongate with mechanical loading, providing the tendon with some of its elasticity (Kastelic et al., 1978), (Wilmink et al., 1992). With age, the collagen fibrils have a bi-modal distribution in the adult tendon with two major fibril diameters. The larger diameter fibrils provide the tendons' tensile strength due to the formation of intra-fibrillar covalent cross-links between fibrils and the smaller diameter fibrils provide inhibition of increased deformation under constant load which contributes to the tendons' elasticity (Parry et al., 1978b), (Parry et al., 1978a).

In the adult horse, the collagen fibrils make up 75-80% of the dry weight of the tendon (Birch et al., 1999). The predominant form of collagen fibril is type I, which makes up 95% of the total collagen mass (Goodship, 1993). Other collagen isoforms include type III, a smaller, weaker fibrillar collagen more commonly associated with immature and damaged tendons (Dahlgren et al., 2005a), (Birk and Mayne, 1997), (Williams et al., 1984). Small amounts of type V collagen are found in normal tendon, mostly in the endotenon. Type II collagen is located in fibrocartilaginous regions exposed to large compressive forces e.g. in those areas found close to joints (Buckley et al., 2013). The collagen fibrils are embedded in an extracellular matrix composed of water and other non-collagenous macromolecules including proteoglycans, glycoproteins and elastin (Smith and Webbon, 1996). Although the function of the non-collagenous components has not been fully elucidated, they do play an important role in tendon biomechanics. For example, the proteoglycan decorin strengthens the electrostatic cross-links between fibrils, participates in fibrillogenesis and binds growth factors (Vogel et al., 1984), (Yamaguchi et al., 1990), (Smith and Webbon, 1996).

Collagen fibrils are synthesised by tendon fibroblasts (tenocytes). The pre-cursor collagen fibril exists as 300nm pro-collagen molecules with N- and C-propeptides flanking the collagen domain. The pro-collagen is initially produced in the endoplasmic reticulum, extensive post-translational modifications occur in the Golgi complex followed by removal of the N- and C-propeptides. The N-propeptide has been shown to be removed by N-proteinases including ADAMTS-2 in the Golgi or ER- Golgi intermediate compartment and the C-propeptide is removed by C-proteinases including BMP1 tolloid proteinases in the post-Golgi compartment. The latter removal is an important step in the formation of fibrils required to initiate transport to the cell surface (Canty-Laird et al., 2012), (Bellamy and Bornstein, 1971), (Bonfanti et al., 1998), (Colige et al., 2005), (Scott et al., 1999), (Colige et al., 1997). During development, tendons have been shown to exhibit a plasma membrane protrusion (fibropositor) which excretes collagen fibrils into the ECM in parallel directions to maintain the parallel geometry of the tendon. Fibropositors have been shown to be absent in post-natal mice, where an increase in collagen fibril diameter takes place by accretion of collagen from extracellular collagen sources (Canty et al., 2004).

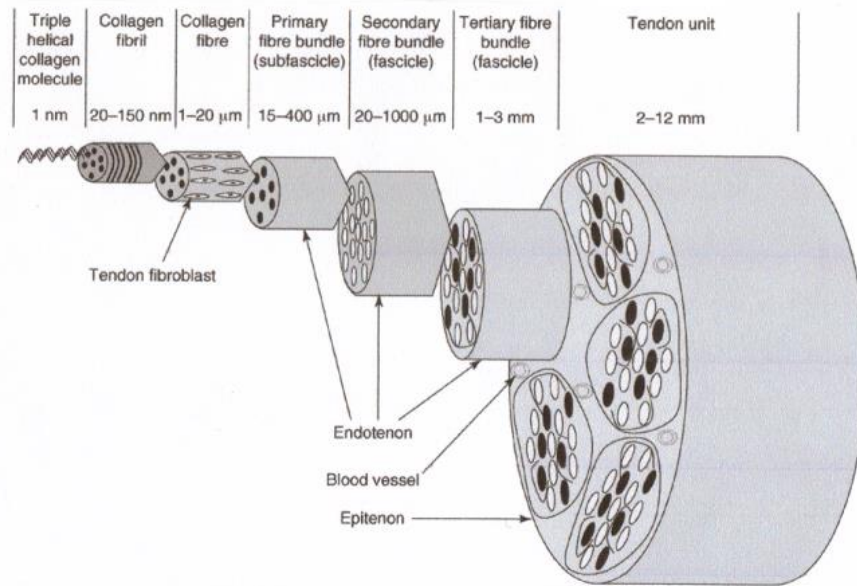


Figure 1-3 The hierarchical structure of the tendon

This figure outlines the hierarchical structure of the equine SDFT. The diagram shows how the collagen fibrils are arranged within the fascicles. The image is reproduced with permission from (Richardson et al., 2007)

1.1.3 Blood supply of the SDFT

The mid portion of the SDFT is supplied with blood from two main sources. The intratendinous component comprises the medial and lateral palmar metacarpal arteries coursing inside the medial and lateral borders of the tendon accompanied by an internal anastomosing network of vessels (Smith, 2003). The extratendinous component supplies blood from the paratenon. The small blood vessels in the paratenon run in a transverse direction then branch several times into smaller vessels coursing longitudinally along the tendon. These vessels eventually enter the tendon via the endotenon. The intratendinous component has been shown to be the main supply to the tendon area as ligation of these vessels has resulted in lesions similar to those found in tendonitis (Kraus-Hansen et al., 1992), (Stromberg, 1973), (Smith, 2003), (O'Brien, 2005).

1.1.4 Cell populations within the equine SDFT

The tenocytes (tendon fibroblastic cells) are the most common type of cell found in tendon and are responsible for the synthesis, remodelling and repair of the collagen matrix in response to mechanical load (Patterson-Kane et al., 2012), (Waggett et al., 2006). Other cell types present in tendon include the fibroblasts found in collagenous tendon sheaths, endotenon, epitenon and paratendon in addition to endothelial cells and some chondrocytes in areas of compression (Magnusson et al., 2003).

Mesenchymal stem cells are multi-potent cells capable of differentiating into a number of different mesenchymal cell types (Lui, 2013) They have been isolated from tendon tissue and induced to form various cell types including osteogenic, chondrogenic and adipogenic lineages in vitro. No specific markers exist for tendon stem cells in vivo which makes the localisation and utilisation of these cells very difficult (Lui, 2013). In the rat Achilles tendon, tendon stem cells have been localised to the peritenon, tendon-bone junction and the mid-substance and in these areas, the labelled tendon derived stem cells were sourced to vascular and non-vascular sites (Tan et al., 2013). The position of tendon stem cells adjacent to the vasculature has been suggested to have important biological implications including the rapid migration of stem cells to distant sites where injury has taken place. Stem cells are able to respond quickly

to immuno-modulatory signals released by the vascular system during the injurious event. These roles are important for tissue healing and repair (Lui, 2013). Tendon-derived stem cells from mice have also been found between the long, parallel collagen fibrils within the ECM (Bi et al., 2007). This latter study was completed in vitro, with tendon stem cells being cultured on synthetic ECM matrices including Matrigel. The localisation of tendon stem cells may differ in vivo. Few studies have investigated the localisation of equine tendon-derived stem cells in vivo and determined the most appropriate markers for their identification.

1.1.5 Tenocytes (tendon fibroblasts)

Tenocytes have been classified into three different phenotypes: type I with thin, spindle shaped nuclei, type II, with more ovoid, cigar-shaped nuclei (Figure 1-4) and type III which retain characteristics of chondrocytes which have round nuclei and visible nucleoli (Smith and Webbon, 1996). Type III tenocytes are typically found in areas where large compressive forces are experienced (e.g. where tendons wrap around joints) (Smith and Webbon, 1996). Type I and II have been labelled tenocytes and tenoblasts respectively. It is thought that type II may be synthetically more active as demonstrated by the production of higher amounts of procollagen type I and MMP1 (matrix metalloproteinase enzyme responsible for the breakdown of type 1 collagen in the ECM) together with higher proliferation and apoptotic indices. This is an indication that this cell phenotype actively participates in the turnover of the ECM (Chuen et al., 2004). Type II tenocytes are predominately found in immature tendons and the proportion of type I tenocytes increases with age in adult tendons. A larger population of type II tenocytes compared to type I in immature tendons suggests that younger horses may demonstrate an increased ability to participate in active remodelling of the tendon in response to mechanical load (Stanley et al., 2008).

The tenocytes are aligned in longitudinal rows alongside the collagen fibrils. Tenocytes are connected to each other within the longitudinal rows via their cell bodies and between rows by long cytoplasmic extensions. At points of contact, there are gap junctions which allow intercellular communication to take place through the movement of ions, amino acids, nucleotides and second

messengers (e.g. Ca^{2+} , cAMP, cGMP, IP_3) (McNeilly et al., 1996), (Fry et al., 2001), (Goldberg et al., 2002). In connective tissues, this form of inter-cellular communication has an important role in synchronizing the response of tendon cells to mechanical load, which is a requirement for load-induced collagen synthesis and matrix modification (Banes et al., 1999), (Waggett et al., 1999).

Gap junctions are composed of hexameric channels; the major structural subunit being connexin proteins (Krysko et al., 2005). In horses, the two major connexin proteins are Cx43 and Cx32 (Stanley et al., 2007), (Young et al., 2009). Research undertaken in avian tendon fibroblasts discovered the two different connexin gap junctions differentially modulate collagen synthesis in response to loading as Cx43 and Cx32 were inhibitory and stimulatory to collagen secretion respectively (Waggett et al., 2006).

The tenocytes are also linked to each other and to the matrix via adherens junctions (Ralphs et al., 2002). Cells can sense mechanical signals from the ECM through integrins, cell surface receptors found on the plasma membrane. Integrins can mediate cellular adhesion to the ECM by binding to junctional proteins (e.g. vinculin) to form focal adhesion complexes and to the cell cytoskeleton. The assembly of focal adhesion complexes are stimulated by the Rho family of GTPases (guanosine triphosphate). Integrins can also transmit intracellular signalling cascades promoting transmission of the mechanical signal (mechanotransduction) (Lee et al., 2002), (Hotchin and Hall, 1995), (Ko and McCulloch, 2001), (Giancotti, 1997). Vinculin together with n-cadherin, are two of the junctional proteins found in adherens junctions. These proteins help tether actin stress fibres, a component of the cell cytoskeleton at cell-cell contacts, which stabilises cells relative to each other and to their matrix (Ralphs et al., 2002).

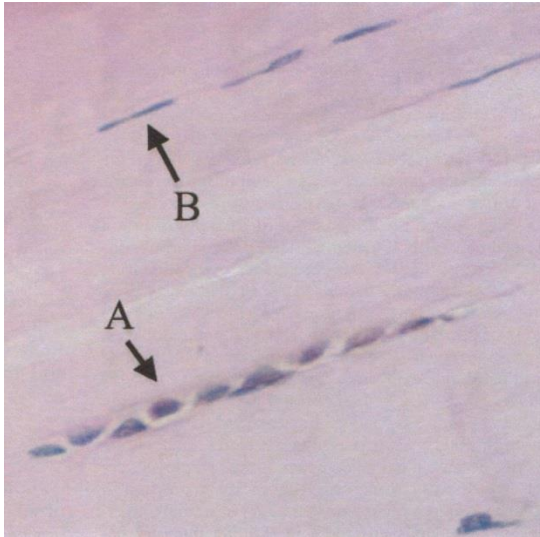


Figure 1-4 Tendon fibroblast phenotypes

The figure shows the two main tendon fibroblast phenotypes, type II (A) and type I (B). Image reproduced with permission from (Chuen et al., 2004).

1.2 SDFT injury

1.2.1 Epidemiology

The most frequently injured tendon in Thoroughbred racehorses is the forelimb superficial digital flexor tendon (SDFT). Injuries can vary from minor partial rupture to complete bilateral rupture of the tendon. Lesions are typically found in the core of the mid-metacarpal region, although they can be located anywhere from the level of the proximal carpus to its branches of insertion (Goodship, 1993), (Gibson et al., 1997), (Chesen et al., 2009). The prevalence of this injury is between 11-30% in athletic horses and the incidence of SDFT injuries in racehorses has been reported as being 0.6%-16.1% per 1000 race starts (Goodship et al., 1994), (Williams et al., 2001), (Kasashima et al., 2004), (Pinchbeck et al., 2004) and (Ely et al., 2009). The risk of injury is higher in older racehorses with a sharp rise in incidence over 5 years of age (Perkins et al., 2005), (Ely et al., 2009). Horses participating in the National Hunt have a higher incidence of injury compared to those on the flat and the increased risk is thought to be linked to the use of older horses, competing over longer distances, racing over a number of seasons. Jumping over hurdles also places increased strain on the tendon (Parkin, 2008), (Williams et al., 2001), (Meershoek et al., 2001).

1.2.2 The concept of microdamage and degeneration of the SDFT with age and exercise

Few cases of tendon rupture are based on a single traumatic incident, instead being caused by numerous, repetitive bouts of high intensity exercise leading to the accumulation of microdamage within the tendon core. Evidence of subclinical age and exercise-induced microdamage has been documented in horses. These include age and exercise associated elevations in type III collagen, age-related increased levels of sulphated glycosaminoclycans (GAGs) and denatured collagen together with decreased exercise-associated collagen mass average fibril diameter, collagen fibril disruption, decline in crimp angle and length and reduced GAG formation in exercised horses (Birch et al., 1999), (Birch et al., 2008a), (Patterson-Kane et al., 1997b), (Patterson-Kane et al., 1997a), (Lin et al., 2005), (Riley, 2005).

A 'tendinosis cycle' or tendonopathy has been reported describing a continuum of pathology in which mechanical overloading and other exercise associated factors can damage the matrix leading to reactive tendinopathy or tendon injury. If the damage is severe enough, it can overwhelm cellular repair processes, leading to irreversible dysfunctional cellular activity which can weaken the matrix and predispose the tendon to rupture. There can be a significant overlap of each of these stages leading to a merging of various macroscopic and microscopic histopathological changes in tendon (Cook and Purdam, 2009), (Leadbetter, 1992), (Patterson-Kane et al., 2012).

There is still some considerable debate as to why cellular repair processes become saturated, whether it results from excessive matrix damage associated with high intensity exercise, insufficient time between episodes of racing/exercise for repair to take place, alterations in cellular synthesis patterns or activity, cellular loss, or even changes to the composition of the matrix (Patterson-Kane et al., 2012).

With increasing age, it has been suggested that SDFT tenocytes 'switch off' their cellular machinery to minimise active tissue remodelling to maintain the tendon within its optimal stiffness, essential for its role as an energy storing tendon (Smith et al., 2002). This cellular "switch off" theory has been supported by a study demonstrating that adult SDFT tenocytes were significantly less active compared with immature tendon and other tendons of the distal forelimb. The synthesis of type I and type III collagens and the expression of Cx43/Cx32 proteins per mm² were all significantly reduced in the SDFT tendon compared to the common digital extensor tendon (CDET), where production of the above proteins increased with maturation (Young et al., 2009).

The turnover of the collagenous matrix is much lower in adult SDFT tendon accompanied by the accumulation of 'old' and denatured collagen together with lower levels of MMPs, the matrix metalloproteinases or enzymes required for breaking down the matrix. Collagen-linked fluorescence shows the levels of collagen glycosylation in the tendon and therefore the age of the tendon. These studies showed that there was a positive correlation of collagen fluorescence with age in SDFT tendons (Batson et al., 2003), (Birch et al., 2008b). The mean collagen half-life has been calculated at 198 years in the SDFT

compared to 34 years in the CDET (Thorpe et al., 2010). The reduced synthetic capacity and cell number of the SDFT have important implications for the ability of the SDFT to repair damage especially in situations of high frequency exercise.

1.2.3 Influence of exercise-associated factors in the injury of SDFT tendon

Many studies have investigated how mechanical and other exercise-associated factors can contribute to matrix and cellular pathology in tendons. All of these factors may directly or indirectly result in cell death and/or lead to cellular dysfunction. Apoptotic cells have been seen in sites of ruptured equine tendon (Hosaka et al., 2005). This may have serious ramifications in a sparsely populated tendon requiring healthy cells for its normal function. High levels of mechanical stress can cause cell death directly in tendon cells. This research group used 20% mechanical strain in rat tail tibialis tendon for 6hrs, the timing of which is non-physiological in vivo (Scott et al., 2005). When the tendon experiences the maximal levels of force, isolated collagen fibril rupture is thought to occur near the end of the linear portion of the load-deformation curve, leading to alterations in cell-matrix interactions in the damaged portion of the tendon. Stress deprivation in cells from the loss of cell-matrix tension has been shown to up-regulate collagenase (MMP-13) expression and Caspase-3, one of the proteases involved in the apoptotic cascade resulting in cell death only in those areas where damaged fibrils are found (Lavagnino et al., 2006) (Egerbacher et al., 2008).

Up to 95% of elastic energy is returned on elastic recoil of the tendon however the remaining 5% is lost as heat leading to hyperthermia. During galloping exercise, measurement of the peak temperature rise within the core of the SDFT tendon has exceeded 43°C in vivo. The temperatures generated in vivo could be higher as a number of factors can significantly increase the magnitude of tendon force such as weight of the jockey, muscular fatigue and track fatigue (Wilson and Goodship, 1994). Heat may also be inefficiently dissipated within the tendon core as studies have shown the mid- to distal portions of the tendon are poorly vascularised (Stromberg, 1973), (Kraus-Hansen et al., 1992), (Zantop et al., 2003). The oxygen tension in the SDFT at rest or during exercise is still unknown, but is thought to be low due to the poor vascular supply.

Equine tendon fibroblasts are susceptible to cell death at temperatures ranging from 45°C to 47°C after 10 mins of heating in vitro (Birch et al., 1997a), (Burrows et al., 2009). This variation in temperature may reflect differences in experimental conditions; Burrows et al used monolayers of tendon cells and Birch et al used cell suspensions. Cell suspensions are known to be more heat-resistant than adherent cells, therefore would require higher temperatures to cause cell death (Smith et al., 1993). Gap junctional communication was instrumental in the spread of heat-induced cell death as blockade of these junctions with 18-β glycerol etheric acid minimised the percentage of apoptosis in tenocytes (Burrows et al., 2009). This propagation of cell death has been seen in other tissue types including burn wounds in murine skin. Connexin 43 specific antisense oligonucleotides have been used to transiently downregulate Cx43 expression. When used for the treatment of burn wounds in mice, they have significantly improved wound healing and minimised the spread of tissue damage (Coutinho et al., 2005).

When the SDFT reaches maximum tensile load, it is thought that the tissue undergoes a period of ischaemia. There is no known data on whether the equine cells experience reduced blood oxygen tension at this time. Equine cells do exhibit aerobic metabolism in vitro (Birch et al., 1997b). Reperfusion of the tissue with restoration of normal oxygen tension following ischaemia will produce elevated levels of reactive oxygen species (ROS) which may not be harmful in normal tendon as the cells produce antioxidants to neutralise the effects of the ROS. It may however be harmful to dysfunctional tenocytes and/or the matrix when microdamage is present. ROS are known to damage the connective matrix, affect the synthesis of matrix proteins and lead to decreased tenocyte viability (Longo et al., 2008), (Tanaka et al., 1993), (Liang et al., 2012). Exposure of human dermal fibroblasts to xanthine, a stimulant of ROS release led to significantly lower collagen synthesis and increased GAG production (Tanaka et al., 1993). A reduction in collagen synthesis was also noted in rabbit anterior and posterior cruciate ligaments when treated with an exogenous source of nitric oxide, however the medial cruciate ligament was not affected, thus demonstrating that there are potential differences between connective tissues in their response to ROS (Cao et al., 2000). When human hamstring tendon fibroblasts were exposed to hypoxia (0.1% oxygen) for 48hrs,

apoptosis was induced in 7.5% compared with 1.6% normoxic controls. Hypoxia with serum starvation for 48hrs increased the percentage of apoptotic cells to 19.5% (Liang et al., 2012). All of the studies outlined above were conducted in vitro: the situation with in the vivo environment may well be different.

Although the mechanical, temperature and oxygenation influences on the cells and the matrix have been assessed as independent stresses, in vivo they will all converge and the occurrence of more than one damaging pathway may be more likely to lead to cell death and/or overwhelm the tendon fibroblasts' ability to repair damage. The application of a double stress, mechanical stress at 9% cyclic strain with hyperthermia at 42°C for 6hrs or 24hrs in canine patellar cells induced a significant increase in Caspase-3 activation and DNA fragmentation. The length of experimental hyperthermia was non-physiological, however shorter bouts of hyperthermia associated with repetitive exercise in a tendon with microdamage may predispose it to rupture (Tian et al., 2004).

1.2.4 Does inflammation play a role in tendinopathy?

There has been some speculation as to whether inflammation plays a strong role in the degenerative process of tendons. In studies of injured human tendons, few inflammatory cells have been found, leading to the belief that tendon injury is primarily a degenerative condition (Leadbetter, 1992), (Järvinen et al., 1997). Few subclinical tendon injury samples are available for examination as they are rarely symptomatic in patients. A recent study demonstrated an influx of inflammatory cells including mast cells and macrophages in matched asymptomatic human subscapularis tendon from patients with torn supraspinatus tendons. The histologic appearance of the subscapularis tendon was suggested as being a model of early human tendonopathy (Millar et al., 2010). In the horse, mast cells have been localised to sub-acute SDFT injuries (3-6 weeks post injury) and the phenotype of the mast cells have been characterised as the M1 MØ class which play a predominately pro-inflammatory role in tissues (Dakin et al., 2012). Dakin et al found there was a population change or alteration of phenotype in chronic injuries where there were more M2 MØ mast cells (Dakin et al., 2012). This latter group is associated with the dampening of the inflammatory response through the production of anti-inflammatory cytokines such as Il-1 receptor

antagonist (Mantovani et al., 2002). The persistence of an anti-inflammatory influence in chronic injuries has been suggested as a potential cause of incomplete resolution of the inflammation in tendons (Dakin et al., 2012).

Inflammatory mediators may have a role in the pathogenesis of tendon injury and there is some evidence for this. Application of cyclic loading to human patellar tendon cells led to the production of cytosolic phospholipase-A₂, prostaglandin E₂ and cyclo-oxygenases 1 and 2 (Wang et al., 2004). Heat stress in equine tendon fibroblasts at 42°C can elevate the production of several pro-inflammatory cytokines including TNF-α. Heating was applied for 30-60 mins (which is non-physiological in vivo) (Hosaka et al., 2006). The pro-inflammatory cytokines IL-1 and TNF and prostaglandin E₂ are known to activate the production of MMPs (Riley, 2005). Breakdown of the ECM by the MMPs will normally allow the turnover and subsequent repair of the damaged tendon but in tendons with microdamage caused by repetitive exercise, the production of pro-inflammatory cytokines and MMPs may be harmful.

1.2.5 Clinical rupture: the problem with regeneration

Healing of an injured tendon is a lengthy process taking up to 9-18 months depending on the severity of the initial injury (Smith et al., 2002). The resultant scar tissue has reduced tensile strength and elasticity which persist for long periods making it susceptible to re-injury. Areas adjacent to the scar tissue are placed under higher compensatory stresses and strains and rupture typically occur at the junction between damaged tissue and this compensatory, normal tendon (Crevier-Denoix et al., 1997), (Oryan et al., 2012). Re-injury rates of 23-67% have been recorded in various equine athletic sports, which have both financial and welfare concerns (Marr et al., 1993), (Dyson, 2004), (O'Meara et al., 2010).

There is no single effective treatment to repair tendon lesions, lacerations and/or rupture. Many medical and surgical therapies have been used with varying success including controlled exercise regimes, rest, ice therapy, injection of recombinant growth factors, autologous plasma concentrates, hyaluronan and polysulphated glycosaminoglycans together with superior check

desmotomy amongst others (Petrov et al., 2003), (Dyson, 2004), (Dowling et al., 2002), (Argüelles et al., 2008), (Bosch et al., 2010), (Fulton et al., 1994).

In recent years, there has been a strong interest in the use of stem cells to recapitulate tendon development and growth as a form of regenerative medicine. Stem cells have produced improvements in the histological appearance of damaged tendons and re-injury rates are reportedly significantly lower following their use. Study sizes have been small and stem cells injected into adult tendons do not appear to revert to the regenerative capacities seen in fetal tendon (Watts et al., 2011), (Marfe et al., 2012), (Smith, 2008), (Beredjiklian et al., 2003), (Smith et al., 2013). A recent study showed there was an improvement in the gross, functional and histological features of injured tendon following treatment with equine bone marrow derived mesenchymal stem cells suspended in marrow supernatant resulting in a smaller cross-sectional area of the affected SDFT in comparison with saline injected controls, better organisation of the collagen fibrils in the treated tendons, lower cellularity of the affected area and reduced tendon stiffness (i.e. improved elasticity) (Smith et al., 2013). One of the problems in interpretation of this work is the lack of a third control containing mesenchymal stem cells in a unconditioned supernatant as it is unknown whether the improvement in histological features could be directly attributed to the effects of the mesenchymal stem cells or the bone marrow supernatant which is known to contain significant quantities of growth factors and other immuno-modulatory agents (Takahashi et al., 2006). Another study demonstrated poor survival of mesenchymal stem cells injected in vivo with less than 5% of stem cells being detected in the tendon 10 days following injection. In contrast, the use of fetal equine embryonic stem cells resulted in improved survival rates with at least 60% of injected cells being detected at the lesion sites (Guest et al., 2010). The failure of complete regeneration of the tendon tissue gives credibility to the fact that prevention of tendon injury will have a greater clinical impact than therapy alone (Patterson-Kane et al., 2012).

1.3 Cellular injury and cell death pathways

Most of the current treatments for tendon injury and inflammation have had mixed success rates and an understanding of how tendon fibroblasts respond

to various exercise-related stresses will allow a hierarchy of cellular injury pathways to be mapped out so that key areas can be identified and potentially manipulated for the prevention of tendon injury.

As the use of large animal studies has significant technical, animal welfare and cost issues, *in vitro* experimental systems are preferentially used to investigate a number of stress associated pathways in equine tendon fibroblasts. They are easy to use, tractable and amenable to both molecular and cellular analyses especially when being used in a time-dependent manner (Patterson-Kane et al., 2012).

Growth of cells in two- dimensional culture systems can place large stresses on tendon cells as the supportive tissue micro-environment is lost. The natural micro-niche which the tenocytes share with the ECM is diminished; the tendon fibroblasts are grown in sheet like monolayers rather than in longitudinally arranged rows and the cells are immersed in a highly oxygenated liquid containing many nutrients and chemicals which differ from those present *in vivo* (Rubin, 1997), (Halliwell, 2003). For example, there is a high sugar content in cell culture media. Standard DMEM (Dulbecco's Modified Eagle Medium) contains 4.5g/L (25mM) glucose and *in vivo* this blood sugar level is seen in diabetic horses. The normal blood sugar values in horses are between 3.4 mmol/L and 7.4mmol/L. (Aiello, 2012). The culture of rat Achilles tendon fibroblasts in high glucose (12mM or 25mM) has been shown to lead to increased expression of MMP-9 and -13 mRNA, the enzymes responsible for the degradation of collagen (Tsai et al., 2013). Cell culture is routinely performed at ambient oxygen (21%), however the oxygen tension in mammalian tissues is thought to range from 1-6% (Halliwell, 2003). High oxygen tensions in culture can generate genotoxic stress in cells which can ultimately lead to growth arrest and premature cell senescence. A hostile tissue culture environment which induces DNA damage to cells resulting in growth arrest and premature cell senescence is known as "cell culture shock" (Wright and Shay, 2002).

A greater understanding of the mechanisms by which certain cell culture cues can stress the tendon fibroblasts prior to the investigation of how exercise-associated factors affect these cells would be beneficial and additionally provide opportunities for the optimisation of the most appropriate culture conditions.

1.3.1 DNA damage response

Phosphorylation of H2AX in cells

One of the most damaging insults to cells is double stranded breaks (DSBs) in DNA. The formation of DSBs can occur in healthy cells as a result of normal replication stress, however it can also be seen in response to insults including UV light, radiation, drugs and hyperthermia (Ichijima et al., 2005), (Rogakou et al., 1998), (Hunt et al., 2007), (Kurz et al., 2004). If left unrepaired or repaired incorrectly, chromosomal aberrations, genomic instability and cell death can result (Mah et al., 2010). Cells react to this threat by activation of the DNA damage response (DDR) which detects DNA lesions and mediates the signalling and recruitment of a host of proteins involved in the DNA damage checkpoint and repair of the lesion. Key signalling proteins activated in response to DSB induction are the protein kinases ATM (Ataxia telangiectasia mutated) and ATR (ATM and Rad3-related). These two kinases mediate the activation of a number of downstream signalling proteins, including the phosphorylation of the histone H2AX at serine 139 (Rogakou et al., 1998), (Ward and Chen, 2001), (Burma et al., 2001). H2AX is a variant of histone H2A in mammalian cells and phosphorylation of this complex is one of the earliest events in the DNA damage response to injury (Rogakou et al., 1999). In the first 30 mins of an injury, phosphorylated H2AX stimulates the recruitment of a number of downstream repair proteins to the site and allows chromatin restructuring to take place to accommodate the extra proteins required for repair of the lesion. Each γ H2AX focus has several hundred γ H2AX molecules at the DSB site, and the number of foci has a strong correlation with the number of DSBs. This has been used to quantify the latter in many experimental conditions. The γ H2AX puncta are lost as the DNA damage is resolved and repaired correctly (Rogakou et al., 1999), (Paull et al., 2000), (Sedelnikova et al., 2002), (Bonner et al., 2008), (Rich et al., 2013). The phosphorylation of H2AX also provides a generic downstream readout of multiple cell stresses including inflammatory cytokine secretion and the production of reactive oxygen species (Han et al., 2006). The investigation of this injury response in SDFT fibroblasts is of value in evaluating the health of the cells.

1.3.2 Heat shock response

The heat shock response is one of the most important cellular defence mechanisms protecting against an insult. It was originally described in 1962 following puffing of salivary gland chromosomes in *Drosophila* in response to heat shock at 30°C (Ritossa, 1962). This appearance was caused by the activation of genes in response to the heat stress and has since been correlated with the production of heat shock proteins (Moran et al., 1978). The heat shock response is not unique to heat stress and can be precipitated by other stimuli including oxidative stress (Ahn and Thiele, 2003).

The transcriptional activation of heat shock proteins is controlled by a family of heat shock factors (HSFs). The major isoform involved in the classical heat shock response is HSF-1 in vertebrates as knockout mice homozygous for HSF-1^{-/-} were unable to produce inducible heat shock proteins in response to heat stress (Xiao et al., 1999), (McMillan et al., 1998). One of the inducible heat shock proteins in equine cells is Hsp-72 which has been shown to be up-regulated in skeletal muscles during exercise (Poso et al., 2002).

HSF-1 exists in a monomeric form through its association with HSP 90 and other co-chaperones in a multimeric complex which keeps it in its inactive form (Zou et al., 1998), (Guo et al., 2001). The presence of unfolded proteins during periods of cellular stress will compete for the HSP 90 binding sites, leading to release of HSF-1, trimerization and its subsequent activation. Active HSF-1 has the ability to bind to heat shock elements which ultimately leads to the transcription of the heat shock proteins (Ananthan et al., 1986), (Baler et al., 1993). HSPs can also act in a negative feedback loop by inhibiting HSF transactivation capacity, an important control step in the modulation of the duration and intensity of HSF activity correlating with the levels of protein damage present (Baler et al., 1992), (Shi et al., 1998).

The rate of temperature increase may be important for the induction of heat shock proteins as the rate of protein accumulation has been suggested to be dependent on the number of working ribosomes, the rate at which the ribosomes are working and the rate of protein degradation (Farewell and Neidhardt, 1998). This suggests the rate of heating is an important concept in

the study of heat shock protein induction, however there is very little data in the literature on this topic.

A study has shown the peptide elongation rate of *E. coli* increased with temperature from 25-44°C and it was suggested an increase in the presence of unfolded proteins induced the production of heat shock proteins (Farewell and Neidhardt, 1998). Another study has shown the higher the temperature used, the faster the kinetics of Hsp-72 production. The time taken for Hsp-72 protein levels to exceed the control values in A549 cells was 1hr for 41°C, 6hr for 39.5°C and 24hrs for 38.5°C. These values may differ according to species (Tulapurkar et al., 2009). The expression of Hsp-72 was quantified as being 0.5 fold/1°C between 37-41°C. When the temperature was increased by one degree from 41 to 42°C, the expression increased to 2.4 fold/1°C (Tulapurkar et al., 2009). These studies suggest that the higher the temperature used and the time taken to achieve this temperature will lead to increased levels of unfolded proteins and therefore lead to faster induction of heat shock proteins which will be critical for the survival of cells exposed to a stressor.

Heat stress can shift the equilibrium between the level of normal and denatured protein resulting in an accumulation of misfolded proteins in the cell. To minimize the build-up of aggregated proteins, cells have adopted a universal prosurvival strategy to protect themselves through the expression of the heat shock proteins (HSPs) which can disaggregate and refold damaged proteins (Samali and Orrenius, 1998). However, if the damage is too severe, it will result in the activation of stress associated pathways resulting in cell death (Fulda et al., 2010). Additionally, if the accumulation of damaged proteins exceeds proteasomal capacity (HSPs are thought to target damaged proteins to this site) it can lead to apoptosis as a study has shown that proteasomal inhibition led to apoptosis in Ewing's sarcoma cells (Soldatenkov and Dritschilo, 1997).

HSP-72 can protect against stress-induced cell death by inhibiting integral proteins associated with Caspase dependent and independent apoptosis. The abnormal accumulation of denatured proteins has been shown to activate the stress associated kinase pathways, JNK and p38 kinases and the presence of HSP-70 can prevent the activation of these pathways when cells are subjected to heat stress (Gabai et al., 1997). HSP-72 can bind to proCaspase-3, the inactive

form of Caspase-3 responsible for the proteolysis of many structural and functional proteins as well as nucleic acids during apoptosis (Jaattela et al., 1998), (Komarova et al., 2004). The expression of HSP 72 can also block and/or antagonize the recruitment of proCaspase-9 into the apoptosome (an activation platform required to activate Caspase-9) and the release of apoptosis-inducing factor from the mitochondria (Beere et al., 2000), (Ravagnan et al., 2001).

1.3.2.1 Thermotolerance associated with HSP-72 production

Induction of the heat shock proteins leads to the development of “thermotolerance” which enables cells to adapt or withstand subsequent hyperthermia or insults which would otherwise be lethal. Many studies have demonstrated this adaptive ability in a range of cell types. U937 cells (histiocytic lymphoma cell line) were exposed to a period of heat stress at 42°C for 1hr before being recovered at 37°C for 6-8 hrs. Up-regulation of heat shock proteins 70, 90 and 27 was detected by western blot. Thermotolerance was demonstrated when resistance to apoptosis (drop from 80% to 35%) was seen after the heat shocked cells were then exposed to a range of damaging agents including actinomycin-D, camptothecin and etoposide (Samali and Cotter, 1996). The thermotolerance phenomenon appears rapidly, with the expression of HSP-72 peaking within 4-6 hours followed by a gradual decline following exposure to the event, often lasting 4-5 days (Laios et al., 1997), (Landry et al., 1982).

1.3.3 Promyelocytic leukaemia (PML) sensing systems

1.3.3.1 PML nuclear bodies (PML-NBs) and DAXX

PML NBs are spheres of approximately 0.1-1.0µm in diameter and are seen in the nuclear matrix of most cell lines. The PML protein is the key organiser of the PML nuclear body and recruits a large number of partner proteins to this sub nuclear hub (Figure 1-5). The ubiquitin-like SUMO-1 protein is essential for the conjugation of the PML protein to the PML NB. Sumoylated PML in turn is required for the interaction and tethering of partner proteins to the PML NBs, one of which includes DAXX, (Zhong et al., 2000b), (Lallemand-Breitenbach and de The, 2010), (Lin et al., 2006). PML NBs have a multitude of roles in the cell including the regulation of transcription, apoptosis, senescence and are also

involved in the DNA damage response and resistance to micro-organisms (Lallemand-Breitenbach and de The, 2010). PML NBs are sensitive to cellular stress and studies have shown that these sub-nuclear hubs are structurally altered in response to viral infections (Maul et al., 1993), heavy metals and heat shock (Nefkens et al., 2003). For example, exposure to arsenic trioxide led to an increase in the size of each PML NB due to an increase in PML SUMOylation (Maroui et al., 2012) and heat shock has been shown to result in dispersal of PML protein and some of its partner proteins including DAXX into the nucleoplasm (Nefkens et al., 2003).

In unstressed cells, DAXX is co-localised with SUMOylated PML protein at PML nuclear bodies. In immunofluorescent images, it can be visualised as speckles within the nucleus (Zhong et al., 2000b). DAXX is a multi-functional protein with roles as a transcriptional co-repressor, participation in cellular stress response pathways and in apoptosis (Khelifi et al., 2005), (Kim et al., 2003). It was first identified as a pro-apoptotic protein specifically binding to the Fas death domain, a plasma membrane death receptor (Yang et al., 1997b). DAXX has been shown to activate the JNK (c-Jun-N-terminal kinase) pathway downstream of Fas by binding to ASK1 (apoptosis signal- regulating kinase 1) leading to Caspase-8 initiated apoptosis in response to various stimuli such as UV irradiation and hydrogen peroxide treatment (Chang et al., 1998), (Song and Lee, 2003). Upon exposure to 80J/m² UV, DAXX depleted cells were more resistant to cell death and the activation of the JNK pathway was significantly impaired (Khelifi et al., 2005).

DAXX is known to repress the transcriptional activity of a number of genes including that of p53 (Kim et al., 2003). During periods of cellular stress which lead to DNA damage, ATM kinase has been shown to phosphorylate DAXX at Ser564 which disrupts the ability of DAXX to stabilise Mdm2, (a ubiquitin ligase complex which keeps p53 at low levels during basal conditions) thus promoting the activation of p53 (Tang et al., 2013). Depending on the severity of the genotoxic stress experienced by cells, p53 can activate the transcription of genes which can determine cell fate e.g. at times of lethal stress, p53 can be phosphorylated at Ser46 resulting in the induction of pro-apoptotic genes including Puma and Bax (Oda et al., 2000).

Dispersal of DAXX from the PML nuclear bodies has been shown to occur following exposure of cells to various stressors including hyperthermia (Nefkens et al., 2003). Heat shock causes the release of DAXX from the PML bodies via enzymatic removal of SUMO-1 from PML by a SUMO-1 isopeptidase such as SENP-1 (Nefkens et al., 2003) (Figure 1-5). Thermal stress was shown to induce the rapid release of DAXX from HEp-2 cells in less than 12mins when heated to a non-lethal temperature at 42°C for one hour. DAXX dispersal was reversible after recovery at 37°C (Nefkens et al., 2003). During the heat shock response, the dispersal of DAXX into the nucleoplasm was shown to oppose the repression of HSF-1 activation through its affinity for binding to trimerised HSF-1 i.e. DAXX shifts the equilibrium from inactive to active HSF-1 resulting in the subsequent production of heat shock proteins (Boellmann et al., 2004).

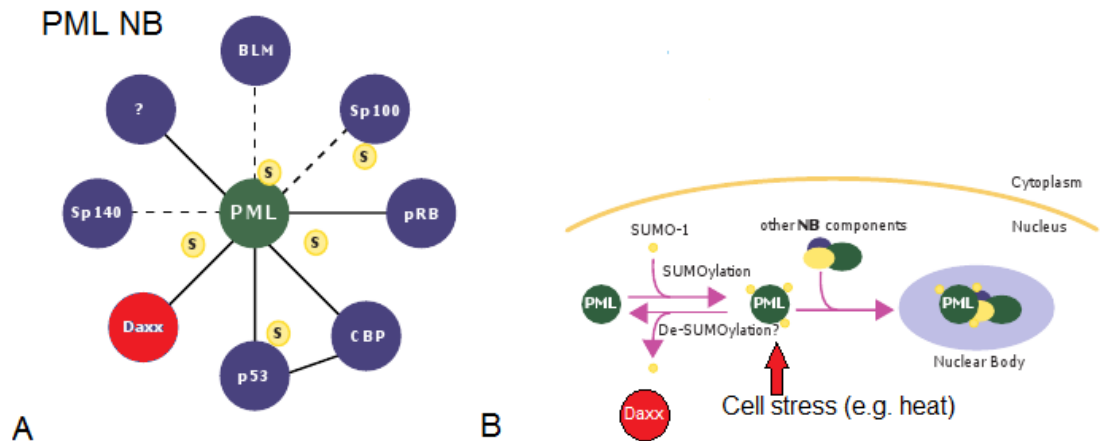


Figure 1-5 PML NB and its response to cell stress

PML protein is the key organiser of the PML NB. The SUMOylation of PML (yellow S circles) is essential for the interaction and tethering of partner proteins including DAXX to the site (A) When the cells are exposed to cell stress e.g. heat de-SUMOylation of the PML protein releases DAXX into the nucleoplasm (B). Image modified from (Zhong et al., 2000a).

1.3.3.2 Caspase-2

Caspase-2 has been shown to co-localise to PML nuclear bodies and it is tethered to this hub protein through its prodomain and its protease domains (Tang et al., 2005). Caspase-2 is activated in response to various stressors; most notably in response to heat shock in addition to cytoskeletal disruption and DNA damage (Bouchier-Hayes et al., 2009). Caspase-2 is a member of the Caspase family which participates in cellular apoptosis. The recruitment of Caspase-2 to a multimeric complex is essential for the dimerization of the pro-form of Caspase-2, a requirement for Caspase-2 activation and subsequent cellular apoptosis (Bouchier-Hayes et al., 2009), (Tu et al., 2006). A lethal heat shock at 45°C for 1hr in HeLa cells has been shown to lead to the activation of PIDD (p53 induced protein with a death domain), RAIDD (receptor-interacting protein (RIP)-associated ICH-1/CED-3 homologous protein with a death domain) and Caspase-2 into the PIDDosome (the multimeric complex) (Bouchier-Hayes et al., 2009). The production of stress-induced heat shock proteins is mediated by the activation of HSF-1. The knock-out of HSF-1^{-/-} in mouse embryonic fibroblasts led to these cells being more sensitive to heat shock induced apoptosis compared to wild type cells. Further work by the group showed that HSF-1 mediated Hsp-90 production inhibited Caspase-2 activation in response to heat shock (Figure 1-6) demonstrating the important influence the heat shock proteins play in cellular fate (Bouchier-Hayes et al., 2009).

1.3.4 Cell death pathways

1.3.4.1 Apoptosis

Apoptotic cells have been seen in horses with clinical SDFT lesions (Hosaka et al., 2005). Caspase-3 is the main executioner protein responsible for the breakdown of the cell during apoptotic cell death and this protein has been used to identify apoptotic cells in tissue lesions (Pearce et al., 2009), (Yuan et al., 2002). Formal validation of Caspase-3 antibodies is lacking in equine studies. Two commercial cleaved Caspase-3 antibodies used in equine tissue studies have not provided any convincing labelling of apoptotic cells in immunocytochemistry or immunohistochemistry work by our lab group (Patterson-Kane et al., 2012).

Apoptosis is a precise, co-ordinated energy-dependent mode of cell death occurring during development, aging and the maintenance of normal cell populations in tissues. Apoptotic cell death can be triggered by a number of cellular insults, both physiological and pathological (Elmore, 2007). The morphological changes of apoptosis are typically characterised by the appearance of small, shrunken cells. Nuclear and cytoplasmic condensation is a key feature of apoptotic cell death and the pyknotic nucleus often becomes crescent shaped, after which nuclear fragmentation takes place. This is followed by extensive plasma membrane blebbing, resulting in small membrane bound fragments (apoptotic bodies) containing cytoplasmic organelles and pyknotic nuclei (Rello et al., 2005), (Kerr et al., 1972), (Taatjes et al., 2008).

The deconstruction of the cell during the apoptotic cascade is typically executed by a family of cysteine proteases -the Caspases. The Caspase family can be classified into two groups depending on its mode of activation. The initiator Caspases (e.g. Caspase-2, -8, -9, -10) contain a long pro-domain region which is required for its oligomerization -facilitated autoactivation at multi-protein complexes. In general they are responsible for the activation of the executioner Caspases (e.g. Caspases-3,-7) and it is the latter group which directly or indirectly cleaves key proteins and nucleic acids in the cell resulting in cell death (Stennicke and Salvesen, 1998),(Elmore, 2007), (Sakahira et al., 1998),(Boatright et al., 2003).

1.3.4.2 Intrinsic apoptotic pathway

The intrinsic apoptotic pathway is activated by various stimuli which initiate a cascade of intracellular signals ultimately targeting the inner mitochondrial membrane resulting in the opening of the mitochondrial permeability transition pore, loss of mitochondrial transmembrane potential and release of pro-apoptotic proteins sequestered within the inter-mitochondrial membrane (Figure 1-6). The control and regulation of mitochondrial membrane permeability is undertaken by the B cell lymphoma-2 (Bcl-2) family of proteins which either promote or inhibit the release of proteins within the inter-mitochondrial membrane, the most widely known being cytochrome c (Elmore, 2007), (Desagher et al., 1999), (Kluck et al., 1997), (Yang et al., 1997a). Once in the cytosol, cytochrome c will activate the formation of the 'apoptosome', a

large protein scaffold mainly composed of an adaptor protein Apaf-1 and proCaspase-9. The apoptosome is the key scaffold platform essential for the dimerization of proCaspase-9, a requirement for its subsequent recruitment and activation in apoptosis. Caspase-9 has the ability to cleave Caspase-3 precursors into its active form resulting in execution of the cell (Bratton et al., 2001), (Zou et al., 1997) (Renatus et al., 2001).

1.3.4.3 Extrinsic apoptotic pathway

The extrinsic apoptotic pathway is characterised by activation of trans-membrane receptors with their specific ligands resulting in the transduction of pro-apoptotic signals from the cell surface into the intracellular environment (Figure 1-6). The death receptors belong to the tumour necrosis factor (TNF) receptor gene superfamily. Clustering of their associated ligands in an autocrine or paracrine fashion at the cell surface is one of the essential features of this mode of apoptotic cell death. Binding of the receptors with their ligands leads to the recruitment of adaptor proteins on the cell surface, such as FADD which can bind to pro-Caspase-8, which subsequently undergoes auto-catalytic activation at a scaffold (DISC-death-inducing signalling complex). Caspase-8 has the ability to activate the executioner Caspases and interact with various proteins involved in the mitochondrial apoptotic cascade as there is some convergence of the intrinsic and extrinsic apoptotic pathways (Elmore, 2007), (Locksley et al., 2001), (Hsu et al., 1995), (Bajt et al., 2000), (Grunert et al., 2012), (Dickens et al., 2012).

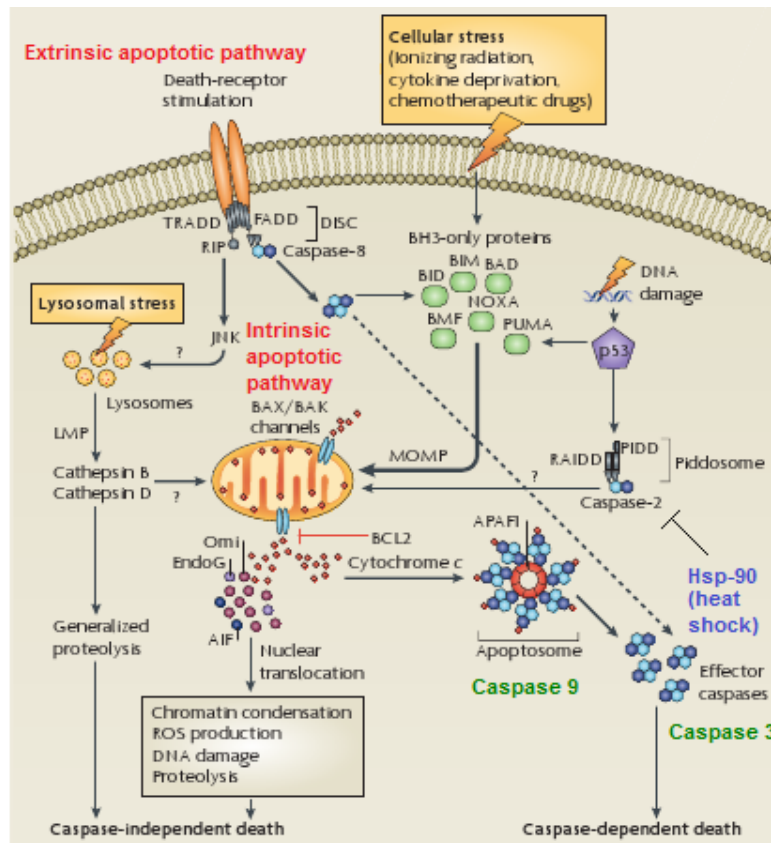


Figure 1-6 The intrinsic and extrinsic apoptotic pathways

This figure outlines a diagrammatic overview of the extrinsic and intrinsic apoptotic pathways in the cell. Image modified from (Maiuri et al., 2007).

1.3.4.4 Necrosis

Necrosis is an uncontrolled passive mode of cell death utilizing energy independent mechanisms resulting in morphological changes including, cell swelling, karyolysis, generalized distention of the internal organelles and loss of cell membrane integrity (Elmore, 2007). As necrosis can refer to the degradative or autolytic processes after cell death has occurred, the term “oncosis” has been proposed to describe a non-apoptotic mechanism of cell death where karyolysis and cell swelling takes place prior to necrosis (Majno and Joris, 1995). Rupture of the plasma membrane associated with necrosis releases the cells’ nuclear and cytoplasmic contents into the extracellular environment, a potent chemotactic signal for the recruitment of inflammatory cells and mediators leading to a widespread inflammatory cascade in the tissue (Hanus et al., 2013), (Scaffidi et al., 2002), (Cohen et al., 2010).

1.3.5 Pro-survival pathways

1.3.5.1 p62 (sequestosome 1)

Autophagy is a “self-eating” process where the cell undergoes catabolic degradation of its own cellular constituents. In healthy cells, autophagy is responsible for the turnover of long-lived proteins or damaged organelles in the cell. Autophagy can be activated by various types of cellular stress including nutrient deprivation, oxidative stress and heat stress (Ishii et al., 1997), (Bjørkøy et al., 2005) (Mizushima et al., 2004), (Nivon et al., 2012). When autophagy is activated, the cells form double membraned vesicles known as autophagosomes which sequester damaged cell organelles or proteins for subsequent transport to the lysosomes (Figure 1-7). The autophagosomes fuse with the lysosomes which contain lysosomal acid proteases promoting the breakdown of cellular constituents into ATP or compounds such as amino acids (Bjørkøy et al., 2005). As a result of this, autophagy is thought of as a “cellular recycling factory” which aids in the protection of cells against an insult and mediates damage control by the removal of non-functional organelles and proteins (Glick et al., 2010).

One of the key proteins involved in autophagy is p62. In the cytoplasm, p62 targets polyubiquitinated proteins for degradation by binding non-covalently to ubiquitin via a C-terminal UBA domain (Vadlamudi et al., 1996). p62 acts as

an adaptor protein, transferring its cargo to the autophagosome through its attachment with LC3B-II, a receptor on these double membraned bodies via the LC3-interaction region (LIR). (Bjørkøy et al., 2005), (Pankiv et al., 2007).

Autophagy is one of two protein turnover pathways employed by the cell. The other is the ubiquitin proteasome system. This system consists of a series of enzymes (E1-E3) linking chains of ubiquitin to proteins for degradation within the 26S proteasome. p62 is linked to this pathway through its ability to transport K63 polyubiquitinated proteins (attached to the C terminal UBA domain) to the proteasome through a second motif at the N terminal PB1 domain (Seibenhener et al., 2004).

p62 acts as a proteotoxic cell sensor as it prevents the build-up of protein aggregates in the cytoplasm because these aggregates are cytotoxic for the cell. The depletion of p62 in cultured neonatal rat ventricular myocytes expressing mutant desmin protein was shown to decrease cell viability and exacerbate cell injury through the accumulation of aggregated mutant protein (Zheng et al., 2011). This protective response is especially relevant during periods of increased protein misfolding which occurs in cells exposed to hyperthermia which causes protein denaturation.

The expression of p62 has been shown to increase after exposure to various stressors including oxidative stress, heavy metals and proteasomal inhibition (Aono et al., 2003), (Ishii et al., 1997), (Pankiv et al., 2010). During oxidative stress, p62 has been shown to activate NRF-2, a stress responsive transcription factor responsible for the expression of anti-oxidant and detoxification enzymes. NRF-2 is normally degraded very quickly via the proteasome to keep it in its inactive form by attaching it to an adaptor protein KEAP1. p62 binds KEAP1 during oxidative stress, allowing NRF-2 to escape from the nucleus where it binds to the antioxidant response elements (Jain et al., 2010), (Lee et al., 2003), (Watai et al., 2007). p62 also acts as an adaptor protein in various intracellular signalling cascades such as linking aPKCs (atypical protein kinase C) to NF- κ B through its interaction with TRAF-6 which can enhance cellular survival and proliferation (Sanz et al., 2000). Hence p62 plays an important role in promoting cell survival during periods of cell stress and acts as an important marker protein evaluating the cells' response to injury.

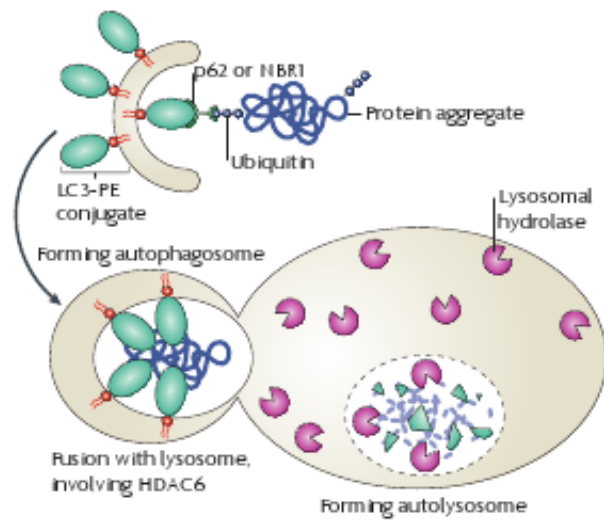


Figure 1-7 p62 transports ubiquitinated protein to the autophagosome

This figure shows the role p62 plays in transporting ubiquitinated protein to the autophagosomes. This is achieved through its interaction with LC3B, one of the receptors found on the autophagosome. The ubiquitinated proteins are eventually degraded in the lysosomes by lysosomal hydrolases. Image reproduced with permission from (Tyedmers et al., 2010).

1.3.5.2 The Unfolded Protein Response (UPR)

The endoplasmic reticulum is an organelle in mammalian cells responsible for the synthesis, folding, modification and quality control of a number of proteins that are destined for the secretory pathway or for the extracellular environment (Cao and Kaufman, 2012), (Kaufman, 2002). This organelle is therefore especially important in secretory cells such as connective tissue fibroblasts which produce large amounts of extracellular matrix proteins (Boot-Handford and Briggs, 2010). The endoplasmic reticulum contains a number of high fidelity processes such as the presence of protein chaperones (e.g. BiP/Grp98) to prevent the accumulation of unfolded proteins in the lumen of the ER. The accumulation of misfolded proteins in the ER leads to the activation of the UPR, where signalling cascades activates an increase in ER folding capacity, decreases protein synthesis within the ER and stimulates ERAD (ER-associated degradation), the targeted destruction of misfolded proteins via the proteasomes (Kaufman, 2002), (Cao and Kaufman, 2012).

There are three transmembrane protein sensors that detect the presence of unfolded proteins in the lumen, the inositol-requiring kinase (IRE1), pancreatic ER eIF2a kinase (PERK) and activating transcription factor 6 (ATF6) (Cao and Kaufman, 2012). All three protein sensors are kept in an inactive state by binding to BiP, a protein chaperone and upon the presence of increased amounts of unfolded proteins in the ER, become dissociated from BiP (Cao and Kaufman, 2012). Once activated these kinases have important roles in the adaptive response to misfolded proteins, e.g. the IRE1 kinase catalyses the splice of X-box binding protein1 (XBP1) to XBP1s (s for spliced) and the latter is responsible for the transcription of genes that increase the protein folding capacity of the ER or those involved in ERAD. IRE1 has also been shown to be associated with TNF- α , which can then lead to the downstream activation of Jun-N-terminal kinase (JNK) and subsequent apoptosis of the cell or autophagy.

ER stress can occur with a number of insults including heat shock, hypoxia and metabolic dysfunction as a result of an increase in the concentration of misfolded proteins and this in turn leads to the activation of the UPR to help maintain protein homeostasis within the cell (Boot-Handford and Briggs, 2010). The exposure of cells to persistent ER stress can lead to the activation of

apoptosis to remove the damaged cells, through the up-regulation of IRE1 mediated JNK activation and additionally through the up-regulation of C/EBP-homologous protein (CHOP, a transcription factor that activates several pro-apoptotic factors such as Bim, a Bcl-2 family member) via PERK activation. Studies have shown that ER stress can lead to pathology of connective tissues including osteoarthritis. One study showed there was an increase in the expression of ER stress associated proteins including phosphorylated PERK and CHOP in addition to increased Caspase-3, an apoptotic marker in degenerate osteoarthritis. Additionally, it was shown there was an increase in the levels of these markers with the severity of the osteoarthritis (Takada et al., 2011), (Guo et al., 2014). It is unknown whether ER stress plays an important role in SDFT tendon pathology, however it is hypothesised that it will be playing a part, as racehorses subjected to repetitive exercise will generate lots of damaged proteins through exposure to heat stress.

1.4 The effects of cooling and the up-regulation of key cold shock proteins

1.4.1 The use of cryotherapy

Various forms of cryotherapy such as ice baths and cooling wraps are commonly used in the equine field. They can aid in treatment and prevention of acute musculoskeletal and tendon injuries. The use of cryotherapy provides analgesia, relieves swelling and inflammation of the affected tissue through vasoconstriction, reduced cellular metabolism and reduction of the production of inflammatory cytokines (Petrov et al., 2003), (Speer et al., 1996), (Van Eps et al., 2012), (Van Eps and Pollitt, 2009), (Zhang et al., 2014).

There is no definitive method outlining the duration, required temperature or the most appropriate application of cold shock therapy for the treatment of tendon injuries and even less on whether injuries can be minimised through preventative cryotherapy (Petrov et al., 2003). A number of experimental studies have shown hypothermia can provide neuroprotection to sensitive regions of the brain exposed to ischaemic injuries. Exposure of rat brains to 30°C during 15 mins of forebrain ischaemia (induced by bilateral occlusion of the common carotid arteries) prevented neuronal cell damage as

shown by reduced alkalosis and reactivity of astrocytes compared to their normothermic counterparts (Chen et al., 1992). There appears to be a window of opportunity during which hypothermia can exercise its protective effects in damaged neuronal cells. When hypothermia was instituted after a 5 min ischaemic event for varying lengths of time, the protection afforded to the neuronal cells was proportional to the duration of hypothermia received. When the hypothermic treatment was delayed for 1 and 3hrs following the ischaemic event, the survival of the neuronal cells dropped from 77% to 49% with a 1hr delay and no survival at all with a 3hr delay (Carroll and Beek, 1992). Improved neuroprotection and functional outcome has been seen when the period of hypothermia is extended for longer durations; even up to 48hrs (Yanamoto et al., 2001), (Clark et al., 2008). There has been no published work on the protective effects of cryotherapy on tendons in vivo and in vitro.

1.4.2 The cold shock protein RBM3 and its roles

Protection of cells with increasing length of cooling time is believed to correlate with the production of cold shock inducible proteins including RBM3 (RNA binding motif protein 3) and CIRP (cold-inducible RNA binding protein) (Dresios et al., 2005). A mild temperature downshift from 37°C to 32°C leads to the expression of RBM3 mRNA, the maximal levels of which are produced at 18hrs of continuous cold shock and lasts for up to 36hrs (Danno et al., 1997).

Although cooling of cells leads to a general inhibition of protein synthesis with a concomitant decrease in the metabolic rate, RBM3 can enhance the translation of certain proteins allowing the cells to tolerate cold shock conditions (Dresios et al., 2005), (Chappell et al., 2001). This protective effect is not restricted to cooling as hypoxia can also increase RBM3 activity in cells (Wellmann et al., 2004). Lowering the temperature not only subjects cells to cold stress, it also increases the dissolved oxygen concentrations in the blood, potentially leading to metabolic stress (Al-Fageeh and Smales, 2006). If metabolic stress is able to up-regulate RBM3 expression, the subsequent rewarming period following cold shock could induce free radical oxygen species production and increased expression of RBM3.

1.4.3 Hsp-72 and cold shock

Protection of cells through the activation of heat shock proteins may also occur during the rewarming period from cooling to 37°C. A number of studies have demonstrated Hsp-72 induction following cold shock in neonatal rat cardiomyocytes and IMR-90 human diploid fibroblasts. The maximal expression of Hsp-72 in neonatal rat cardiomyocytes after cooling (4°C for 1hr) was not as high compared to heat shock (42°C for 1hr) (Laios et al., 1997), (Liu et al., 1994), (Tveita et al., 2012). There is a paucity of data on whether thermotolerance can be instituted following cold shock. The induction of thermotolerance is known to take place following heat shock and it would be of interest to see if this could occur with cold shock. If cold shock is able to protect cells from a subsequent lethal stimulus, the application of ice packs prior to a race would be an easy method to administer to horses in the field.

1.5 Aims of this work

The main focus of my research was to investigate the sensitivity of SDFT-derived fibroblasts to hyperthermia *in vitro* (as this stressor is thought to be one of the major contributors to cell death in tendon fibroblasts in racing Thoroughbreds) and to compare this with the DDFT, a non-injury prone tendon.

1) My first aim prior to the investigation of heat shock in SDFT and DDFT tendon fibroblasts was to quantify the basal cellular injury levels (by measuring the percentage of DNA damage) acquired from culturing cells *in vitro*, as certain environmental cues including high oxygen tensions (21%) can result in “cell culture shock”. The use of high oxygen tensions was hypothesised to lead to elevated levels of DNA damage in SDFT and DDFT fibroblasts and this response may be mitigated or amplified with certain matrix types including collagen type I and fibronectin.

2) For the heat shock work, I aimed to examine the expression pattern of heat shock protein-72 in SDFT and DDFT fibroblasts by western blot over a range of heat and cold shock temperatures ranging from 26-52°C and to determine if thermotolerance could be induced in these cells following both heat shock and cold shock. The SDFT was predicted to be faster to mobilise Hsp-72 production in

comparison with the DDFT and as a result of this, be better at surviving a lethal heat shock.

3) The identification and expression of protein markers (e.g. DAXX) which are up-regulated during the early stages of heat and cold shock were also determined. This could enable preventative strategies to be devised to minimise cell death in tendon fibroblasts. It was hypothesised that the size of DAXX puncta would be different when exposed to heat and cold shock i.e. smaller during heat shock due to loss of DAXX into the nucleoplasm and larger with cold shock as protein production is suppressed at cold shock temperatures.

Chapter 2) Materials and Methods

2.1 Collection of tendon samples

The incidence of SDFT injuries increases with age in Thoroughbred horses with a sharp rise in incidence over 5 years of age. For this reason, I sourced SDFT and DDFT tendons from Thoroughbred horses between the ages of 2-7. Two Thoroughbred (TB) racehorses were sourced from Weipers Equine Clinic at the University of Glasgow. These horses were euthanased for reasons other than tendon injury. One was a 6 year old TB gelding that presented for an over-reach injury (not tendon related) and the other was a 7 year old TB racehorse that presented for colic. The forelimbs of one foal that presented for a fracture was also collected.

Two more TB horses (aged 5 and 7 years old) were collected from an abattoir in Cheshire as the sample population at the University of Glasgow were scarce. The disadvantage of obtaining horse legs from the abattoir were; the history of the horses were unknown (medical and race history were not known), only one set of horse legs (two forelimbs) could be transported back to the lab at one time and the long time between transport of the limbs (5-6 hours) and processing of the legs. A summary of all the horses collected during my thesis is outlined in Table 1 below.

Following euthanasia of the horses (according to the most appropriate welfare protocols), both forelimbs were severed at the radiocarpal joint. For horses sourced from the abattoir, the whole leg (including the hoof) was kept, wrapped in a number of tea towels then placed in a polystyrene box containing ice. The ice was used to keep the limb cold and prevent post mortem degeneration of the cells and tissues. For horses sourced from Weipers Equine Clinic, the legs were processed straight away.

Horse/Foal	Age	Gender	Racehorse	Reason for euthanasia	Chapter of thesis
Horse 1	7 years	Gelding	No	Unknown (abattoir)	Chapter 3
Horse 2	5 years	Mare	No	Unknown (abattoir)	Chapter 3
Horse 3	6 years	Gelding	Yes	Over-reach injury	Chapter 4
Horse 4	7 years	Gelding	Yes	Colic	Chapter 5
Foal 1	2 days	Female	No	Fracture	Chapter 3

Table 1: List of the horses (and foal) used in my thesis

This table outlines the age, signalment, gender, whether it was a racehorse, reason for euthanasia, and which chapter of my thesis the extracted cells were used for.

2.2 Preparation of tendon specimens for cell culture

2.2.1 Tendon specimens

5 cm mid-metacarpal segments of the SDFT and of the underlying DDFT were aseptically retrieved from both forelimbs of four TB horses (not occurring at the same time). To retrieve the tendon segments aseptically, the mid-metacarpal region of the forelimbs were shaved using electric clippers (Oster A5 Turbo 2 Speed) to remove all the hair then scrubbed with chlorhexidine (HiBiScrub) to clean and sterilise the skin. Sterilising the skin minimises the transfer of bacterial and fungal organisms from the skin to the tendon segments. Following this, the limb was covered with surgical drapes and the skin was incised with sterilised scalpel blades and forceps. The outermost connective

tissues were removed to expose the SDFT tendon. Following the removal of the SDFT tendon, the DDFT tendon was excised (it is found underneath the SDFT). Following the excision of the tendon segments, they were placed into pre-warmed DMEM (Dulbecco's Modified Eagle's Medium) (37°C) and harvested for tendon fibroblasts immediately.

2.2.2 Extraction and culture of tendon fibroblasts by enzymatic digestion

In a sterile cell culture hood, the tendon segments were washed with PBS (Phosphate Buffered Saline) three times to remove any excess debris and hair. Tendon fibroblasts were retrieved from the core of the mid-metacarpal region. The exterior surfaces of the tendons were excised using a sharp single edged blade (HD Hardware, #PS01). The exposed core was diced into 2mm³ pieces before being added to a 100ml flask containing a media solution consisting of pre-warmed DMEM (37°C) and 1mg/ml pronase (Sigma, #P8811), a proteinase enzyme derived from *Streptomyces griseus* which breaks down peptide bonds in proteins into individual amino acids (Frackenpohl et al., 2001). This enzymatic solution was placed on a magnetic stirrer at 37°C for 1 hour in an incubator (21% oxygen, 5% CO₂) to ensure adequate mixing and to facilitate mechanical breakdown of the tendon tissue. The media solution was decanted and discarded after one hour. Fresh media was added to the tendon pieces (40mls) followed by 0.25mg/ml collagenase type VIII (Sigma, #C2139) and 0.55mg/ml dispase (Gibco/Life Technologies, #17105041) for another hour. Collagenase type VIII cleaves the main polypeptide bonds within the native triple helical structure of collagen (Harper, 1980). Dispase, a neutral protease or metalloprotease (from *Bacillus polymyxa*) has a high efficiency facilitating the disassociation of fibroblast cells from the extracellular matrix (Cruz et al., 1997). After the digestion, the cell solution was strained through a 70µm cell strainer (VWR UK, #734-0003). The cells were pelleted by centrifugation at 1000rpm for 15 mins and then re-suspended in pre-warmed DMEM (37°C). The remaining tendon pieces were re-used and added to fresh media and enzymes, collagenase type VIII and dispase to obtain maximal numbers of cells.

The harvested tendon cells were maintained in DMEM supplemented with 10% heat inactivated foetal bovine serum (FBS, Gibco/Life Technologies, #10270-

106) and 1% penicillin/streptomycin (P/S, Life Technologies, #15140-122). Throughout my experimental work, DMEM with reduced glucose (1g/L) was used (marketed as DMEM with low glucose, Life Technologies, #21885108). Standard DMEM contains 4.5g/L glucose which approximates 25mM glucose and in contrast there is only 5mM in low glucose DMEM. The normal blood glucose range for horses is between 3.4mmol/L and 7.4 mmol/L (Aiello, 2012). Culturing horse tendon fibroblasts in standard DMEM media is therefore abnormal as it would mimic diabetic blood horse sugar levels. The culture of rat Achilles tendon fibroblasts in high glucose (12mM or 25mM) has been shown to lead to increased expression of MMP-9 and -13 mRNA, two of the enzymes responsible for the degradation of collagen (Tsai et al., 2013).

The tendon fibroblasts were cultured in 60 mm cell culture dishes coated with either 10ug/cm² type 1 collagen (Sigma, #C3867) or 1ug/cm² fibronectin (Sigma, #F4759). When approximately 80% confluent (which took 7 days for SDFT fibroblasts and 10-12 days for DDFT fibroblasts), the cells were passaged using trypsin/EDTA 0.05% (Ethylenediaminetetraacetic acid, Life Technologies, #25300054). The cells were either maintained in ambient oxygen by culturing them in a standard incubator (37°C, 21% O₂ and 5% CO₂) or in 2% oxygen and 5% CO₂ with the balance provided by Nitrogen.

2.2.3 Extraction and culture of tendon fibroblasts by tendon explant

After removing the external peripheral tissue from the tendon samples as outlined above, the exposed tendon core was diced into 2mm tendon pieces. The tendon pieces were placed onto collagen type I or fibronectin coated 60mm cell culture dishes. The bottom of each cell culture plate was scored with a scalpel blade to create 5 or 6 parallel lines to increase surface-adhesion of the tendon pieces. Pre-warmed (37°C) complete DMEM containing 10% FBS and 1% P/S (and reduced glucose) was added to the dishes. The dishes were then transferred either to a standard incubator at 37°C (21% O₂, 5% CO₂) or in 2% oxygen, 5% CO₂ with the balance provided by Nitrogen. The normal time for explanted cells to achieve confluency was approximately 14 -21 days.

2.2.4 Cell culture: “normoxic” oxygen (2% oxygen)

Culture of tendon fibroblasts in “normoxic” oxygen was performed by placing the cell culture dishes inside commercially available plastic wide-mouth containers which were subsequently gassed with a gaseous mixture containing 2% oxygen, 5% CO₂ and a nitrogen balance at 2 p.s.i. for 2 mins (Wright and Shay, 2006) (Figure 2-1). Flushing the containers with this gaseous mixture for greater than 1 min was required to purge the atmospheric gas within the containers. The containers were re-gassed one hour later (again using 2 p.s.i. for 2 mins) to remove any remaining atmospheric gas in the containers (Wright and Shay, 2006). When not being used, the gaseous mixture was stored in a 50L tank provided by BOC Industrial Gases (# 226943-L). 90% gaseous equilibration of 10cm cell culture dishes was shown to occur within 15 mins, however gas-liquid equilibration was not achieved for at least 3 hours (Allen et al., 2001). To minimise gas leakage from the containers, the rim of each of the containers was smeared with silicon grease (Wright and Shay, 2006). These containers were kept inside a standard CO₂ gassed incubator at 37°C. Media colour change (phenol red) was checked daily to ensure non-leakage of the gaseous mixture from the containers. Loss of the gaseous mixture, especially carbon dioxide would make the media more alkaline thus changing media colour from red to yellow (Wright and Shay, 2006). The 2% oxygen gas mixture was only used for the DNA damage, replication and binucleate cell work as the cost of the tanks were too expensive to use for all of the experiments in my thesis.

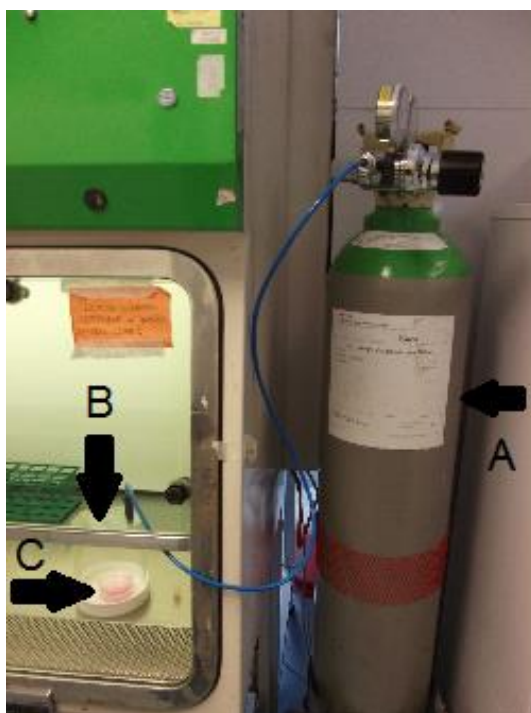


Figure 2-1 “Normoxic” oxygen (2%) incubators

This figure shows the tendon fibroblasts being gassed with normoxic (2%) oxygen.

2.3 Immunocytochemistry

Tendon fibroblasts were seeded (3×10^5 cells) onto type I collagen- or fibronectin-coated glass coverslips inside cell culture dishes and cultured until 80% confluent (for immunocytochemistry work, the cells were cultured on coated coverslips as this facilitated easy fixing and staining of cells).

To collagen coat glass coverslips (or cell culture dishes for experiments not involving immunocytochemistry), a Type I collagen solution (Sigma, #C3867) was diluted to a working concentration of 0.01% with sterile distilled water. Following this, $10 \mu\text{g}/\text{cm}^2$ collagen was used to coat 60mm cell culture dishes. The collagen solution inside the dishes was left at room temperature (RT) (inside the cell culture hood to maintain sterility) for several hours to allow the collagen to bind to the bottom of the dish. At the end of this period, excess fluid was removed and the collagen-coated dishes were left to dry for an hour.

To coat the dishes with fibronectin (Sigma, #F4759), the stock solution was diluted with HBSS (Hanks' Balanced Salt Solution) (Life Technologies, #14060040) and $1 \mu\text{g}/\text{cm}^2$ was used to coat 60mm cell culture dishes. Once the fibronectin solution was added to the dishes, they were left at RT for approximately 1 hr to allow the fibronectin to bind to the bottom of the dish. At the end of this period, the fibronectin had dried onto the surface of the dish. If there was any excess fluid, the solution was aspirated.

At the end of the experiments, the cells were fixed with 4% paraformaldehyde/PBS for 5 min followed by permeabilization with 0.25% Triton-X 100/PBS for 5 min. Blocking of non-specific binding was carried out using 10% milk/PBS for 30 min at room temperature (RT). Primary and secondary antibody incubations were carried out overnight at 4°C and 1 hr at RT respectively. Secondary antibody reagents used were Alexa Fluor 555 and/or 488 conjugates (dilution 1:1000). Samples were washed using 0.2% Tween-20/PBS throughout the protocol. Slides were mounted using Prolong-Gold anti-fade DAPI (DAPI: 4',6-diamidino-2-phenylindole) (Life Technologies, #P36931). A negative control was carried out with the immunocytochemistry experiments to make sure no false positive results were generated. To achieve this, a couple of coverslips were fixed and stained as per the immunocytochemistry protocol

described above however, no primary antibodies were used, just secondary antibodies.

2.3.1 Immunocytochemistry methods for Chapter 3

2.3.1.1 Quantification of DNA damage and cell proliferation

To examine the basal cellular injury levels in passage 1 (P1) and passage 2 (P2) SDFT and DDFT fibroblasts from two horses, DNA damage was detected by immunolabelling for phospho- γ H2AX antibody in cells exposed to various cell culture environments including two different oxygen tensions (20% and 2% oxygen) and two matrix types (collagen type I and fibronectin). All antibody details for immunocytochemistry work are recorded in Table 1 at the end of this thesis chapter.

The link between DNA damage and replication is well- known to be bi-directional (Burhans and Weinberger, 2007) & (Burhans and Heintz, 2009). Therefore, TPX2, a marker for the G2, S and M stages of the cell cycle was used as a single stain by immunocytochemistry to assess the replicative fraction in both P1 and P2 SDFT and DDFT fibroblasts in different oxygen tensions (20% and 2% oxygen) and matrix surfaces (collagen type I and fibronectin). Bromodeoxyuridine (BrdU) labelling was not used to quantify the replicative fraction in tendon fibroblasts as it is toxic to cells and can induce multiple types of DNA lesion resulting in premature senescence (Masterson and O'Dea, 2007)

There was a strong correlation between the percentage of DNA damage and the percentage of replicating cells (see Chapter 3) therefore P1 and P2 SDFT and DDFT fibroblasts were double stained for both phospho- γ H2AX and TPX2.

The fluorescent single stain images were examined and imaged using an inverted DM IRE2 confocal laser scanning microscope (Leica, Milton Keynes, UK). Individual images were viewed using the x40 1.25 oil immersion lens and scanned using the xyz mode creating a z-stack from two different lasers for two different fluorescent wavelengths, a Helium Neon laser to detect 555nm (γ H2AX or TPX2) and UV laser to detect DAPI (461nm wavelength). Up to 5 fields of view were imaged for each coverslip representing the different experimental conditions.

Total numbers of cells positive for either phospho- γ H2AX or TPX2 were counted using ImageJ digital software for each field of view (Abramoff et al., 2004). Low levels of DNA damage can occur normally during replication in cells, therefore cells containing 7 or more γ H2AX puncta were classified as DNA damaged. To obtain the mean percentage of DNA damage or replication, the number of cells positive for γ H2AX or TPX2 was divided by the total number of cells for each field of view followed by averaging each percentage from five fields of view.

2.3.1.2 **Binucleate counts**

A binucleate cell is formed when two daughter cells fail to undergo cytokinesis (Wong and Stearns, 2005). SDFT and DDFT fibroblasts were retrieved from two horses for this experiment. To assess the percentage of binucleate cells at two different oxygen tensions (20% and 2% oxygen), cultured on two different matrix types (collagen type I and fibronectin), P1 and P2 SDFT and DDFT fibroblasts were fixed with 4% paraformaldehyde/PBS for 5 mins and then treated with 5 μ g/ml CellMask (Life Technologies, #C10046) for 5 mins at 37°C to demarcate the plasma membranes of the cells. After the staining procedure, the cells were washed several times in PBS and 10 μ l of DAPI was added to detect nucleic acid. The coverslips were imaged with the inverted DM IRE2 confocal laser scanning microscope and a z-stack was generated as outlined in section 2.2.1.1 above. 5 fields of view were recorded for each experimental condition and the number of binucleate cells was measured by counting the total number of cells with two nuclei within one CellMask positive cell. For each field of view the percentage of binucleate cells was calculated (number of binucleate cells divided by the total number of cells) and this was averaged to obtain the mean binucleate percentage.

2.3.1.3 **p21 expression in SDFT fibroblasts**

Replication-induced DNA damage may lead to the activation of DNA damage checkpoints and an effector of this response is p53 phosphorylated at serine 15. One of p53' transcriptional targets is p21, a cyclin dependent kinase inhibitor. A single immunostain for p21 was performed in SDFT foal fibroblasts. Qualitative assessment of the single stain was made in triplicate.

2.3.2 Immunocytochemistry methods for Chapter 4

2.3.2.1 RBM3 expression in SDFT fibroblasts

Immunocytochemistry was used to assess RBM3 expression during heating and cooling of SDFT fibroblasts. SDFT derived fibroblasts from one horse were cultured on collagen type I coated glass coverslips in 60mm cell culture dishes until 80% confluent. At this point, each of the dishes was sealed with parafilm (Sigma, #P7793) to prevent water leaking into the dishes and then subsequently heated at 43°C for 15 mins in a waterbath (Grant, Cambridge). After the heating period, the cells were left to recover at 37°C for 72hrs. A separate group of SDFT derived fibroblasts was chilled continuously at 26°C or 32°C for 72hrs in the water bath. At 1hr, 4hr, 24hr, 48hr and 72hrs of cold shock or in the recovery phase post heating, the cells were fixed and stained with an anti-RBM3 antibody. The SDFT fibroblasts were imaged with an inverted DM IRE2 confocal laser scanning microscope using the x40 1.25 oil immersion lens as outlined in section 2.2.1.1. To quantify the mean intensity of RBM3 staining for each of the heating or cold shock times, the nuclear RBM3 intensity of 20 random cells was measured with the Leica confocal software. Using the profile function to measure pixel intensity across a line segment, it allows the area of interest to be measured, for example, the width of individual nuclei, where RBM3 intensity was greatest. The mean pixel intensity from 20 cells was then calculated for each time point.

2.3.3 Immunocytochemistry methods for Chapter 5

2.3.3.1 Validation of DAXX and Caspase-2 in foetal Equine Palate fibroblasts

To investigate whether there was immuno-positivity of equine PalF (foetal palate fibroblasts) to DAXX or Caspase-2, PalF cells were cultured on glass coverslips until 80% confluent and then heated at 46°C in the waterbath for 3 and 10 mins. At these times, the cells were fixed and stained for DAXX and Caspase-2. All images were viewed and imaged using a 63x objective lens on an inverted phase contrast Axiophot 2 microscope (Zeiss).

2.3.3.2 Translocation of DAXX with heating and cooling

SDFT fibroblasts were cultured on collagen coated coverslips. Once 80% confluent, they were heated on the heating rig (Figure 4-3) at 43°C for 3, 10 and 15 mins. At each of these time points, the cells were fixed and stained for DAXX immediately using the immunocytochemistry protocol outlined above (section 2.2). These time points were chosen to see if DAXX would escape from the PML nuclear bodies, a known feature of the heat shock response (Nefkens et al., 2003). To ensure DAXX returned to its position at the PML bodies, a separate group of SDFT fibroblasts was heated for 15 mins at 43°C and left to recover at 37°C for 10 mins, 15 mins, 1hr and 4hrs. The cells were fixed and stained for DAXX at each of these time points.

To investigate whether DAXX has the ability to disperse from the PML bodies during cold shock, SDFT fibroblasts were placed into a pre-chilled gassed incubator at 26°C for 30 mins or 1hr then fixed and stained for DAXX immediately at these times. To determine whether DAXX translocated into the nucleoplasm during the rewarming period, another group of SDFT fibroblasts was chilled at 26°C for 1hr then allowed to recover at 37°C for 15 mins, 1hr and 4hrs. At each of these time points, the cells were fixed and stained for DAXX. Once the cells had been stained, they were viewed and imaged with an inverted phase contrast Axiophot 2 microscope (Zeiss).

2.3.3.3 Quantification of DAXX puncta using Image J

To quantify DAXX puncta size in Image J, the image was split into three channels, a red, blue and green. The image comes up as black and white, however the red channel was used as this corresponded to the colour of the fluorescent stain used and the puncta inside the nuclei could be visualised at a bright intensity. The threshold value of the DAXX puncta was calculated (Image->Adjust->Threshold) and standardised for all of the experiments. To quantify DAXX puncta size, the area of the DAXX puncta was calculated. To achieve this, the area function was chosen from the Set Measurement tool (Analyse-> Set Measurement) and the scale had to be set (Analyse->Set scale) by choosing the unit of length (μm) and the known distance was 0.00. Following this, the Analyse Particles icon was used. The size range of the particles had to be standardised.

To minimise the quantification of minute specs due to background noise and extra-large particles (not DAXX puncta) caused by very bright patches of secondary antibody, the particle size range was set (20-500 pixels). The resultant summary table gave the average size of DAXX puncta. This quantification step was repeated for each experiment (with five fields of view for each). The data was added to Prism (GraphPad Prism, version 5.00), a software program which calculated the mean DAXX particle size for each experiment then graphed the data.

2.3.3.4 The expression of p62 in SDFT fibroblasts

Validation of the p62 antibody was carried out in equine SDFT fibroblasts by fixing the cells followed by immunostaining with anti-p62 antibody. Different batches of a rabbit polyclonal p62 antibody were shown to result in a different distribution in SDFT tendon fibroblasts. Use of lot 14 or 15 p62 antibody showed a predominately nucleolar distribution and in contrast, lot 16 was predominately cytoplasmic. These differences can be seen in Figure 5-8. To highlight the nucleolar expression of p62 with lot 14 or 15 antibody, SDFT fibroblasts were fixed and stained followed by imaging with the inverted confocal laser scanning microscope to achieve a single equatorial image of p62 in these cells. The confocal laser scanning microscope was chosen to depict the localisation of nucleolar p62 clearly. For all of the other images in Figure 5-8, an inverted phase contrast Axiophot 2 microscope was used.

2.3.3.5 Bortezomib treatment

SDFT derived fibroblasts were cultured on collagen type I coated glass coverslips until 80% confluent. Bortezomib, a proteasomal inhibitor leads to the accumulation of lysine-48 linked polyubiquitinated proteins together with an increase in the expression of p62 in cells (Jia et al., 2012). To determine whether p62 was responsive to bortezomib (LC Laboratories, #B-1408) in a dose dependent manner, 1 nM, 5nM, 10nM and 100nM were added to monolayers of SDFT fibroblasts overnight. Following treatment, the SDFT fibroblasts were fixed and stained for p62 expression using the above protocol (section 2.2). All images were captured with an inverted phase contrast Axiophot 2 microscope (Zeiss).

2.3.3.6 N-Acetyl Cysteine (NAC) treatment of SDFT fibroblasts and concurrent NRF-2 staining

To determine the distribution of NRF-2 in control SDFT fibroblasts, a group of SDFT fibroblasts from one horse was grown on collagen coated coverslips until 80% confluent and then fixed and stained for NRF-2 (section 2.2). A separate group of SDFT fibroblasts from the same horse was treated with 200 μ M hydrogen peroxide, a source of oxygen free radicals as a positive control. A third group of SDFT fibroblasts was treated with 1mM NAC (N-acetyl cysteine) (Sigma, #A7250), an anti-oxidant, for 48hrs to determine whether NRF-2 would be prevented from translocating to the nucleus. At the end of each treatment, the SDFT fibroblasts were fixed and stained for anti-NRF-2 antibody. Five fields of view were captured from each coverslip (one representing each experimental group) with the x40 objective on an inverted phase contrast Axiophot 2 microscope (Zeiss). To quantify the mean intensity of nuclear NRF-2 staining, five fields of view from each coverslip were imaged with an inverted DM IRE2 confocal laser scanning microscope to create a z stack. The quantification of 75 cells for nuclear NRF-2 pixel intensity was completed with the Leica Confocal software as described in section 2.2.2.1.

2.3.3.7 NRF-2 and Cx43

To verify NRF-2 co-localisation to gap junctions, a double stain using both NRF-2 and Cx43 (one of the connexin proteins present in gap junctions) was performed. SDFT cells were cultured on collagen coated glass coverslips until 80% confluent. The cells were fixed and stained for NRF-2 and Cx43 (section 2.2). The cells were viewed on an inverted DM IRE2 confocal laser scanning microscope using x40 1.25 oil immersion lens and scanned to give a single equatorial image.

2.4 Senescence staining

SDFT and DDFT derived fibroblasts were obtained from an adult Thoroughbred horse (aged 10 years). SDFT derived fibroblasts were also retrieved from a stillborn foal. The fibroblasts were cultured on glass coverslips inside 6 well plates until 70% confluent. The DMEM media was removed from the

6 well plate and the wells were washed with PBS twice. The protocol from a senescence histochemical staining kit from Sigma (#CS0030) was followed. After the cells had been fixed, stain was added to the cells and left to incubate at 37°C overnight without CO₂. Positive cells stained blue. The SDFT and DDFT fibroblasts were visualised and imaged using a 40x objective lens on an inverted phase contrast Axiophot 2 microscope (Zeiss).

2.5 Comet assay

To determine whether replication induced DNA damage affects the reparative ability of tendon fibroblasts, they were cultured on: 1) collagen type I coated 60mm dishes until confluent 2) fibronectin coated 60mm dishes until confluent 3) fibronectin coated dishes until 50% sub-confluent. Sub-confluent tendon fibroblasts were maintained on a fibronectin matrix as the SDFT fibroblasts were particularly susceptible to replication-induced DNA damage on this matrix type as shown in our results in Chapter 3. Confluent cultures were chosen to minimise replication induced DNA damage in cells that may otherwise increase the basal levels of DSB damage and potentially affect the reparative ability of the tendon fibroblasts.

DNA damage was induced by incubation with 200µM hydrogen peroxide (H₂O₂) for 5 min on ice. To assess repair capacity, a separate group of tendon fibroblasts was treated with H₂O₂ (Sigma, #H1009) followed by a 1 hr recovery period at 37°C. Both treatment groups were compared with a control (untreated) group. An alkaline comet assay was performed according to the manufacturers' instructions (Trevigen Inc, Gaithersburg, MD, USA, #4252-040-K). This assay was chosen as it is a more sensitive method for detecting the presence of both single and double strand breaks, a feature of hydrogen peroxide induced DNA damage (Driessens et al., 2009). All experiments were completed in triplicate.

The control (untreated) cells were trypsinised (0.05% trypsin/EDTA, Life Sciences) immediately, re-suspended in PBS and 1X10⁵ cells were embedded in molten agarose at a dilution of 1:10 and placed onto individual sample areas on a Trevigen Comet Assay slide. The cells had to be lifted and embedded in agarose as quickly as possible to prevent trypsin induced DNA damage. The "treated" SDFT and DDFT fibroblasts were incubated with 200µM H₂O₂ for 5 mins

on ice and processed immediately as described above. The “recovery” group of fibroblasts were treated with H₂O₂, rinsed with PBS and fresh media was added to the cells. The cells were then maintained in an incubator for 1hr at 37°C before being processed as above.

To allow the LMAgarose (low melting point agarose)/cell mixture to solidify into a gel-like consistency, the slide was placed at 4°C for 10 mins. To achieve gentle cell lysis, the slide was placed in a pre-chilled Lysis Solution (Trevigen Inc, Gaithersburg, MD, USA) at 4°C for at least 30 mins, followed by unwinding and denaturation of the DNA with an alkali for approximately 40 mins (200mM NaOH, 1mM EDTA). Electrophoresis was used to migrate out the damaged DNA from the “nucleoid” (a term used to describe the agarose encapsulated DNAs from each individual cell). If a Trevigen Comet Assay ES II tank is used for electrophoresis, it is important to ensure that only 850ml of electrophoresis buffer solution is used to achieve a buffer height above the slides of 0.4cm. Otherwise, the efficiency of electrophoresis will be poor. Each run was standardised with control etoposide “damaged” cells with expected comet tail grades (Trevigen Inc, Gaithersburg, MD, USA).

After 30 mins of electrophoresis (at 21V constant), the slide was washed twice with distilled water and fixed with 70% ethanol for 5 mins. The slide was dried at room temperature for 10-15 mins before staining with a fluorescent dye (SYBR Green I) for 5 mins at 4°C to enable visualisation of the DNA (30ul/ sample area). To achieve maximal resolution of each sample the slide was left at 4°C overnight to allow the agarose to dry completely. Images were viewed and captured using a using a 40x objective lens on an inverted phase contrast Axiophot 2 microscope (Zeiss).

2.5.1 Quantification of oxidatively damaged cells via comet assay

100 comets (individual cells) were randomly chosen from the control, treatment and repair groups for both the SDFT and the DDFT. The degree of DNA damage for each comet was quantified using a visual scoring system employing 5 categories ranging from 0 (no tail) to 4 (almost all DNA in tail). Summing the scores of each of the individual comet values (0-4) gives an arbitrary total score between 0-400, with the highest values representing the most severe damage

(Collins, 2004). The total arbitrary scores taken from two TB horses were averaged for the control, treatment and repair groups on both collagen and fibronectin respectively. The data was added to Prism which graphed the mean arbitrary scores for all of the experiments.

2.6 Choice of heat rig equipment

Much difficulty was experienced in finding the most appropriate heating apparatus, the ideal qualities being low cost, accuracy, ease of use and reproducibility. The first basic heating apparatus we considered for use in the experiments was the unstirred standard laboratory water bath.

The advantages of the water bath were its ease of use and the fact that a large number of cell culture dishes could be heated simultaneously. A type K thermocouple attached to a digital reader (RS Components) was used to measure media temperature inside control cell culture dishes through a small hole in the top. The experimental heating of equine tendon fibroblasts was completed simultaneously in separate test dishes as the creation of a hole on the top of the dishes could have introduced bacterial contamination in the cell dishes. This experimental set up only indirectly measured the temperature of the test dishes.

Readings taken from the centre and edges of the control dishes suggested that there was a temperature variation across the plate by as much as 2 degrees. There was also a clear difference in the morphology of the SDFT fibroblast monolayer across the culture dishes, when heated up to 45°C for 10 mins in the water bath (Figure 2-2). At one end of the dish, the SDFT derived fibroblasts were morphologically normal with isolated clusters of rounded up cells. In the middle of the plate, there was an increase in the number of rounded up cells and at the other end of the dish, where the temperature was highest, the majority of the cells had become permanently detached from the surface into the media which suggested that cell death had taken place (Figure 2-2).

We had a heating rig made to suit our specific needs by the Bioelectronics group at the University of Glasgow. It was composed of 4 Peltier elements positioned underneath a metal plate (Figure 2-3). The Peltier elements use the

principle of the “thermoelectric effect” whereby there is a difference in voltage across the element creating a temperature gradient. The arrangement of the four Peltier elements allowed rapid heating or cooling of the metal plate to take place.

The Peltier elements were connected to a controller responsible for temperature regulation by altering the voltage across the elements. A set of pre-engineered temperature settings was used. In control dishes, the temperature of the media was monitored constantly by a thermocouple inserted through a small hole of the cell culture dish lid. The thermocouple was directly connected to the controller through a port. One of the biggest limitations of this apparatus was poor temperature regulation by the controller because fluctuations in the temperature (by as much as one degree) were seen within control dishes. The fluctuations in temperature were believed to be caused by electronic noise as a result of random fluctuations in the electronic signal possibly through poor insulation of the electronic circuits (pers.comm N.Mirzai). As a result, unacceptable variation in temperature was recorded in replicate dishes.

Due to the significant limitations of the two sets of apparatus described above, we decided to purchase a resistive heater from Cell MicroControls (Norfolk, VA). This device uses current flow through a conductor to release heat. The amount of current applied across the conductor can be varied and the heat given off is proportional to the current and the electrical resistance of the conductor. A glass plate coated with indium tin oxide (ITO) was the conductor unit. This plate was enclosed to minimise changes to airflow which would otherwise affect the temperature of the plate (Figure 2-4).

Two thermistors were used in this experimental set up. One was attached to the glass plate using latex based glue (Copydex) and was thermally coupled to the plate using a silicone based thermal compound. The second thermistor was inserted through a minute hole in the cell culture dish lid where it measured the temperature at the bottom of the dish (Figure 2-4). Both thermistors were attached to a mTCII micro-Temperature Controller (firmware version V49H) (Figure 2-4). For our purposes, a thermistor was chosen for its accuracy in the detection of the temperature range being used in the experiments (37°C- 52°C). Thermistor accuracy of the set temperature between 37°C and 50°C has been

recorded as being approximately 0.2°C (pers comm H.Cornell). During the calibration of the temperatures used in my experiments, there was greater fluctuation in the temperatures measured so thermistor accuracy was slightly lower (approximately 0.5°C).

The mTCII micro-Temperature Controller was connected to the serial port of a computer via a RS232 cable with a DB9 serial adaptor and the temperature from the two thermistors was recorded every 5 seconds. This data was entered into a software program (RealTerm version 2.0.0.70- Figure 2-5) which enabled close monitoring of the temperature inside the cell culture dishes and furthermore at the end of the heating period, a txt file with this data could be downloaded into Microsoft Excel 2003. One of the advantages of this software program was the ability to calibrate the heating rig prior to the experimental work to calculate the accuracy of media temperature inside the cell culture dishes. Each of the set temperatures being used for the experiments was calibrated and graphed (Figure 2-6). The rate of temperature used in my experiments was approximately 1-2°C/min as a study by Wilson and Goodship showed there was a 2°C/min temperature rise within the SDFT during a galloping session (Wilson and Goodship, 1994). The graphs in Figure 2-6 show the reproducibility of the temperatures being used. There were two major limitations of the apparatus, the first being the small size of the glass plate allowing only one 60mm cell culture dish to be heated at one time. The second was residual temperature variation across the plate as different morphological changes were evident in cells at the centre of the dish versus the edge, as reported previously with the other heating systems. For the cell death experiments only the cells in the centre were counted as this was where the thermistor was placed during the calibration of the rig. Despite the limitations of the heating rig, it was easy to use, accurate, reproducible and the advantages outweighed those of the two other sets of apparatus.

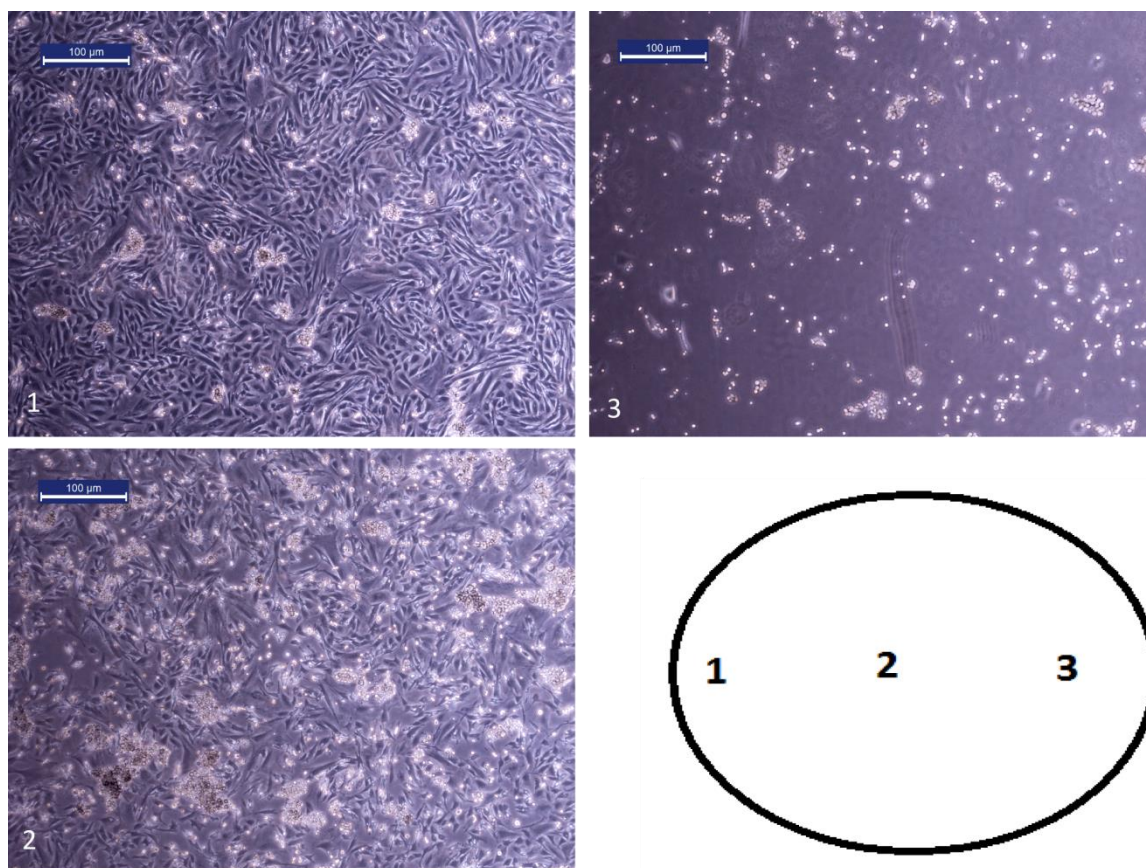


Figure 2-2 Difference in cell morphology across the cell culture dish

There was a clear difference in the cell morphology across a 60mm cell culture dish. At position 1 the majority of SDFT fibroblasts were morphologically normal with small numbers of rounded up cells on the dish. In position 2, which corresponds to the middle of the dish, there is an increase in the number of rounded up cells. At the other end of the dish, in position 3, most of the SDFT fibroblasts have permanently detached from the dish. Images were given with permission from T. Rich.

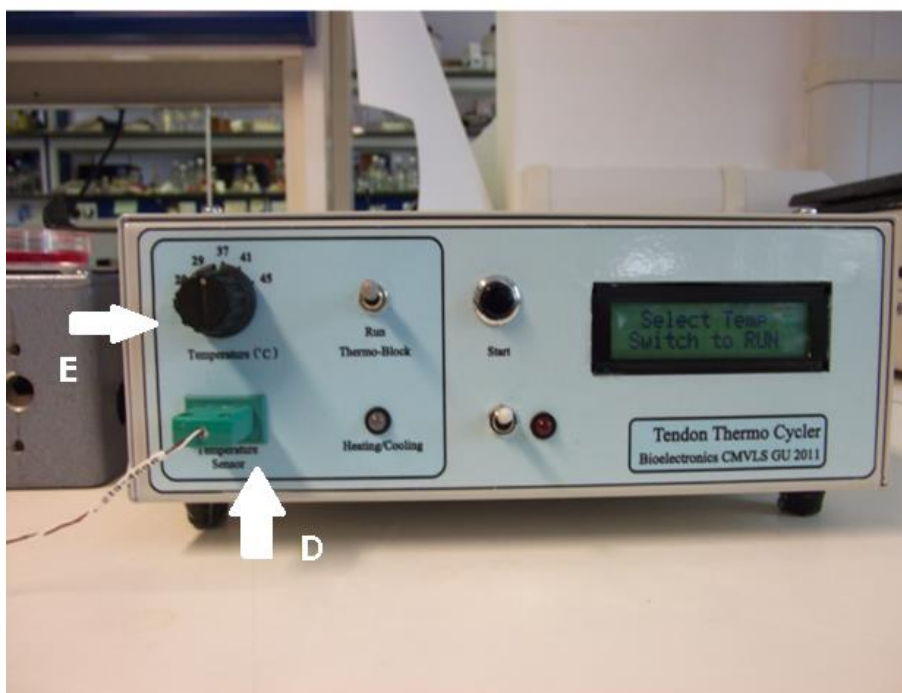
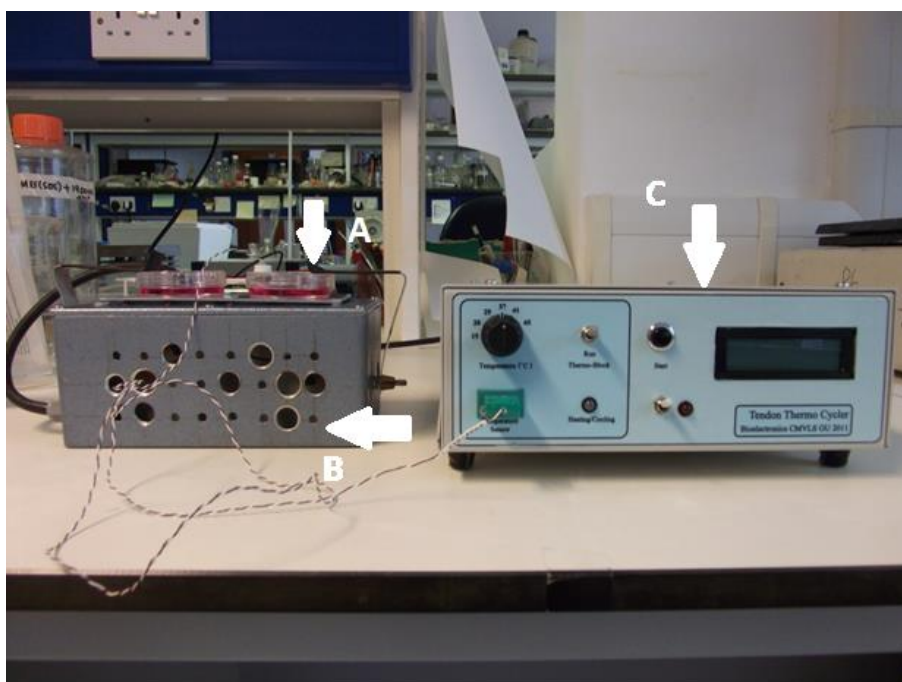


Figure 2-3 The tendon thermocycler heating apparatus

This heating apparatus was designed by the Bioelectronics group at the University of Glasgow. The cell culture dishes (A) rest on a metal plate which is heated by 4 Peltier elements (B). The controller (C) was responsible for temperature control by altering the voltage across the Peltier elements. A thermocouple measured the temperature of the media and this information was relayed to the controller through a port (D) on the controller. Only set temperatures could be used with this equipment ranging from 20°C, 29°C, 37°C, 42°C, 45°C (E).

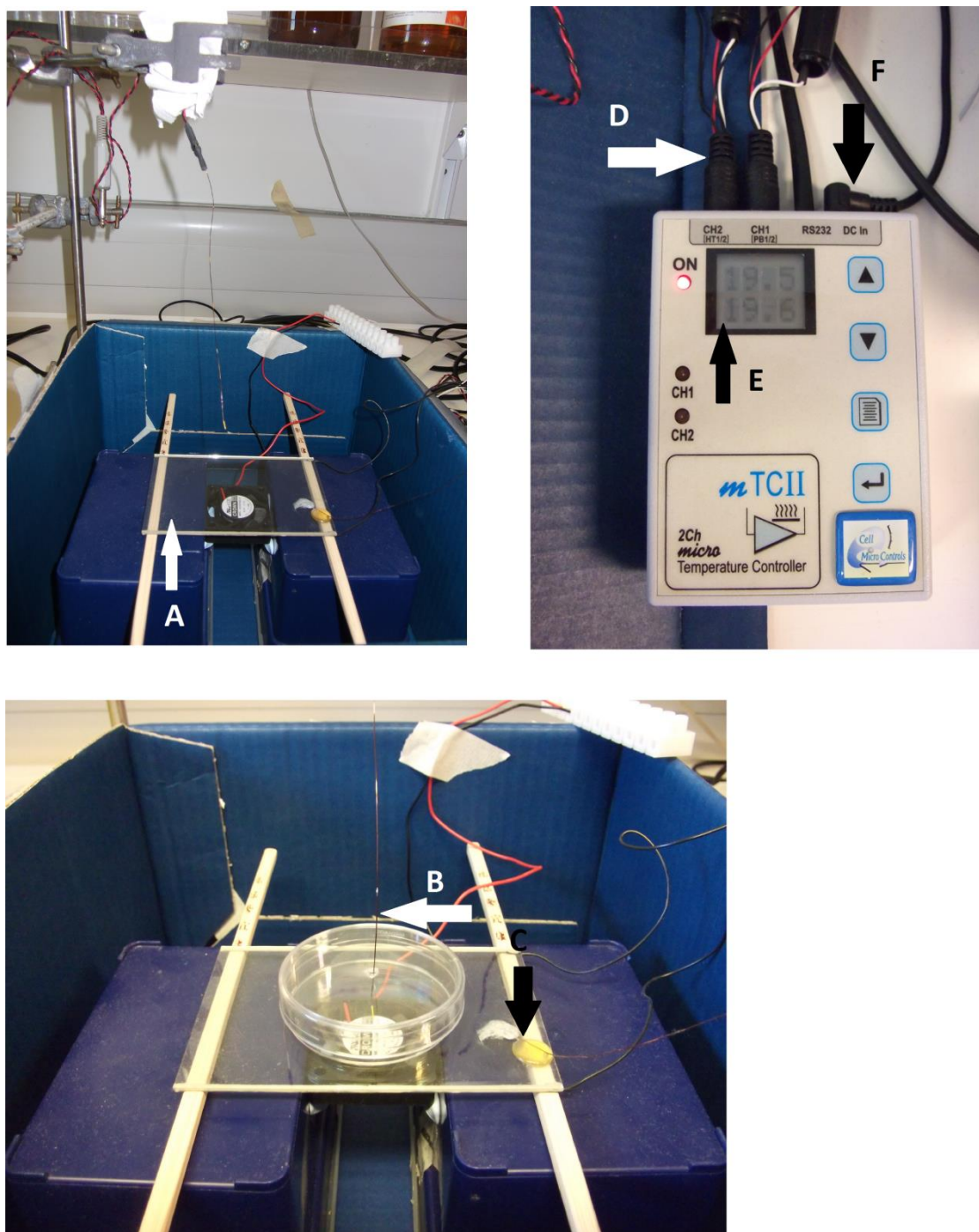


Figure 2-4 Resistive heating rig from Cell MicroControls

This resistive heater was composed of a glass plate (A) coated with indium tin oxide (ITO), a good conductor of heat. The plate was enclosed to minimise temperature fluctuations. Two thermistors were used to calibrate the temperature of the liquid/media inside the cell culture dish (B) and the glass plate (C). These two thermistors were attached to the mTCII micro-Temperature Controller (D). The controller was able to monitor the temperature of both surfaces (E). A RS232 cable relayed 5s temperature readings from the controller to a computer (F).

2.6.1 Calibration of the Cell MicroControls heating rig

One of the most important steps prior to the start of experimentation with heat shock was calibration of the heating rig. The Cell MicroControls heating rig (Norfolk, VA) had two thermistors, one attached to the glass plate of the conductor unit and the other measuring media temperature through a minute hole on the top of the cell culture dish. The thermistors would record the temperature from these two areas every 5 seconds and transmit this data to a software program (RealTerm (Version 2.0.0.70)). A snapshot of the RealTerm software program can be viewed in Figure 2-5. At the end of the experiment, the data was saved as a txt file which was then transferred to Microsoft Excel.

The first five rows (A-E) in Microsoft Excel contained A) data on the time recorded B) the symbol T1 (1st thermistor recording media temperature) C) the temperature recorded by T1 at that moment in time D) the symbol T2 (2nd thermistor- recording the temperature of the glass plate) and E) the temperature recorded by T2 at that moment in time.

To place time 0 in a cell e.g. K1, the following calculation was put in the fx icon of Excel =A1-(the data recorded in the first cell). This was repeated for the whole A column e.g. for time 5 seconds, the calculation used was A2- (data recorded) etc.

The temperatures recorded by the two thermistors did not have decimal points. To correct this, a new column had to be created. In a new cell e.g. L1, the following calculation was completed: =C1/10. By doing this, it would convert a temperature reading of 351 to 35.1°C. This calculation was repeated for all temperatures, e.g. =C2/10 etc.

All of the temperatures used in the experiments were calibrated 3 times. For each temperature used in the experiments, (43°C, 47°C, 52°C) all three runs were graphed (Figure 2-6).

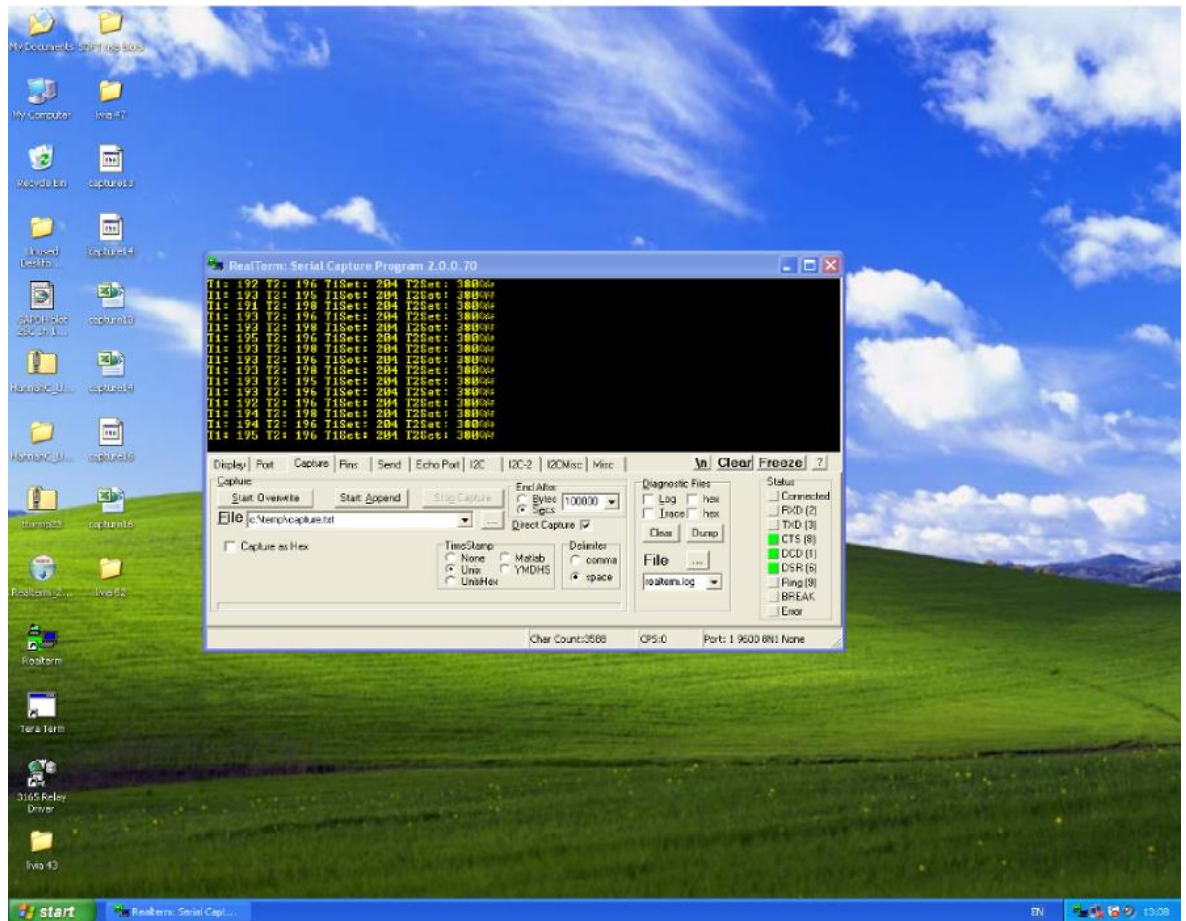


Figure 2-5 A snapshot of the RealTerm software program

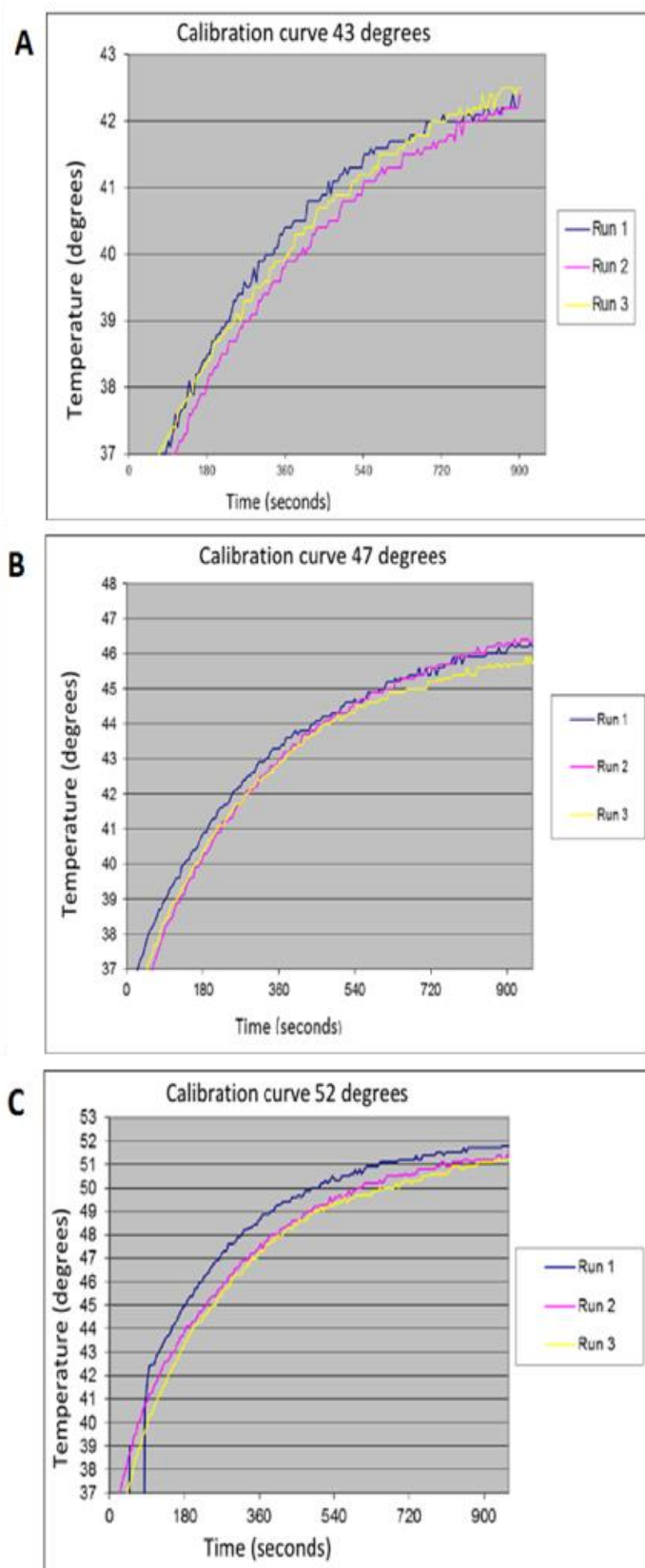


Figure 2-6 Calibration curves for the Cell MicroControls heating rig

SDFT fibroblasts were heated to (A) 43°C, (B) 47°C and (C) 52°C with the Cell MicroControls heat rig. The temperature was recorded every 5 seconds for a period of 15 mins (900secs). These calibration experiments were run in triplicate. A line graph was constructed outlining the temperature in degrees over time in seconds. The rate of temperature increase was between 1-2°C/min (see section 2.6).

2.7 Measurement of Hsp-72 expression in SDFT and DDFT fibroblasts with heating and cooling

2.7.1 Heat shock protocol

SDFT and DDFT tendon fibroblasts were seeded (1×10^5 cells) onto type I collagen coated 60mm plates and cultured until confluent. The cells were initially maintained in 5ml complete DMEM with 10% serum and 1% P/S (and low glucose). 24 hours prior to the commencement of experiments, the serum levels were dropped to 1%. Both low serum conditions and confluent cultures were introduced to minimise replication induced DNA damage in the SDFT and the DDFT. Throughout the heating experiments, the media (with 1% serum and 1% P/S) was sourced from one bottle to minimise any variations between batches that could have an effect on the experiments. The media was kept constant during the heating and the recovery period i.e. it was not changed as this also minimised any effect of new media on the experimental results.

Confluent cultures of tendon fibroblasts were heated for 15 minutes at 43°C, 47°C or 52°C on the heating rig. Following the heating period, the cells were left to recover at 37°C for 1, 4, 24, 48 and 72 hrs. At each of the recovery times the cells were detached by trypsin/EDTA 0.05% (Invitrogen), pelleted by centrifugation (1000rpm for 5 mins) and lysed using RIPA buffer (Radioimmunoprecipitation assay buffer) for western blot analysis.

2.7.2 Cold shock protocol

Confluent tendon fibroblasts were cooled in dishes inside a pre-chilled gassed incubator set at 26°C. All cells were maintained in 20% O₂, 5% CO₂ with the balance provided by Nitrogen i.e. atmospheric oxygen. 3 separate groups of SDFT or DDFT derived tendon fibroblasts were cultured at 26°C for 1hr or 4hr or 16hrs then left to recover at 37°C for 1hr, 4hr, 24hr, 48hr and 72hrs. To determine whether the tendon fibroblasts were capable of expressing Hsp-72 protein without a recovery period, SDFT and DDFT derived fibroblasts were cultured at 26°C continuously for 1hr, 4hr, 24hr, 48hr and 72hrs. The tendon fibroblasts were trypsinized (as above) and analysed for Hsp-72 expression by western blot at each of the recovery time points or in the case of the cold shocked cells, at each of the cold shock time points.

2.8 Western blotting

2.8.1 Preparation of the cell lysate(s)

The cells were gently trypsinized from the plates (0.05% trypsin/EDTA). The media from each plate was also collected to ensure any floating/detached cells were included in the cell pellet following centrifugation at 1000rpm for 5 minutes. The resultant pellet was re-suspended in 100µl RIPA buffer (50mM Tris-HCL pH 7.4, 150mM NaCl, 1mM EDTA, 1% v/v Triton X-100, 1% w/v sodium deoxycholate, 0.1% w/v SDS) to ensure sufficient lysis of the cell membranes, thus allowing proteins to be released from the cells. The RIPA buffer contains a protease inhibitor cocktail (Roche #11836170001) to minimise endogenous protease activity which could damage and/or denature the proteins in the sample. The lysate was also kept on ice for 30 mins to minimise endogenous protease activity during lysis of the cells. The cell lysate was centrifuged at 13,000rpm for 20 mins at 4°C and the supernatant was collected into a 1.5ml Eppendorf. All samples were stored at -80°C when not being used. Freezing of the samples at this temperature inhibited protease activity and allowed the samples to be stored for longer periods of time.

2.8.2 The BCA Assay

The Bicinchoninic assay (BCA) was used to measure the total protein concentration of each sample to ensure equal amounts of protein were loaded in the western blot. This assay relies on the formation of a Cu^{2+} -protein complex in alkaline conditions resulting in the conversion of this cation to Cu^+ . The absorbance (562nm) of this chromogenic agent (Cu^+) is directly proportional to the amount of protein in the sample (Walker, 1996).

A standard protein concentration curve was constructed using BSA (bovine serum albumin) to increase the accuracy of protein measurement. A stock solution of BSA at 1mg/ml was used to generate a range of dilutions at 200, 400, 600, 800 and 1000ug/ml. A 4% w/v solution of CuSO_4 (Sigma, #BCA-1) was diluted 1:50 with bicinchoninic acid (Sigma, #BCA-1). 25ul of each protein sample and each BSA protein standard were added into individual wells of a 96 well plate, followed by the addition of 200ul of the bicinchoninic acid solution. A negative control consisting of 25ul of RIPA buffer and 200ul of bicinchoninic acid solution

was included. The 96 well plate was kept at 37°C for 30 mins to catalyse the Cu^{2+} reduction by the proteins in the sample. At the end of this period, the absorbance of each protein sample was measured by a 96 well plate reader (MultiSkan Ascent 96/384 plate reader, VA). Calculation of the final protein concentration in mg/ml is achieved using the formula $y=mx+c$, where x is the protein concentration.

2.8.3 Preparation of the SDS-polyacrylamide gel(s)

SDS-PAGE electrophoresis separates proteins out according to their molecular weights. This process involves the migration of charged proteins through a porous matrix (acrylamide gel) in the context of an applied electric field. There are two gels used in SDS-PAGE electrophoresis, a stacking gel and a resolving gel. The stacking gel has a lower pH and larger pore size in comparison with the resolving gel. The pH, the ionic strength of the buffers used in the stacking gels and pore size help to concentrate the protein samples into a tight band. The pH of the resolving gel is higher, pore size is smaller and the ionic voltage gradient is lost therefore the proteins are separated out according to size (Srinivas, 2012).

The resolving polyacrylamide gel (10% polyacrylamide) was composed of the following chemical ingredients: (3.3ml 30% Bis-acrylamide solution, 2.5ml Tris-HCl buffer (pH8.8), 4.1ml distilled water, 0.1ml 10% SDS detergent, 100ul 10% ammonium persulphate (APS) and 10ul TEMED (N,N,N,N - tetramethylethylenediamine). This chemical mixture was poured between two 75mm glass plates until the mixture polymerised and solidified. A stacking polyacrylamide gel (5% polyacrylamide) was then poured on top of the resolving gel.

The stacking gel was composed of the same ingredients as the resolving gel but with different quantities which gives a different polyacrylamide gel percentage (0.83ml 30% Bis-acrylamide solution, 1.26ml Tris-HCl (pH 6.8), 2.14ml distilled water, 0.05ml 10% SDS detergent, 100ul 10% APS and 10ul TEMED). Electrophoresis was performed with a Tris-glycine buffer (pH 8.3, 25mM Tris, 192mM Glycine and 0.1% SDS) (Biorad, #161-0732EDU).

2.8.4 Preparation of the protein samples followed by SDS-electrophoresis

Each protein sample was diluted 50:50 with a Laemmli sample buffer (277.8mM Tris-HCL (pH 6.8), 4.4% LDS (Lithium dodecyl sulphate), 44.4% (w/v) glycerol, 0.02% bromophenol blue) (Biorad, #161-0747) followed by heating at 95°C for 5 mins. Heating the samples causes denaturation of the protein mixture thus breaking down the 3D conformation of the protein and allowing the antibody to access the epitope of interest (Simpson, 2006). 20µg of each protein sample were pipetted into separate lanes. 5µl of a protein standard (Biorad, #161-0374) was used. This product contains various molecular weight markers and provides an indication of protein size on the gel. The electrophoresis was commenced at 100V and allowed to run for one hour or until the proteins were seen to reach the bottom of the gel.

2.8.5 iBlot of the polyacrylamide gel and preparation of the nitrocellulose membrane

The proteins on the gel were “blotted” onto a nitrocellulose membrane using an iBlot machine (Life Technologies). This procedure uses an electroblotting technique where an electric field is applied to the gel which then mediates the transfer of proteins from the gel to the membrane (Kurien and Scofield, 2006). Following transfer of the proteins onto the nitrocellulose membrane (Life Technologies, # IB301001), 15ml of 5% milk/PBS was added to the membrane for 30 mins to allow blocking of non-specific binding to take place. The primary antibody, Hsp-72 was added to 5% milk and left at 4°C overnight with gentle agitation. The complimentary HRP-conjugated 2° antibody was used at 1:1000 (Dako) for 1hr at room temperature. Washing of the membranes was completed throughout the protocol with 0.2% Tween-20/PBS. To allow visualisation of the protein bands, a chemilumiscent HRP substrate (Immobilon, #WBKLS0500) was added to the nitrocellulose membrane for 5 mins. The membrane was covered in cling film and exposed to x-ray film for approximately 30 seconds.

2.8.6 Loading control

Alpha Tubulin, a 50kDa cytoskeletal protein, is commonly used as a loading control to ensure equal loading of protein samples has been achieved. The following protocol was used to probe for alpha Tubulin: To remove the chemiluminescent HRP-substrate, the membranes were stripped with 0.2M sodium hydroxide for 15 mins before being re-blocked with 10% milk for 30 mins to exclude non-specific binding of antibody. The primary antibody was left on the membrane at a dilution of 1: 100,000 in 10% milk at 4°C overnight. The membrane was then washed, probed for secondary antibody (Dako) at a dilution of 1:1000 and processed as outlined above.

During the investigation of Hsp-72 expression in SDFT and DDFT fibroblasts, it was discovered that there were differences in the expression of alpha Tubulin in cold shocked lysates. Two bands were visualised on the western blots, one at 50kDa and another at 55kDa. The band at 55kDa corresponded to acetyl Tubulin, a cold shock post translational modification (Figure 2-7). As a result of these differences, Amido Black was used as a loading control for all the cold shock experiments. To keep the loading control the same, Amido Black was also used for the heat shocked lysates, with one exception, for SDFT fibroblasts heat shocked to 43°C. This experiment was the first of the Hsp-72 experiments and due to insufficient time, it was not repeated to accommodate the Amido Black loading control. Alpha Tubulin was used as a loading control for all other experimental work in my thesis including Caspase-3 in Chapter 4 and p62 in Chapter 5.

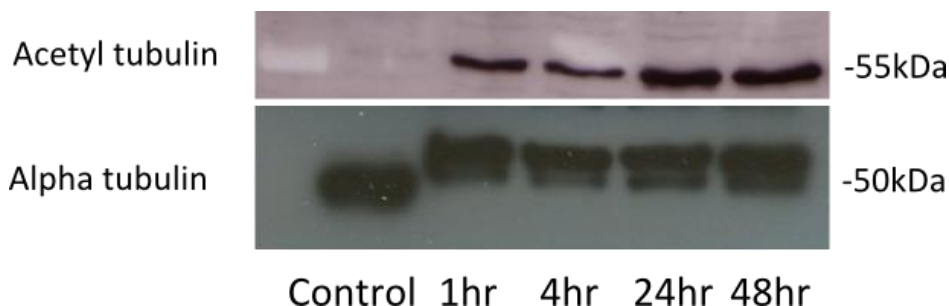


Figure 2-7 Post translational modification of alpha Tubulin with cooling

SDFT fibroblasts were exposed to 26°C for 1hr, 4hr, 24hr and 48hrs. Control cells were maintained at 37°C. A western blot was carried out with the cold shocked lysates using two different antibodies, an anti-alpha Tubulin antibody and an anti-acetyl Tubulin antibody. Alpha Tubulin was identified as two bands at approximately 50kDa (lower panel). The slight increase in molecular weight for these bands following cooling was attributed to acetylation, as confirmed by immunostain (upper panel). The same amount of protein (20µg) was loaded into each lane.

2.8.7 Amido Black protocol

Amido Black (40ml methanol, 10ml acetic acid and 0.1g w/v Amido Black) was used to stain total protein on nitrocellulose membranes. The membrane was rinsed with distilled water three times before 10ml Amido Black was added. The stain was left for 5 mins at room temperature before it was destained with several washes of distilled water. The images of the membranes were captured using a scanner (Epson Perfection V33).

2.8.8 Caspase-3 western blot

To induce apoptosis in equine SDFT fibroblasts, two different drugs were used namely, 20µg/ml etoposide (Sigma, #E1383), 0.5µM staurosporine and 1µM staurosporine (Sigma, S4400). Each of these drugs was added to 60mm dishes containing confluent SDFT fibroblasts overnight. At the end of the treatment period, the cells displayed the features of apoptotic cell death including cytoplasmic shrinkage, pyknotic nuclei and permanent cell detachment. Following treatment with these drugs, the medium was removed from the cell culture dishes and placed into a 50ml Falcon tube to collect all the floating dead cells. The few remaining attached cells were removed with trypsin and added to the 50ml falcon tube. The cells were pelleted by centrifugation (1000rpm for 5 mins) and lysed using 100µl RIPA buffer.

L540 cells, a human Hodgkin lymphoma cell line, were used as a positive control as the anti- Caspase-3 antibodies specifically recognises the amino acid residues 165-175 in the human version of cleaved Caspase-3. Various drug treatments including 0.1µg/ml and 0.5µg/ml etoposide and 5nM bortezomib were used to induce apoptosis in 3 separate groups of L540 cells cultured in T75 flasks. The drugs were added to 3 T75 flasks overnight. At the end of the treatment period, the L540 cells were pelleted by centrifugation and 100µl RIPA buffer was added to create a lysate. All lysates were stored at -80°C when not being used. The western blot for Caspase-3 was carried out according to the protocol outlined above. Two anti-Caspase-3 antibodies were used in the western blot, one from Cell Signalling and the other from R and D Systems (The details of antibodies used for western blot work are included in Table 2).

2.8.9 p62 western blot

SDFT fibroblasts were grown in collagen type I dishes and cultured at 37°C (21% O₂, 5% CO₂) until confluent. Once confluent, the cells were trypsinized and spun down into a pellet by a centrifuge (1000rpm for 5 mins) before being added to a RIPA buffer lysate. The expression of p62 was examined by western blot using the above protocol (section 2.8).

2.8.10 REAP (Rapid, Efficient and Practical) cell fractionation

This method of cell fractionation splits cells into nuclear and cytoplasmic components (Suzuki et al., 2010). This method was used to fractionate SDFT tendon fibroblasts from one horse into 3 components: a whole cell lysate, a cytosolic fraction and a nuclear fraction. SDFT fibroblasts were cultured on collagen coated 10cm dishes until confluent. The media from the dishes was removed and the cells were gently washed with ice-cold PBS to minimise endogenous protease activity. The cells were scraped away from the surface of the dish using a plastic cell scraper. 1ml of cell-rich PBS fluid was pipetted into a 1.5ml Eppendorf tube and then centrifuged for 10 sec in a table top Eppendorf microfuge. The supernatant were removed from the sample and the cell pellet was re-suspended with 900µl ice cold 0.1% NP-40 buffer followed by pipetting x 5 to ensure good mixing of the samples. 300µl of cell lysate was removed and labelled as whole cell lysate (WCL). 100µl of 4x Laemmli sample buffer was added to the WCL and then left on ice. The remainder of the NP-40 cell lysate (600µl) was centrifuged for 10 secs and 300µl of the resultant supernatant was removed and labelled as the cytosolic fraction. 100µl of 4x Laemmli sample buffer was added to the cytosolic fraction followed by boiling of the sample at 95°C for 1 min which aids in the denaturation of proteins in the cytosolic fraction. At the end of the boiling period, the cytosolic fraction was kept on ice. The cell pellet of the initial NP-40 cell lysate was re-suspended in 1ml of ice-cold 0.1% NP40 lysis buffer. The cell lysate was centrifuged for 10 sec then the supernatant was removed. The cell pellet was re-suspended in 180µl of 1x Laemmli sample buffer and labelled as the nuclear fraction. This fraction was kept on ice. The WCL and the nuclear fractions were sonicated for approximately 5 secs to help break up the DNA followed by boiling of the fractions at 95°C for 1 min. 10µl of the WCL fraction, 10µl of the cytosolic

fraction and 5 μ l of the nuclear fraction were loaded into a 10% polyacrylamide gel and electrophoresed for 1hr at 100V. The membranes were western blotted for p62 protein according to the protocol described above (section 2.8). Alpha Tubulin, a cytoskeletal protein was used to ensure there was clean separation of the nuclear and cytosolic fractions i.e. no contamination of fractions.

2.9 Thermotolerance in tendon fibroblasts associated with heating and cooling

2.9.1 Protocol for heating and cooling SDFT and DDFT fibroblasts

The lethal temperature required to kill SDFT cells was consistently 52°C (see Chapter 4). Confluent SDFT and DDFT tendon fibroblasts were heated at 52°C for 15 mins on the Cell MicroControl heating rig and then left in recovery at 37°C for 1hr, 4hr, 24hr, 48hr and 72hrs. At each of these recovery times, the cells were viewed and imaged using a 40x objective lens on an inverted phase contrast Axiophot 2 microscope (Zeiss).

To determine whether thermotolerance would occur in response to a lethal heat shock, a separate group of SDFT and DDFT fibroblasts were heated at a sub-lethal temperature of 47°C for 15 mins followed by a short recovery at 37°C for 4hrs. Recovery at 37°C for 4hrs was chosen as this time co-incided with high Hsp-72 expression levels in both SDFT and DDFT cells- see Chapter 4). The pre-conditioned group was then exposed to a lethal temperature (52°C for 15 mins) followed by recovery at 37°C for 1, 4, 24, 48 and 72hrs. Throughout the experimental work, a control group of cells kept at 37°C was used.

As it is unknown whether thermotolerance can be induced in equine tendon fibroblasts in response to cold shock, SDFT and DDFT tendon fibroblasts were pre-chilled by exposure to 26°C for 16hrs followed by 48hrs in recovery at 37°C. The length of recovery period at 37°C was chosen as it co-incided with high Hsp-72 expression levels in both tendons-see Chapter 4). At the end of the 48hr period, the cells were exposed to a lethal temperature at 52°C for 15 mins and left in recovery for 1hr, 4hr, 24hr, 48hr and 72hrs.

2.9.2 Quantification of cell death

Once the unconditioned or preconditioned SDFT and DDFT fibroblasts were exposed to a lethal heat shock and left to recover at 37°C for the required time, the media from each 60mm cell culture dish was removed and replaced with 1ml 4% trypan blue (Sigma, #T8154) for 3 mins. After this period, the trypan blue was emptied and rinsed with PBS several times. Fresh PBS was added to each dish and the cells were viewed using a 20x objective lens on an inverted phase contrast Axiophot 2 microscope (Zeiss). Each experiment was repeated three times.

To determine the percentage of attached cells, the number of attached cells was counted in 5 fields of view and this included all the cells with normal morphology in addition to the refractile, rounded up cells. The number of trypan blue positive cells was also counted. Trypan blue traverses compromised cell membranes, one of the features associated with dead cells (Strober, 2001). The percentage of attached cells at each experimental time point was calculated by dividing the number of attached cells by the mean number of control cells. This calculation was repeated for each of the five fields of view and then averaged to provide the mean percentage of attached cells for that experimental time point. This method was repeated for the percentage of trypan blue positive cells. A representative 3-D column graph showing the mean percentage of attached cells and positive trypan blue cells over 72hrs of recovery time for both the unconditioned and preconditioned groups was created in Excel.

2.10 Protein sequence alignments

To determine whether there was protein sequence conservation between species, an alignment of one or more sequences can be generated and differences in the numbers and type of individual amino acids can be seen. Protein sequence alignment was completed for the Caspase-3 protein in Chapter 4 and p62 protein in Chapter 5.

In Chapter 4, two anti- cleaved Caspase-3 antibodies from R&D Systems and Cell Signalling (which specifically recognises the amino acid residues at 165-175 in human Caspase-3) were used to determine whether there was species

cross-reactivity of these antibodies in the horse. If validation of these antibodies was achieved, one of these antibodies could be used to measure apoptosis in equine tendon fibroblasts in response to a lethal heat shock. To determine whether there was sequence conservation of cleaved Caspase-3 at the peptide epitope (amino acid residues 165-175) in the horse and humans, an alignment of the sequences was created.

In Chapter 5, to determine whether the NES (nuclear export signal) and the two NLS (nuclear localisation signals) within the p62 protein sequence of the human, mouse and the horse was conserved, a multiple protein sequence alignment of the p62 protein was carried out.

To achieve alignment of the protein sequences between species, the FASTA protein sequences were retrieved from the NCBI website (<http://www.ncbi.nlm.nih.gov/pubmed>) and put into the ClustalW software program (<http://www.ebi.ac.uk/Tools/msa/clustalw2/>) which aligns multiple amino acid sequences together and highlights differences in individual amino acids. Each species has a NCBI reference sequence code for each protein and this was recorded in Table 1 below).

Protein	NCBI Reference sequence code
Caspase-3 (Human)	CAC88866.1
Caspase-3 (Equine)	NP_001157433.1

Protein	NCBI Reference sequence code
p62 (Human)	NP_003891.1
p62 (Equine)	XP_005599229.1
p62 (Mouse)	AAH06019.1

Table 2: The NCBI reference sequence codes for the proteins used in multiple sequence alignment work

The classic leucine rich NES sequence typically displays an amphipathic alpha helical secondary structure with three hydrophobic residues on one side of the helix and the fourth hydrophobic residue on the other side (la Cour et al., 2004). To investigate whether the equine p62 NES sequence follows this classic pattern, a helical wheel was created as this allows the proteins' alpha helical secondary structure to be viewed. The NES sequence of the equine p62 protein was entered into the sequence icon of the following website (http://www.tcdb.org/progs/helical_wheel.php) and a helical wheel was created. In the helical wheel, the hydrophobic residues were outlined in blue.

2.11 Immunohistochemistry

Three Thoroughbred SDFT tendons with lesions of varying severity were obtained from biopsy samples with permission from Professor Janet Patterson-Kane. All of the samples were formalin fixed paraffin embedded tissues and prior to fixation, all the samples had to be deparaffinised and rehydrated. The samples were hydrated three times with a Tris buffer (pH7.5 with 0.05% Tween) for 5 mins each. Dewaxing of the tendon sections was achieved by immersing them three times in CitrocLEAR (HD Supplies, #HC5005) for 2 mins each followed by immersion through graded alcohols (2 x absolute alcohol then 1x 70% methylated spirits for 3 mins each). At the end of this, cold tap water was used to rinse the alcohol from the tendon sections. Antigen retrieval is a technique employed to break down the cross-linkages between proteins created during formalin fixation. The presence of cross-links between proteins can mask the epitope of interest (Syrbu and Cohen, 2011), (McNicol and Richmond, 1998). Heat-mediated antigen retrieval was performed with a pressure cooker (Menarini Access Retrieval Unit (Menarini Diagnostics, UK)). The tendon sections were submerged in sodium citrate buffer (pH 6.0) for 1 min 40s at 125°C at full pressure in the pressure cooker. The sections were then given a 5 min buffer rinse (Tris pH7.5 with 0.05% Tween), before being loaded onto a Dako Autostainer (Dako, UK) and given another buffer rinse. Blocking of endogenous peroxidase activity was employed to reduce background staining by the addition of Dako Real TM Peroxidase blocking solution (Dako, #S2023) for 5 mins followed by another 5 min buffer rinse. The primary antibody, p62 was diluted 1:2000 with Dako Real Antibody Diluent (Dako, #K8006) and placed onto the tendon sections for 30 mins at room temperature. The primary antibody solution was removed and the sections were washed twice for 5 mins each using the Tris-buffer. The secondary antibody, an anti-rabbit HRP (horseradish peroxidase) conjugate (Dako Real Envision, #K4065) was added to the tendon sections for a further 30 mins at room temperature followed by another 2 x 5 mins buffer rinse. A chromogenic agent, DAB (3,3'-Diaminobenzidine) (Dako, # K4065) which recognises the HRP conjugated substrate was applied to the tendon sections twice for 5 mins each to allow visualisation of the antigen complex in the tendon. Excess agent was rinsed off with water three times. A counterstain, Gills Haematoxylin, was added for 27 seconds to allow visualisation of the nuclei in

the tendon, facilitating viewing of the surrounding cells. The slides were rinsed in water and then dehydrated by passing them through alcohol of increasing grades, in a reversal of the previous procedure i.e. 1x 70% methylated spirits and then twice in absolute alcohol. The slides were cleared using CitrocLEAR (3x for a few seconds each) and mounted using DPX (a mixture of distyrene, a plasticiser and xylene) mounting media (CellPath, #SEA-1304-00A).

2.12 Statistical analysis

2.12.1 Chapter 3

Calculated results in this chapter were recorded as the mean value. As the data was not normally distributed, the following non-parametric test was conducted, the Mann-Whitney U test for comparing the percentage of DNA damage in different oxygen tensions and on different matrix types. This test was also repeated for the percentage of replicative and binucleate cells respectively in these different environmental conditions. Error bars in the graphs represented the standard error. Statistical significance between results was represented by *** p-value<0.001, ** p-value<0.01 and *p-value<0.05.

2.12.2 Chapter 4

The data in this chapter subjected to statistical analysis was the expression of RBM3 in SDFT fibroblasts with heat and cold shock and the lethal heat shock experiments in SDFT and DDFT fibroblasts. All of the result values given were recorded as the mean value. The non-parametric Kruskal Wallis test was used to compare statistical differences between the expression of RBM3 in control cells with each of the recovery times following heat and cold shock. The Kruskal Wallis test was also used to compare the percentage of attached cells at each of the recovery time points following a lethal heat shock in comparison with the control. The Mann Whitney was used to determine significant differences in the percentage of attached cells between the unconditioned versus preconditioned heat and cold shocked SDFT and DDFT fibroblasts. Statistically significant results were represented by P-values as described in the previous section.

2.12.3 Chapter 5

In this chapter, two sets of data underwent statistical analysis, the first being the comparison of DAXX puncta size in heat and cold shocked SDFT fibroblasts versus those from unheated control cells. The second set of data being analysed was the expression of nuclear NRF-2 in SDFT fibroblasts exposed to various environmental conditions. To determine whether there were any statistically significant results, the non-parametric Kruskal-Wallis test was used for both sets of data. Error bars in the graphs represented the standard error. Statistically significant results were represented by P-values as described in the previous section.

Antibody	Manufacturer	Clone	Source	Dilution
γH2AX (Ser 139)	Millipore	JBW301	mouse monoclonal	IC: 1:1000
KiS2 (also known as TPX2)	1: Abcam (ab:32795)	18D5-1	mouse monoclonal	1C: 1:250
	2: Abcam (ab:71816)	-	rabbit polyclonal	IC: 1:100
phospho-p53 (Ser15)	Abcam (ab:1431)	-	rabbit polyclonal	IC: 1:200
p21	Calbiochem	EA10	mouse monoclonal	IC: 1:100
RBM3	Abgent (AP7397c)	RB18776	rabbit polyclonal	IC: 1:100
DAXX	Santa Cruz (M-112)	-	rabbit polyclonal	IC: 1:100
Caspase-2	Santa Cruz (C-19)	-	rabbit polyclonal	IC: 1:100
NRF-2	Abcam (ab:31163)	-	rabbit polyclonal	IC: 1:200
Cx43	Chemicon	RN26	mouse monoclonal	IC: 1:100
p62	MBL (PM045)	-	rabbit	IC: 1:500
			polyclonal	IHC: 1:2000

Table 3: Antibodies used for immunocytochemistry

The table provides comprehensive antibody details for immunocytochemistry experiments throughout the thesis.

Antibody	Manufacturer	Clone	Source	Dilution
Hsp-72	Enzo Life Sciences	C92F3A-5	mouse monoclonal	WB: 1:1000
Alpha tubulin	Abcam (ab:18251)	-	rabbit polyclonal	WB: 1:100,000
Acetyl-tubulin	Abcam (ab:24610)	6-11B-1	mouse monoclonal	WB: 1:1000
Caspase-3	1: Cell Signalling (#9611)	-	rabbit polyclonal	WB: 1:1000
	2: R&D Systems (AF835)	-	rabbit polyclonal	WB: 1:100
p62	MBL (PMO45)	-	rabbit polyclonal	WB: 1:1000

Table 4: Antibodies used for western blot

The table provides comprehensive antibody details for western blot experiments throughout the thesis.

Chapter 3) The influence of the cell culture environment on tenocytes from two tendons with different injury susceptibilities

3.1 Introduction

Energy storing tendons including the superficial digital flexor tendon (SDFT) are subject to high failure rates associated with exercise. These tendons are finely-tuned “biological springs” which are also designed to withstand high levels of force. The maintenance of tendon stiffness is paramount to this function (Alexander, 2002), (Butcher et al., 2009), (Stephens et al., 1989), (Riemersma and Schamhardt, 1985), (Wilson and Goodship, 1991). Reduced matrix turnover and decline in the cellular activity of SDFT tenocytes occur with maturity. It has been suggested that the tenocytes may ‘switch off’ their cellular machinery to minimise tendon remodelling and maintain the matrix within narrow optimal limits for strength and elasticity; this fine tuning comes at the expense of adequate tendon repair in response to injury (Goodman et al., 2004), (Birch, 2007), (Birch et al., 2008a). Repetitive loading of the SDFT together with other exercise related factors such as hyperthermia and ischaemia/reperfusion are thought to overwhelm the tenocytes’ reparative processes and/or induce their dysfunction or death, leading to a weaker tendon predisposed to rupture (Wilson and Goodship, 1994), (Farris et al., 2011), (Millar et al., 2012), (Leadbetter, 1992), (Patterson-Kane et al., 1997b), (Maffulli et al., 2000), (Pearce et al., 2009), (Flick et al., 2006), and (Jones et al., 2006).

The removal of cells (i.e. by enzymatic digestion or explant culture) from their in vivo three-dimensional, mutually contacting arrangement within an extracellular matrix (ECM) to in vitro culture in two-dimensional cell monolayers leads to the generation of cellular stress as a result of radical changes in the physical environment (Rubin, 1997). Cell culture is an inherently stressful event generating multiple stresses including altered oxygen tensions, different matrix types and/or stiffness, loss of mechanical signals and exposure to unphysiological growth stimuli (Halliwell, 2003), (Hadjipanayi et al., 2009), (Egerbacher et al., 2008), (Rubin, 1997).

Prior to my study of the effects of exercise-related stress such as hyperthermia on SDFT and DDFT fibroblasts, the basal behaviour of tendon fibroblasts in standard cell culture conditions are required to be established. The detection of subtle differences in damage readout in response to hyperthermia using two biologically different tendons could be masked by substantial cell culture induced injury. Understanding the levels of this culture induced 'noise' and how it could be minimised was critical. Although there are no published studies on the effects of culture conditions on markers of cell stress in equine tendon fibroblasts, current culture protocols have been shown to lead to rapid phenotypic drift (Yao et al., 2006b) and slow growth rates in human tendon stem cells (Zhang and Wang, 2013). The underlying reasons for the rapid phenotypic drift are unknown. Monolayer cell culture can generate genotoxic stress leading to premature senescence (also known as "culture shock") (Halliwell, 2003), (Wright and Shay, 2002). Senescence is characterised by a reduction in cellular proliferation eventually leading to irreversible growth arrest. It can be caused by shortening of the telomeres (replicative senescence) as a result of repeated cellular divisions or from cellular stress caused by serum starvation or oxidative stress (Yang and Hu, 2005), (Cristofalo, 2005), (Ye et al., 2007), (Herbig et al., 2004). One of the primary causes of culture shock is the use of ambient (atmospheric) oxygen tensions (21%) (Wright and Shay, 2006). Virtually every published tenocyte study to date has employed cell culture under oxygen tensions of 21% although in vivo oxygen tensions in tendon, a poorly vascularised tissue, are only thought to approximate to 2-3% (Zhang et al., 2010b), (Wright and Shay, 2006). Elevated levels of oxygen free radicals can provoke DNA damage and/or alter the replicative characteristics of cells (Burhans and Weinberger, 2007). These effects can be species specific. For instance, murine fibroblasts cultured in 21% oxygen accumulated 3-4 fold more DNA damage compared to growth at 3% oxygen, resulting in their premature senescence (Parrinello et al., 2003). Immature cell types are equally susceptible to oxidative stress. Mouse embryonic fibroblasts expressed 3-fold more DNA damage at ambient oxygen and entered senescence more rapidly than WI-38 human fibroblasts (derived from foetal lung) (Parrinello et al., 2003). In general, murine fibroblasts exhibited greater susceptibility to cell culture induced stress than human fibroblasts.

Composition of the matrix can also alter the behavioural characteristics of tenocytes e.g. human tenocytes showed differences in proliferative rates and matrix protein production when cultured on a variety of commercially available extracellular matrix patches (Shea et al., 2010). Matrix stiffness has been shown to be critical for cellular proliferation as human dermal fibroblasts cultured free-floating in 3D collagen matrices showed no proliferation even after 8 days of culture. On the other hand, attached fibroblasts seeded at the same density initiated proliferation after a lag period of 4 days. Stiffer matrices with a density of 20% collagen w/w led to rapid proliferation of dermal fibroblasts with no lag phase (Hadjipanayi et al., 2009). Cells are able to sense mechanical signals through a family of integrin receptors on the cell surface which closely connect the actin cytoskeleton to the ECM through focal adhesion complexes. The integrins can transmit intracellular signalling cascades into the cell, potentially influencing cell fate. When GD25 fibroblasts (derived from murine embryonic stem cell line) were cultured on fibronectin, collagen type III or laminin, integrin B1A promoted pro-survival signals in response to radiation genotoxicity (Cordes et al., 2005).

It is unknown whether the effects of different matrix proteins such as collagen type I or fibronectin found in normal and injured tendon respectively can modulate or mitigate the effects of DNA damage caused by high levels of oxygen free radicals in vitro. Similarly, data is lacking on whether these matrix proteins can also influence the repair of damaged cells.

Binucleate cells were evident in equine tendon fibroblast monolayers during my preliminary work with these cells. Although binucleate cells may arise in cell culture, their frequency was abnormally high when culturing tendon derived fibroblasts. Binucleation is a replicative stress occurring when there is a failure of cells to undergo cleavage during mitosis (Wong and Stearns, 2005). While karyokinesis occurs to replicate the genome, cytokinesis fails. A number of mitotic defects were believed to potentiate binucleate cell formation leading to G1 arrest (Wong and Stearns, 2005). Wong and Stearns showed that the G1 arrest arising in binucleate cells was not provoked by aberrant centrosome number, increased cell size and/or tetraploidy. Instead it was suggested that the addition of anti-cytoskeletal drugs causing microtubule depolymerisation (typically used in studies of binucleation) together with other cellular manipulations led to

increased DNA damage that triggered cell cycle arrest (Wong and Stearns, 2005). G1 arrest was attributed to the activation of a p53 associated DNA damage checkpoint caused by the cytotoxicity of the drugs (anti-cytoskeletal drugs) used, as less toxic doses led to the generation of binucleate cells which subsequently re-entered the cell cycle and completed mitosis (Uetake and Sluder, 2004), (Wong and Stearns, 2005). Some studies have shown that the type of matrix surface is of importance in promoting the re-entry of binucleate cells into the cell cycle and producing two monoclear, daughter cells (Uetake and Sluder, 2004). This would suggest that there is some influence of matrix protein on DNA damage, acting either by altering susceptibility to injury or its repair.

Regardless of the source of stress, DNA damage is a highly conserved end product between species and therefore provides a useful method for measuring the endogenous injury in cells exposed to 'complex stress' environments. Whilst there are multiple types of DNA lesion, the double strand break (DSB) constitutes the most lethal form of DNA damage in the cell which, if left unrepaired, leads to apoptosis, genomic instability and cellular arrest (Rogakou et al., 1999), (Gentile et al., 2003). One of the earliest biochemical events in the DNA damage response is the phosphorylation of H2AX, a histone variant of H2A in mammalian cells. Phosphorylated H2AX occurs for a megabase on either side of a DSB (to induce an 'open-chromatin' state for repair) and serves as a reliable and useful marker for the measurement of DSBs. Each γ H2AX focus has several hundred γ H2AX molecules at the DSB site, and studies using irradiated cells have shown there is a link between the number of γ H2AX foci and the number of DSBs. This has been used to quantify the latter in various experimental studies. The γ H2AX puncta are lost as the DNA damage is resolved and repaired correctly. It has therefore been used to monitor DNA repair which is experimentally useful (Rogakou et al., 1999), (Sedelnikova et al., 2002), (Paull et al., 2000), (Leatherbarrow et al., 2006), (Rich et al., 2013).

Oxidative damage to DNA can impair the replication of the genetic material during the cell cycle and replicative stress in turn can damage DNA. Exposure of cells to reactive oxygen species can spontaneously result in single strand DNA breaks. In replicating cells, the double helix is unwound to allow DNA strand template synthesis to take place. Inefficient DNA replication causes replication forks to stall or stop because of genomic lesion repair. Single strand

breaks at a replication fork can then lead to the production of double strand breaks (Sirbu et al., 2011), (Burhans and Heintz, 2009), (Burhans and Weinberger, 2007). As there is a close relationship between oxidative stress and the acquisition of DNA damage, we predicted that replicating cells would be most sensitive to cell culture induced stress. The monoclonal Ki-S2 is specific for the microtubule-associated protein TPX2 (also known as p100). This reagent was used to assess the replicative fraction in SDFT and DDFT fibroblasts. Unlike the commonly used Ki-67 clone, Ki-S2 does not stain cells in the G1 phase, which helps us to avoid overestimation of the replicative fraction through inclusion of damage-induced G1 arrested cells (Rudolph et al., 1998).

There have been no published studies on the reparative ability of SDFT fibroblasts in response to an exogenous oxidising genotoxic agent (such as hydrogen peroxide). These data would be of value as defective repair in the SDFT, in comparison to a second functionally distinct tendon, would suggest a mechanistic route to microdamage accumulation leading to tendon failure.

The aims of this chapter were:

- 1) To establish the basal DNA damage and replicative fraction for cells cultured from two functionally distinct tendons with different injury susceptibilities at different oxygen tensions and on different matrix surfaces (collagen type I and fibronectin). It was hypothesised that high oxygen tensions would increase the percentage of DNA damage in both SDFT and DDFT fibroblasts.
- 2) To understand if environmental cues (matrix/oxygen tension) influence binucleation. As oxidative damage is thought to lead to DNA damage and cell cycle arrest, it was hypothesised high oxygen tension would increase the percentage of binucleates in SDFT and DDFT fibroblasts. The use of certain matrix substrates e.g. fibronectin would reduce binucleation.
- 3) To determine DNA reparative ability following challenge by a DNA damaging agent. As SDFT fibroblasts are known to have a poor healing rate in vivo, it was hypothesised that the reparative ability of the this tendon would be less than that of the DDFT, a non-injury prone tendon.

3.2 Results

3.2.1 Tendon specific susceptibility to DNA damage

To test whether environmental variables such as oxygen tension and/or matrix type could lead to “culture shock” and the accumulation of cellular injury, the acquisition of DNA damage was measured. Immunostained γ H2AX was chosen as a reliable and sensitive marker of DSBs. The S-phase transition in fibroblasts is known to result in low levels of reparable DNA damage which is visible in these cells as low numbers of large γ H2AX puncta. Therefore, only cells containing 7 or more large γ H2AX puncta were classified as severely damaged and included in the quantification of DNA damaged cells (Ichijima et al., 2005), (Rich et al., 2013). The quantification of immunostained γ H2AX was used in preference to binary live/dead biochemical assays including Annexin V/PI staining as it provides a more sensitive and versatile indication of ongoing stress in cells which may otherwise appear healthy by Annexin/PI. Importantly, the DDR injury response also provides a global downstream read-out of multiple relevant cell stresses, including inflammatory cytokine secretion (Han et al., 2006), (Rodier et al., 2009).

The levels of DNA damage were quantified in passage 1 (P1) and passage 2 (P2) SDFT and DDFT fibroblasts cultured on two different matrix types (collagen type 1 and fibronectin) and two oxygen tensions (20% and 2%). This experiment was completed in two sets of horse tendons and the data obtained from them were comparable. There were no significant differences in the percentage of DNA damage between the two horses suggesting there was no inter-horse variation in their susceptibility to DNA damage. Figure 3-1 shows the data from both horses.

The culture of SDFT fibroblasts on fibronectin in ambient oxygen (21% oxygen) was shown to result in a significant increase in DNA damage with increasing time in culture, from passage 1 (P1) to passage 2 (P2) in both horses (P-value: 0.0079) (Figure 3-1A). In contrast, the opposite was found in SDFT fibroblasts cultured on collagen where the levels of DNA damage significantly decreased with culture time (P1 to P2) (P-value: 0.0079 for horse 1 and P-value: 0.0317 for horse 2). In normoxic oxygen (2% oxygen), there was a trend for a

decrease in DNA damage from P1 to P2 irrespective of matrix type in SDFT fibroblasts (Figure 3-1A). As sample size was small, future experiments would require larger numbers of horses to detect any potential significant differences in the percentage of DNA damage with passage number in normoxic oxygen.

There were no significant differences in the DNA damage levels for DDFT fibroblasts cultured on either matrix type or oxygen tension. However, there was a trend for an increase in DNA damage from P1 to P2 irrespective of matrix type or oxygen tension (Figure 3-1C). Again, sample size was small in these experiments. A larger number of horses would be required for future experiments to detect significant differences between different environmental cues.

In general, when comparing the levels of DNA damage between the SDFT and DDFT, initially the P1 SDFT fibroblasts contained higher levels of DNA damage in comparison with the DDFT for either matrix type or oxygen tensions. This is reversed in P2, where the levels of DNA damage in the SDFT fibroblasts was lower than the DDFT cells, especially for those cultured on collagen in ambient oxygen conditions. There was one exception to this rule: SDFT fibroblasts cultured on fibronectin in ambient oxygen conditions exhibited significantly higher DNA damage levels than the DDFT fibroblasts.

Two potential causes for the DNA damage detected by γ H2AX are the enzymatic digestion process used to extract the tendon fibroblasts from the tissue and infection with *Mycoplasma sp.* (Sun et al., 2008). All testing for *Mycoplasma sp.* was negative in our tendon fibroblast cultures. To assess whether DNA damage could have been caused by the extraction of tendon fibroblasts using enzymes, an alternative method of tendon cell isolation was chosen. An explant method, where tendon fibroblasts migrate outwards from tissue fragments into the surrounding environment was employed. The DNA damage levels in SDFT fibroblasts cultured from explants were not significantly different from those harvested by enzymatic means. For example, the percentage of DNA damage in P1 SDFT fibroblasts cultured on collagen in ambient and normoxic oxygen levels was 12.8% and 6.2% for the explants and 17.4% and 11.7% for harvested cells respectively.

3.2.2 DNA damage is enriched in the proliferative fraction

When culturing the SDFT and DDFT fibroblasts in vitro, the growth rate of the two different tendons were noted to be different. Following extraction of tendon fibroblasts from the tendon core, the DDFT cells were slower to grow at first then overtook their SDFT counterparts. This suggests that the increase in DNA damage, at least in the DDFT may be attributed to replicative rate. To investigate whether the replicative rate was causative in the acceleration of DNA damage in both SDFT and DDFT fibroblasts, immunolabelling with a mouse monoclonal antibody, clone KiS2, was used to assess the replicative fraction under the same set of oxygen tension and matrix conditions.

There was a strong link between the replicative fraction and the acquisition of DNA damage in both tendons (SDFT and DDFT) especially for those cultured on collagen. For example, the percentage of replicating cells was shown to be significantly lower in P2 compared with P1 for SDFT fibroblasts cultured on collagen irrespective of oxygen tension (P-value: 0.0079). This replicative profile was similar to that of DNA damage. This finding was seen in both horses (Figure 3-1B).

For DDFT fibroblasts, there was a trend for an increase in the percentage of replicating cells in P2 compared with P1 (irrespective of oxygen tension) and this matched the DNA damage profile. However, the only significant difference in the replicative profile between P1 and P2 was seen in those fibroblasts from horse 1 cultured on collagen in ambient oxygen (P-value: 0.0079) (Figure 3-1D). This again reflects a lack of sample size in these experiments.

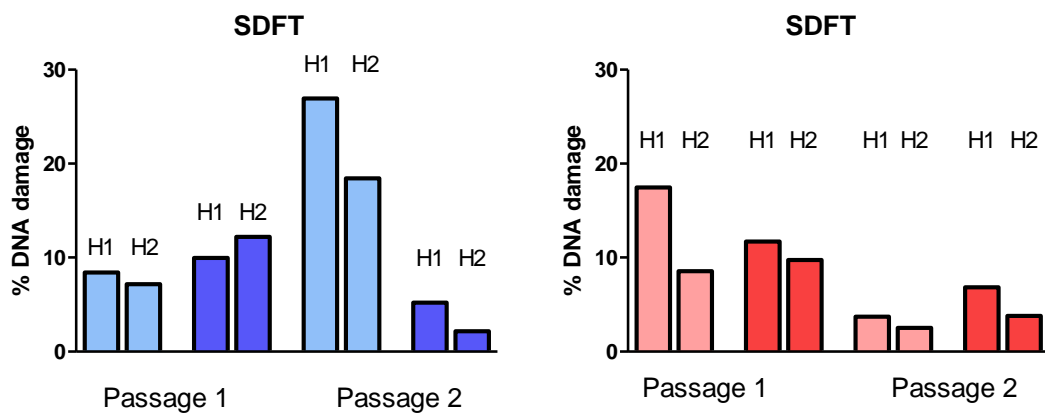
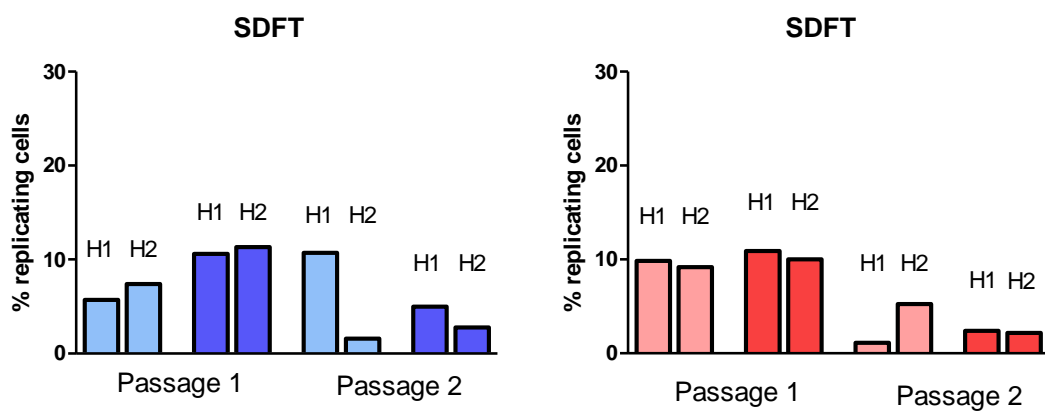
When SDFT fibroblasts were cultured on fibronectin, the replicative profile was similar to those of the DNA damage with one exception. P2 fibroblasts from horse 2 had a very low percentage of replicating cells when cultured in ambient oxygen in comparison with horse 1. This may be an outlier finding and could be related to experimental anomalies (Figure 3-1B). The replicative fraction of P2 horse 1 fibroblasts in ambient oxygen was not as high as expected as the DNA damage levels on this matrix was 2-3 times higher.

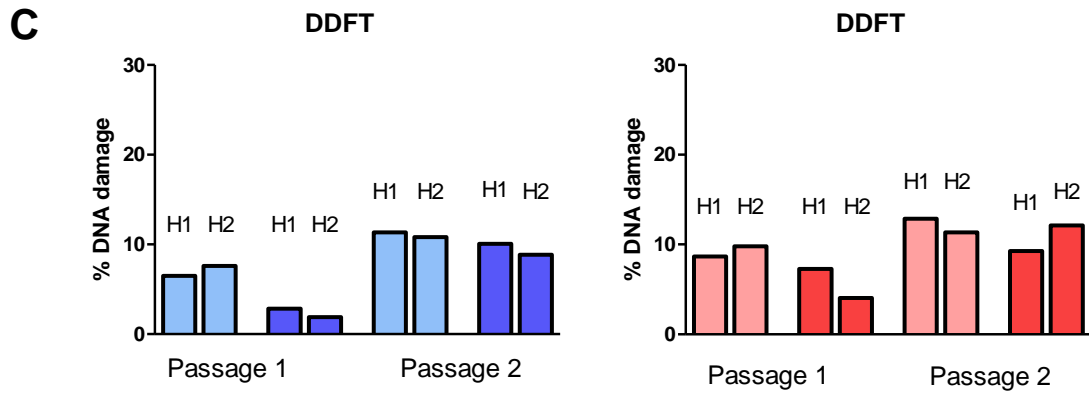
For DDFT fibroblasts, there was a significantly higher percentage of replicating cells in P2 compared with P1 in both horses when they were cultured on fibronectin in ambient oxygen (P-value: 0.0317 for horse 1 and P-value: 0.0159 for horse 2) (Figure 3-1D). This matched the DNA damage profile where there was an increase in the percentage of damaged cells with culture time.

In normoxic oxygen, the percentage of replicating cells does not increase in horse 1 DDFT fibroblasts with culture time (one set of data is missing in horse 2) (Figure 3-1D). In contrast, the DNA damage levels were shown to increase from P1 to P2 in the same oxygen tension. This suggests that replication associated DNA damage response may be uncoupled on a fibronectin matrix in both the DDFT and SDFT (where the DNA damage levels were also higher than expected) irrespective of the oxygen tension. However, the significance of these findings would need to be investigated by more work on a larger sample size.

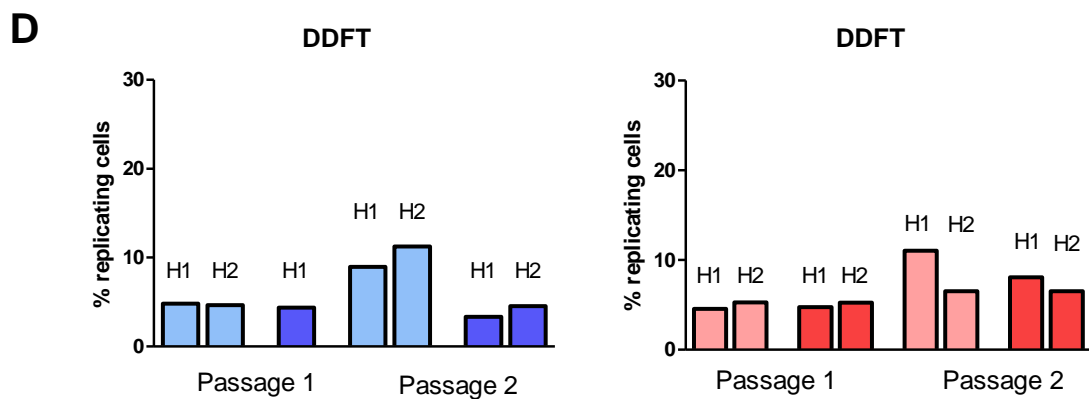
The correlation between DNA damage and the percentage of replicating tendon fibroblasts suggested that replication-induced genotoxic stress was occurring in both tendons. To verify whether DNA injury occurred in the replicative fraction of SDFT derived fibroblasts, a double stain of the DNA damage marker γ H2AX and the replicative marker TPX2 was chosen (Figure 3-2). A polyclonal rabbit anti-TPX2 antibody was purchased for the co-localisation experiments as KiS2 is a mouse monoclonal antibody specific for p100/TPX2/REPP68 (γ H2AX is also a mouse monoclonal antibody).

Very few non replicating cells were found to express puncta of γ H2AX. To extend these data further, the γ H2AX/TPX2 fraction was assessed in SDFT fibroblasts extracted from a foal; we hypothesised that cells derived from a very young horse might express a greater replicative fraction and therefore acquire a greater proportion of DNA damaged cells. For the foal, there was a 19% dual replicative and damaged fraction as opposed to 13% in adult SDFT fibroblasts taken from a 5 year old horse. The γ H2AX/TPX2 fraction was also examined in older horses; at 10yrs and 14yrs of age, where the fraction was calculated as being 7% and 5% respectively.

A**DNA damage****B****Replication**



DNA damage



Replication

Figure 3-1 Measurement of DNA damage and replication in SDFT and DDFT fibroblasts

Graphs A and B show the percentage of DNA damage and the percentage of replicating cells in SDFT fibroblasts over two passages (P1 and P2). Graphs C and D show the percentage of DNA damage and the percentage of replicating cells in DDFT fibroblasts over two passages. Two horses were used for this experiment (Horse 1: H1 and Horse 2: H2). SDFT and DDFT fibroblasts were cultured on fibronectin (blue) and collagen (red). The experiments were conducted in ambient oxygen (light blue and light red respectively) and normoxic oxygen (dark blue and dark red respectively). The percentage of DNA damage and replication was counted in 5 fields of view for each experimental condition for both horses. The columns in the above graphs represent the mean percentage of DNA damage or replication respectively.

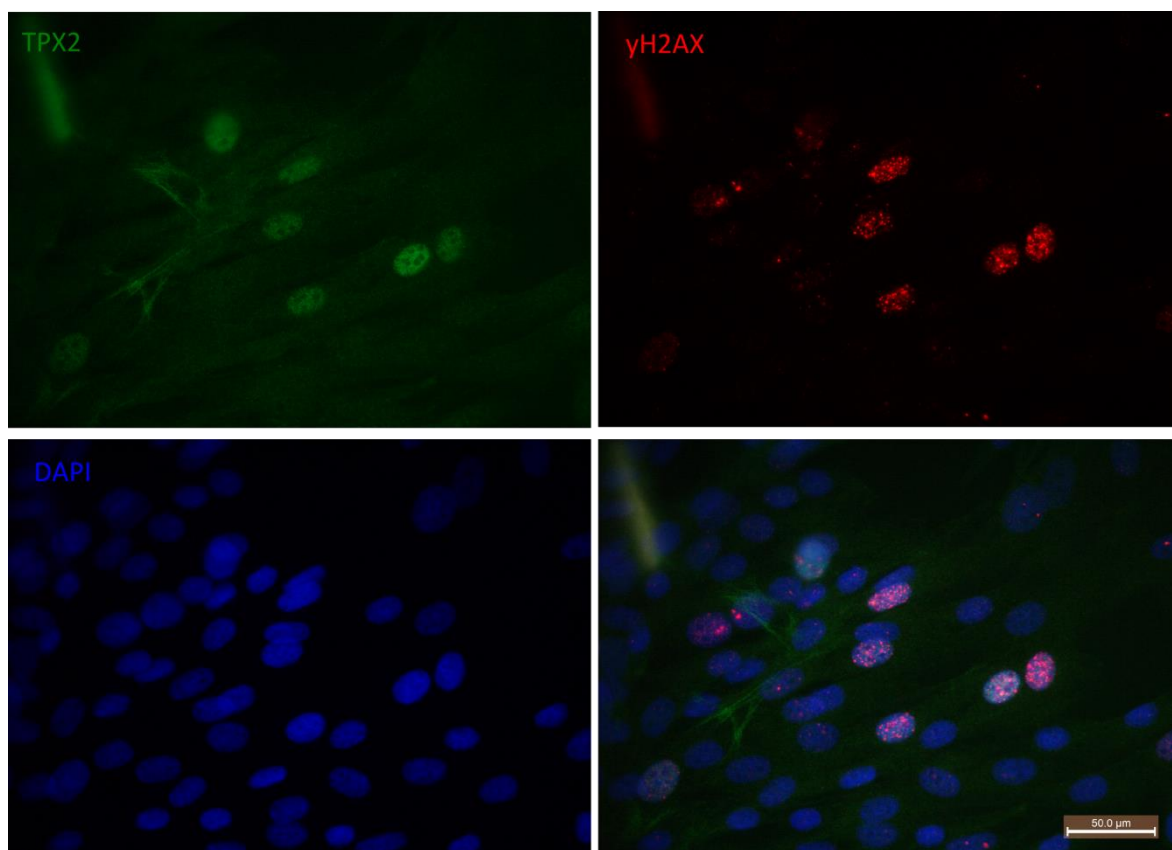


Figure 3-2 Dual stain for both γ H2AX and TPX2 demonstrates the significant association between replication and DNA damage.

SDFT fibroblasts were co-immunostained for TPX2 (green) and γ H2AX (red) with a DAPI co-stain (blue). The replicating SDFT fibroblasts (TPX2) expressed multiple γ H2AX foci suggesting replication induced DNA damage. Scale bar: 50 μ m.

3.2.3 Evidence of aberrant cytokinesis in SDFT fibroblasts

Genotoxic stress can be indicated by a number of different phenotypes including micronuclei, stabilised p53 and abnormal mitoses. DNA damage can lead to aberrant cytokinesis resulting in binucleation of cells (Wong and Stearns, 2005). Micronuclei are small extra-nuclear structures containing chromosomal DNA thought to be created from mitotic errors producing lagging chromosomes which are then ejected from the nucleus (Crasta et al., 2012). Replication-induced DNA damage may also lead to the activation of DNA damage checkpoints. A typical effector of this response is p53 phosphorylated at serine 15 (a phosphorylation specifically occurring in response to a DNA damage activated kinase). p53 in turn activates the transcription of downstream targets including that of p21, a cyclin dependent kinase inhibitor which ultimately leads to cell cycle arrest (Loughery et al., 2014). The detection of injury (genotoxic or cytoskeletal) can occur during interphase as well as at the latter stages of mitosis. Injury detection at mitosis (for example unrepaired lesions or de-novo breaks) can delay cytokinesis which then gives rise to binucleation (Wong and Stearns, 2005), (Ichijima et al., 2010). Given the link between DNA damage and binucleation, it was of interest to determine whether any of these phenotypes could be detected and whether they were influenced by environmental cues- namely the two different oxygen tensions and matrix surfaces. Data was collected from two horses.

Binucleate cells (BN) were evident in all cultures (Figure 3-3). The percentage of binucleate cells was significantly different between the two horses. It is unknown whether this is due to inter-horse susceptibility to the formation of binucleate cells or whether there were experimental differences (Figure 3-4). Further work would have to be carried out with larger sample sizes.

The oxygen tension and matrix type did not influence the percentage of binucleate cells with passage number (culture time). There was a significant increase in the percentage of binucleate cells from P1 to P2 for horse 2 SDFT and DDFT fibroblasts cultured in ambient oxygen irrespective of matrix type. This data indicates this horse may be more susceptible to binucleate formation in this oxygen tension.

Aberrant nuclear morphology was detected in binucleate cells, by the presence of micronuclei containing small amounts of damaged DNA. Figure 3-5 shows a binucleate cell with two blebs (containing damaged DNA positive for γ H2AX) extruding from its edges. Once these blebs have detached completely from the nucleus, they will become micronuclei.

Further confirmation of p53 induced DNA damage checkpoint activation was examined by investigating whether a transcriptional target of p53, p21 was up-regulated. As seen in Figure 3-6, p21 was clearly expressed in SDFT cells, not just in binucleate cells, but also in mononuclear cells.

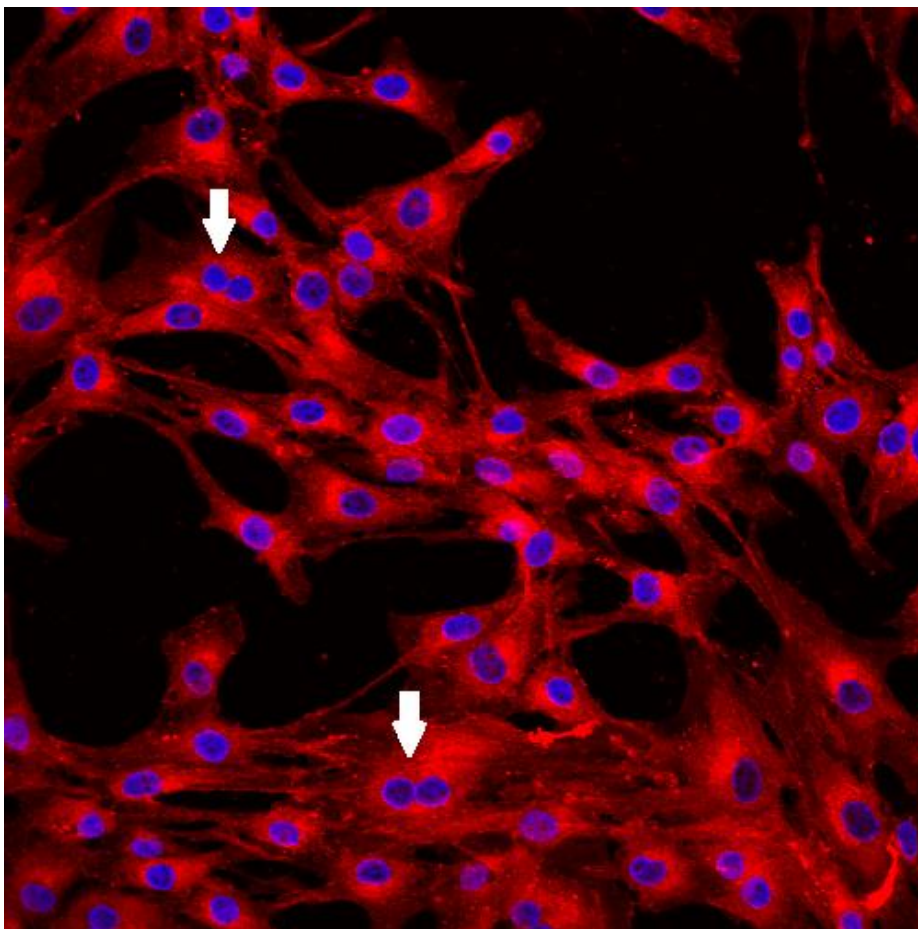


Figure 3-3 Binucleate SDFT fibroblasts

Binucleate cells in a monolayer of SDFT derived tenocytes (white arrows). Binucleate cells contain two nuclei within one daughter cell. The SDFT fibroblasts were stained with CellMask which outlined the cytoplasmic contents of the cells (red) and DAPI (blue) to stain nucleic acid.

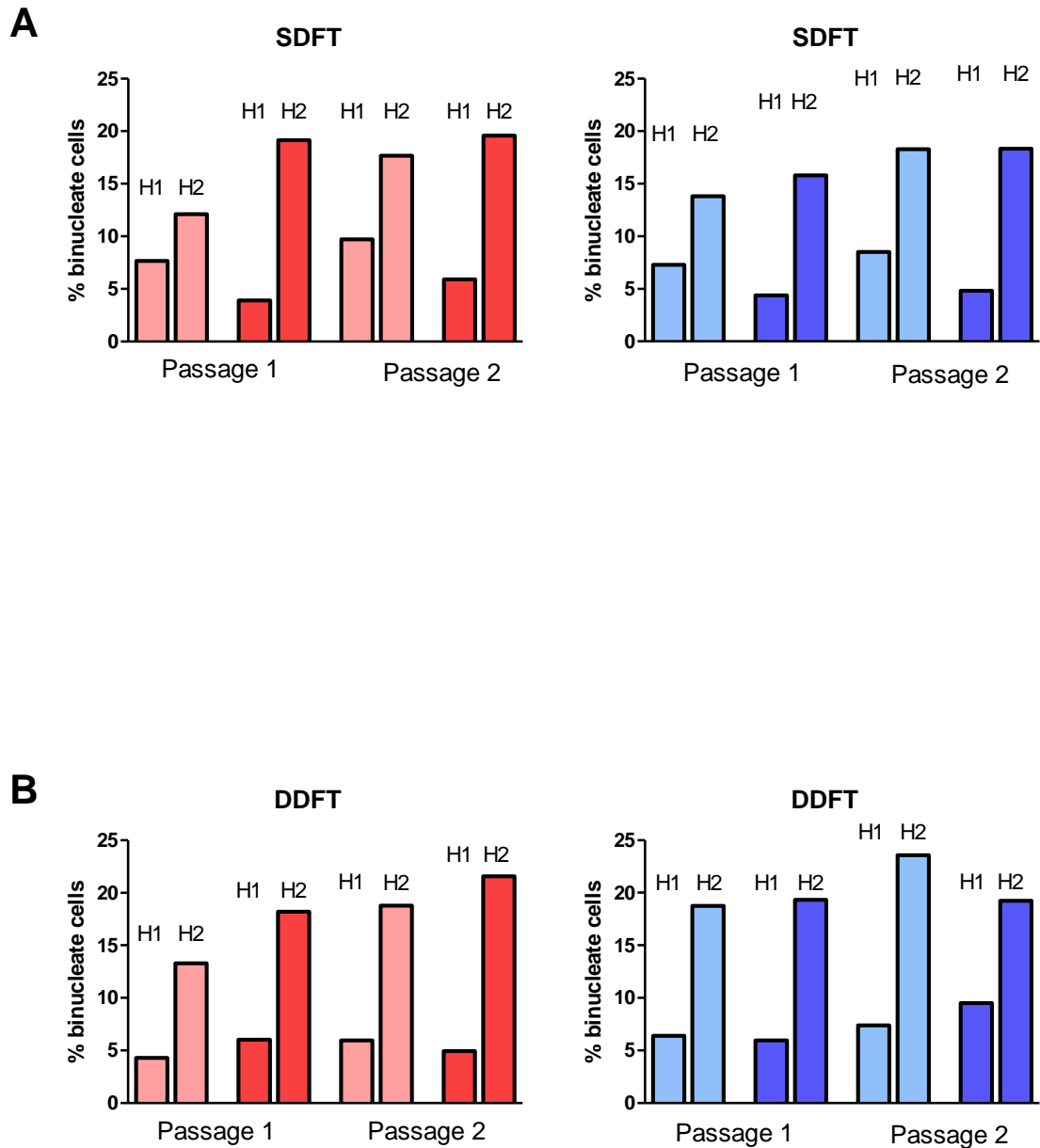


Figure 3-4 Binucleate cells were detected in all culture environments

The percentage of binucleate cells (BN) was recorded in two different oxygen tensions and matrix types in SDFT (Graph A) and DDFT fibroblasts (Graph B) over two passages (P1 and P2 respectively). Two horses were used for this experiment (Horse 1: H1 and Horse 2: H2). SDFT and DDFT fibroblasts were cultured in fibronectin (blue) and collagen (red) in either ambient (light blue and light red respectively) or normoxic oxygen tensions (dark blue and dark red respectively). The percentage of binucleate cells was recorded in five fields of view for each experimental condition for both horses. The columns in the above graphs represent the mean binucleate percentage for each experiment.

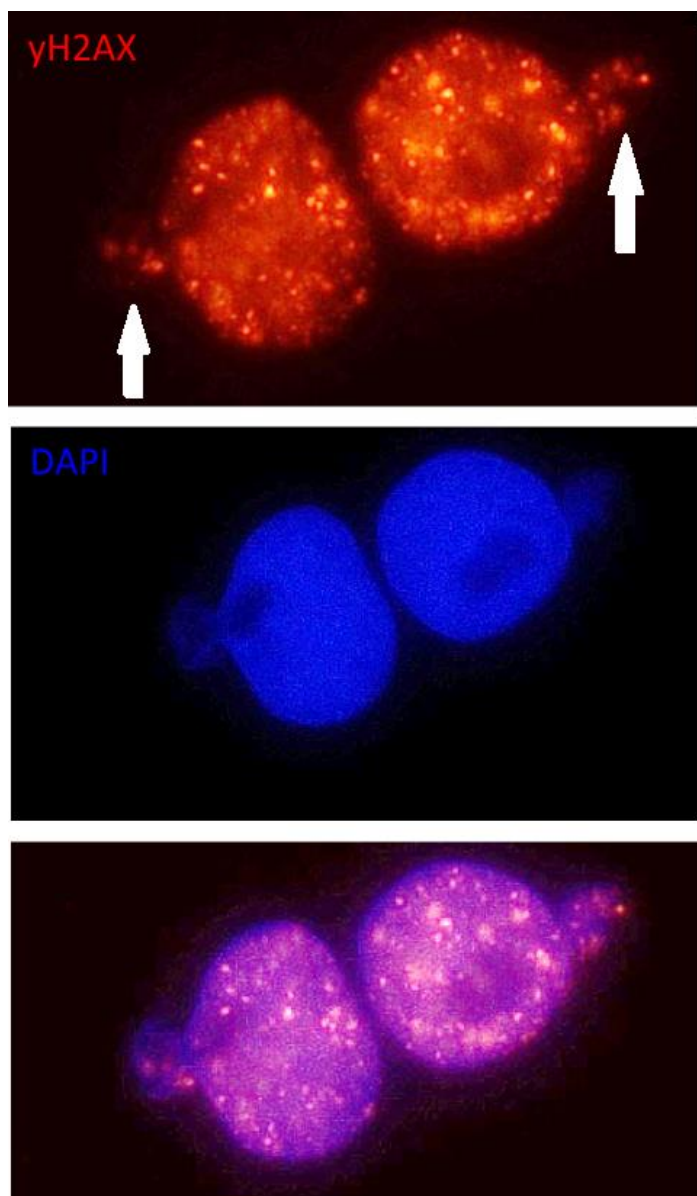


Figure 3-5 Binucleate cell with bleb containing damaged DNA

Image shows binucleate cell positive for γ H2AX (red). The cell was also co-stained with DAPI to detect nucleic acid (blue). The binucleate cell contains two blebs attached to the nuclei (white arrows). The blebs contain damaged DNA, as shown with the γ H2AX stain.

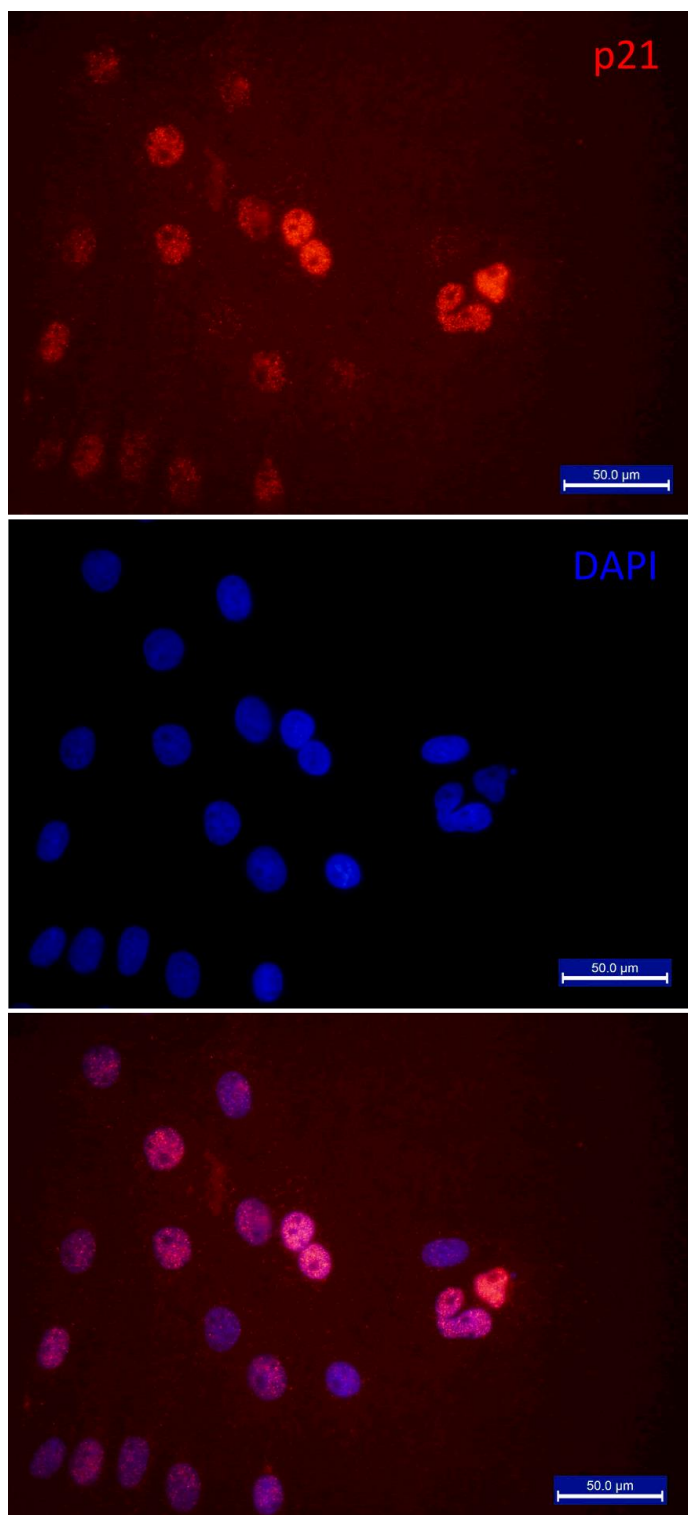


Figure 3-6 p21 expression in SDFT fibroblasts

SDFT fibroblasts were stained for p21 (red) and DAPI (blue). The two images were merged (bottom box). Scale bar: 50μm

3.2.4 Increased lysosomal enzyme activity in tendon cells

Continued or chronic DNA-replication stress and the formation of DSBs is believed to induce p53 mediated cell cycle arrest and senescence, thus preventing the proliferation of damaged cells (Zheng et al., 2012), (Marusyk et al., 2007). A senescent state implies the increased expression of lysosomal degradation and therefore lysozyme (Lee et al., 2006). This can be detected by a pH dependent beta-galactosidase stain. A senescence-associated beta galactosidase stain therefore was used to indicate lysosomal activity in SDFT fibroblasts from an adult horse. The majority of SDFT cells were positively stained (Figure 3-7A). For DDFT cells from the same horse, the uptake of stain was much lower and in positive cells, the staining was less intense (Figure 3-7B). For fibroblasts from a foal SDFT, only one or two cells were positive per x20 magnification field for the senescence-associated beta-galactosidase stain (Figure 3-7C).

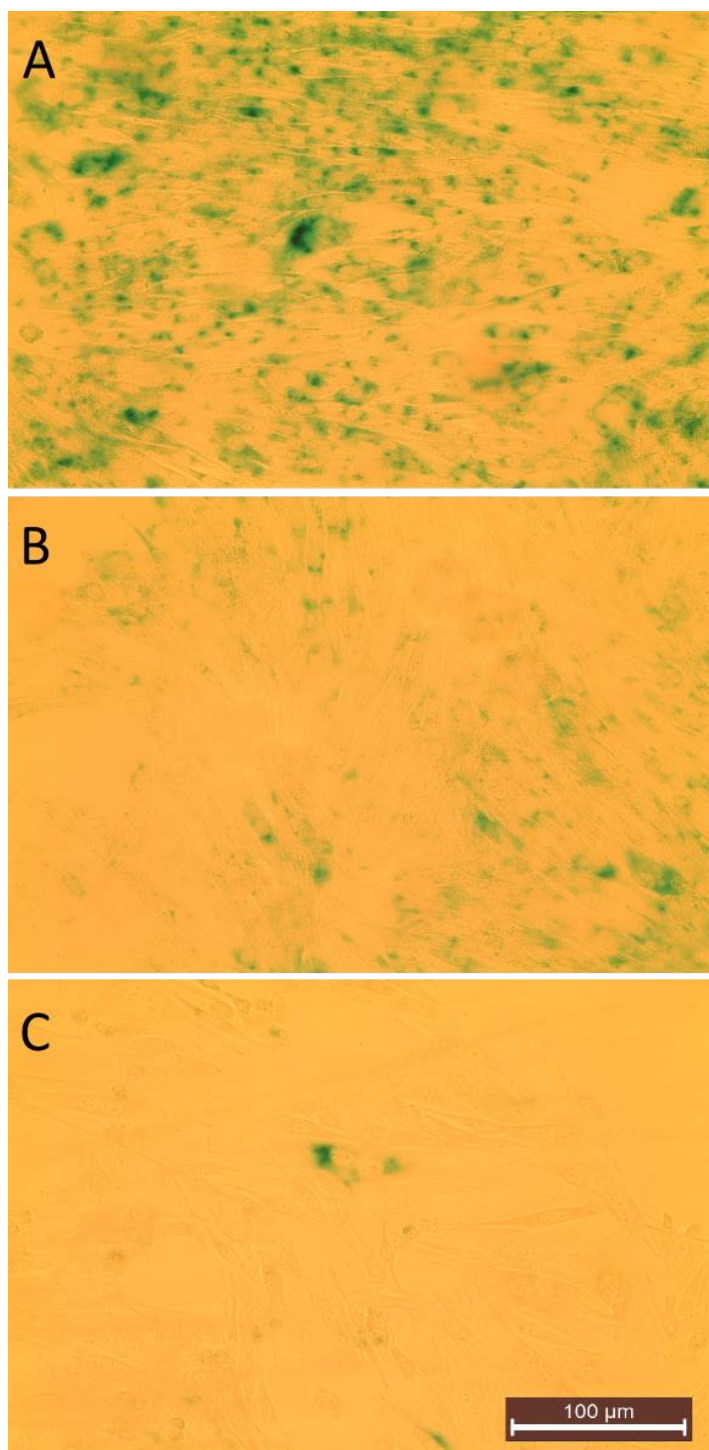


Figure 3-7 Senescence-associated beta galactosidase stain was strongest in adult SDFT

SDFT adult fibroblasts were positive for lysosomal activity following staining with a senescence-associated beta galactosidase stain (Panel A). In comparison, staining was less intense in DDFT derived fibroblasts from the same horse (Panel B) SDFT foal fibroblasts were almost entirely negative for the stain (Panel C). SDFT fibroblasts were seeded at the same density for all samples being compared. Scale bar: 100 μ m

3.2.5 SDFT and DDFT fibroblasts showed comparable repair capacities following exogenous oxidative DNA damage

Foci of γ H2AX arise initially because of DNA breaks and will persist if these breaks are not repaired (Löbrich et al., 2010). High numbers of foci may therefore represent ineffective repair of these lesions, rather than increased damage detection as high levels of DNA damage in our equine tendon fibroblast monolayers did not result in cell death. To determine whether DNA repair was defective in SDFT and DDFT fibroblasts, these cells were cultured until confluent on both collagen and fibronectin at ambient oxygen. Confluency was chosen to minimise replication induced DNA damage in the monolayers as hydrogen peroxide (H_2O_2) was used as an injury stimulus to generate both single-stranded and double stranded breaks (Driessens et al., 2009). Critically, oxidative damage is also implicated in exercise-induced microdamage as it is believed ROS are generated within the tendon tissue during high speed exercise (Millar et al., 2012), (Longo et al., 2008).

The assessment of DNA repair in two functionally different tendons was therefore assessed using the comet assay which is a sensitive and direct biophysical method for detecting multiple types of DNA lesion and repair rates (Collins, 2004). Detection of γ H2AX foci in cells is an indirect method of measuring DNA repair in cells as it primarily detects genomic injury at the DSB site and its presence also indicates that modification of the chromatin has taken place to allow the accumulation of repair proteins to the site (Paull et al., 2000). Knock -out mice lacking H2AX have been shown to repair DSBs at a less efficient rate (Celeste et al., 2002), (Kinner et al., 2008). Therefore, the use of anti- γ H2AX antibodies by immunocytochemistry was not used to monitor DNA repair.

DNA damage was induced by incubation with 200 μ M hydrogen peroxide (H_2O_2) for 5 min on ice. To assess repair capacity, the H_2O_2 treatment was followed by a 1 h recovery period. Both treatment groups were compared with untreated controls. Damaged DNA migrates away from the nucleoid (a term used to describe the agarose encapsulated DNAs from each individual cell) following the application of an electric field. When the damaged DNA was fluorescently labelled, a 'comet' shape was visualised for each cell (Rich et al., 2013). The

comet shape and tail size has been shown to correlate with the severity of DNA damage (Collins, 2004). A visual scoring system employing 5 categories ranging from class 0 (no tail) to class 4 (almost all DNA in tail) was used to quantify the degree of damage in the SDFT and DDFT fibroblasts following treatment with H₂O₂ (Figure 3-8). Summing the scores of each of the individual comet values (0-4) gave an arbitrary total score between 0-400, with the highest values representing the most severe damage (Collins, 2004).

Control cells were in class 0 as expected for both the SDFT and DDFT fibroblasts cultured on collagen and fibronectin matrices (Figure 3-8). Following a short burst of oxidative stress caused by 5 min of 200µm H₂O₂ treatment, confluent SDFT and DDFT cells on fibronectin and collagen showed similar levels of DNA damage with the majority of scores in the '3' range. The mean arbitrary score for DNA damaged SDFT cells on collagen and fibronectin were 299 and 185 respectively. For DNA damaged DDFT fibroblasts on collagen and fibronectin, the mean arbitrary score was 306 and 212 respectively (Figure 3-9). Following one hour of repair, the DNA damage scores had fallen into the '1' range for both tendons (Figure 3-8). The 'patterns' of DNA damage induction and repair were the same for either matrix protein using the SDFT or DDFT.

As replicative stress appears to have a role in the propagation of DNA damage in both SDFT and DDFT cells, the comet assay was repeated using sub-confluent fibroblasts (i.e. replicating) on a fibronectin matrix to determine whether the cells' replicative status would affect the repair of lesions caused by H₂O₂. (Figure 3-9). There was a higher level of (basal) damage in control, treated and recovered subconfluent cells for both the SDFT and the DDFT fibroblasts on fibronectin in comparison to confluent cells cultured on the same matrix. As sample size was small, samples from a larger number of horses would be required to determine whether this is a significant finding in subconfluent cells.

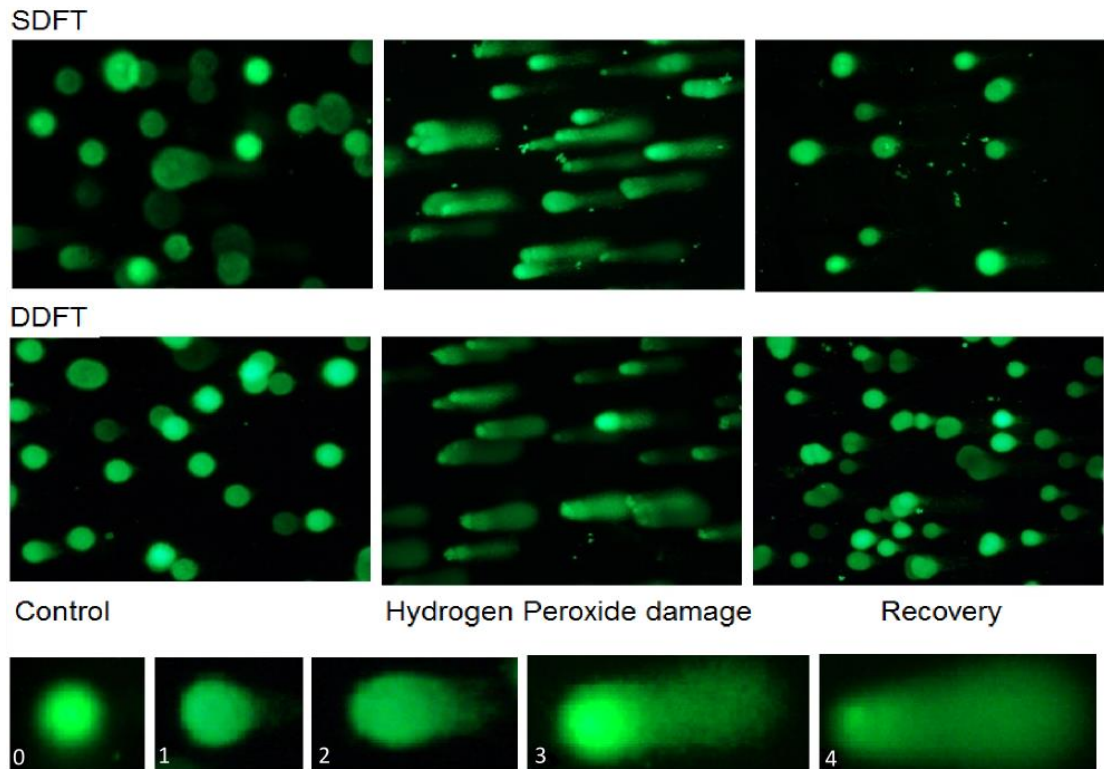


Figure 3-8 Comet assay in SDFT and DDFT fibroblasts

Comet assay using SDFT and DDFT derived fibroblasts. Three treatment groups were used for each tendon, a control group where cells were maintained at 37°C only, a treatment group where cells were exposed to hydrogen peroxide for 5 mins on ice and a recovery group where the cells were treated with hydrogen peroxide followed by one hours' recovery at 37°C. The cells were graded on the severity of DNA damage using a visual scoring system that employs 5 categories from 0 (nothing in tail) to 4 (almost all DNA in tail). Images shown at x63 magnification.

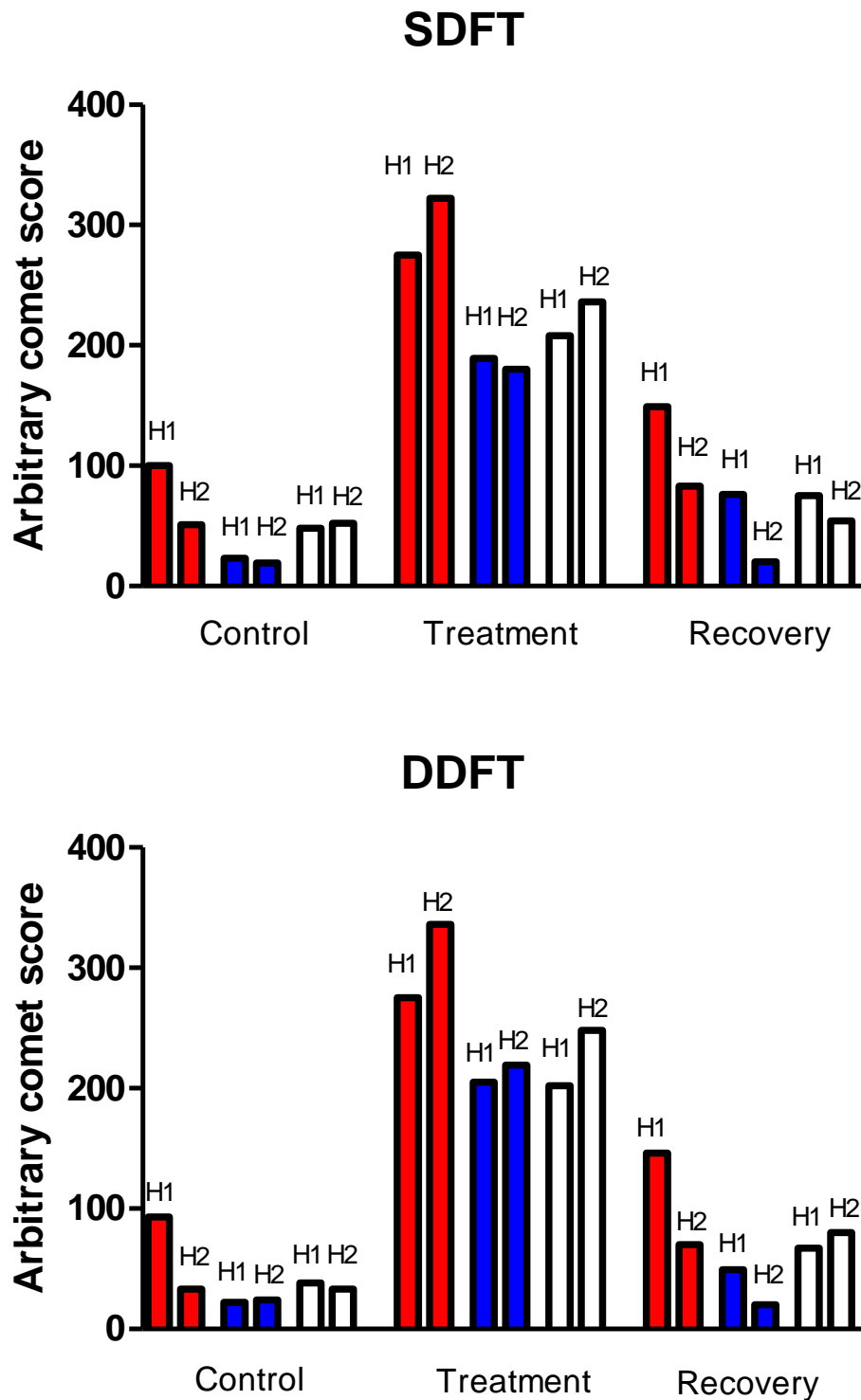


Figure 3-9 Quantification of DNA damage associated with the comet assay

Confluent SDFT (Graph A) and DDFT (Graph B) fibroblasts were cultured on collagen (red) and fibronectin (blue). Subconfluent SDFT and DDFT fibroblasts were also cultured on fibronectin (white) to determine whether the replicative rate of these cells would affect the repair of DNA damaged cells. Two horses was used in this experiment (Horse 1: H1 and Horse 2: H2). The DNA damage levels were quantified using the visual scoring system as shown in Figure 3-8. 100 cells from the control, treatment and recovery groups were each quantified for both horses. Summing the scores of 100 individual comet values (0-4) gives an arbitrary score of 0-400 with the highest scores representing the most severe damage.

3.3 Discussion

3.3.1 SDFT fibroblasts are sensitive to replication-induced stress in certain culture conditions

One of the main findings in this section was that equine tendon fibroblasts were very susceptible to replication induced DNA damage in vitro. Matrix type appeared to have an important influence on the DNA damage response in both tendons. My data suggests that there is a strong link between replication induced DNA damage on a collagen matrix, however on fibronectin, replication may be uncoupled with the DNA damage response. This latter statement was based on my findings where the DNA damage levels would be higher than the replicative fraction in both SDFT and DDFT fibroblasts e.g. in SDFT fibroblasts cultured on fibronectin in ambient oxygen, the DNA damage levels were 2-3 times higher than those of the replicative profile. However, sample size was very small and a larger number of animals would be required to determine whether this is a significant biological finding or not.

The exact cause for replication induced DNA damage is still unknown, although the cell culture environment was thought to be a damaging influence in both the SDFT and the DDFT. Two factors potentially causing DNA damage in the monolayers were ruled out, one being the enzymatic extraction of tendon fibroblasts as the tendon explants displayed comparable levels of damage. The other possible factor was *Mycoplasma sp.* infection of the cultures. *Mycoplasma sp.* can cause DNA damage detectable by γ H2AX immunostaining (Sun et al., 2008). All testing for infection was negative.

It is possible that the delay in processing of tendon samples and/or transport conditions for bringing back horse tendons from the abattoir to the laboratory (6-7 hour drive) was sub-optimal as the DNA damage levels were high for both the enzymatically extracted cells and the explanted cells (derived from the same horse). Work completed by my colleagues (post thesis) indicated that the speed of enzymatic processing may be important for minimising the DNA damage levels in equine tendon fibroblasts as cells enzymatically extracted from a horse within 1 hour of death had a smaller number of large γ H2AX puncta (Rich et al., 2013).

Despite the high levels of replication induced DNA damage in these cells, very little cell death was present in the cell monolayers i.e. no apoptotic bodies were visualised and there was an absence of the pan-nuclear γ H2AX immunostaining associated with cellular apoptosis (de Feraudy et al., 2010). These results indicate that although the tendon monolayers appeared healthy as cell death was sparse in the cultures, the growth of cells in vitro was still a stressful environment for the tendon fibroblasts. This underlying cell culture stress may easily be missed and more tests may be required to check the overall health status of the cells.

As discussed above, the influence of matrix type played a strong role in amplifying or mitigating the replication induced DNA damage response in SDFT fibroblasts especially when cultured in ambient oxygen. P2 SDFT fibroblasts expressed high levels of phosphorylated γ H2AX when cultured on fibronectin in ambient oxygen and by contrast, reduced levels of DNA damage when cultured on collagen at the same oxygen tension. This suggests the SDFT may be more sensitive to injury on a fibronectin matrix. Alternatively, it has been suggested that fibronectin may promote increased DNA damage response signalling. De Wever has recently demonstrated that fibronectin promotes DNA damage recognition (DDR) in an α 5 integrin dependent fashion together with increased stimulation of the phosphatidylinositol 3-kinase pathway, one of the kinases responsible for mediating the phosphorylation of H2AX at serine 139, resulting in γ H2AX foci formation (De Wever et al., 2011).

Two studies have shown that fibronectin has the ability to override cell cycle entry checkpoints by suppression of the cyclin-dependent kinase 2 (Cdk2) inhibitors p21cip/waf and p27Kip1 and induction of cyclin D1 (Jang and Chung, 2005), (Roy et al., 2002). This was not backed up in my data where quantitative replication KiS2 studies showed the percentage of KiS2 positive SDFT fibroblasts did not match the percentage of DNA damaged cells, the latter being 2-3 times higher. This suggests fibronectin may potentiate the DNA damage signalling response in SDFT fibroblasts. Again, a larger sample size would be required to determine whether fibronectin does have the ability to amplify the DNA damage response in equine fibroblasts.

Conversely, fibroblast adhesion via $\alpha 1$ integrin to polymerised type I collagen has been shown to inhibit the G1/S phase transition, repressing cellular proliferation (Xia et al., 2008). These findings are consistent with the decreased replicative fraction in P2 SDFT tendon fibroblasts on collagen.

The SDFT fibroblasts initially had a higher replicative fraction in P1 on both matrices and oxygen tensions in comparison with DDFT fibroblasts. This was reversed in P2 (with the exception of fibronectin at ambient oxygen for the SDFT). One potential reason for the difference in the replicative fractions between passages in SDFT and DDFT derived fibroblasts may result from the greater number of SDFT cells extracted from the tissue during the enzymatic extraction procedure. The extraction of DDFT derived cells from the tissue was poor and resulted in very low cell numbers. As there was a difference in the seeding density between tendons, the growth of the DDFT may lag behind those of the SDFT and as proliferation of the cells correlated with DNA damage, this could explain the pattern of damage in the two tendons with increasing culture time. The enzymatic extraction protocol for DDFT derived fibroblasts will have to be improved for future studies to optimise cell numbers at the start of all experimentation work. During the preparation of the tendon core prior to enzymatic extraction, it was noted that the DDFT tendon tissue was much softer than the SDFT therefore a more gentle enzymatic digestion may be required, either by shortening the time of digestion and/or using more appropriate enzymes suitable for the extraction of DDFT derived fibroblasts from the tendon core.

3.3.2 Binucleation was influenced by oxygen tension in SDFT fibroblasts only

Binucleation is normally a rare event in mammalian cell culture (with the exception of cardiomyocytes) and occurs when there is a failure of cytokinesis in the later stages of mitosis (Stephen et al., 2009), (Wong and Stearns, 2005). The use of cell synchronisation treatments in human diploid fibroblasts has been shown to induce p53 associated G1 arrest in BN cells as a result of DNA damage caused by the drugs used (Wong and Stearns, 2005). Our experimental work demonstrated up-regulation of stabilised p53 and its transcriptional target, p21,

in BN cells; however, the numbers of BN cells formed were not influenced by the DNA damage levels (γ H2AX levels).

The percentage of BN cells was shown to accumulate with culture time in horse 2 SDFT and DDFT fibroblasts which indicates that this horse may be more susceptible to the formation of BN cells. This horse also displayed an increased BN number in comparison with horse 1. Further studies are required to determine whether these differences between horses are due to different injury susceptibilities between horses or whether there was a difference due to experimental nuances.

The culture of rat embryonic fibroblasts on matrix coated surfaces especially those using fibronectin, have been shown to rescue binucleate cells and favour their re-entry into the cell cycle (Uetake and Sluder, 2004). Our experimental work did not reveal any influence of matrix type on BN number, but this may be a reflection of species specific differences in their predisposition to BN formation (Uetake and Sluder, 2004), (Stukenberg, 2004).

3.3.3 Increase in lysosomal enzyme activity in adult SDFT fibroblasts

Adult SDFT fibroblasts showed increased staining with senescence-associated beta galactosidase (SA- β gal) in comparison to the DDFT and the foal SDFT. The SA- β gal activity at pH 6.0 has been used as a marker of cell aging in vitro (Dimri et al., 1995). One of the features of senescent cells is a reduction in proliferation eventually leading to irreversible growth arrest (Maehara et al., 2010). During our experimental studies, SDFT derived fibroblasts continued to proliferate despite a large number of cells staining positive for the SA- β gal marker. Other senescent phenotypes such as an increase in cell size (by two fold) and a flattened morphology were not present in the SDFT cells (Lee et al., 2006). Therefore, we propose that the SA-beta gal positive cells have not entered a state of irreversible cell cycle arrest but instead are likely to be expressing increased lysosomal activity (Lee et al., 2006).

The reliability of the aging assay has been questioned by a number of authors for its lack of specificity as SA- β gal staining has been shown to be

increased not only in cells with increased replicative age but also in quiescent cells or serum starved cells. In senescent cells or in hydrogen peroxide treated cells the increase in SA- β gal staining has been shown to be irreversible but reversible in serum starved cells and other conditions (Yang and Hu, 2005), (Cristofalo, 2005). The activity of SA- β gal has been attributed to the lysosomal β -D galactosidase enzyme that is localised to the lysosomes. Maximal activity of this enzyme occurs at pH 4.0-4.5. At pH 6.0, its activity is much lower (Zhang et al., 1994). Senescent cells display higher levels of lysosomal β -galactosidase activity due to an increase in lysosomal number and content, thus exceeding a threshold level where the expression of this enzyme will be higher at pH 6.0 (Kurz et al., 2000), (Lee et al., 2006).

The reason for the increase in lysosomal activity in adult SDFT fibroblasts is unknown. It could be caused by cell culture related stress producing an increase in protein damage which is then targeted for degradation. Adult SDFT fibroblasts retrieved from the in vivo environment where subclinical microdamage could be present may be more likely to be aged or injured as a result of repetitive exercise. As damaged proteins are more commonly found in aged or injured cells, up-regulation of the autophagosome- lysosome systems would already be in place to remove these proteins (Bjørkøy et al., 2005). This test needs to be repeated with more animals to determine whether this is a true biological finding and most importantly, a more reliable marker for lysosomal activity needs to be used.

3.3.4 The SDFT and DDFT had similar rates of repair

Comparable rates of DNA repair were noted in both SDFT and DDFT fibroblasts irrespective of matrix type which suggests the SDFT does not exhibit an impairment or deficiency in DNA repair due to intrinsic endogenous injury caused by free radicals. Most of the DNA damage caused by hydrogen peroxide treatment was repaired within one hour. Complete repair may have occurred if the cells had been left to recover for longer. In general, these results show the SDFT can repair genotoxic damage in response to a stressor, however this does not equate to the complete repair of matrix damage which may potentially be sub-optimal, especially when matrix turnover is known to be very slow (Thorpe et al., 2010). Furthermore, my results are based on a small sample size and a

larger study would be required to determine whether both the SDFT and the DDFT show a comparable rate of repair on these matrix types in response to an oxidative stress.

The DNA damage levels in confluent SDFT monolayers cultured on fibronectin were much lower than the sub-confluent cells on the same matrix which suggests that the replicative status of the tendon cells may have an effect on the ability of the tendon fibroblasts to repair damage. The tendon fibroblasts are believed to have a low replicative rate in vivo as the turnover of the ECM is very low (Batson et al., 2003). The introduction of SDFT tendon fibroblasts into the cell culture environment may induce a de-differentiation state in vitro producing a replicative phenotype (Zhang et al., 2010a) susceptible to genotoxic stress and thus the repair processes may become overwhelmed. The influence of small differences in the basal levels of DNA damage may alter the injury threshold for these cells and as such future work will be required to minimise the levels of genotoxic stress in replicating cells (Rich et al., 2013). For example, the use of low serum (1%) in cell culture media may slow down tendon fibroblast proliferation through a reduction in the availability of growth factors and nutrients thus minimising replication induced DNA damage (Rhudy and McPherson, 1988). Another method for reducing tendon fibroblast proliferation would be to culture tendon cells on slices of tendon matrix taken from the tissue itself or use 3-D synthetic matrices that closely resemble the ECM in vivo. Within the tendon, the tendon fibroblasts are located in small niches where they interact with the collagenous and non-collagenous components of the ECM and additionally with each other via a number of communication channels including gap junctions and adherens junctions (Ritty et al., 2003), (McNeilly et al., 1996), (Ralphs et al., 2002), (Rich et al., 2013). These interactions may be required for tendon derived fibroblasts to maintain their differentiated status (i.e. slow replicative state) in vitro.

There was a marked difference in results when comparing the low injury levels of SDFT fibroblasts as assessed by the comet assay and the high levels of immunostained γ H2AX foci in P2 SDFT fibroblasts when cultured on fibronectin. This difference may be a reflection of the methods used. Measurement of γ H2AX foci in cells may indicate that there is increased sensitivity to an injury rather than an increase in DSBs. Phosphorylation of H2AX is mediated by ATM kinase in

response to DNA DSBs leading to the activation and recruitment of a number of repair proteins to the site of the break (Burma et al., 2001), (Paull et al., 2000). Phosphorylation of H2AX has also been shown to occur when stress-induced chromatin re-organisation takes place i.e. often without DNA breaks (Ichijima et al., 2005). In contrast, the comet assay is a method which directly measures multiple types of DNA lesions, such as single and double strand breaks, incomplete excision repair sites and cross-links (Rich et al., 2013).

In summary, the data presented in this chapter suggests that both SDFT and DDFT equine tendon fibroblasts are susceptible to replication induced cellular injury in cell culture and this in turn could lead to rapid phenotypic drift, slow growth rates, premature senescence (Yao et al., 2006b), (Zhang and Wang, 2010), (Tsai et al., 2011). Genotoxic stress in tendon fibroblasts also gave rise to a number of phenotypes including micronuclei, stabilised p53 and binucleation. Tendon fibroblasts are commonly expanded in vitro to increase the yield of tendon fibroblast-like cells for investigative purposes (Durgam et al., 2011), (Taylor et al., 2009). Early passage cells with high levels of DNA damage would not be suitable for experimental purposes and further investigation will be required to find the most appropriate culture conditions for growing tendon fibroblasts in vitro (Rich et al., 2013). Finally, the SDFT and DDFT fibroblasts exhibited comparable repair capacities. This suggests the SDFT does not have any deficiency in the repair of genotoxic DNA lesions.

Chapter 4) Heat Shock Protein-72 and thermotolerance in tenocytes

4.1 Introduction

Tenocytes are tendon fibroblasts responsible for the synthesis, degradation, turnover and repair of the collagen rich tendon extracellular matrix. Tendons are sparsely populated with less than 300 tenocytes per mm² in the SDFT. A range of exercise-associated factors including tendon core hyperthermia is known to have detrimental effects on tendon fibroblasts by directly or indirectly causing cell death and/or cellular dysfunction (Wilson and Goodship, 1994), (Farris et al., 2011), (Millar et al., 2012), (Leadbetter, 1992), (Patterson-Kane et al., 1997b), (Maffulli et al., 2000), (Pearce et al., 2009), (Flick et al., 2006), (Jones et al., 2006). Loss of tenocytes in a sparsely populated tendon as a result of hyperthermia (Stanley et al., 2007) would be predicted to have significant effects on the reparative and regenerative ability of energy storing tendons.

The SDFT acts as an energy storing tendon by converting both kinetic and potential energy into elastic energy during weight bearing associated deformation. This increases the efficiency of locomotion. Approximately 5% of elastic energy is lost as heat during elastic recoil of the tendon during exercise. Heat generated within the tendon is inefficiently dissipated due to its poor vascular supply resulting in temperatures as high as 45°C being recorded in the tendon core of the SDFT in the distal forelimbs of galloping racehorses (Wilson and Goodship, 1994), (Alexander, 2002). In contrast, the DDFT is not an energy storing tendon, does not experience the same strain values (percentage elongation) during exercise compared to the SDFT and as a consequence, is not believed to be exposed to hyperthermic temperatures during exercise. This has never been recorded in vivo, however.

Hyperthermic stress induces a variety of intracellular changes including membrane fluidisation, transient cell cycle arrest and a change in cell form manifested as rounding and shrinkage of cells caused by modifications in the cellular cytoskeleton (Balogh et al., 2005), (Luchetti et al., 2004), (Bellmann et al., 2010), (Gabai et al., 2000), (Zölzer and Streffer, 1995). One of the adaptive

cellular responses to stress is the production of heat shock proteins. These molecular chaperones aid in the refolding of damaged proteins and protect against Caspase dependent and independent cell death (Chow et al., 2009) (Gabai et al., 2000), (Jaattela et al., 1998). The production of inducible heat shock protein 72 has been shown in several studies to participate in the development of thermotolerance, a transient resistance to stress induced by prior exposure to heat or other stressors. This provides cells with a survival advantage against subsequent stresses, (Gabai et al., 2000), (Chow et al., 2009), (Cheng et al., 2011).

There are no published studies to date which have quantified how heat stress affects two biologically distinct equine tendons, the SDFT and DDFT e.g. the induction and kinetics of Hsp-72 protein are unknown. There may be differences between SDFT and DDFT fibroblasts in their ability to protect themselves from a damaging heat shock. As the SDFT is routinely exposed to elevated temperatures during high intensity exercise, it might be predicted that it may be preconditioned (thermotolerant) and therefore less sensitive to a subsequent lethal heat shock. Then again, the SDFT is notoriously injury prone which suggests that preconditioning may be inadequate in these cells.

Whilst thermal preconditioning is well-known to provide a survival advantage to cells prior to a lethal heat shock, it is not known whether thermotolerance can also be achieved using cooling methodologies in equine tendon fibroblasts e.g. a preconditioned cold shock prior to a lethal heat shock. Cooling of IMR-90 human diploid lung fibroblasts and other cell types such as neonatal rat cardiomyocytes has been shown to induce heat shock protein 72 in the recovery phase following cold shock, however there was no data on whether there was up-regulation of Hsp-72 during cold shock itself (Liu et al., 1994), (Laios et al., 1997). Roobol and coworkers demonstrated that Hsp-72 induction was not detectable in CHO-K1 (Chinese Hamster ovary) cells during cold shock or its recovery (Roobol et al., 2009). There may be species specific differences in Hsp-72 induction during cold shock and recovery. No data exists on whether Hsp-72 induction takes place during cold shock in equine tendon fibroblasts.

Another reason for the poor induction of Hsp-72 during cold shock and recovery may be due to the suppression of protein translation during cold shock

which therefore limits the production of de-novo heat shock proteins. Cells generally respond to moderate hypothermia (25°C-35°C) by suppressing protein transcription and translation, reducing the metabolic rate in addition to inhibition of ATP expenditure and consequent reduction in oxygen free radicals (Al-Fageeh and Smales, 2006), (Neutelings et al., 2013). One of the survival mechanisms cells employ during cooling is up-regulation of RBM3 (RNA binding motif protein 3), a cold-shock inducible protein which has the ability to enhance the translation of certain proteins (Dresios et al., 2005), (Pilotte et al., 2011). Maximal levels of RBM3 mRNA production at moderate hypothermia (32°C) has been shown to occur at 18hrs of cooling in NC65 cells (human renal carcinoma cell line) which suggests that there may also be a time-dependent effect of de-novo protein synthesis (Danno et al., 1997).

The up-regulation of RBM3 mRNA was shown to occur in murine organotypic hippocampal slice cultures following exposure to moderate hypothermia at 32°C but not severe hypothermia at 17°C. An increase in PI (propidium iodide), a marker of cell death was visible in brain sections cooled at 17°C for 24hrs which implies RBM3 may provide an important survival advantage in cells exposed to cold shock (Tong et al., 2013).

Investigation into therapeutic hypothermia has been carried out in areas of cardiology and neurology, for example in the treatment of strokes aiming to reduce infarct size caused by ischaemia (Shintani et al., 2011). Recent studies have shown that cold-shock induced neuroprotection from ischaemic injuries to the brain was only instituted after prolonged periods of cooling (24hrs hypothermia) (Shintani et al., 2011), (Maier et al., 2001) (Colbourne et al., 2000).

Ice is commonly used to treat equine SDFT lesions to provide analgesia and reduce swelling and inflammation of the tendon (Petrov et al., 2003). Ice may be used to induce thermotolerance in the SDFT to aid in the protection of tendon fibroblasts against various exercise-associated stresses including hyperthermia. As neuroprotection associated with cold shock has been shown to occur only with prolonged periods of cooling in rats (Shintani et al., 2011), it might be predicted that the induction of thermotolerance in equine tendon

fibroblasts would only occur following a long pre-conditioned exposure to cold shock i.e. greater than 24hrs.

The aims of the work in this chapter were:

- 1) To determine the levels of induction and kinetics of Hsp-72 and RBM3 expression in SDFT and DDFT fibroblasts following heat shock and cold shock. The SDFT was hypothesised to have a faster induction of Hsp-72 protein in response to heat and cold shock as it is regularly exposed to heat stress in vivo and in contrast, the DDFT is not.
- 2) To quantify cell death in SDFT and DDFT fibroblasts when exposed to a lethal heat shock at 52°C. As the SDFT is routinely exposed to heat stress in vivo, it was predicted the percentage of cell death would be less in comparison with the DDFT.
- 3) To determine whether a pre-conditioning episode of heating at 47°C or cooling at 26°C can provide a survival advantage when tendon fibroblasts are exposed to a lethal heat shock. It was hypothesised that only a pre-conditioned heat shock and not a pre-conditioned cold shock would protect SDFT and DDFT fibroblasts from a lethal heat shock.

4.2 Results

4.2.1 The tendon of origin and the Hsp-72 expression pattern associated with heating

One of the aims of the work described in this chapter was to investigate the induction and kinetics of Hsp-72 expression in the SDFT and the DDFT. In vivo work completed in the SDFT tendon by Wilson and Goodship in 1994 showed the mean peak temperature rise in the central core of the tendon was 43.3°C and the highest temperature recorded in one horse was 45.4°C. No data exists on whether a similar temperature rise occurs in the DDFT, although it would not be expected to be as high because this tendon does not act as a “biological spring”. Approximately 5% of the SDFT tendon’s elastic energy is lost as heat which is dissipated in the tendon core during exercise (Alexander, 2002).

To determine the expression of Hsp-72 protein at 43°C, the average temperature experienced in the SDFT, both SDFT and DDFT derived fibroblasts were enzymatically retrieved from the tendon core and passage 3 (P3) cells were heated to 43°C for 15 mins followed by recovery at 37°C. A western blot was used to assess the expression of Hsp-72 protein over 72hrs of recovery. All experiments were retrieved from one horse and conducted in triplicate. All three replicates for this experiment are shown in Figure 4-5. When the western blots were completed, little to no protein expression was present in the control lysates. The pattern of Hsp-72 induction over 72hrs of recovery at 37°C was achieved by comparison with the first heated sample at 1hr of recovery.

Tendon dependent differences in the expression of Hsp-72 were identified when SDFT fibroblasts were heated to 43°C for 15 mins. At 43°C, the DDFT derived fibroblasts did not induce Hsp-72 expression regardless of the length of recovery time at 37°C (Figure 4-1). In contrast, there was induction of Hsp-72 from 4hrs post heating at 43°C in the SDFT with the expression levels remaining high for a further 72hrs post heating (Figure 4-2).

To determine whether the induction pattern of Hsp-72 was similar in both tendons when a higher temperature was used, SDFT and DDFT fibroblasts were heated to 47°C for 15 mins. At this temperature, both the SDFT and the DDFT expressed increased Hsp-72 levels at 4hrs post heating and the Hsp-72 protein

levels remained elevated for a further 72hrs (Figure 4-3 and Figure 4-4 respectively).

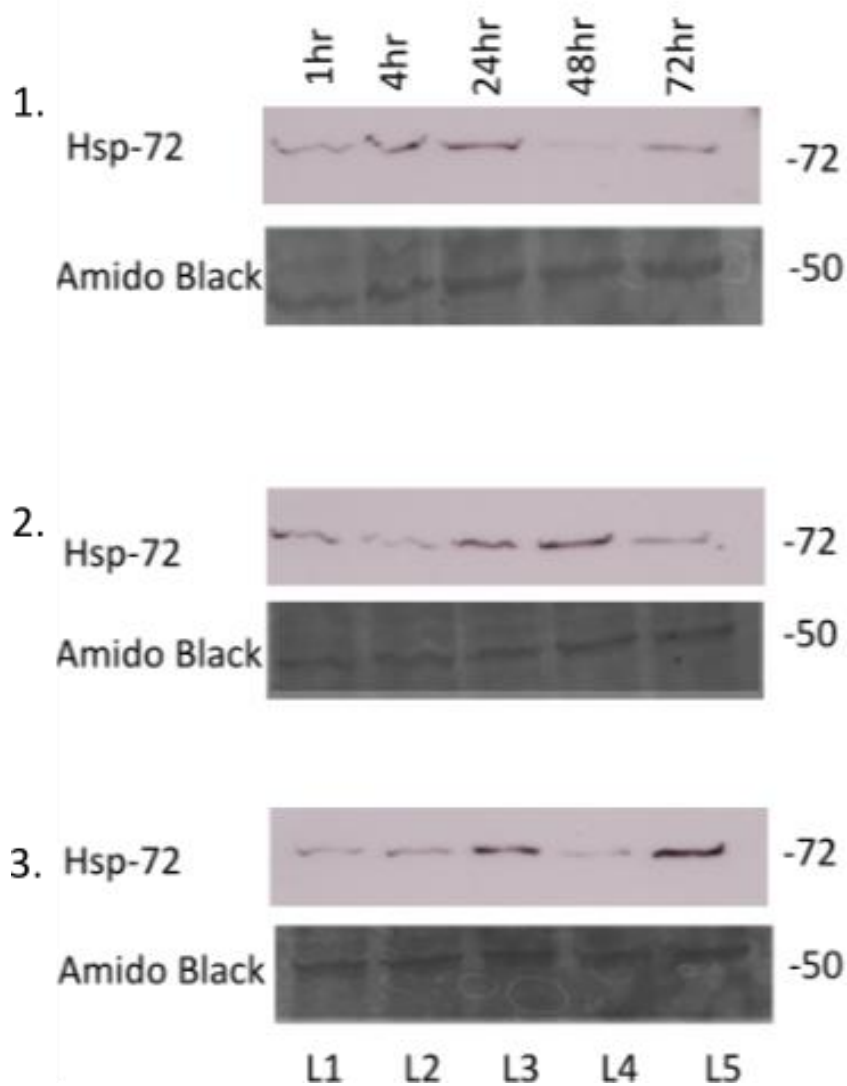


Figure 4-1. The expression of Hsp-72 protein in DDFT fibroblasts heated to 43°C.

DDFT fibroblasts were heated at 43°C for 15 mins and then recovered at 37°C for 1hr, 4hr, 24hr, 48hr and 72hrs. A western blot was created from the heated lysates at each of the recovery times and immunostained for Hsp-72 protein (72kDa). The same amount of protein (20µg) was loaded into each lane. This experiment was taken from one horse and repeated in triplicate.

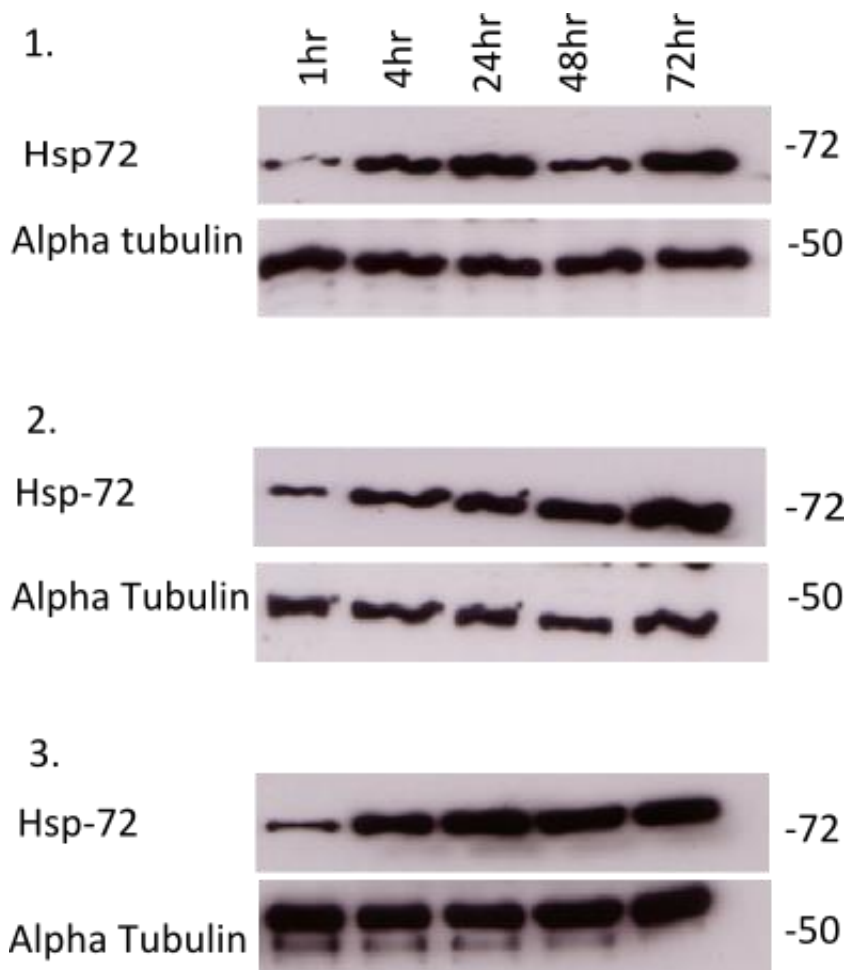


Figure 4-2. The expression of Hsp-72 in SDFT fibroblasts heated to 43°C

SDFT fibroblasts were heated at 43°C for 15 mins and then recovered at 37°C for 1hr, 4hr, 24hr, 48hr and 72hrs. A western blot was created from the heated lysates at each of the recovery times and immunostained for Hsp-72 protein (72kDa). The same amount of protein (20µg) was loaded into each lane. This experiment was taken from one horse (the same horse as for the SDFT) and repeated in triplicate.

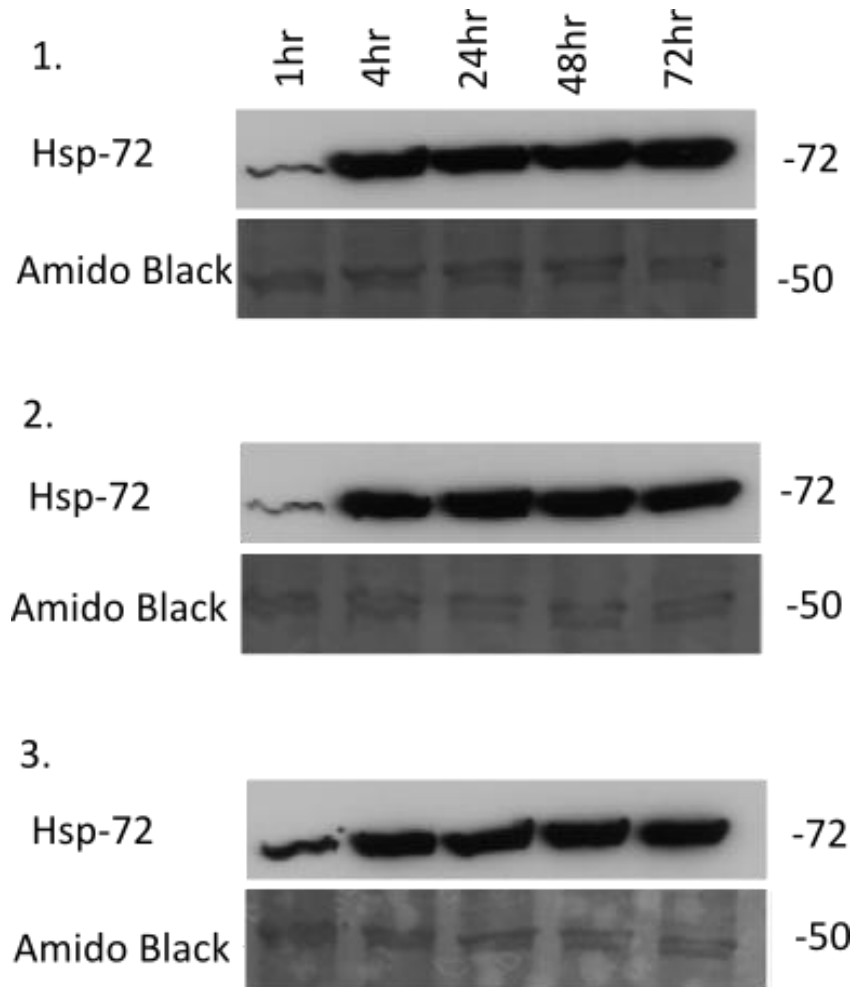


Figure 4-3. The expression of Hsp-72 in SDFT fibroblasts when heated to 47°C

SDFT fibroblasts were heated at 47°C for 15 mins and then recovered at 37°C for 1hr, 4hr, 24hr, 48hr and 72hrs. A western blot was created from the heated lysates at each of the recovery times and immunostained for Hsp-72 protein (72kDa). The same amount of protein (20µg) was loaded into each lane. This experiment was taken from one horse (the same horse as for the above experiments) and repeated in triplicate.

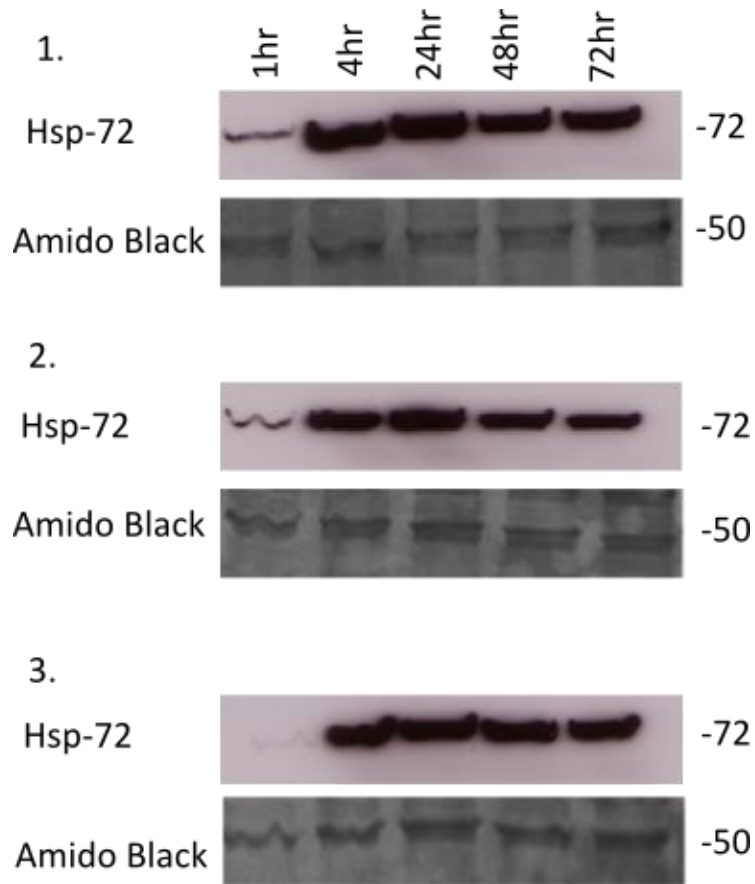


Figure 4-4. The expression of Hsp-72 protein in DDFT fibroblasts exposed to 47°C

DDFT fibroblasts were heated at 47°C for 15 mins and then recovered at 37°C for 1hr, 4hr, 24hr, 48hr and 72hrs. A western blot was created from the heated lysates at each of the recovery times and immunostained for Hsp-72 protein (72kDa). The same amount of protein (20µg) was loaded into each lane. This experiment was taken from one horse (the same horse as for the above experiments) and repeated in triplicate.

4.2.2 The tendon of origin and the Hsp-72 expression pattern associated with cooling

No data exists on whether equine tendon fibroblasts are able to express Hsp-72 during cold shock or its recovery. Previous studies have shown poor induction of Hsp-72 with cold shock in comparison with heat shock in rat cardiomyocytes and CHOK1 cells (Laios et al., 1997), (Roobol et al., 2009). Protein transcription and translation are thought to be suppressed with cold shock, therefore it is possible that longer exposure to cold shock may be required for Hsp-72 production to occur. For this reason, during the investigation of Hsp-72 expression with cold shock in equine tendon fibroblasts, a period of up to 72hrs was chosen.

To investigate whether Hsp-72 could be induced during a period of cold shock with no recovery, P3 SDFT and DDFT derived fibroblasts were continuously chilled at 26°C for 72hrs in a gassed incubator. A western blot was used to examine the expression of Hsp-72 at 1hr, 4hrs, 24hrs, 48hrs and 72hrs of cooling. There was induction of Hsp-72 at 4hrs of cooling for the SDFT followed by a sudden increase in the expression of Hsp-72 at 72hrs of cooling (Figure 4-5). In the DDFT, the induction of Hsp-72 expression was much later, starting at 48hrs of cold shock. (Figure 4-6). No cell death was visualised at any of the cold shock time points, as there was no significant irreversible cell detachment or any of the morphological features of cell death including shrinkage of cells or pyknotic nuclei.

To determine whether there was a similar induction pattern of Hsp-72 expression when a recovery period was given after cold shock, SDFT and DDFT derived fibroblasts were chilled at 26°C for 1 hr or 4hrs or 16hrs then allowed to recover at 37°C for 72hrs. When the SDFT fibroblasts were chilled for 1hr at 26°C and the cells recovered, significant Hsp-72 induction occurred at from 1-4hrs post cooling and the levels remained high for a further 72hrs (Figure 4-7). When 4hrs of cold shock at 26°C was administered to SDFT derived fibroblasts and the cells recovered, there was no increase in Hsp-72 expression levels with recovery i.e. Hsp-72 levels remained high throughout the recovery period and were already expressed at 4hrs of recovery (Figure 4-8).

In comparison to the SDFT, there was delayed Hsp-72 expression for DDFT fibroblasts exposed to 1hr or 4hrs of cold shock at 26°C followed by recovery (Figure 4-9 and Figure 4-10 respectively). The expression of Hsp-72 protein in DDFT fibroblasts was not seen until 48-72hrs post cooling. In contrast, there was no Hsp-72 induction when either the SDFT or the DDFT were chilled at 26°C for 16hrs followed by 72hrs at 37°C (Figure 4-11 and Figure 4-12 respectively). High levels of Hsp-72 levels were present in the early recovery period which indicates that the levels of Hsp-72 may have already reached a plateau which was then maintained throughout the entire recovery period. For SDFT fibroblasts, it was noted there was a reduction in the Hsp-72 levels at 72hrs of recovery which suggests the SDFT may have recovered from cold shock by this point in time.

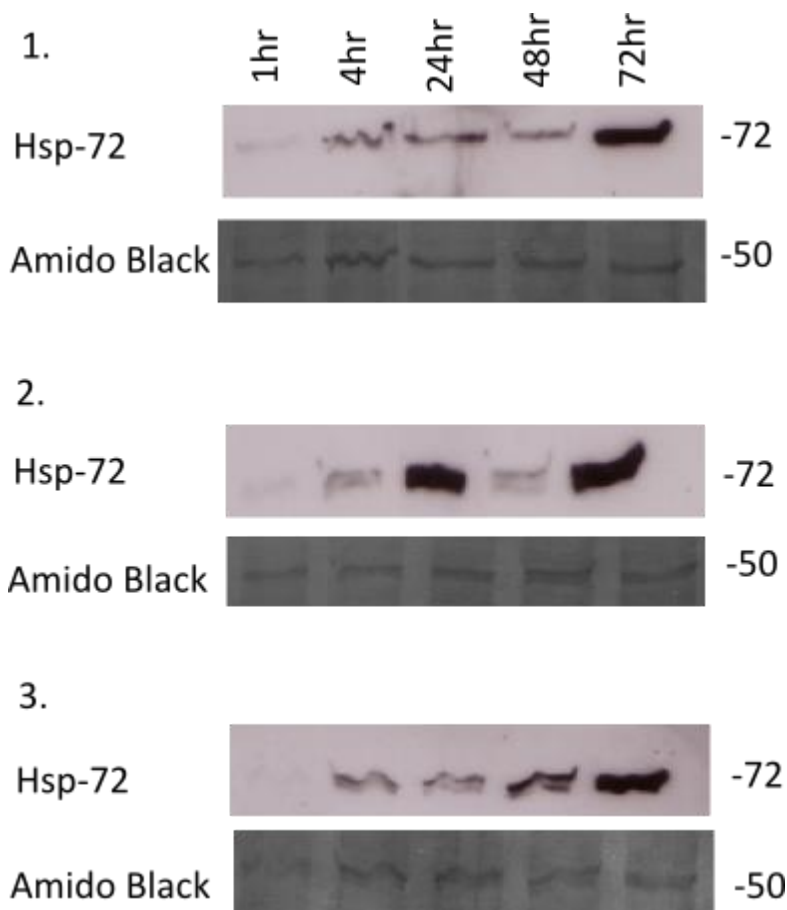


Figure 4-5. The expression of Hsp-72 protein in SDFT fibroblasts cooled at 26°C continuously for 72hrs.

SDFT fibroblasts were exposed to 26°C continuously for 72hrs. A western blot was created from cooled lysates at 1hr, 4hr, 24hr, 48hr and 72hrs and then immunostained for Hsp-72 protein (72kDa). All data was retrieved from one horse (same as for above experiments) and experiments repeated in triplicate. Amido Black was used as a loading control.

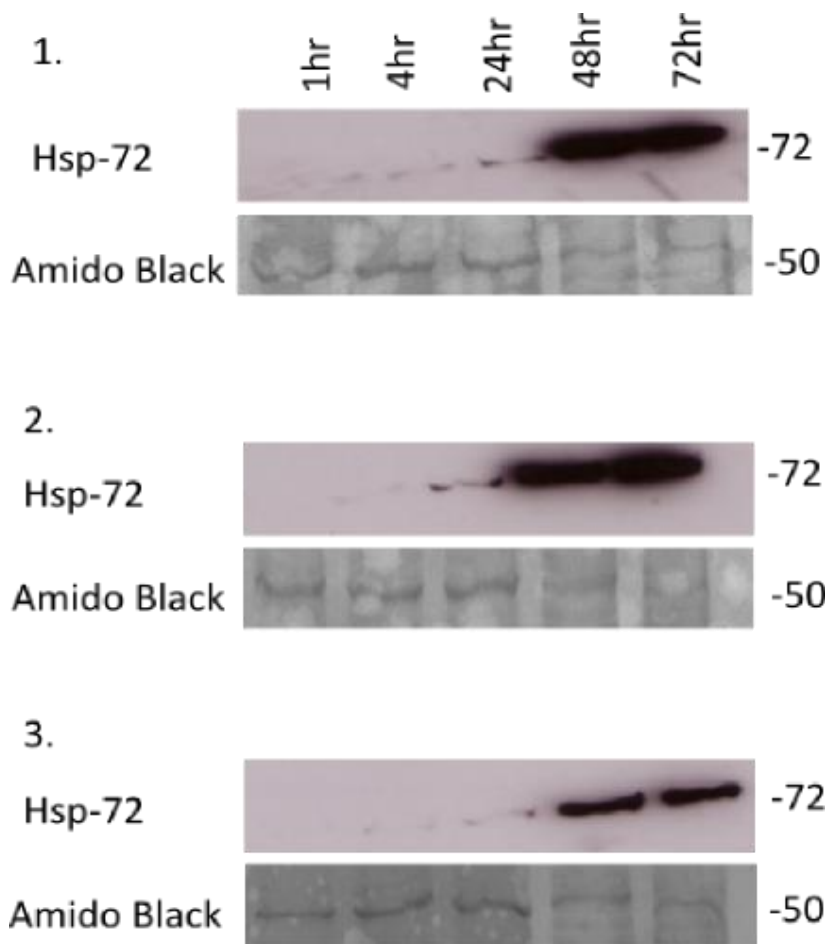


Figure 4-6. The expression of Hsp-72 in DDFT fibroblasts cooled continuously at 26°C for 72hrs.

DDFT fibroblasts were exposed to 26°C continuously for 72hrs. A western blot was created from cooled lysates at 1hr, 4hr, 24hr, 48hr and 72hrs and then immunostained for Hsp-72 protein (72kDa). All data was retrieved from one horse (same as for above experiments) and experiments repeated in triplicate. Amido Black was used as a loading control.

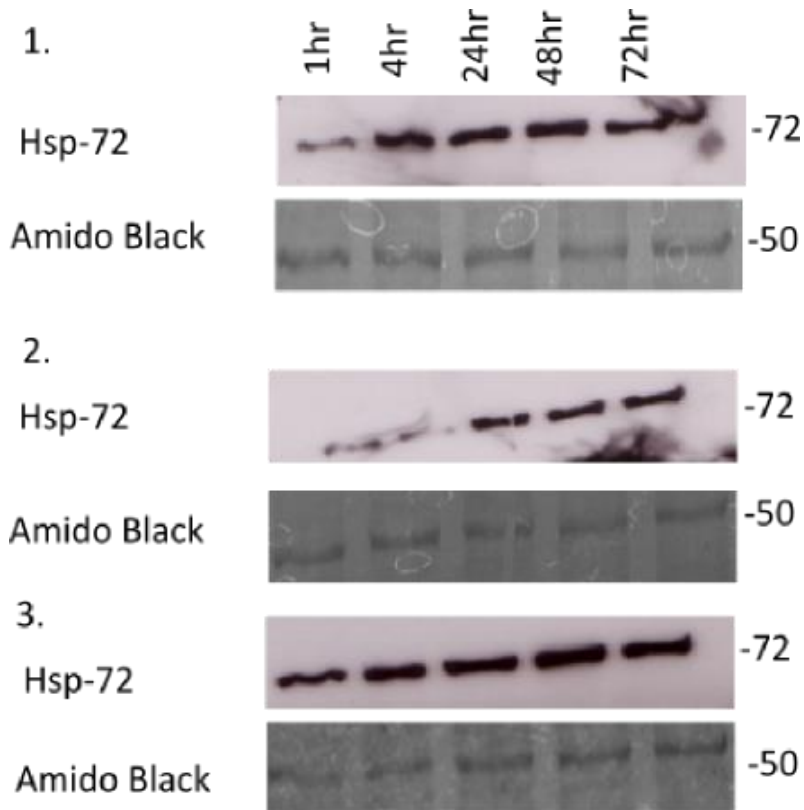


Figure 4-7. The expression of Hsp-72 protein in SDFT fibroblasts given 1hr of cold shock at 26°C followed by 72hrs of recovery at 37°C

Following the exposure of SDFT fibroblasts to 1hr of cold shock at 26°C, the fibroblasts were recovered for 1hr, 4hr, 24hr, 48hr and 72hrs at 37°C. A western blot was created from lysates generated at each of the recovery time points. All data was retrieved from one horse (as above) and repeated in triplicate. Amido Black was used as a loading control.

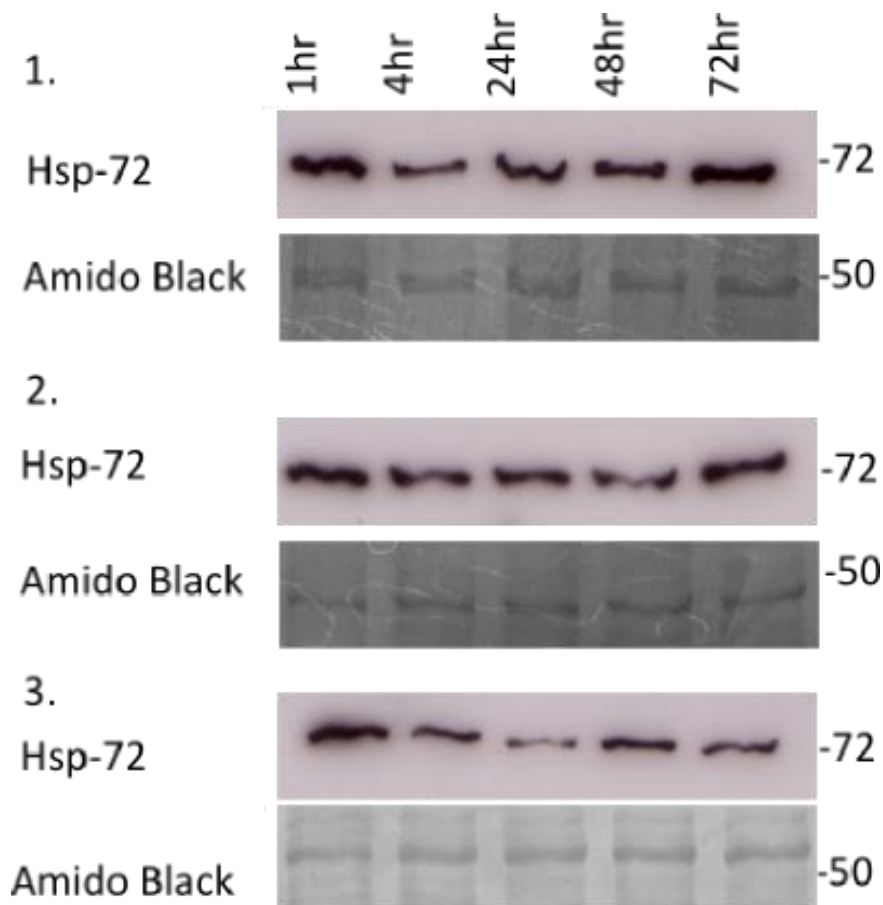


Figure 4-8. The expression of Hsp-72 protein in SDFT fibroblasts cold shocked at 26°C for 4hrs followed by recovery at 37°C

Following the exposure of SDFT fibroblasts to 4hr of cold shock at 26°C, the fibroblasts were recovered for 1hr, 4hr, 24hr, 48hr and 72hrs at 37°C. A western blot was created from lysates generated at each of the recovery time points. All data was retrieved from one horse (as above) and repeated in triplicate. Amido Black was used as a loading control.

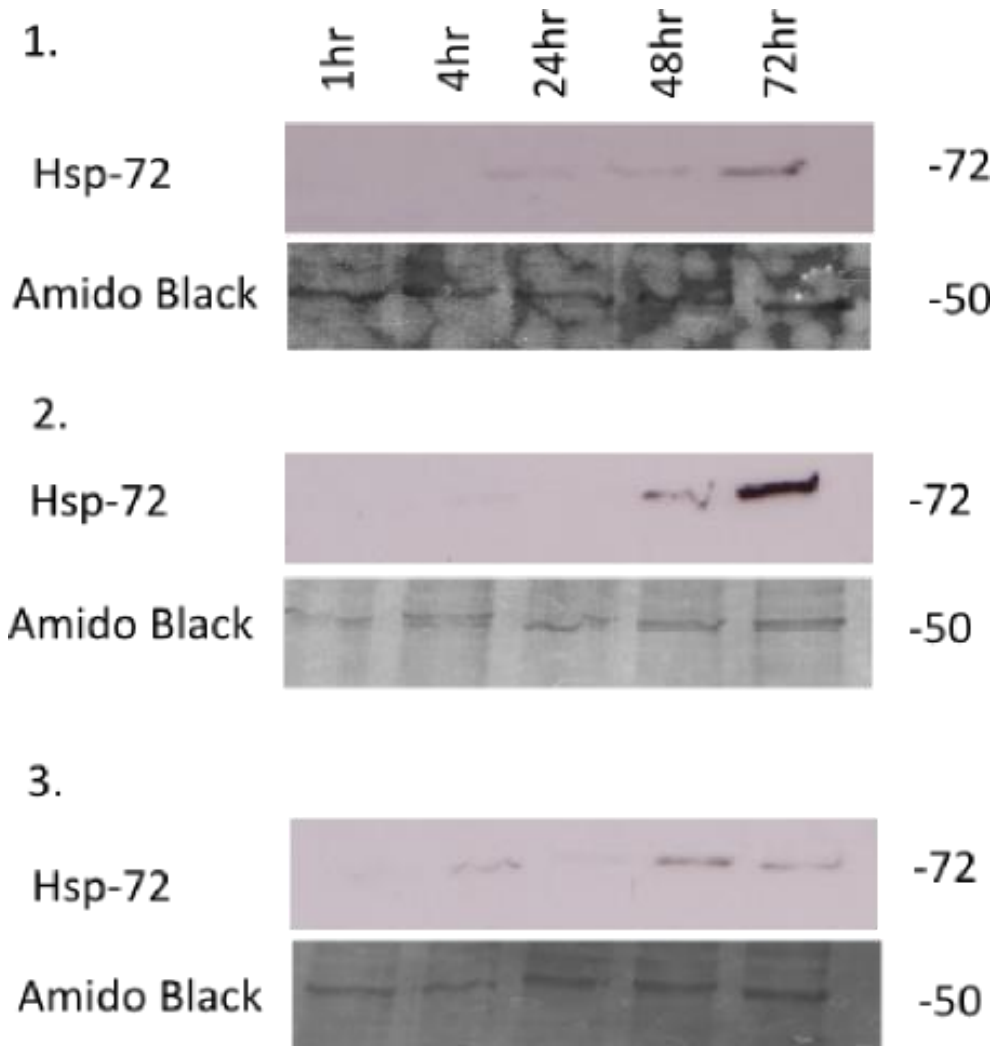


Figure 4-9. The expression of Hsp-72 protein in DDFT fibroblasts exposed to 1hr of cold shock at 26°C followed by recovery at 37°C

Following the exposure of DDFT fibroblasts to 1hr of cold shock at 26°C, the fibroblasts were recovered for 1hr, 4hr, 24hr, 48hr and 72hrs at 37°C. A western blot was created from lysates generated at each of the recovery time points. All data was retrieved from one horse (as above) and repeated in triplicate. Amido Black was used as a loading control.

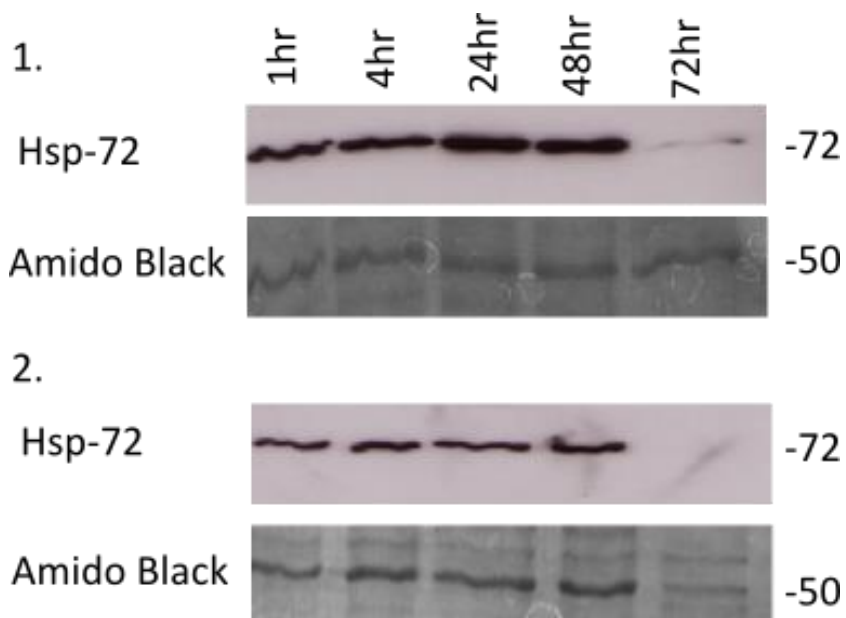


Figure 4-11. The expression of Hsp-72 protein in SDFT fibroblasts following an overnight cold shock at 26°C followed by recovery at 37°C

SDFT fibroblasts were exposed to 26°C overnight in a gassed incubator then left to recover at 37°C for 1hr, 4hr, 24hr, 48hr and 72hrs. A western blot was created from lysates generated at each of the recovery time points. All data was retrieved from one horse (as above) and repeated in duplicate (The third blot and control for this experiment were too smudged for use and therefore were omitted). Amido Black was used as a loading control.

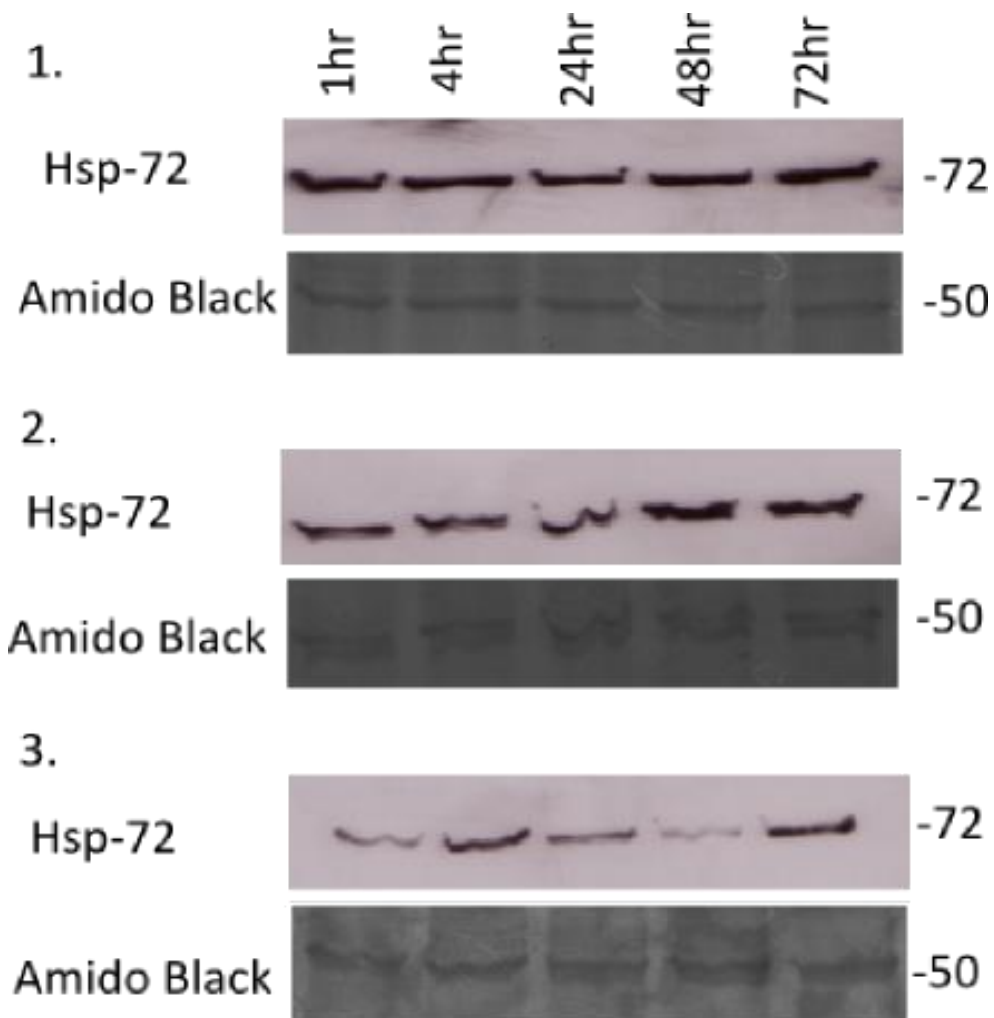


Figure 4-12. The expression of Hsp-72 protein in DDFT fibroblasts exposed to 26°C overnight then recovered at 37°C.

DDFT fibroblasts were exposed to 26°C overnight in a gassed incubator then left to recover at 37°C for 1hr, 4hr, 24hr, 48hr and 72hrs. A western blot was created from lysates generated at each of the recovery time points. All data was retrieved from one horse (as above) and repeated in triplicate. Amido Black was used as a loading control.

4.2.3 The expression of the cold-shock protein, RBM3 in heated and chilled equine tendon fibroblasts

To determine the pattern of RBM3 induction in equine tendon fibroblasts, P3 SDFT monolayers were chilled continuously at either 26°C or 32°C in a water bath for up to 72hrs. At 1hr, 4hr, 24hrs, 48hrs and 72hrs of cooling, the SDFT fibroblasts were stained for anti-RBM3 antibody by immunocytochemistry. Two hypothermic temperatures were chosen for this experiment to determine if there would be any differences in the expression of RBM3 at the lower (26°C) and upper (32°C) ends of the moderate hypothermic temperature range. It was predicted that higher expression levels of RBM3 would be produced at a lower temperature (26°C) in equine tendon fibroblasts. A water bath was used for these experiments as rapid temperature changes were not required (i.e. from 37°C to 43°C in 15 mins as required in the heating experiments) and the cells could be fixed and stained for RBM3 straight from the water bath. To determine whether the expression of RBM3 was significantly higher with cold shock in comparison with the control (cells maintained at 37°C), the Kruskal-Wallis non-parametric test was employed.

The expression patterns for RBM3 at two mild cold shock temperatures were different. At 32°C, the expression of RBM3 was biphasic. In the first hour of cooling there was a significant increase in the expression of RBM3 from control values (P-value: <0.05) and this was followed by a steep decrease in the expression of RBM3 at 4hrs of cooling. The second increase in RBM3 expression occurred at 24hrs of cooling and was significantly higher than the control (P-value: <0.05). After 24hrs the expression of RBM3 decreased again (Figure 4-13A).

In contrast, when SDFT derived fibroblasts were chilled at 26°C continuously, RBM3 expression increased gradually from 1hr to 48hrs of cooling, followed by a decrease by 72hrs of cooling (Figure 4-13B) With the exception of the first hour, the expression levels of RBM3 during cold shock at 26°C were significantly higher than the control levels.

To investigate whether RBM3 was induced with heating as well as cooling, SDFT fibroblasts were heated at 43°C for 15 mins followed by recovery at 37°C

for 72hrs. The expression of RBM3 at this temperature was also biphasic, with expression peaks at 4hr and 48hrs post heating. Maximal expression of RBM3 occurred at 48hrs post heating (Figure 4-13C). The expression of RBM3 was significantly higher at 4hrs, 48hrs and 72hrs of cooling in comparison with the control.

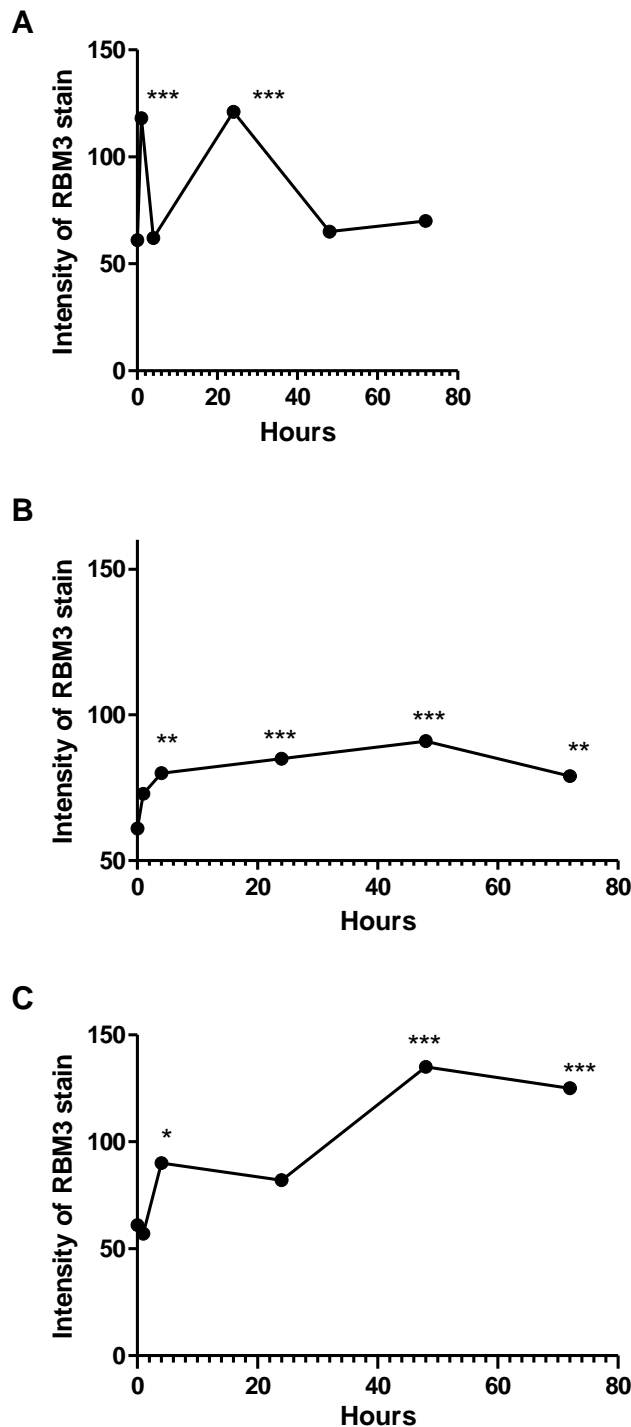


Figure 4-13. The pattern of RBM3 expression with heating and cooling in SDFT fibroblasts

SDFT fibroblasts were chilled continuously at 32°C (graph A) or 26°C (graph B) for 1hr, 4hr, 24hr, 48hr and 72hrs in the water bath. Another group of SDFT fibroblasts (graph C) were heated at 43°C for 15 mins then given 1hr, 4hr, 24hr, 48hr and 72hrs recovery at 37°C. Control cells were maintained at 37°C. The cells were immunostained for RBM3 at each of the cooling times (or recovery times for heat shock) and the mean expression levels of RBM3 were measured from 20 cells for each time point. All data were retrieved from one horse. Kruskal Wallis was used to determine any significant differences in RBM3 expression between cold shock (or heat shock recovered cells) and the control. Error bars represent the standard error. Stars represent P-value: <0.05).

4.2.4 Choosing a lethal temperature for SDFT and DDFT fibroblasts

One of the main focuses of the work in this chapter was to investigate whether SDFT and DDFT fibroblasts can be protected from a lethal heat stimulus using either a preconditioned heat or cold shock. Prior to this investigation, we had to determine the lethal temperature resulting in significant cell death in the equine tendon fibroblast monolayers. A number of assays were trialled to quantify cell death in equine tendon fibroblasts. Hyperthermia is a well-known inducer of apoptosis (Bellmann et al., 2010), (Chow et al., 2009), (Mosser and Martin, 1992) resulting in morphological changes such as reduction in cell size, condensed chromatin and fragmented nuclei (Mosser and Martin, 1992).

Caspase-3 is one of the major executioners responsible for driving apoptotic cell death as it activates various proteases such as CAD (Caspase-activated deoxyribonuclease) which breaks down chromosomal DNA resulting in chromatin condensation (Sakahira et al., 1998). To determine whether there was cross-reactivity of two anti- cleaved human Caspase-3 antibodies from R&D Systems and Cell Signalling (which specifically recognises the amino acid residues at 165-175 in human Caspase-3) with equine tendon fibroblasts, a western blot was carried out. These two antibodies worked well when used with human L540 cells (Hodgkin lymphoma cell line) but in contrast, did not work in equine SDFT fibroblasts. The SDFT fibroblasts were treated with a range of drugs known to induce cellular apoptosis including staurosporine, a competitive protein kinase inhibitor which binds to the ATP components of protein kinases resulting in inhibition of enzymatic activity (Prade et al., 1997) and etoposide, a drug causing DNA breaks by inhibiting topoisomerase II associated re-ligation of DNA strands (Muslimović et al., 2009). Following treatment with the drugs, the equine tendon fibroblasts displayed features of apoptotic cell death as there was cell shrinkage, pyknotic nuclei and permanent cell detachment. No visible protein bands were seen on the resultant western blot (Figure 4-14). There is a single amino acid difference when comparing the peptide epitope in human and equine Caspase-3 (Figure 4-15). This single difference may be the cause of the epitope not being conserved between species.

Upon the activation of apoptosis, the inactive pro-Caspase-3 is cleaved into the large (17kDa) and small (12kDa) fragments of active Caspase-3 respectively (Nicholson et al., 1995). Human L540 cells were used as a positive control for the detection of the cleaved Caspase-3. In this cell line, the larger cleaved fragment of Caspase-3 is constitutively expressed and cell death is prevented by continual proteolysis of the smaller fragment. Upon the induction of apoptosis in L540 cells, treated cells contain both the larger and smaller fragments of Caspase-3. When two apoptotic drugs, etoposide and bortezomib, (a proteasomal inhibitor which leads to the build-up of aggregated proteins in cells leading to cell death) were used in L540 cells there was a strong apoptotic response. This was verified by seeing both the larger and smaller fragments of cleaved Caspase-3 in the western blot (Figure 4-14).

As there was poor cross-reactivity of anti-cleaved Caspase-3 antibodies in equine cells, other methods were used to measure apoptosis. Externalisation of the phosphatidylserine residues on the outer plasma membrane is a classic feature of apoptosis and can be detected using Annexin V in cultured cells (Bratton et al., 1997). Annexin V-FITC worked well in SDFT tendon fibroblasts using immunocytochemistry, however the membrane permeant nucleic acid dye, propidium iodide, a marker for the detection of non-viable cells worked poorly and bleached rapidly when attempting quantification of the number of positive cells during fluorescence microscopy in these cells.

Thermal stress can induce alterations in cellular morphology characterised by rounding and shrinkage of the cells as a result of modifications to the cytoskeleton. Restoration of normal cellular morphology can occur following exposure to heat stress, but if temperature magnitude and/or duration is lethal, it will result in permanent cell detachment (Luchetti et al., 2004), (Coss et al., 1996). As cell rounding and detachment was a consistent event in both SDFT and DDFT tenocytes following heating, these morphological features were used to measure sensitivity to heat. An advantage of using this method for detecting cell death was that there was no presumption on the mechanism of cell death taking place.

P3 SDFT fibroblasts were cultured on collagen coated matrices until confluent to minimise replication induced DNA damage in the tendon

monolayers. When these cells were heated at 43°C for 15 mins on the Cell MicroControls heating apparatus, there were minimal effects on the cell morphology of SDFT monolayers. Only small numbers of rounded up cells were visible at 24hrs post heating as seen by the presence of bright refractile bodies in the monolayers (Figure 4-16). These bodies may represent replicating cells undergoing the process of mitosis and have 'lifted' from the plate during this time.

Higher temperatures were employed to determine the "lethal" temperature where cells would permanently detach from the cell surface. When SDFT fibroblasts were heated to 47°C and 49°C for 15 mins, small numbers of rounded up cells were attached to the cell surface at 1hr and 4hrs post heating. Recovery from heat shock at these temperatures was rapid as there were few rounded up cells present at 24hrs post heating (Figure 4-16).

At 52°C, the cells showed more pronounced hyperthermia-related changes such as marked cell shrinkage, distortion of cell shape and blebbing. There were numerous refractile rounded up cell bodies throughout the entire recovery period. There was also evidence of cells detaching permanently from the dish as the number of cells with normal fibroblast-like morphology was fewer with increasing length of recovery time (Figure 4-16).

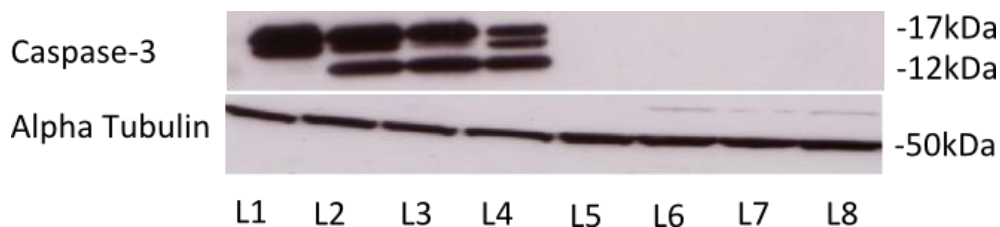


Figure 4-14. Two anti-Caspase-3 antibodies from Cell Signalling and R and D Systems did not detect cleaved equine Caspase-3

To determine whether Caspase-3 antibodies from Cell Signalling and R and D Systems cross-react with equine SDFT fibroblasts, a range of overnight drug treatments were used to induce cell death in both SDFT fibroblasts and L540 cells, a human Hodgkin lymphoma cell line (positive control). Lane 1 represents control L540 cells (no drug treatment). The larger cleaved fragment (17kDa) of Caspase-3 is constitutively expressed in these cells. L540 cells were given 0.1 μ g/ml etoposide (Lane 2), 0.5 μ g/ml etoposide (Lane 3) and 5nM bortezomib (Lane 4). The treated L540 cells have two cleaved fragments of Caspase-3 (17kDa) and (12kDa). Lane 5 represents control equine SDFT fibroblasts (no treatment). For the equine SDFT cells, a higher concentration of etoposide was used to induce cell death at 20 μ g/ml (Lane 6). In addition to this, 0.5 μ M (Lane 7) and 1.0 μ M staurosporine (Lane 8) were also used. No cleaved Caspase-3 fragments were detected in equine SDFT fibroblasts. Alpha Tubulin (50kDa) was used as a protein loading control.

```

Human (CAC88866.1)    MENTENSVDSKSIKNLEPKIIHGSESMDSGMSWDTGYKMDYPEMGLCIII 50
Horse (NP_001157433.1) MENSKISVDSKSIKNSETKILHGSKSMDSGISLDSSYKMDYPEMGLCIII 50

Human (CAC88866.1)    NNKNFHKSTGMTSRSGTDVDAANLRETFRNLYEVRNKNDLTREEIVELM 100
Horse (NP_001157433.1) NNKNFHKSTGMASRSGTDVDAANLRETFRNLYEVRNKNDLTGEEIVALM 100

Human (CAC88866.1)    RDVSKEDHSKRSSFVCLLSHGEEGIIFGTNGPVDLKKITNFFRGDRCRS 150
Horse (NP_001157433.1) RSVSKEDHSKRSSFICVLLSHGEEGIIFGTNGPIDLKKLTCFFKGDCCRS 150

Human (CAC88866.1)    LTGKPKLFIIQACRGTELDGIETD SGVDDDMACHKIPVDADFLYAYSTA 200
Horse (NP_001157433.1) LAGKPKLFIIQACRGTELDSGIETD SGIEDDMACQKIPVEADFLYAYSTA 200

Human (CAC88866.1)    PGYYSWRNSKDGSWFIQSLCAMLKQYADKLEFMHILTRVNRKVATEFESF 250
Horse (NP_001157433.1) PGYYSWRNSKDGSWFIQSLCAMLKLYAHKLELMHILTRVNRKVAMEFESY 250

Human (CAC88866.1)    SFDATFHAKKQIPCIVSMLTKELYFYH 277
Horse (NP_001157433.1) CLDPTFHGKKQIPCIVSMLTKELYFYH 277

```

Figure 4-15. Protein sequence similarity between equine and human Caspase-3

There is a single amino acid difference (highlighted in green) when comparing the peptide epitope 165-175 (red) in human and equine Caspase-3. The NCBI reference sequence code for the human and equine Caspase-3 protein has been outlined adjacent to the species of interest.

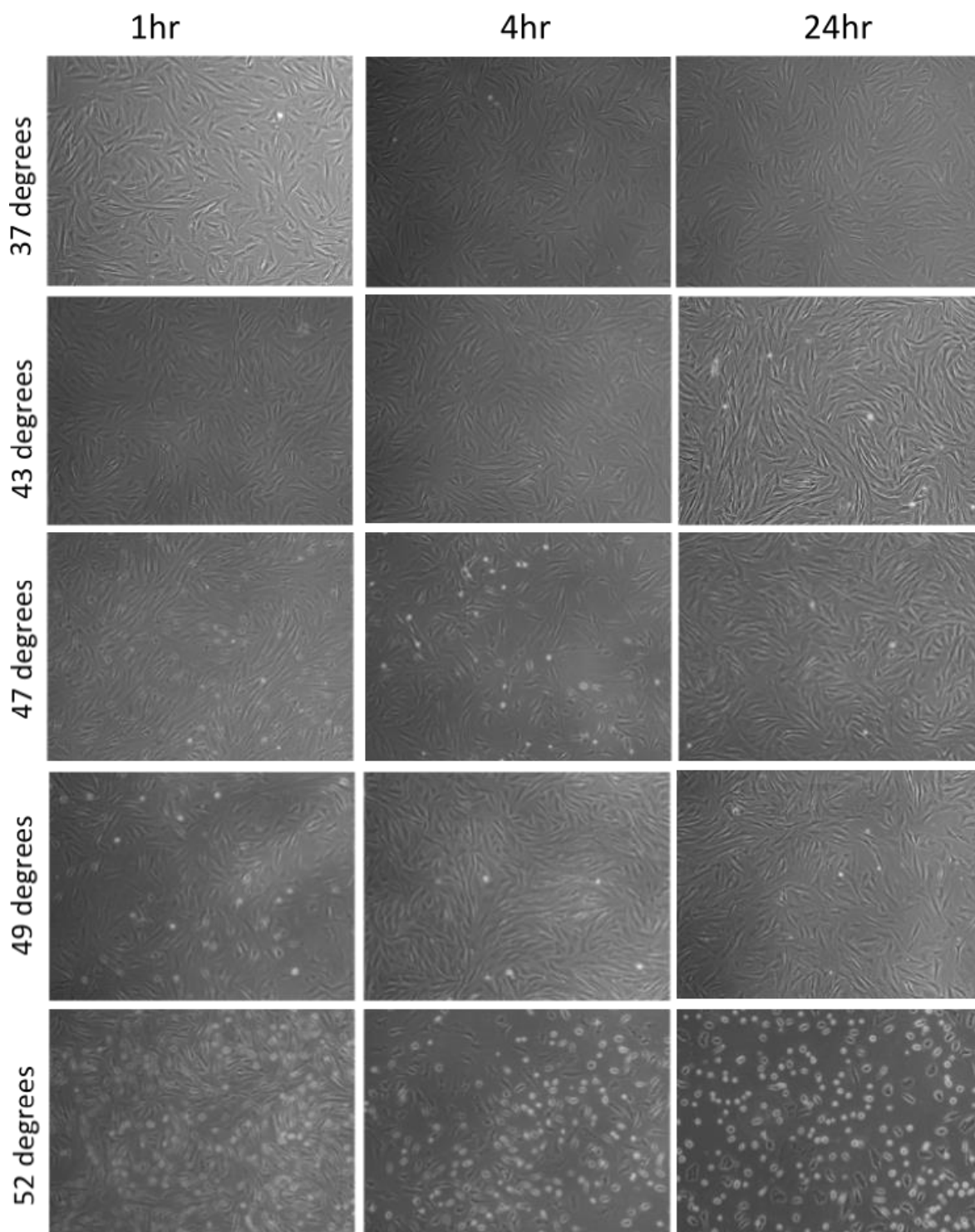


Figure 4-16. Differences in cellular morphology in SDFT fibroblasts according to temperature

SDFT fibroblasts were heated on the Cell MicroControls heating rig at 43°C, 47°C, 49°C and 52°C for 15 mins followed by recovery at 37°C for 1hr, 4hr and 24hrs. At each of the recovery times, the morphology of the cells was viewed with a phase contrast microscope at 10x magnification. Control cells were maintained at 37°C.

4.2.5 “Thermotolerance” associated with the heat shock response in SDFT and DDFT fibroblasts.

Thermotolerance is a well-known phenomenon which protects cells from a subsequent lethal shock and is dependent on the production of heat shock proteins (Chow et al., 2009), (Gabai et al., 2000). My previous set of experiments showed high levels of Hsp-72 protein at 4hrs post heating for both the SDFT and DDFT fibroblasts following exposure to 47°C for 15 mins. We predicted the induction of thermotolerance in the tendon fibroblasts at this time due to the high levels of Hsp-72 protein in these cells. Thus, for the pre-conditioned heat shock experiments, both the SDFT and DDFT fibroblasts were heated at 47°C for 15 mins followed by 4hrs of recovery at 37°C.

Quantification of the attached cell population following heat shock was a good indicator of cell loss as permanent cell detachment resulted in cell death. This was proved when the media containing detached cells (from a culture that had been heated up to 52°C) was re-plated onto a fresh cell culture dish and none of the detached cells re-attached to the cell surface (despite being left for up to a week).

P3 SDFT fibroblasts were cultured on collagen coated matrices until confluent. Unconditioned SDFT and DDFT fibroblasts were heated at a lethal temperature of 52°C for 15 mins followed by recovery at 37°C for 1hr, 4hr, 24hrs, 48hrs and 72hrs. A separate group of SDFT monolayers was pre-heat conditioned at 47°C for 15 mins (followed by 4hrs of recovery at 37°C) before being exposed to the lethal temperature as outlined above.

To determine whether thermal preconditioning was able to minimise cell death following a lethal heat shock in both SDFT and DDFT tendon fibroblasts, the percentage of viable, attached cells was quantified over a period of 72hrs after heating in preconditioned cultures and this was then compared with the unconditioned cultures. The percentage of attached positive trypan blue cells, a marker for the detection of non-viable cells was also calculated. Each experiment was done in triplicate and the data was comparable between experiments. A representative 2-D column graph showing the mean percentage

of attached cells and positive trypan blue cells over 72hrs of recovery time for both the unconditioned and preconditioned groups is shown in Figure 4-17.

When unconditioned SDFT derived fibroblasts were heated to 52°C for 15 mins, there was minimal cell loss in the first hour post heating. Although not significant, there was a decrease in the percentage of attached cells from approximately 100% to 72% in the first 4 hours post heating. Following this, the percentage of attached cells continued to significantly decrease for a further 72hrs post heating until only 15% of cells were still attached to the cell culture dish (Figure 4-17A).

When unconditioned DDFT fibroblasts were exposed to a lethal temperature, there was a similar pattern of cell loss to the SDFT. The percentage of attached cells decreased over time starting at 1hr post heating followed by a significant loss of cells after 24hrs of recovery time in comparison with the control (P-value: <0.001). The loss of cells in the DDFT cultures was not as great when compared with the SDFT for example, at 24hrs post heating there was 38% versus 61% of attached cells for the SDFT and DDFT respectively (Figure 4-17B). Sample size was small, so a larger number of animals would be required to determine whether there is a significant difference in the susceptibility of two different tendons to heat stress. There was a low percentage of adherent trypan blue positive cells for both the SDFT and the DDFT during the heating experiments.

Pre-conditioning both the SDFT and the DDFT monolayers with a sub-lethal heat shock conferred a greater survival advantage to a subsequent lethal heat shock. The percentage of attached cells was higher in preheated fibroblasts for the SDFT and the DDFT in comparison with their unconditioned counterparts. This finding was significant for both the SDFT and DDFT after 24 hours of recovery, for example, at 24hrs post heating the percentage of attached cells in preconditioned SDFT fibroblasts was significantly higher at 79% compared with 38% in unconditioned SDFT cells (P-value: <0.001) (Figure 4-17C). For DDFT fibroblasts, the attached cell population at 24hrs post heating was significantly higher at 90% in the preconditioned cultures compared with 61% in unconditioned cultures (P-value: <0.001) (Figure 4-17D).

In cold shocked cells, high levels of Hsp-72 protein were seen in SDFT and DDFT cells exposed to 26°C overnight (16hrs) followed by 48hrs of recovery at 37°C. This cold shock protocol was used with the aim of inducing thermotolerance in these cells prior to their exposure to a lethal heat shock at 52°C.

The mean percentage of attached cold shock conditioned SDFT fibroblasts decreased with recovery time from 95% at 1hr of recovery, to 83% at 4hrs of recovery, to 78% at 24hrs of recovery to 50% at 48hrs of recovery and 33% at 72hrs of recovery (Figure 4-17E). This experiment was done on a separate occasion from that of the unconditioned SDFT cells. The mean percentage of attached cells in the unconditioned group was 95% of cells at 1hr of recovery, 72% at 4hrs, 38% at 24hrs, 18% at 48hrs and 15% at 72hrs. When comparing the cold conditioned cultures with the unconditioned cultures, the data indicates there was some protection from cell death following a lethal heat shock in the cold conditioned fibroblasts as cell loss was not as great in the first 24-48hrs of recovery time. More data would have to be collected in side by side experiments to confirm the significance of these findings.

When the percentage of attached cells was quantified over 72hrs of recovery time in cold conditioned DDFT fibroblasts, it was calculated as being 90% at 1hr of recovery, 90% at 4hr of recovery, 70% at 24hrs of recovery, 54% at 48hrs of recovery and 41% at 72hrs of recovery (Figure 4-17F). In contrast, in the unconditioned cold shocked DDFT fibroblasts, it was 86% at 1hr of recovery, 78% at 4hr of recovery, 61% at 24hrs of recovery, 55% at 48hrs of recovery and 36% at 72hrs of recovery. These data indicate there was no protection conferred from cooling at all in DDFT fibroblasts although a greater sample size would be needed to confirm the significance of this finding in the DDFT.

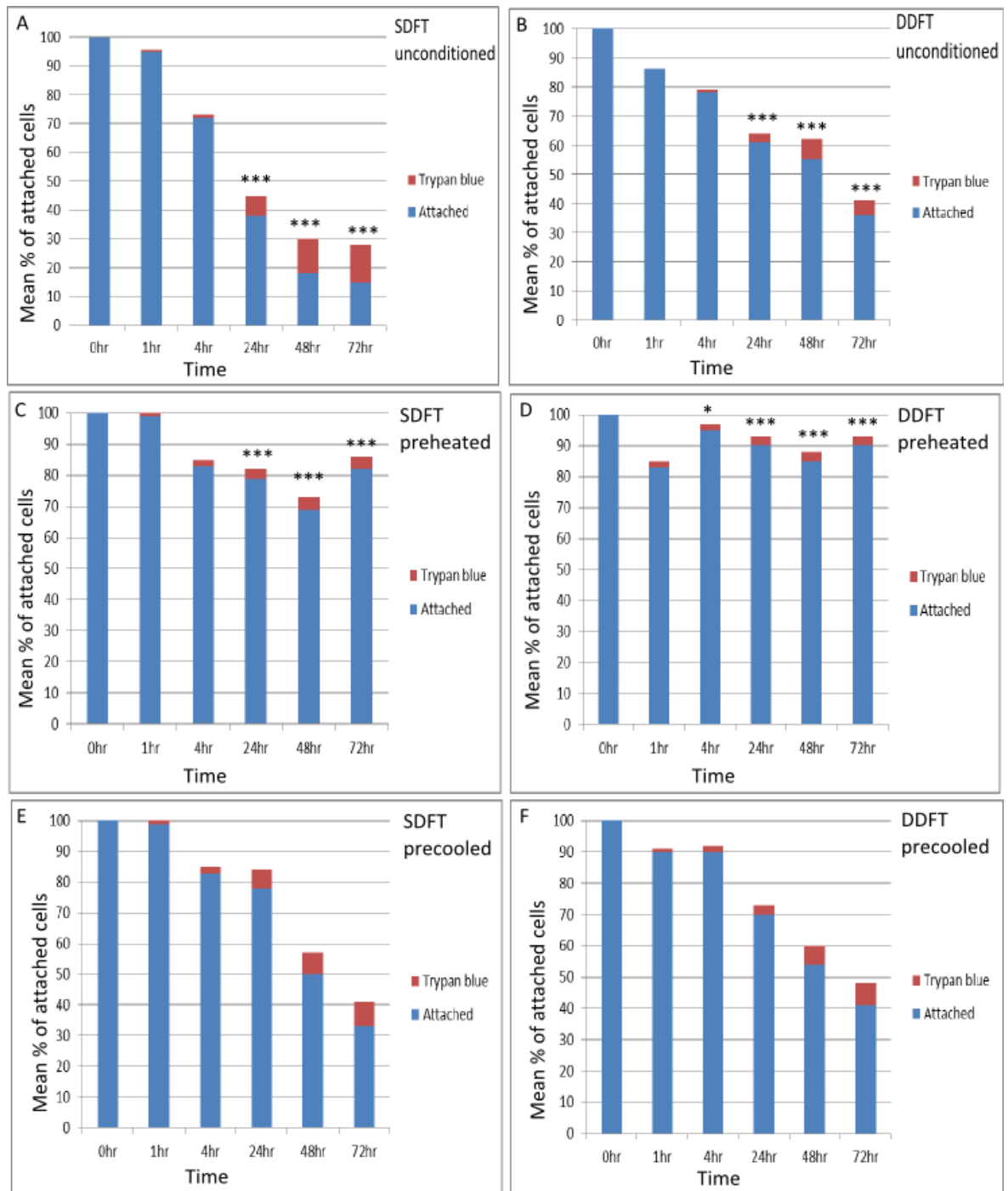


Figure 4-17. The percentage of attached SDFT and DDFT fibroblasts when exposed to pre-conditioned heat and cold shock.

SDFT and DDFT fibroblasts were exposed to 3 different experimental conditions (1) an unconditioned heat shock at 52°C for 15 mins (graphs A and B respectively) (2) a preconditioned heat treatment (47°C for 15 mins followed by recovery at 37°C for 4hrs prior to exposure to 52°C for 15 mins (graphs C and D respectively)) (3) a preconditioned cold treatment (26°C overnight followed by recovery at 37°C for 48hrs prior to exposure at 52°C for 15 mins (graphs E and F respectively)). The mean percentage of attached cells (blue) and trypan blue positive cells (red) was quantified over 72hrs post heating in SDFT and DDFT fibroblasts. All data was retrieved from one horse and repeated in triplicate. The Kruskal-Wallis test was used to determine whether there were any significant differences in the percentage of attached cells between the control and recovery times for both the unconditioned SDFT and DDFT fibroblasts. The Mann-Whitney test was used to determine whether there were any significant differences in the percentage of attached cells between the unconditioned and preheated SDFT and DDFT fibroblasts at time 4hr, 24hr, 48hrs and 72hrs. Significant differences at any of these time points are highlighted with stars (P-value: * <0.05 , *** <0.001).

4.3 Discussion

4.3.1 Calibration of the heating rig is an important criterion when choosing a suitable apparatus for heating cells.

Before starting the research into the heat shock response in equine tendon fibroblasts, a lot of time was devoted to finding an appropriate heating apparatus that was reliable, easy to use and produced reproducible results. The apparatus which best fulfilled these criteria was a resistive heater (Cell MicroControls, (Norfolk, VA)). Ability to calibrate the heating rig was very important especially for the measurement of cell culture media temperature. The media temperature was only able to be indirectly measured in control cell culture dishes heated simultaneously with the test dishes because the introduction of a small hole on the top of test dishes would have introduced a high risk of bacterial contamination of the cultures. The thermistor was very thin and could easily fit inside a minute hole thus minimising heat loss compared to other measuring probes including thermocouples which are significantly larger in size. Thermistor accuracy has been recorded at $\pm 0.2^{\circ}\text{C}$ by the company that manufactured it (pers.comm H.Cornell). In my experiments, the accuracy of the temperatures being measured was lower than reported values (approximately 0.5°C) and this difference in thermistor accuracy may have been caused by a number of factors including the type of experimental set up and variations in environmental temperature. It was noted that the placement of the thermistor tip on the bottom of the dish was important for the measurement of temperature as slight tipping of the thermistor edge led to greater variations in temperature by as much as $0.5\text{-}1.0^{\circ}\text{C}$.

There is large variation in the literature describing the variety of heating equipment used for in vitro work. The most common heating apparatus used is the water bath (Chow et al., 2009), (Kubo et al., 2005), (Bellmann et al., 2010), (Roobol et al., 2009), (Wu et al., 2009), (Maytin et al., 1990), (McMillan et al., 1998). Some authors do not mention whether any temperature calibration was used (Wu et al., 2009), (Roobol et al., 2009), (McMillan et al., 1998). Other groups record temperature calibration of the water bath only which does not

equate to the temperature of the media surrounding the cells (Chow et al., 2009), (Bellmann et al., 2010), (Kubo et al., 2005). Rarely has the media temperature itself been recorded (Maytin et al., 1990). The time spent in choosing the most appropriate heating apparatus was therefore a very useful exercise as it exposed the pitfalls of temperature calibration on a wider scale. In conclusion, the absolute values hitherto reported in the literature are probably unreliable as accurate temperature readings were rarely available.

Although the final choice of heating rig best fitted our criteria, there were still some limitations with this piece of equipment. These centred on the small number of cell culture dishes which could be heated at any one time and the temperature differential across the plate. One of the reasons for the temperature differential could be due to a difference in the rate of heat transfer at the edge versus the centre of the plate. The bottom of the cell culture dish is not uniformly flat, the edge has a rim or lip leaving a hollow area in the centre of the dish which traps air. The transfer of heat through plastic is typically slower than through air and therefore could contribute to the observed temperature differential across the cell culture plate.

4.3.2 The induction of Hsp-72 protein with heat shock in SDFT and DDFT fibroblasts

There were tendon dependent differences when SDFT and DDFT fibroblasts were heated to 43°C. At this temperature, there was no up-regulation of Hsp-72 in the DDFT and in contrast there was rapid induction of Hsp-72 protein at 4hrs post heating in the SDFT. The Hsp-72 induction timeframe for the SDFT corresponds with published data where peak induction of this protein has been shown to occur at 4-6 hours post heating in neonatal rat cardiomyocytes (Laios et al., 1997). This indicates that the induction of Hsp-72 in SDFT fibroblasts is consistent with other sensitive cell types (i.e. cells that may be more prone to injury).

Since the ability of a cell's response to stressful stimuli is dependent on the mobilisation and activation of stress responsive pathways to ensure the organism's survival (Judy et al., 2013), it may be that the more rapid the response, the more sensitive the cells are to an injury. The SDFT is routinely

exposed to various repetitive stresses associated with exercise including hyperthermia and oxidative stress *in vivo*. As the heat shock proteins are responsible for the refolding of damaged proteins in response to an insult and additionally aid in the protection of cells against apoptosis (Mosser et al., 1997), (Saleh et al., 2000), (Samali and Orrenius, 1998), (Samali and Cotter, 1996) it is not surprising that the injury-prone SDFT was able to rapidly activate HSP-72 in response to heat stress in comparison with the DDFT in these experiments. This difference in Hsp-72 induction between the SDFT and the non-injury prone DDFT also indicates that there is conservation of the two different phenotypes *in vitro*. These preliminary experiments were based on the results of samples from one horse and to confirm whether there are differences in the induction pattern of Hsp-72 protein between the SDFT and DDFT in the wider Thoroughbred horse population, a larger group of animals would need to be tested.

4.3.3 The induction of Hsp-72 protein with cold shock in SDFT and DDFT fibroblasts

The experimental work in this chapter provides convincing evidence that equine tendon fibroblasts were able to produce Hsp-72 protein during cold shock itself and in the rewarming period post cooling. Although these findings are completely novel in this area of research, they are based on the data from one horse. There is large variation in the literature regarding the expression of Hsp-72 during cold shock. Most studies have shown that Hsp-72 is only expressed during the rewarming period following the cold shock and not during cold shock itself. For example, in neonatal rat cardiomyocytes, maximal induction of Hsp-70 was shown 4-6hrs post cooling (Laios et al., 1997). This most likely reflects the type of experimental set up where measurements of Hsp-72 expression were only recorded during the rewarming period. Another study in CHO-K1 (Chinese Hamster Ovary cells) cells showed that there was no Hsp-72 production either during cold shock or its recovery period (Roobol et al., 2009). Cullen and Sarge, (1997) demonstrated that Hsp-72 mRNA levels can be increased in response to cooling in mice, the extent of which differed according to the type of tissue (Cullen and Sarge, 1997). This may indicate that there may be species specific and tissue differences in the induction of Hsp-72. Another explanation for these differences may be that the length of cold shock exposure in these cells was not long enough e.g. the CHO-K1 cells were only exposed to 6hrs of cold shock

(Roobol et al., 2009). My results showed that the production of Hsp-72 protein only occurred after a prolonged exposure time (especially for DDFT fibroblasts) at 48-72hrs of continuous cold shock at 26°C.

Although the reasons for the prolonged induction time for Hsp-72 protein in cold shock temperatures are unknown, a number of factors may be involved. The activation of HSF-1, a key transcription factor involved in the production of heat shock proteins, may use different mechanisms of activation during cooling, as hyperphosphorylation of HSF-1 which is important for heat shock was shown not to occur with cold shock (Cullen and Sarge, 1997).

It is possible that the production of heat shock proteins is delayed during hypothermic conditions. DAXX, a protein which is normally localised to the PML NBs (Promyelocytic leukaemic nuclear bodies) in the nucleus of unheated cells has been shown to oppose the repression of HSF-1 during heat shock through its affinity to bind trimerised HSF-1. This prevents interaction of HSF-1 with its multichaperone complex thus keeping it in the inactive state. On release from this complex, HSF-1 is able to bind to heat shock elements leading to the transcription of the heat shock proteins (Boellmann et al., 2004), (Zou et al., 1998). DAXX has been shown to disperse from the PML NBs during heat shock in human cells which is thought to allow its interaction with HSF-1 (Nefkens et al., 2003). Hitherto there has been no data in equine tendon fibroblasts. DAXX dispersal with heat and cold shock in SDFT and DDFT fibroblasts is described in Chapter 5. As there was a delay in the production of Hsp-72 protein at hypothermic temperatures in these cells, we have predicted DAXX dispersal from the PML NBs does not take place at cold shock temperatures in equine fibroblasts.

When a recovery period following cold shock was allowed, there was much more rapid induction of Hsp-72 protein in the SDFT compared with the DDFT. Numerous physiological changes occur during cooling which enable cells to survive hypothermic conditions, such as lowering of protein synthesis, reduced metabolic rate, inhibition of ATP expenditure and disassembly of the cytoskeletal architecture (Dresios et al., 2005), (Al-Fageeh and Smales, 2006), (Roobol et al., 2009). When cells are rewarmed, the resumption of metabolic activities will enhance the levels of cellular oxygen free radicals in the cell

which can damage proteins and organelles (Neutelings et al., 2013), (Rancourt et al., 2002). This indicates that the SDFT may be more sensitive to the damage associated with rewarming leading to faster Hsp-72 activation and mobilisation. These results follow a similar trend to the heat shocked SDFT fibroblasts where Hsp-72 activation was more rapid than in the DDFT.

With longer exposure to cold shock, especially overnight incubation (16hrs) in the tendon fibroblasts, there were high levels of Hsp-72 protein in the early recovery period post cooling in both tendons. This suggests that adaptation to the cold shock may have occurred with the production of Hsp-72 taking place during the cooling process.

4.3.4 Tendon-dependent difference in thermotolerance in response to heat shock

Thermotolerance is a well-known phenomenon known to protect cells against various types of stress and is attributable to the action of the heat shock proteins (Chow et al., 2009), (Gabai et al., 2000). Both the SDFT and the DDFT were able to exhibit thermotolerance in response to a lethal heat shock when the cells were preconditioned at 47°C. The SDFT should be adapted to heat stress as temperatures as high as 45°C have been recorded in vivo (Wilson and Goodship, 1994). Despite high levels of Hsp-72 in SDFT fibroblasts, these cells were more susceptible to a lethal heat shock in comparison with the DDFT fibroblasts. Again, with the small sample size (one horse) more confirmatory studies will be required in a larger population.

In vivo, SDFT fibroblasts are exposed to the effects of hyperthermia and other exercise associated factors including oxidative stress. These may have detrimental effects on the tendon fibroblasts including the induction of irreversible cellular dysfunction, aging of the cells, overwhelming of the reparative processes and/or cell death (Patterson-Kane et al., 2012). In chapter 3, we demonstrated that the SDFT fibroblasts had higher levels of lysosome activity in comparison to the DDFT in standard cell culture conditions. This was believed to be caused by high levels of protein damage as a result of the cell culture environment. The exposure of cells to heat stress is well known to result in oxidative stress, protein denaturation and phosphorylation of p53, all of which

can lead to cell death (Mustafi et al., 2009), (Kim et al., 2005), (Neutelings et al., 2013), (Lepock, 2003). The high levels of aggregated protein in the SDFT fibroblasts caused by hyperthermic stress (in addition to those caused by the cell culture environment) may lead to saturation of the autophagy pathways thus sensitising these cells to heat shock related cell death (Bellmann et al., 2010), (Nivon et al., 2009). The application of heat stress (40°C for 60-90 mins) in rats was shown to result in the time-dependent activation of autophagy. Inhibition of autophagy by 3-methyladenine (3-MA) led to aggravation of heat-induced neurodegeneration of neurons in the cerebral cortex indicating that autophagy plays a protective role in the survival of cells to an insult (Liu et al., 2010).

4.3.5 Thermotolerance only occurred for the first 24hrs post heating in preconditioned cold shocked SDFT fibroblasts

When pre-conditioned cold shocked SDFT fibroblasts were exposed to a lethal heat shock, there was some protection from cold shock in the first 24hrs post heating. In contrast, this did not occur in the DDFT. This may be a reflection of the differences in the amount of Hsp-72 protein between the SDFT and the DDFT. The SDFT has been shown to mount a rapid response to Hsp-72 induction in the early rewarming period post cooling and this may result in a time-related accumulation of Hsp-72 protein in these cells, thus providing a greater advantage against a lethal heat shock compared with the DDFT.

In my results on equine tendon fibroblasts, the amount of heat shock protein induced with cold shock in the SDFT and the DDFT was not as great when compared with heat shock (this awaits verification as the data will have to be collected in side by side experiments). The rate of temperature induction may be an important requisite for the production of HSPs. Tulapurkar showed that the expression of Hsp-72 protein was increased linearly in A549 lung epithelial cells, where there was a 0.5 fold induction in Hsp-72 protein/1°C from 37-41°C. In contrast, there was a 2.4 fold induction in Hsp-72 protein between 41°C- 42°C. This suggests that there is a difference in the kinetics of Hsp-72 production according to the temperature being used (Tulapurkar et al., 2009).

4.3.6 The expression of RBM3 occurred with both heat and cold shock in SDFT fibroblasts.

In our studies, the up-regulation of RBM3 protein was shown to occur not only in cold shock but also with heat shock. RBM3 was strongly up-regulated during moderate hypothermia, the pattern of which was discovered to be biphasic at 32°C. At 26°C, there was an increase in the expression of RBM3 which was maintained for a much longer period of time. The increase in RBM3 expression at lower temperatures may be an important determinant for cell survival as lower temperatures result in a reduction in cellular proliferation, reduction in ATP expenditure and protein translation (Al-Fageeh and Smales, 2006). One of the major roles of RBM3 is the ability to restore the translation of proteins during a period of protein suppression (Dresios et al., 2005), (Chappell et al., 2001). A recent study has shown RBM3 to be instrumental in the control of miRNA biogenesis, a family of RNA proteins involved in the regulation of mRNA, an important precursor step to protein production (Pilotte et al., 2011).

RBM3 has been shown to be up-regulated in response to various types of stress including cold shock, serum deprivation and hypoxia (Chappell et al., 2001), (Wellmann et al., 2004), (Wellmann et al., 2010). Two studies have shown that an increase in RBM3 expression helps to protect cells against apoptosis caused by serum starvation and exposure to hydrogen peroxide, a source of ROS species in cells (Ferry et al., 2011) (Wellmann et al., 2010). Heat shock is thought to induce oxidative stress in cells and this may in turn stimulate RBM3 expression (Kim et al., 2005). Our studies showed the expression of RBM3 protein to be biphasic in SDFT fibroblasts following heating at 43°C. The biphasic expression of RBM3 was slower in comparison with cold shock at 32°C (peaks of expression occurred at 4hrs and 48hrs post heating compared with 1hr and 24hrs during cold shock).

Heat stress (39°C) has been shown to down-regulate RBM3 mRNA and protein production in BMA-1 bone marrow stromal cells, 3T3 fibroblasts and TAMA26 Sertoli cells (Danno et al., 2000). Another study showed the expression of RBM3 mRNA to be increased at 1hr of cold shock at 25°C and following rewarming, there was a gradual decline in the RBM3 mRNA levels until 24hrs post cooling where it returned to control levels (Neutelings et al., 2013). These

findings are in contrast to our studies where heat stress led to an increase in RBM3 protein expression. This may be a reflection of species specific or tissue differences in RBM3 protein production. Additionally, Neutelings only investigated the mRNA levels of RBM3 and these levels do not always correlate with protein levels due to the varied post-translational modification of proteins, differences in the half-lives of proteins and the significant amount of error/background noise in mRNA and protein experiments (Greenbaum et al., 2003). The sample size in my experiments was small and future experimental work in this area will require larger numbers of animals to determine the impact of heat stress on RBM3 expression.

4.3.7 Restoration of normal cellular morphology is a useful predictor of cell fate following heat shock

One of the characteristic reactions to temperature stress in SDFT and DDFT fibroblasts was an alteration in cellular morphology as result of modifications to the cytoskeleton. Two of the main morphological alterations visible in equine tendon fibroblasts were cell rounding and shrinkage. Cell rounding typically arose at 1hr post heating and lasted until 24 hours post heating and if the temperature was not lethal, the cells returned to their normal cellular morphology (spindle shaped cells). The restoration of normal cellular morphology following heat shock has been described as a useful predictor of cell survival (Coss et al., 1996). If the temperature stress induced lethal injury, cell rounding and shrinkage would lead to permanent cell detachment and death. Loss of cell-ECM attachment is part of the apoptotic heat shock response and has been termed anoikis (Frisch and Francis, 1994), (Luchetti et al., 2003). This morphological response could be useful in future studies as a method of detecting cell death in tendon monolayers without having to presume the exact mechanism of cell death.

Cytoskeletal changes are thought to contribute to cell rounding during heating. Collier demonstrated that there was generalised loss of intermediate filament structure when chicken embryonic fibroblasts were exposed to heat shock at 45°C for 3hrs that was reversible on recovery from stress (Collier and Schlesinger, 1986). When a similar temperature was used in Chinese Hamster ovary cells, actin microfilaments were found to be disrupted and microtubule

disassembly was also prominent following hyperthermia (Coss et al., 1982), (Glass et al., 1985).

Cold shock has also been shown to lead to depolymerisation of the microtubules (Terasaki et al., 1986). One of the problems in our western blot work was that alpha Tubulin displayed a different expression pattern in cold shocked lysates with two bands, one at 50kDa and the other at 55kDa. Further investigation of this additional band led to the conclusion that the 55kDa was acetylated alpha Tubulin. The acetylation of alpha Tubulin has been shown to occur in cold shocked cells (Piperno et al., 1987) however the function of acetylated tubulin in cells is still yet to be understood. The acetylation of microtubules has been shown to recruit Hsp-90 and its target proteins to the microtubules which suggests that the microtubules are involved in the transport of Hsp-90 chaperone proteins in the cell (Giustiniani et al., 2009). Alpha tubulin would not be useful as a protein loading control for the quantification of protein in cold shocked cells.

The heat shock proteins may play an important role in the stabilization of the cytoskeleton and/or refolding of damaged cytoskeletal proteins following heat stress. Exposure of human mesothelial cells to a noxious agent, peritoneal dialysis fluid, led to significant disruption of the cytoskeleton. When cell lysates were created using these cells, Hsp-72 was shown to re-localise from the Triton soluble supernatant in control cells into the cytoskeletal fraction following exposure to the peritoneal dialysis fluid. Re-exposure of mesothelial cells to the same toxic agent did not prevent disruption of the cytoskeleton, but did speed up its restoration within 4hrs of recovery (Endemann et al., 2007). This result was similar to our research findings as cell rounding was not prevented in the pre- heated SDFT and DDFT fibroblasts and indicates that this process is a constitutive component of the cellular response to heat stress. Induction of Hsp-72 occurred at 4hrs post heating for both 43°C and 47°C which closely approximates the restoration of normal cellular morphology in tendon fibroblasts suggesting that Hsp-72 plays an important role in the maintenance of cytoskeletal function. Further work will be required to investigate this link more closely.

The percentage of trypan blue positive cells was very low in the heat and cold shock experiments which suggests that the majority of these cells may have washed away into the surrounding media. The trypan blue positive cells could not be harvested from the supernatant when the cell culture media underwent centrifugation, therefore very few injured and still attached cells were dye permeant.

In summary, although the sample size was limited, the data presented in this chapter suggested that there were tendon dependent differences in the expression of Hsp-72 at both heat shock and cold shock temperatures. In general, the SDFT displayed faster induction of Hsp-72 protein in comparison with the DDFT. Despite high levels of Hsp-72 protein in SDFT fibroblasts, these cells were more susceptible to a lethal heat shock compared with the DDFT. This may be a reflection of the inability of the SDFT to cope with a lethal stimulus and furthermore may indicate that in vivo, heat stress related cell death in a sparsely populated tendon may be detrimental for the repair of tendon lesions. Additionally, pre-conditioned cold shocked SDFT fibroblasts were able to protect themselves for the first 24hrs following exposure to a lethal heat shock. In contrast, no thermotolerance was seen in preconditioned cold shocked DDFT fibroblasts. Finally, up-regulation of RBM3 was seen with both heat and cold shock in SDFT fibroblasts. This protein may be important for the survival of these cells in response to various temperature changes, although future research will be required to determine its exact roles.

Chapter 5) Markers of injury sensing in equine tendinopathy

5.1 Introduction

Complex biological defence mechanisms protect cells against various types of stress. The heat shock response, a focus of the last chapter, is one of these. Understanding the physiological mechanisms in the early phase of heat shock and other injurious processes such as oxidative stress should enable the future manipulation of these pathways to protect susceptible tendon fibroblasts from injury and/or death. One of the ways to achieve this is to examine the distribution and expression of various reporter proteins involved in these stress-associated pathways.

PML NBs are stress-responsive nuclear hub proteins which become structurally altered in response to various types of insults. PML protein is one of the scaffold proteins required for the binding and retention of a number of partner proteins at this nuclear hub, one of which is DAXX (Zhong et al., 2000b) (see Figure 1-5). One of the earliest changes induced by heat shock is the rapid dispersal of PML and DAXX from the PML NB into the nucleoplasm. One study showed DAXX release from the PML NB took place within 12 mins of heating at 42°C in HEp-2 cells (human epithelial laryngeal carcinoma contaminated with HeLa cells) and reformation of the PML NB was equally rapid as this was shown to occur within 30-45 mins after heat shock (Maul et al., 1995), (Nefkens et al., 2003). This stress responsive pathway has not been investigated in equine cells and it would be of great interest to see if DAXX dispersal occurs in response to heat shock in equine tendon fibroblasts. Furthermore, no data exists on whether DAXX dispersal from the PML NBs also occurs with cold shock in human, mice or equine cells.

The production of heat shock proteins is regulated by HSF-1 (heat shock transcription factor 1). Certain proteins can enhance the transcription capacity of HSF-1 including DAXX which has a strong affinity for trimeric HSF-1, the activated form of the HSF-1 transcription factor (Boellmann et al., 2004). Previous work described in this thesis (chapter 4) demonstrated the strong association between the production of heat shock proteins and the acquisition of

thermotolerance in equine tendon fibroblasts exposed to a lethal heat shock at 52°C. The presence of increased levels of heat shock proteins in human cells has been shown to have a negative feedback effect on HSF-1 activity and its subsequent production of heat shock proteins (Shi et al., 1998). The negative feedback effect on HSF-1 activity may in turn lead to a stress adaptable response in which the release of DAXX from the PML NBs is inhibited in equine tendon fibroblasts to prevent its nucleoplasmic association with trimeric HSF-1. The production of Hsp-72 was delayed following cold shock especially with prolonged cooling; therefore it was also predicted that DAXX would not be available to regulate Hsp expression, possibly by being retained at the PML bodies.

Exposure of mammalian cells to heat stress results in extensive protein denaturation (Lepock, 2003). Protein denaturation is known to result in activation of the heat shock proteins which are responsible for the refolding of damaged proteins (Chow et al., 2009), (Madden et al., 2008). The presence of denatured proteins following heat stress in HeLa cells has also been shown to lead to the activation of NFκB transcription factor which in turn resulted in the activation of autophagy and increased survival of the HeLa cells (Nivon et al., 2009). The clearance of aggregated proteins and the refolding of damaged proteins are of great importance in cells following exposure to an insult as these proteins are cytotoxic and can trigger cell death (Bucciantini et al., 2002). The protein turnover pathways such as autophagy could therefore be relevant pro-survival mechanisms during hyperthermia in equine tendon fibroblasts.

One of the attractive reporter protein candidates for the investigation of proteotoxic stress is p62 as it binds to protein aggregates in the cell and transports them to the lysosomes for degradation. p62 binds to ubiquitinated protein through its C-terminal UBA domain and attaches to the autophagosomes via its interaction with LC3B-II, an adaptor protein on the autophagosomes. The autophagosomes then subsequently fuse with the lysosomes where protein degradation takes place (see Figure 1-7) (Bjørkøy et al., 2005), (Pankiv et al., 2007), (Vadlamudi et al., 1996).

p62 as a proteotoxic cell sensor has been implicated in a number of degenerative conditions including cardiomyopathies and neurodegenerative

diseases such as Alzheimer's or Parkinson's disease. It is thought to have a protective role in promoting cell survival as ablation of p62 in vitro was found to increase cell injury and decrease cell viability as a result of the build-up of aggregated proteins in rat ventricular myocytes expressing misfolded desmin proteins (Zheng et al., 2011), (Schaeffer et al., 2012). p62 is often found in neuronal inclusion bodies in Alzheimer's disease. The sequestration of p62 in these bodies depletes cytoplasmic p62 thus limiting its availability to clear toxic protein aggregates leading to an increase in the levels of damaged proteins in the cell (Kuusisto et al., 2002), (Du et al., 2009a), (Salminen et al., 2012). Metabolic stress in autophagy defective tumour cells resulted in the accumulation of p62 in the cytoplasm together with increased oxidative stress and activation of the DNA damage response. The addition of ROS scavengers led to decreased p62 accumulation in the cytoplasm and increased cell survival (Mathew et al., 2009). In summary, p62 contributes to cytoprotective autophagy functions but can also drive ROS accumulation when autophagy is dysfunctional (Hariharan et al., 2011). SDFT pathology is thought to be caused by high intensity repetitive exercise resulting in dysfunctional cellular activity and/or unrepaired matrix fatigue leading to the accumulation of microdamage in the tendon matrix. Tendon microdamage has been described as a degenerative condition (Patterson-Kane et al., 2012). No data exists on whether p62 is expressed in SDFT lesions. If p62 is up-regulated in these lesions, it may be used as a marker of proteotoxic stress in SDFT tendon injury.

p62 has a strong role in oxidative stress signalling in cells. p62 interacts with NRF-2, a transcription factor mediating the production of anti-oxidants in response to oxidative stress (Jain et al., 2010). Under normal cellular conditions, NRF-2 is bound to cytoplasmic KEAP1 which promotes the degradation of NRF-2 via the proteasome. Under conditions of oxidative stress, p62 binds KEAP1 which frees NRF-2 to translocate to the nucleus where it binds to antioxidant response elements (Jain et al., 2010), (Watai et al., 2007), (Lee et al., 2003) (Theodore et al., 2008), (Sekhar et al., 2002). In chapter 3, the cell culture environment was shown to be conducive to the creation of replication-induced DNA damage in tendon fibroblasts, possibly as a result of increased levels of exogenous and/or endogenous ROS. The localisation of nuclear NRF-2

may therefore be a useful marker of oxidative stress in equine tendon fibroblasts in vitro.

The aims of the work in this chapter were:

- 1) To investigate whether DAXX translocates from nuclear puncta into the nucleoplasm in equine tendon fibroblasts during heat shock and cold shock. As DAXX has been shown in human cells to translocate from PML NBs into the nucleoplasm with heat stress, it was predicted the same response would occur in equine cells and that the opposite would occur with cold shock.
- 2) To determine if DAXX translocation was stress adaptable with a subsequent heat shock in equine tendon fibroblasts. DAXX is thought to play a role in Hsp-72 production, it was hypothesised a negative feedback effect would take place with a subsequent heat shock i.e. DAXX release from the nuclear puncta into the nucleoplasm would be prevented.
- 3) To establish whether p62 was expressed in injured equine SDFT tendon. SDFT pathology is a degenerative condition and proteotoxic stress may contribute to this process therefore it was predicted p62 would be up-regulated in these lesions.
- 4) To verify the localisation of NRF-2 in equine SDFT fibroblasts in a highly oxygenated environment in vitro. The localisation of NRF-2 in SDFT fibroblasts in vitro was predicted to be nuclear as the cell culture environment could play a role in ROS-mediated cellular stress.
- 5) To determine whether the addition of an exogenous anti-oxidant agent would alter the distribution of NRF-2 in SDFT fibroblasts. The addition of NAC was hypothesised to shift NRF-2 from the nucleus back into the cytoplasm.

5.2 Results

5.2.1 Validation of DAXX and Caspase-2 in Foetal Equine Palate fibroblasts

Validation of two protein markers known to localise to the PML NBs, DAXX and Caspase-2 was carried out in foetal equine PalF fibroblasts (PalF) as they may be useful indicators of injury recognition by equine cells (Rich et al., 2013). PalF cells were chosen for the validation experiments to help conserve equine tendon fibroblasts due to small sample size (the PalF cells were kindly provided by Dr. Elizabeth Gault with permission). Monolayers of equine PalF were heated at 46°C for 10 mins and Caspase-2 and DAXX were shown to be up-regulated and/or re-located into the nucleoplasm respectively (Figure 5-1 and 5-2). Caspase-2, a member of the Caspase family critically involved in the initiation of apoptosis in response to heat shock (Bouchier-Hayes et al., 2009) was shown via immunocytochemistry to be up-regulated within 10 mins of heating, as determined by the increased expression of nuclear Caspase-2 (Figure 5-1). DAXX, a protein with multiple roles in the cell including regulation of transcription, differentiation and apoptosis (Yang et al., 1997b), (Khelifi et al., 2005), (Oda et al., 2000), (Kim et al., 2003) was visible in the nucleus as small, discrete puncta in control cells maintained at 37°C. Punctate staining of DAXX in the nucleus was thought to be consistent with its localisation at the PML NBs, however this was not proven. DAXX was shown to disperse rapidly from the nuclear puncta into the nucleoplasm within 3 mins of heating as there was reduced punctate staining. At 10 mins of heating, DAXX punctate staining was still absent (Figure 5-2). These changes induced by heat shock to Caspase-2 and DAXX were very rapid, which exemplifies the potential importance of each of these proteins as early markers in the physiological response to heat.

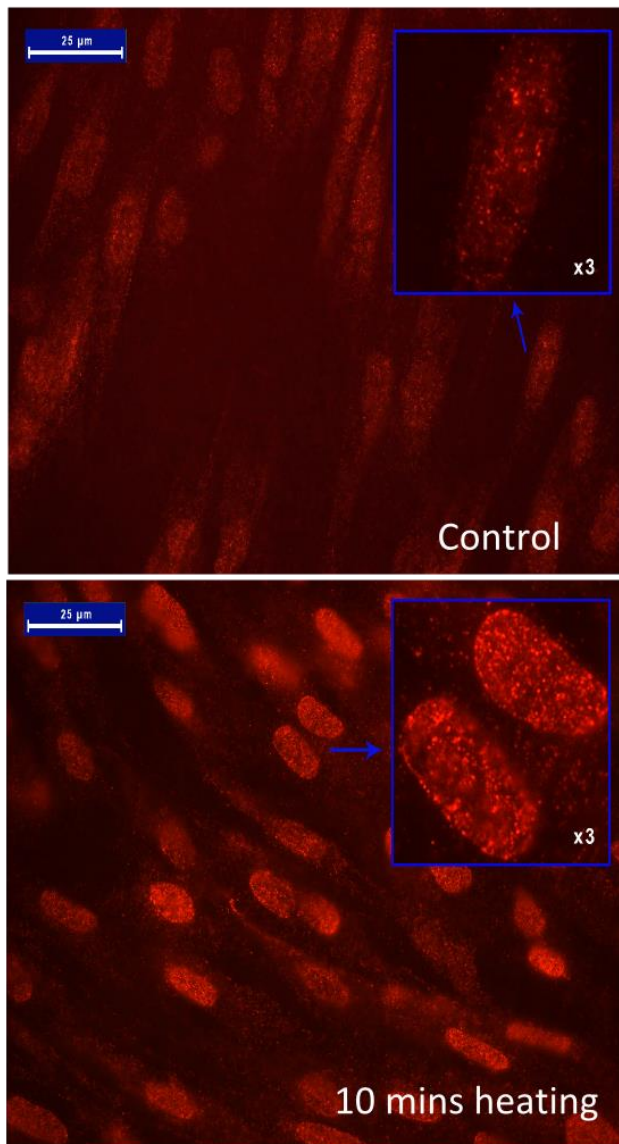


Figure 5-1 Caspase-2 distribution with heating in equine palate (Eq PalF) cells

Eq PalF cells were heated at 46°C for 10 mins. The cells were immunostained for Caspase-2 (red). Control cells were maintained at 37°C. Images shown at x63 magnification. Scale bar: 25µm. Inserts show magnification of individual nuclei x 3.

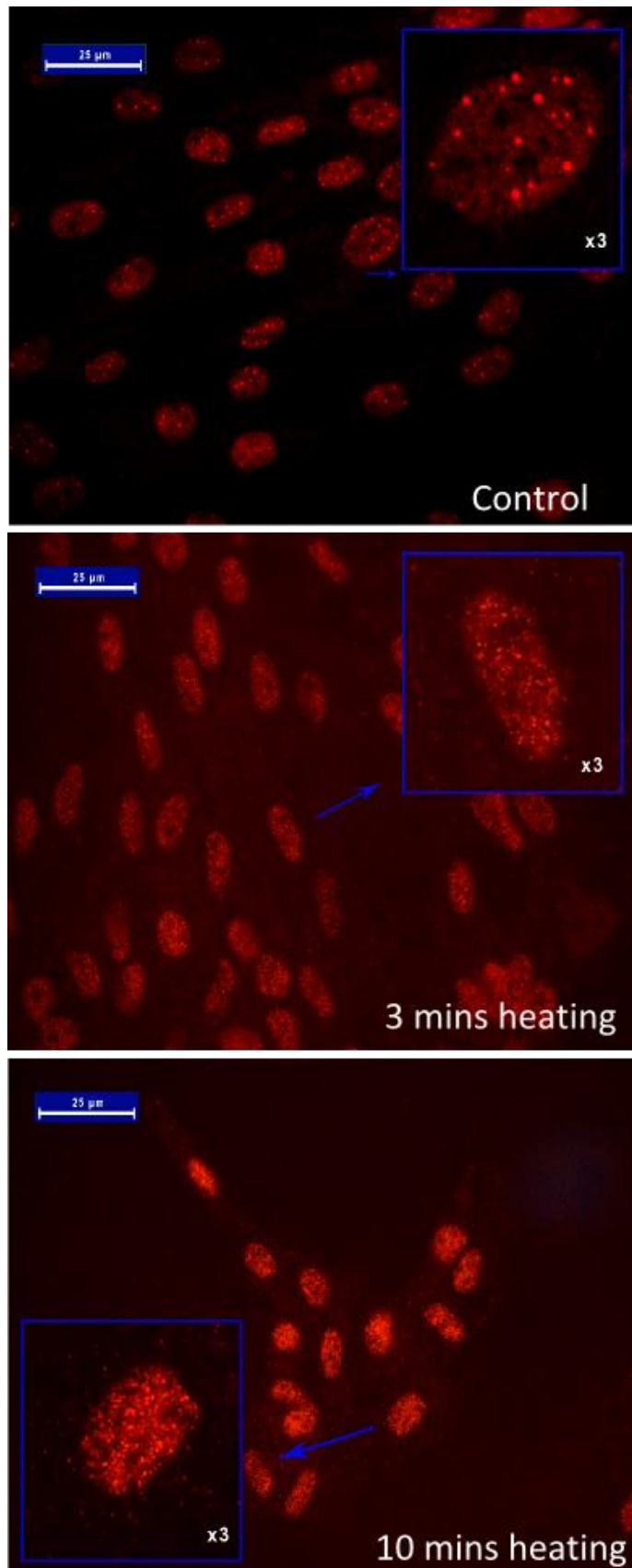


Figure 5-2 DAXX disperses with heating in E. coli PalF cells

E. coli PalF cells were heated at 46°C for 3 mins and 10 mins. Control cells were maintained at 37°C. The E. coli PalF cells were immunostained for DAXX (red puncta). Images shown at x63 magnification. Scale bar: 25µm. Inserts show magnification of individual nuclei x 3.

5.2.2 DAXX immuno-localisation during heat shock

DAXX is known to disperse rapidly from the PML bodies into the nucleoplasm during heat shock in both human and mouse fibroblasts (Nefkens et al., 2003). To verify whether this occurred in equine tendon fibroblasts as it does in PalF fibroblasts, SDFT fibroblasts were heated to 43°C for 3 mins, 10 mins and 15 mins. This temperature was chosen as it corresponds to the mean peak temperature recorded in the tendon core of galloping Thoroughbred racehorses in vivo (Wilson and Goodship, 1994). In the unheated group of tendon fibroblasts, DAXX was easily visualised as discrete puncta within the nuclei (Figure 5-3). At 3 mins of heating, there was a slight decrease in punctate DAXX expression. At 10-15 mins of heating, the majority of nuclei showed little punctate DAXX expression and diffuse nucleoplasmic staining of DAXX predominated. Upon closer examination, micropuncta and speckles of DAXX were also evident (Figure 5-3).

The recovery phase post-heating was examined to see if DAXX returned to its original position, at the nuclear puncta. Recovery from heating was rapid, as DAXX was shown to re-form nuclear puncta as early as 10 mins post-heating (Figure 5-4).

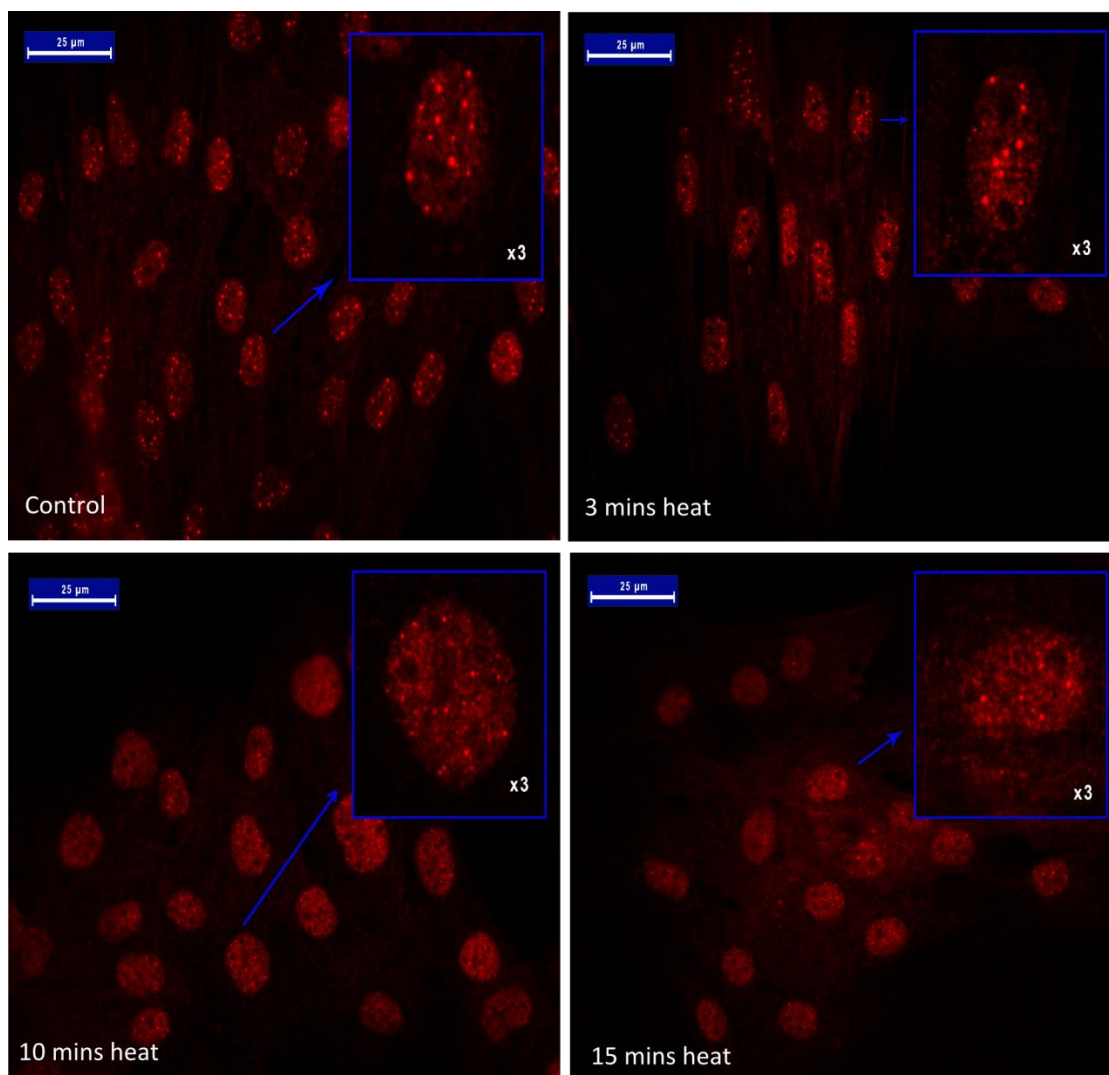


Figure 5-3 DAXX dispersal was very rapid in SDFT tendon fibroblasts

SDFT cells were heated to 43°C for 3 mins, 10 mins and 15 mins. Control cells were maintained at 37°C. The cells were immunostained for DAXX (red puncta). DAXX puncta are larger in unheated compared with heated cells. All data were retrieved from one horse and multiple fields of view for each time point were examined. Images shown at x63 magnification. Scale bar: 25μm. Inserts show magnification of individual nuclei x 3.

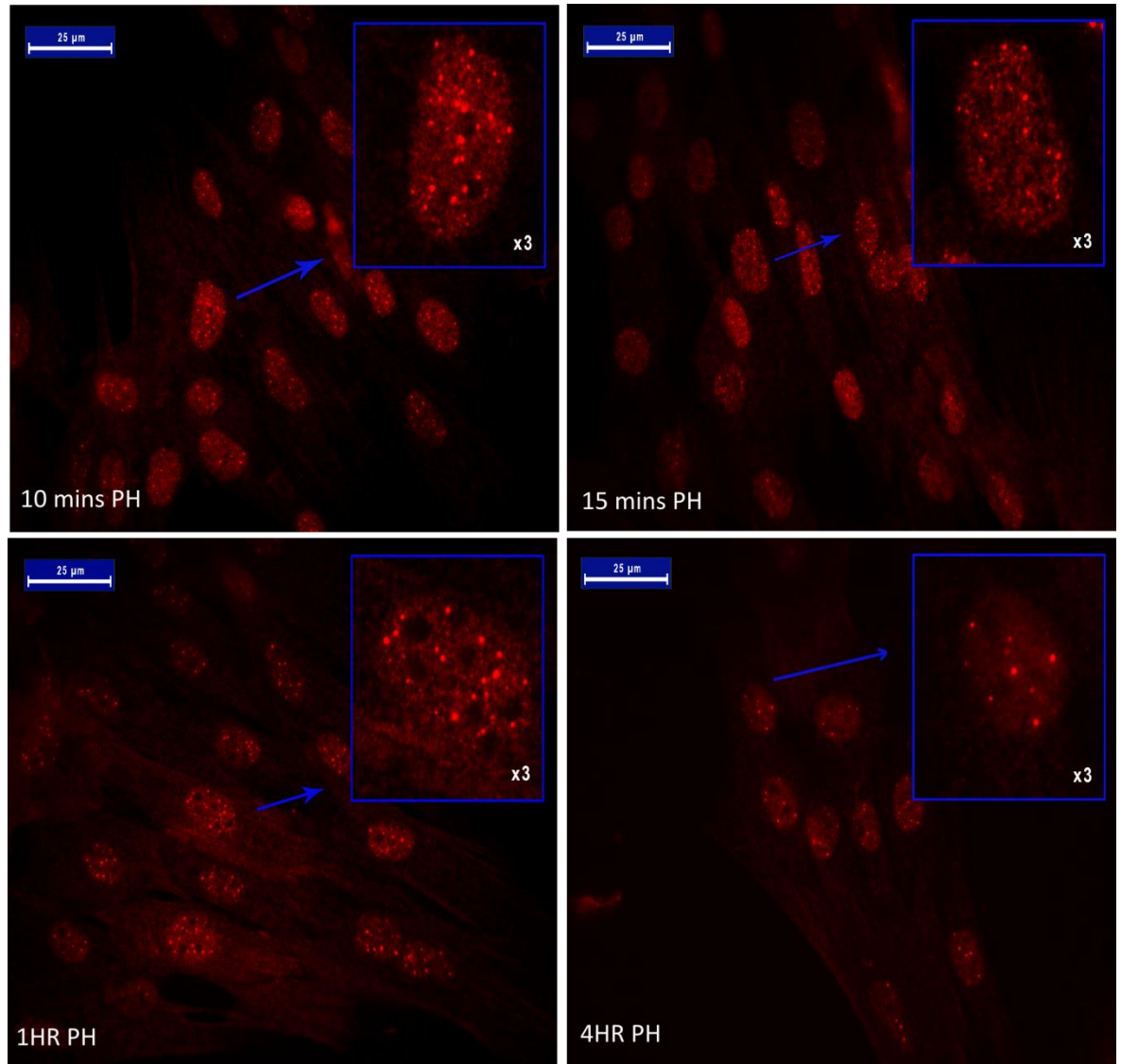


Figure 5-4 DAXX returned to the PML NBs very rapidly post heating

SDFT fibroblasts were heated at 43°C for 15 mins, before being returned to 37°C to recover for 10 mins, 15 mins, 1 hr and 4hr. The cells were stained for DAXX (red puncta). All data were retrieved from one horse and multiple fields of view for each time point were examined. Images shown at x63 magnification. Scale bar: 25μm Inserts show magnification of individual nuclei x 3. PH: post heating.

5.2.3 Re-shocking SDFT fibroblasts did not prevent DAXX dispersal

DAXX plays a central role in the expression of heat shock proteins during heat shock (Boellmann et al., 2004). Increased levels of heat shock proteins in cells are thought to have a negative feedback effect on subsequent HSF-1 transcriptional activity (Shi et al., 1998). Elevated levels of Hsp-72 were shown to promote cell survival following exposure to a subsequent lethal heat shock through the 'thermotolerance effect' in SDFT and DDFT fibroblasts (chapter 4). This protective response may lead to a stress adaptive response where DAXX release from the PML NBs is inhibited. To investigate whether DAXX dispersal would occur following successive heat shocks at conditions under which adaptive responses have previously been shown, monolayers of SDFT fibroblasts were heated at 43°C for 15 mins, left to recover at 37°C and then re-shocked 24 hours later. As shown in figure 5-5, re-shocking the SDFT fibroblasts did not prevent DAXX dispersal from its position at nuclear puncta into the nucleoplasm at 10-15 mins of heating. This suggests DAXX re-localisation into the nucleoplasm is part of the constitutive physiological (i.e. hard wired) injury response of the cell and was not stress adaptable.

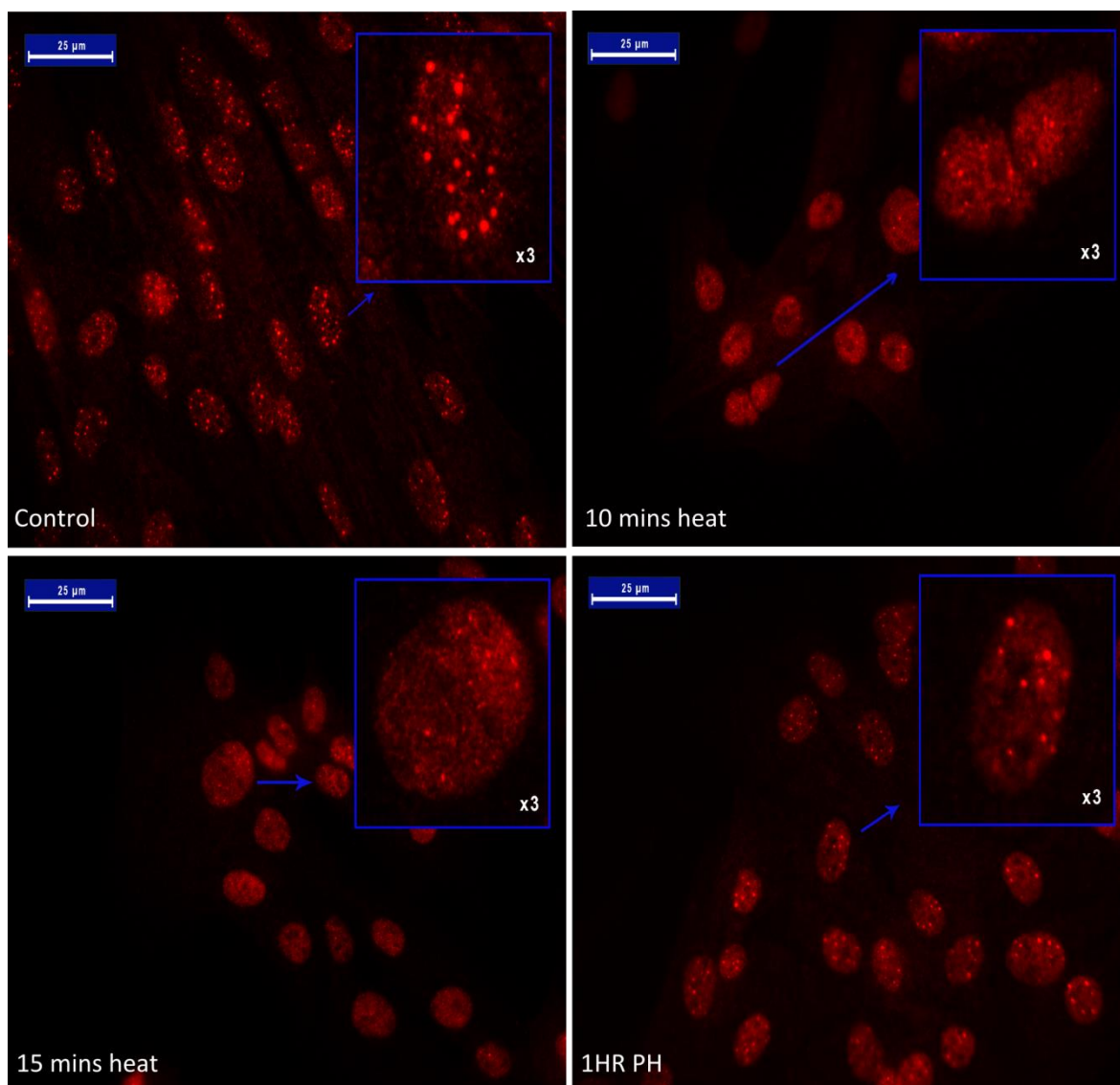


Figure 5-5 Reshocking SDFT fibroblasts did not prevent DAXX dispersal

SDFT fibroblasts were heated to 43°C for 15 mins before being returned to 37°C to recover for 24hrs. After this recovery period they were re-heated at 43°C for 10 mins or 15 mins only or given 1hr recovery at 37°C. Each test group was immunostained for DAXX (red puncta). Control cells were maintained at 37°C. All data were retrieved from one horse and multiple images of each time point were examined. Images shown at x63 magnification. Scale bar: 25µm. Inserts show magnification of individual nuclei x 3. PH: post heating.

5.2.4 DAXX puncta size increased during the early hypothermic period, with dispersal during the rewarming period only.

To determine whether DAXX re-localisation also occurred with cold shock i.e. with a temperature differential and not just absolute temperature, SDFT derived fibroblasts were chilled at 26°C for 10 mins or 30 mins. There was no dispersal of DAXX from its position at nuclear puncta into the nucleoplasm at either of these time points (Figure 5-6). The cold shocked cells were rewarmed following 30 mins of cold shock at 37°C for 15 mins, 1hr or 4hrs. Dispersal of DAXX into the nucleoplasm was thought to have taken place at 15 mins post cooling as some of the DAXX puncta appeared slightly smaller.

To verify whether DAXX dispersal did occur in the rewarmed population of cold shocked fibroblasts, the size of over 500 DAXX puncta was analysed with multiple cells from one horse using the particle analysis function of Image J. The average size of DAXX puncta in control cells was approximately 36 pixels which dropped to 27 pixels at 15 mins post cooling (Figure 5-7). At 1hr post cooling, the size of the DAXX puncta was still lower than control cells, at 30 pixels. However by 4hrs post-cooling, the size of the puncta had completely returned to control values (36 pixels).

As the measurement of DAXX puncta size using the particle analysis function of Image J resulted in useful quantitative information in the rewarmed SDFT fibroblast population, puncta size was also measured in the cold shocked cells. At 10 mins of cold shock, DAXX puncta size was larger than the control cells, increasing from 36 pixels to 45 pixels. However, at 30 mins of cold shock, mean puncta size decreased slightly to 38 pixels (Figure 5-7). To determine whether there were any significant differences between the control and any of the cold shocked or rewarmed population of cells, the Kruskal-Wallis non-parametric test was employed. Although, no statistical differences were seen in these experiments, this could be attributed to small sample size.

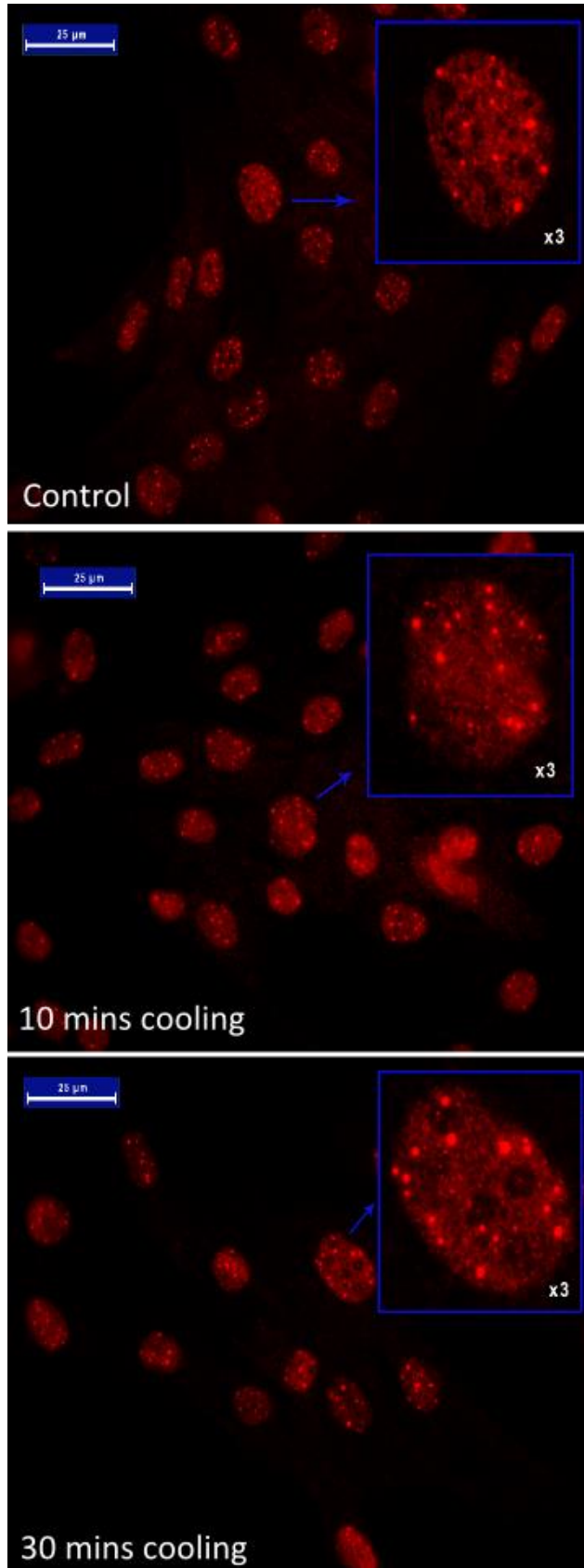


Figure 5-6 DAXX dispersal did not occur with cooling

SDFT fibroblasts were chilled for 10 mins or 30 mins at 26°C. Control cells were maintained at 37°C. At the end of the cooling period, the cells were stained for DAXX (red puncta). All data were retrieved from one horse with multiple images of each time point examined. Images shown at x63 magnification. Scale bar: 25µm. Inserts show magnification of individual nuclei x 3.

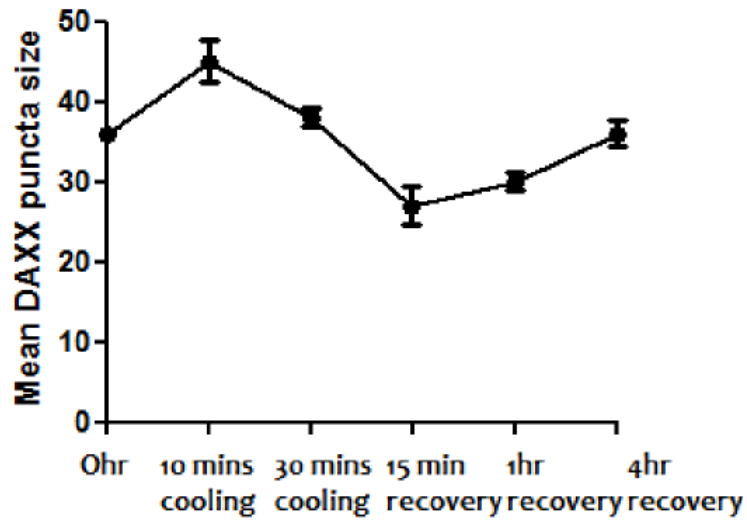


Figure 5-7 DAXX puncta size changed with temperature

SDFT fibroblasts were cold shocked for 10 mins or 30 mins at 26°C with no recovery or given 30 mins of cold shock then left to recover at 37°C for 15 mins, 1hr or 4hrs. The size of over 500 DAXX puncta was measured from multiple cells in one horse using the particle analysis function of Image J for each group and the average was calculated to give the mean puncta size. DAXX puncta size was shown to increase in size with cooling and decrease during the re-warming period. The error bars represent the standard error for each treatment group. The Kruskal Wallis test was used to determine whether there were any statistical differences between the control and any of the cold shocked/rewarmed groups. No statistical differences were found.

5.2.5 Different batches of p62 antibodies displayed different in vitro cellular distributions

Prior to the start of investigative work, validation of the p62 antibody in equine cells was completed as very little data exists on the use of p62 in equine studies. In mouse embryonic fibroblasts, p62 protein has been shown to localise to round bodies in the cytoplasm, the autophagosomes (Itakura and Mizushima, 2011). In HeLa cells, both cytoplasmic and nuclear p62 have also been recorded. In this study, approximately 85% of HeLa cells were positive for cytoplasmic p62 with weaker staining of nuclear p62. 15% of cells were shown to have similar fluorescence intensities for p62 in both the nuclear and cytoplasmic compartments (Bjørkøy et al., 2005). The disadvantage of the latter study is that HeLa cells are an immortal cervical carcinoma cell line and do not represent normal primary fibroblasts. Several batches of a rabbit polyclonal anti-p62 (SQSTM1) antibody were purchased from the manufacturers (MBL International Corporation -rabbit polyclonal, PM045). During the commencement of immunocytochemistry work with p62, it was noted that different lots of this antibody resulted in different distributions of p62 in SDFT fibroblasts. Staining with lots 14 or 15 was found to have a strong nucleolar distribution with some cytoplasmic speckling (Figure 5-8A). The DAPI stain is typically excluded from nucleolar regions which, ordinarily allows their identification in primary cells (Armstrong et al., 2001). The p62 staining pattern was implicated as being nucleolar as p62 was located within DAPI negative nuclear regions only (Figure 5-8B). In contrast, no nucleolar staining was evident with lot 16 and only cytoplasmic staining of p62 could be seen (Figure 5-8C). When the equine SDFT fibroblasts were serum starved (1% fetal bovine serum for 48hrs) there was an increase in the expression of p62 at cytoplasmic puncta which indicates the accumulation of p62 (bound to protein and organellar waste) in autophagosomes (Bjørkøy et al., 2005).

Two different anti-p62 antibody lots were used in a western blot to look for differences in the banding pattern of p62. Multiple bands can indicate multiple target proteins (i.e. isoforms), cross-reactive proteins, post-translational modifications of the same target protein, denaturation and/or aggregation of the protein (Burry, 2010a). Western blots generated from the two anti-p62 antibody lots were compared. The western blot from lot 14 generated

multiple bands clustered between the 64 and 51kDa markers (Figure 5-9). Two higher molecular weight species were also seen at and above the 97kDa marker. There was a similar banding pattern for lot 16, with a strong band at 51kDa and another below the 64kDa marker (Figure 5-9). The two higher weight bands at 85kDa and 97kDa were also visible as well as an even higher molecular weight species (around 191kDa). The high weight species may represent aggregated p62, ubiquitinated p62 or even SDS stable dimers of p62 as the molecular weight of this protein is 47kDa (Bartlett et al., 2011). The most likely explanation for multiple bands of p62 in the western blots is the presence of cross reactive proteins.

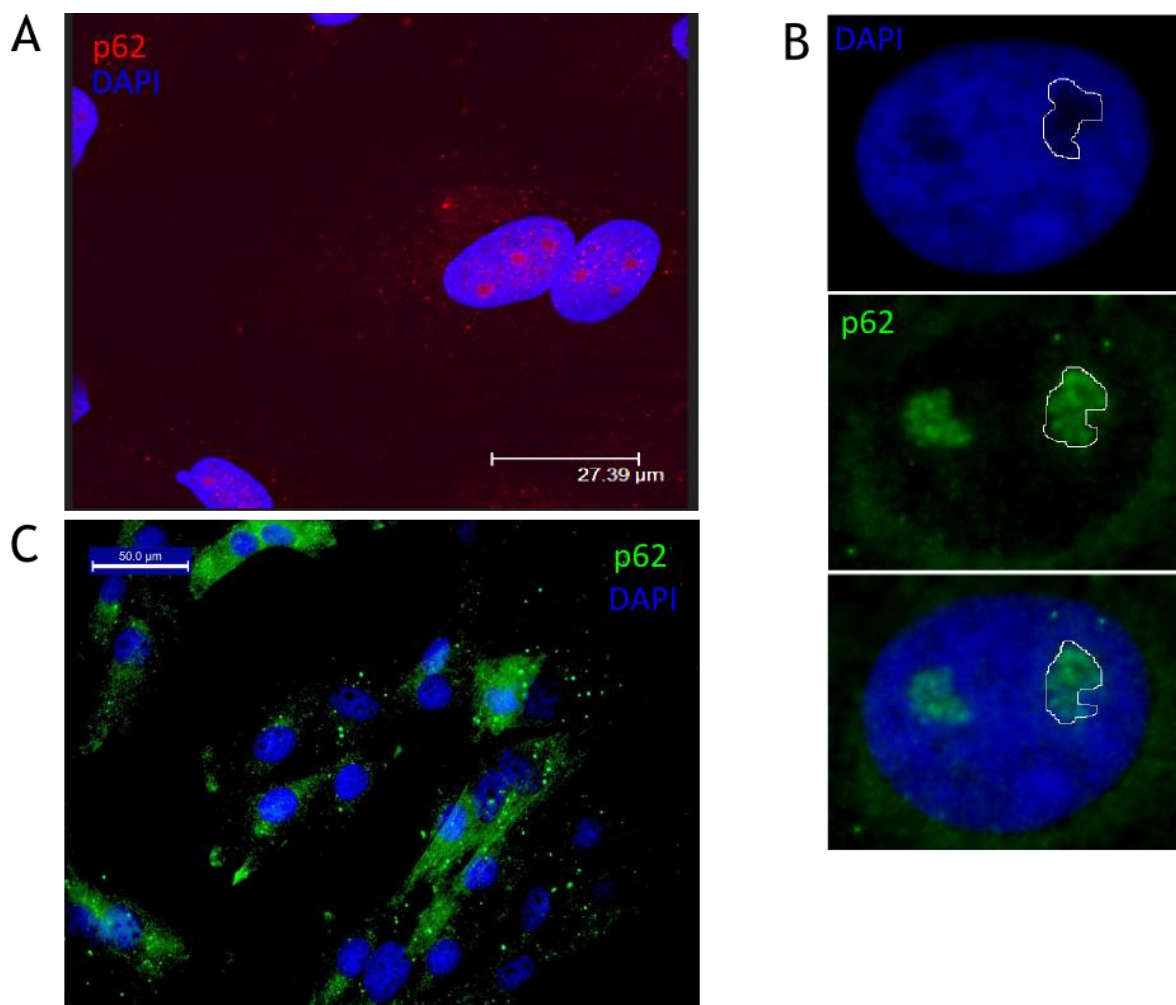


Figure 5-8 The distribution of p62 in SDFT fibroblasts stained with anti-p62 antibody is dependent on batch

SDFT fibroblasts stained with lot 14 or lot 15 anti-p62 antibody by immunocytochemistry showed a predominately nucleolar stain (Image A). Image B shows the overlay of p62 in the nucleolus (outlined in white line). Lot 16 anti-p62 antibody did not show any nucleolar staining and was predominately cytoplasmic (Image C).

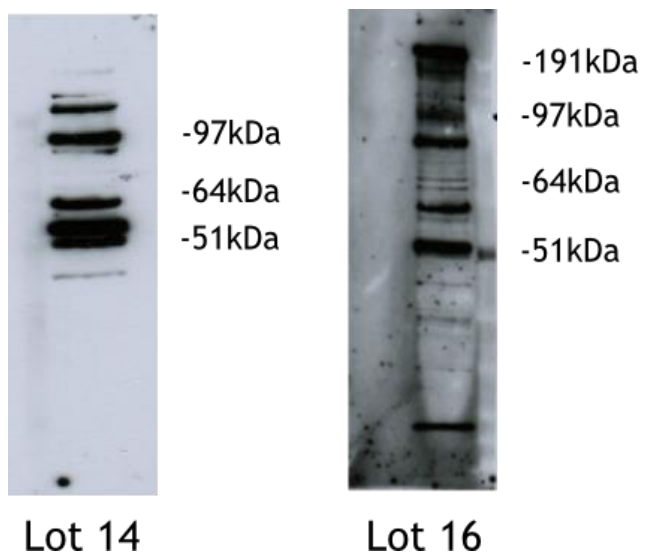


Figure 5-9 A similar banding pattern of p62 protein in a western blot when two anti-p62 antibody batches were used

A western blot was carried out on a single RIPA buffer lysate generated from SDFT fibroblasts to examine the banding pattern of p62 when two different anti-p62 antibody lots were used.

5.2.6 Bortezomib, a proteasomal inhibitor induced the translocation of p62 from the nucleus into the cytoplasm

To determine whether the p62 antibody is able to detect the correct antigen, a functional test was chosen to see if it corresponded with the action of p62 in cells. The increased expression of p62 in cells is typically linked to protein handling stress. To induce a protein handling stress in the cytoplasm, the cells were exposed to bortezomib, a proteasomal inhibitor, which leads to the accumulation of lysine-48 linked polyubiquitinated proteins (Jia et al., 2012). Proteasome inhibition is a useful methodology to generate a transient population of ubiquitinated species in the cell; this population is then ordinarily targeted by p62 for autophagic turnover. Translocation of p62 from the nucleus into the cytoplasm has been shown to occur in L1236 cells (Hodgkin lymphoma cell line) following treatment with bortezomib (R.Dean, pers comm). To test whether the p62 immunopositive material in tenocyte nuclei was responsive to proteasome inhibition, bortezomib was administered at a range of doses (1nM, 5nM, 10nM and 100nM) to SDFT derived monolayers cultured on collagen coated glass coverslips. Following an overnight treatment with bortezomib, the cells were fixed and stained for p62 antibody.

p62 was predominately localised to the nucleoli in control cells (Figure 5-10A). At the lowest dose (1nM) of bortezomib, the p62 signal was present in the nucleoli, however small speckles could be seen throughout the cytoplasm in the vast majority of cells (Figure 5-10B). The cytoplasmic speckles most likely represent the expression of p62 at the autophagosomes (Bjørkøy et al., 2005). At 5nM of bortezomib, the cytoplasmic speckles increased in size (Figure 5-10C). At higher doses of bortezomib, at 10nM and 100nM, large peri-nuclear aggregates of p62 was visible in SDFT fibroblasts (Figure 5-10D and Figure 5-10E respectively). The expression of p62 in the cytoplasm was dependent on the dose of bortezomib and was shown to increase with higher concentrations of the drug. This data indicates that this antibody detected the correct p62 protein, although more tests would need to be carried out, such as the knock -out of the p62 protein in cells. The latter was not completed due to a lack of finances.

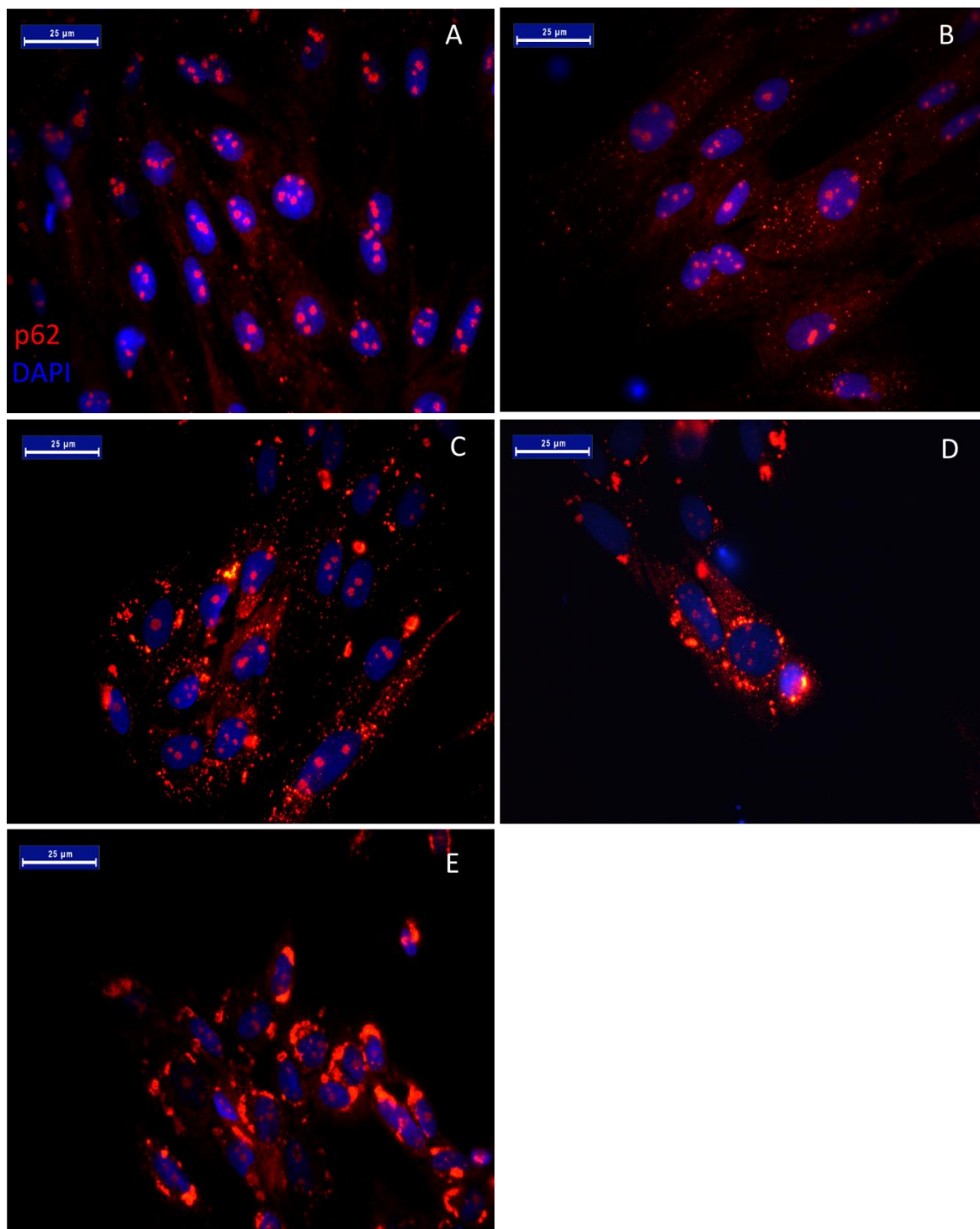


Figure 5-10 The administration of bortezomib provokes p62 expression in the cytoplasm at the expense of the nuclear fraction.

Untreated control SDFT fibroblasts (maintained at 37°C) (Panel A) were compared with SDFT fibroblasts treated with a range of bortezomib doses 1nM (Panel B), 5nM (Panel C), 10nM (Panel D), 100nM (Panel E) to determine the localisation of p62 in the cells.

5.2.7 p62 expression is increased in chronic SDFT lesions.

p62 has been implicated as a proteotoxic cell sensor in a number of degenerative diseases including Alzheimer's disease (Zheng et al., 2011), (Schaeffer et al., 2012), (Salminen et al., 2012), (Du et al., 2009b). The exposure of the SDFT to repetitive exercise associated factors such as heat stress may lead to an increase in protein damage and subsequent p62 expression. To determine whether there was an increase in the expression of p62 in injured SDFT, two SDFT tendons with chronic lesions of several weeks to several months duration were immunostained for p62 by immunohistochemistry. The history of the tendon lesions was unknown for both horses.

Both horses displayed the typical features of chronic lesions in SDFT tendons. There was expansion of the endotenon by differing numbers of small blood vessels. The endotenon contained a few mononuclear cells particularly macrophages and lymphocytes. The adjacent tendon matrix was aligned in a longitudinal axis with minimal loss of collagen fibril alignment. The matrix was highly cellular and the tendon fibroblasts were quite plump with double the amount of cytoplasm than normal cells. The latter cells may represent activated fibroblasts, type 2 tenocytes (Chuen et al., 2004), (Stanley et al., 2007). The severity of the lesions in one of the horses was greater. The tendon matrix of this horse contained areas of acellularity. An example of a chronic SDFT lesion can be seen in Figure 5-11B (This section was retrieved from the horse with the more severe lesion.) This lesion was compared with a section from normal SDFT where the tendon fibroblasts were shown to be oriented longitudinally and the thin, spindle shaped fibroblasts were also sparse within the tendon matrix (Figure 5-11A).

The expression of p62 was predominately nuclear in both horses with some cytoplasmic staining. p62 positive staining was particularly prevalent in the horse with the more severe lesions. p62 positive cells were visualised throughout the lesion, in the tendon matrix and the expanded endotenon (Figure 5-11C). Within the tissue lesion, the connective tissue cells (pericytes) lining the blood vessels, the infiltrative fibroblasts, the small numbers of inflammatory cells and the resident tendon fibroblasts were all positive for p62.

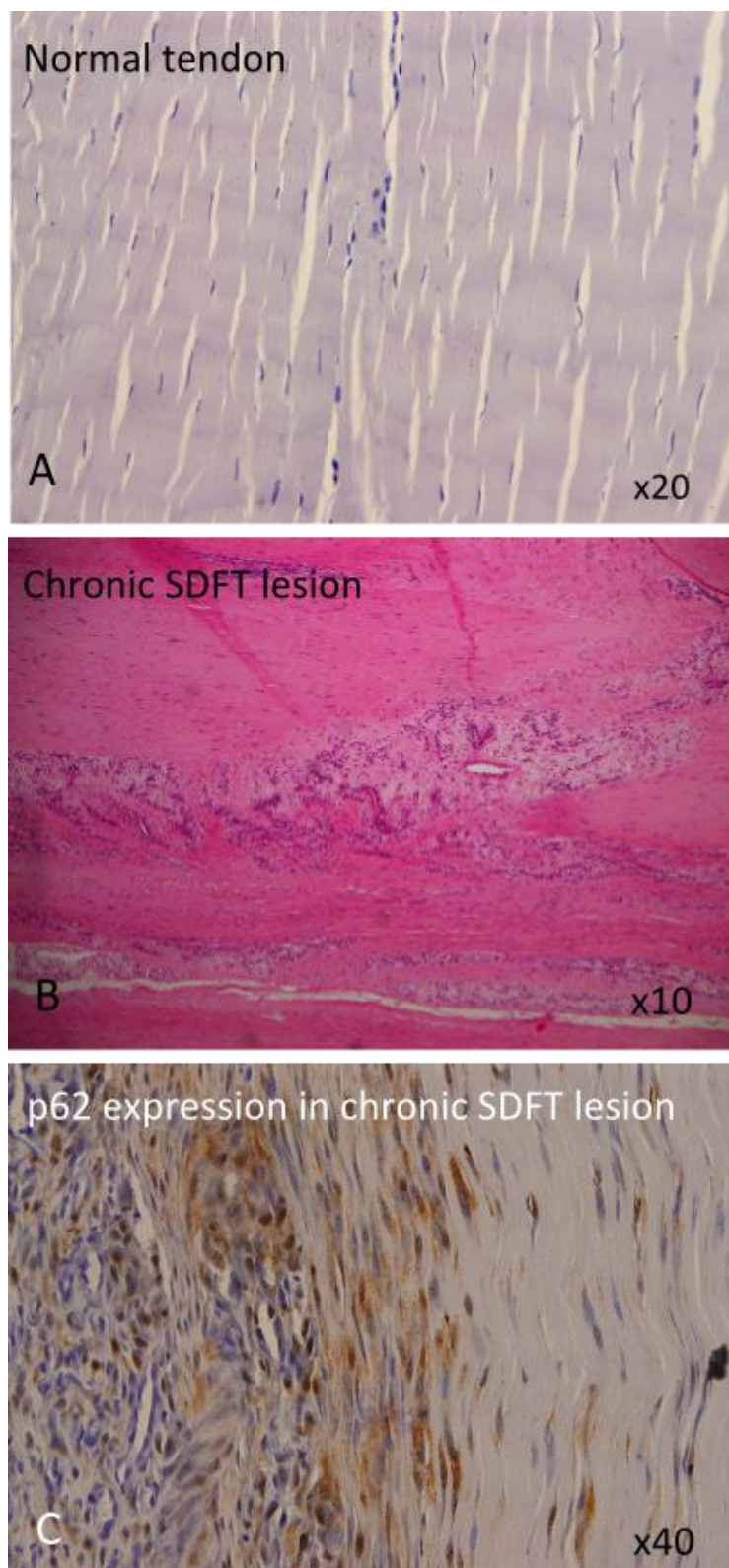


Figure 5-11 The expression of p62 in a chronic SDFT lesion

(A) A section taken from a normal SDFT. The normal tendon matrix shows the tendon fibroblasts aligned in a longitudinal orientation and the fibroblasts are sparse in number within the matrix. There are white tears in the tendon tissue and is the result of artefacts acquired during processing. Image shown at x20 magnification. (B) An H and E section of a chronic SDFT lesion. Image shown at x10 magnification. (C) The expression of positive p62 cells (brown) can be seen in the endotenon and the tendon matrix from the same lesion. Image shown at x40 magnification.

5.2.8 The addition of an exogenous anti-oxidant (N-acetyl cysteine) did not alter the expression or localisation of NRF-2 in SDFT cells

Exposure of cells to oxidative stress results in a cascade of events where p62 binds to cytoplasmic KEAP1, which prevents NRF-2 from being degraded by the proteasomes, allowing NRF-2 to translocate to the nucleus to participate in the transcription of antioxidants (Jain et al., 2010). The localisation of nuclear NRF-2 in cells could therefore indicate that these cells are undergoing a significant oxidative insult. To investigate this, the distribution of NRF-2 was examined by immunocytochemistry in SDFT fibroblasts.

In control SDFT fibroblasts, NRF-2 was predominately localised to the nucleus, although there was some cytoplasmic staining present (Figure 5-12A). This suggests the SDFT fibroblasts may be experiencing oxidative stress in the cell culture environment. The ROS may come from a variety of sources including high oxygen tensions or chemicals within the culture media which can be oxidised (Halliwell, 2003). The NRF-2 was also localised to cytoplasmic puncta and to plaques between SDFT fibroblasts, the latter potentially being sites of gap junctions. The addition of hydrogen peroxide, a source of reactive oxygen free radicals which would be expected to increase the nuclear expression of NRF-2, did not appear to alter the nuclear expression of NRF-2 in SDFT fibroblasts in comparison to the control cells (Figure 5-12B). However, when the expression of nuclear NRF-2 was quantified for both the control and hydrogen peroxide treated fibroblasts by Image J, there was a significant increase in the mean nuclear NRF-2 expression when hydrogen peroxide was added to the SDFT fibroblasts (P-value: <0.05) (Figure 5-13). Treatment with 1mM NAC, a ROS scavenger did not shift NRF-2 from its position in the nucleus (Figure 5-12C). Higher doses of NAC were not used as cellular proliferation and viability were compromised when doses greater than 1mM were used.

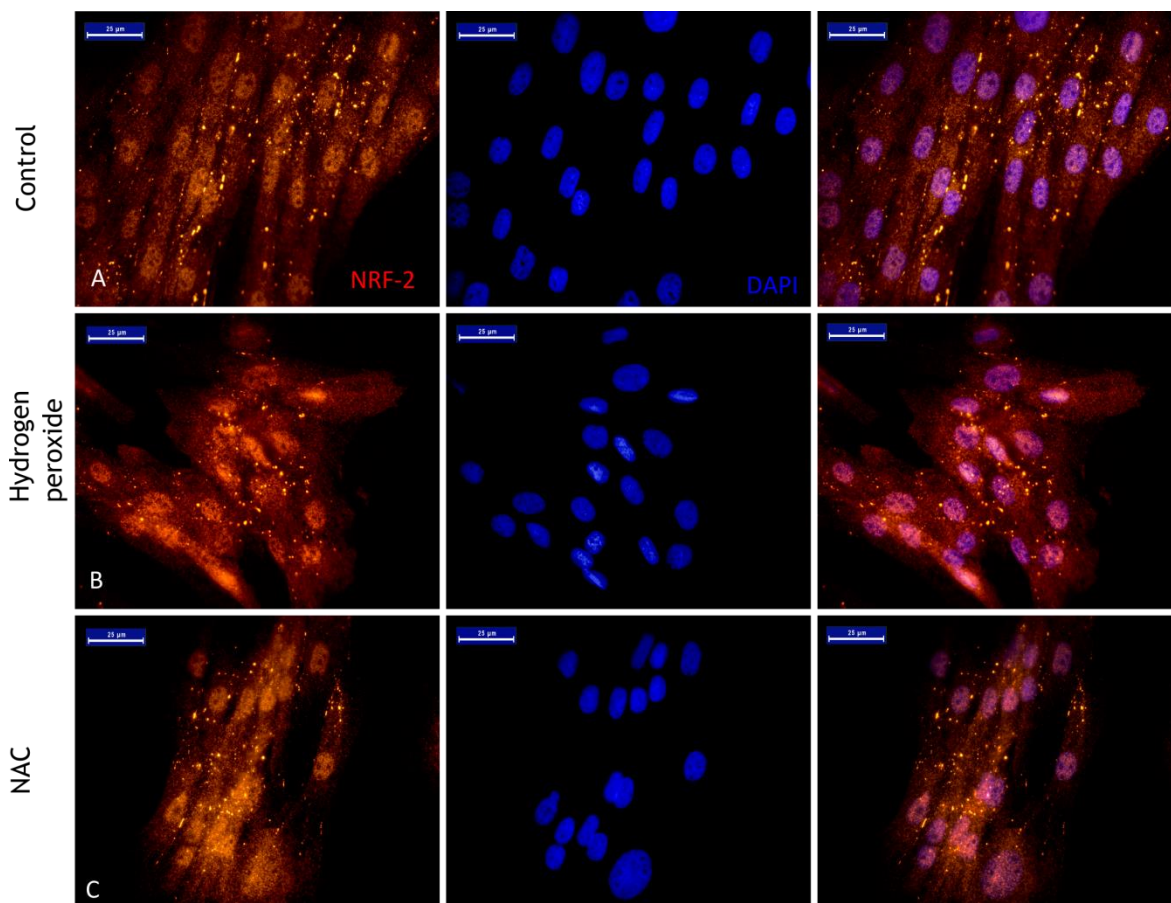


Figure 5-12 The addition of NAC does not alter the distribution of NRF-2

To determine the localisation of NRF-2 in control SDFT fibroblasts, the cells were immunostained for NRF-2 (red) and DAPI (blue). The far right panels show the merged images. The control group of SDFT cells was compared with two groups, one group of SDFT fibroblasts was treated with 200µM hydrogen peroxide and a third group was treated with 1mM NAC only. All data was retrieved from one horse with multiple images examined for each treatment group. Images shown at x63 magnification. Scale bar: 25µm

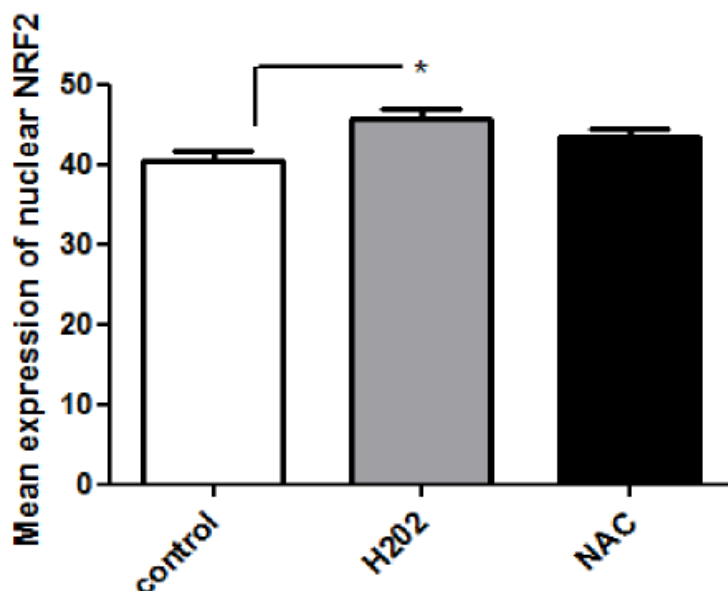


Figure 5-13 Measurement of NRF-2 expression in SDFT fibroblasts

Bar graph depicting the mean nuclear NRF-2 expression in SDFT fibroblasts. Control SDFT fibroblasts were maintained at 37°C. A separate group of SDFT fibroblasts were exposed to 200µM hydrogen peroxide. A third group of SDFT fibroblasts were treated with 1mM NAC only. Data was collected from the one horse. Multiple technical replicates were taken (x75) for each treatment group. To detect whether there were any statistical differences in the expression of nuclear NRF-2 between the control and the two treatment groups, the Kruskal Wallis test was employed. The expression of NRF-2 was higher in the hydrogen peroxide treated group in comparison with the control (P-value: <0.05). Error bars represent the standard error.

5.2.9 Co-localisation of NRF-2 and Cx43 was seen at gap junctions and other intracellular sites

In the last section, plaques of positive NRF-2 expression were visible between cells, potentially in areas where gap junctions are located. To see if Cx43, one of the proteins which make up the gap junction structure, co-localised with NRF-2, a double immunocytochemistry stain was performed. There was a very strong relationship between NRF-2 and Cx43, as NRF-2 was not only present at gap junctions, it also co-localised with many of the intracellular Cx43 cytoplasmic speckles (Figure 5-14).

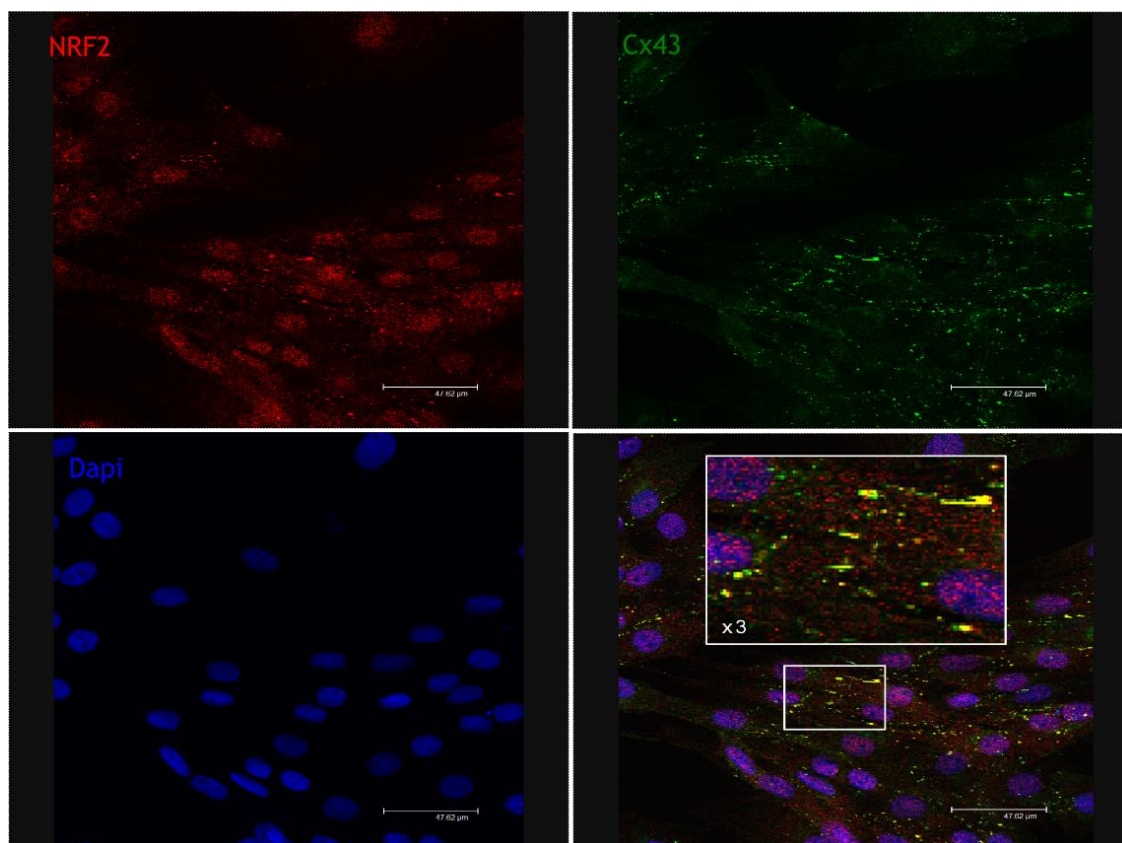


Figure 5-14 Co-localisation of NRF-2 at gap junction plaques and Cx43 foci

SDFT fibroblasts were co-immunostained for NRF-2 (red), Cx43 (green) and DAPI (blue). There was strong co-localisation of NRF-2 with Cx43, at gap junctions and Cx43 foci in the cytoplasm. The merged Cx43 and NRF-2 foci appear yellow. To show the co-localisation of Cx43 and NRF-2 more clearly, an insert box has been added with x3 magnification of the small white box below it. Images shown at x63 magnification. Scale bar: 47.62 μ m.

5.3 Discussion

5.3.1 DAXX re-localisation into the nucleoplasm occurred rapidly during heat shock in SDFT fibroblasts

One of the main aims of this section was to determine whether equine DAXX redistributes from nuclear puncta (thought to be PML NB) into the nucleoplasm during heat shock as has been shown in human cells. This stress response is conserved in equine tendon fibroblasts as DAXX dispersal into the nucleoplasm occurred as early as 3 mins of heating at 43°C where there was a slight decrease in DAXX puncta expression. At 10 mins of heating, in the majority of cells, there was very little DAXX punctate expression. These experiments show that this stress response was very rapid in equine tendon fibroblasts. In human HEP-2 cells, the first recorded time point of DAXX dispersal occurred at 12 mins of heating at 42°C, therefore it is possible that loss of DAXX into the nucleoplasm could take place at a much earlier time (Nefkens et al., 2003). DAXX re-expression of nuclear puncta was equally rapid in SDFT fibroblasts and took place as early as 10 mins post heating. Likewise, the first recorded time point of DAXX re-localisation to the PML NB in HEP-2 cells is 30-45 mins post heating (Nefkens et al., 2003). Again, this response could be even earlier in human cells as was demonstrated in equine tendon fibroblasts.

The rapid re-localisation of DAXX to nuclear puncta following heat shock was a useful marker of the cellular response to a mild heat shock. Future studies will be required to determine whether the distribution of DAXX can be used to predict cell fate when lethal temperatures are used, as failure of re-localisation of DAXX to nuclear puncta and/or re-localisation to the cytoplasm may indicate a threshold dependent response to heat stress. Re-localisation of DAXX to the cytoplasm is thought to be associated with pro-apoptotic pathways including ASK1 mediated cell death that is closely linked with the JNK signal transduction pathways (Ko et al., 2001), (Song and Lee, 2003).

We sought to determine whether DAXX re-localisation was stress-adaptable i.e. that there would be retention of DAXX at nuclear puncta during a second heat shock. My work demonstrated that DAXX re-localisation into the nucleoplasm is part of the constitutive heat shock response and not stress

adaptable as DAXX re-localisation into the nucleoplasm took place with a subsequent heat shock.

It was predicted that DAXX dispersal from nuclear puncta would be inhibited with a second heat shock as studies have shown that increased levels of Hsp-90 and Hsp-70 negatively regulate HSF-1 trimer formation and its subsequent transactivation capacity (Shi et al., 1998), (Baler et al., 1992), (Åkerfelt et al., 2010). It is possible that two heat shock episodes were not enough to generate a negative feedback response in equine tendon fibroblasts. Future work could investigate whether a larger number of heat shock episodes are required for a negative feedback effect to be instituted in these cells, possibly leading to DAXX retention at nuclear puncta. All of my results were obtained from one horse and much more extensive work would be required to determine for example whether DAXX translocates as rapidly from nuclear puncta into the nucleoplasm in a larger population of animals.

McDonough et al, 2009 identified reduced levels of soluble nuclear DAXX in heat shocked mouse embryonic fibroblasts, an effect markedly enhanced by its interaction with CHIP (carboxyl terminus of Hsc/Hsp-70 interacting protein). CHIP was found to regulate the assembly of non-canonical ubiquitin chains which renders DAXX insoluble and resistant to proteosomal degradation. This process was transient, allowing DAXX to return to 'control' levels of soluble protein within 30 mins. These data agree with our findings of DAXX re-expression as nuclear puncta following heat shock (McDonough et al., 2009). Interestingly, this group has also demonstrated CHIP bound to DAXX on its amino terminus preventing the interaction of HIKP2 (homeodomain-interacting protein kinase 2) with DAXX which is known to phosphorylate serine 46 on p53, a known activator of the apoptotic pathway (McDonough et al., 2009). Future research would be required to investigate DAXXs' interaction partners in the nucleoplasm of equine cells to identify how its activity is regulated during heat shock. Understanding how DAXX is regulated during heat shock could allow manipulation of this pathway to be undertaken with the ultimate aim of protecting susceptible SDFT cells from injury.

5.3.2 DAXX puncta size increased with cold shock in SDFT fibroblasts

My experiments provide evidence that DAXX re-localisation into the nucleoplasm did not occur during cold shock as DAXX puncta size was quantifiably increased at 15 mins and 30 mins of cold shock at 26°C. This finding has not been shown before in human or equine studies. The limitation of this work was that it was based on data from one horse. Larger scale experiments would be required to validate whether this is a significant biological response to cold shock.

The reason for the increase in DAXX puncta size is unknown. DAXX has the ability to interact with SUMO non-covalently through a C-terminal SUMO interacting motif (SIM) and the SIM of DAXX is required for its association with SUMOylated PML and localisation to the PML NBs (Lin et al., 2006). Treatment of human cells (U373MG cells, an astrocytoma cell line) with arsenic trioxide has been shown to increase the expression of SUMOylated PML leading to a subsequent increase in size of the PML NBs (Maroui et al., 2012). An increase in SUMOylated PML in turn has been shown to activate the recruitment of DAXX to the PML NBs (Lin et al., 2006). There is some difference of opinion on the role of DAXX function once targeted to the PML NBs. A recent study showed that sorbitol treatment of cells led to CK2 kinase mediated phosphorylation of DAXX SIM resulting in DAXX SUMOylation and increased interaction with SUMOylated proteins. The authors concluded that the recruitment of SUMOylated DAXX to the PML NB resulted in the repression of anti-apoptotic genes thus sensitising the cells to stress induced apoptosis (Chang et al., 2011). In my own work, there was no evidence of cell death in the equine tendon fibroblast monolayers during cold exposure making this scenario unlikely, although repression of other genes may be possible. Finally, Maroui and coworkers have shown that following the treatment of U373MG cells with arsenic trioxide, the SUMOylation of PML and its SIM are required for its interaction with RNF4 (RING (Really interesting New Gene) Finger Protein 4), ubiquitination of PML, recruitment of proteasome components to the PML NBS and proteasomal degradation of PML isoforms (Maroui et al., 2012). This suggests that proteasomal degradation of PML and potentially DAXX could take place at the PML NBs.

The translation of proteins has been shown to be minimised during cold shock with only enough production of essential proteins taking place to allow the cell to function in hypothermic conditions (Dresios et al., 2005). One of the proteins responsible for the regulation of protein translation during this time is RBM3 and in chapter 4 of this thesis, the up-regulation of RBM3 in SDFT fibroblasts first occurred in the first hour of cold shock at 26°C. Retention of DAXX at the PML NBs may be essential for inhibition of its transcriptional activities in cells to allow RBM3 and other cold shock proteins to regulate protein translation during the hypothermic period. Future work will be required to determine the fate of DAXX at the PML NB during the first 30 mins of cold shock. For example, DAXX may be targeted for proteasomal degradation or may undergo transcriptional silencing of its promoter genes.

5.3.3 p62 in injured tendons may be associated with the healing response

My experiments demonstrated up-regulation of p62 in a SDFT lesion with significant scar tissue and enlarged endotenon. Hosaka and coworkers have previously shown immunopositive staining of four cytokines (IL-1 α , IL-1 β , TNF- α , IFN γ) in tenocytes, endothelial cells and vascular epithelial cells in injured equine SDFT (Hosaka et al., 2002). The distribution of p62 positive cells in my work matched the same set of cells in Hosakas' research. p62 has been shown to participate strongly in the regulation of cytokine release (Lee et al., 2011) and also acts as an adaptor protein, linking protein kinase pathways, such as aPKCs (atypical protein kinase C) to TRAF-6 which activates the release of NF- κ B, a major transcription factor involved in the activation of pro-inflammatory cytokines including TNF- α , IL-1 β and IL-6 (Sanz et al., 2000), (Lee et al., 2011), (Tak and Firestein, 2001).

A study using siRNA against p62 in human keratinocytes found there was significant inhibition of the release of inflammatory cytokines in response to MALP-2, a stimulator of TLRs (Toll-like receptors) which are key recognition molecules on the cell surface responding to extraneous stimuli including antimicrobial pathogens. Interestingly, knocking out p62 also reduced the proliferation and cell cycle progression of keratinocytes via reduced phosphorylation of Akt and expression of cyclin D1/Cdk4 respectively (Lee et al.,

2011). It is possible therefore that the presence of p62 in the scar tissue and endotenon of equine tendon could be instrumental in the healing response to injury. Indeed, a number of cytokines play an active role in the healing of equine tendons, for example, TGF- β 1 is secreted by the vascular cells and fibroblasts of the endotenon during the initiation of the inflammatory phase where it encourages matrix gene expression and cellular proliferation and its effects can last for up to 24 weeks (Dahlgren et al., 2005b). Immunohistochemistry studies would be required to confirm whether p62 and various cytokines (TGF- β , IL-1 α , IL-1 β , TNF- α , IFN γ) are produced from the same cell types outlined above by staining equine tendon sections from the same lesion. A limitation of this work was the small sample size and only being able to retrieve tendon biopsy sections from horses with chronic lesions. Early phase tendinopathy lesions are most commonly asymptomatic in both horses and humans and for this reason when biopsy sections are studied from symptomatic equine patients, the material often represents chronic tendinopathy lesions (Millar et al., 2010).

5.3.4 Validation of p62/SQSTM1 antibody

A large component of this section was spent in the validation of our p62 antibody. The distribution of p62 in equine SDFT fibroblasts differed with different batches of p62 antibody, one being predominately nucleolar (lot 14 or 15) and the other cytoplasmic (lot 16). A western blot from the two different p62 antibody lots revealed multiple bands for both antibodies. Reasons for these bands could be due to multiple isoforms, post-translational modifications of the same target protein and aggregation of the protein. The most likely reason was thought to be due to cross-reactive proteins.

Polyclonal antibodies are commonly used in immunocytochemistry work because they are inexpensive to produce and the technology and skills required for their production is not high. They are created when an injection of an antigen into an animal generates a number of different B cell clones which produce antibodies to different epitopes. As living animals only have a finite life, when different animals are injected with the same antigen, the exact epitopes generating antibodies will be different. Additionally, shared epitopes on different proteins may target a protein that is not the antigen of interest. Either of these reasons could explain the differences in my experimental results

(Burry, 2010b). The p62 used in my work was a polyclonal rabbit antibody. Attempts to use a monoclonal mouse antibody failed as no immunopositive reactions to p62 with this antibody were detected in equine SDFT fibroblasts. Due to differences in the distribution of p62 between batches of antibodies, a functional test was carried out (treatment of SDFT fibroblasts with bortezomib to induce a protein handling stress in cells which then activates p62 expression in cells) to determine whether the antibody being used was indicative of p62/SQSTM1 function. The test demonstrated there was every indication that the antibody was detecting the correct p62/SQSTM1 protein as p62 was shown to localise to cytoplasmic puncta which was thought to represent autophagosomes where ubiquitinated proteins are sent to be degraded. Future experiments are required to confirm the presence of autophagosomes alongside p62. Subsequent work by our research group has verified the validation of the same p62/SQSTM1 antibody in equine tendon fibroblasts by knocking out the p62 protein (pers comm, T.Rich).

5.3.5 The localisation of NRF-2 in the nucleus in SDFT fibroblasts was indicative of oxidative stress in vitro

The presence of nuclear NRF-2 in SDFT fibroblasts suggested these cells were undergoing a significant oxidative insult, which was not ameliorated by the addition of an exogenous anti-oxidant agent (NAC). The cell culture environment is strongly suspected to be the cause of the oxidative insult in SDFT fibroblasts. It is not surprising that the SDFT fibroblasts were sensitive to ROS, as these fibroblasts typically reside in an avascular tissue where oxygen levels are not thought to exceed 2-3% (Wright and Shay, 2006), (Zhang et al., 2010b). The reasons for the poor protective ability of NAC may be due to its being an irrelevant protectant and/or the concentration used was insufficient for anti-oxidant protection to take place. Two investigators have shown that it is possible to prevent ROS mediated oxidative DNA damage upon the addition of an anti-oxidant (Yedjou et al., 2010), (Baumeister et al., 2009). Li and coworkers demonstrated a reduction in the translocation of NRF-2 into the nucleus when NAC was added to RAW 264.7 cells (mouse leukaemic monocytic macrophage cell line) after being treated with diesel exhaust particles, a potent oxidant (Li et

al., 2004). The localisation of nuclear NRF-2 was therefore a useful indicator of oxidative stress in SDFT fibroblasts. This data was based on a small sample size, however when collated with the data in chapter 3, it does suggest the need to re-design cell culture protocols for the culture of tendon cells including the use of low oxygen tensions or changing the media type as DMEM (the media used in our studies) contains high levels of iron III nitrate, a pro-oxidant chemical (Halliwell, 2003).

5.3.6 NRF-2 co-localisation with Cx43 protein in SDFT fibroblasts

One surprising finding was the co-localisation of NRF-2 to Cx43 proteins intracellularly and at gap junction plaques. There has been very little work on the link between NRF-2 and gap junctions. One of the major functions of gap junctions is in the transmission of intracellular ions, amino acids, nucleotides and second messengers (e.g. Ca^{2+} , cAMP, cGMP, IP_3) between cells (Goldberg et al., 2002), (Fry et al., 2001). During periods of cellular stress, gap junctions can propagate the spread of cell fate modulators between cells (the bystander effect) which can result in cell death or survival (Lin et al., 1998), (Krysko et al., 2004), (Yasui et al., 2000), (Krysko et al., 2005). The SDFT fibroblasts may be communicating with each other to promote cellular survival whilst experiencing an oxidative insult as no cell death was visualised in the monolayers during the experimental work. Future research will be required to investigate the role NRF-2 plays in Cx43 and/or gap junction expression or signalling.

In summary, DAXX was shown to translocate from nuclear puncta into the nucleoplasm in response to heat shock but NOT cold shock and DAXX release into the nucleoplasm is part of the 'constitutive' heat shock response. p62 was shown to be up-regulated in both the endotenon and the tendon matrix of a chronic SDFT lesion. SDFT fibroblasts were thought to be exposed to a significant oxidative insult in vitro as NRF-2 was predominately found in the nucleus, a marker of oxidative stress in cells. The addition of NAC, an anti-oxidant did not alter NRF-2 distribution away from the nucleus. Additionally, we also discovered co-localisation of NRF-2 at gap junctions, the role of which could be investigated in future studies. The main limitation of my work was the small sample size used in my experiments.

Chapter 6) Limitations of the research in this thesis

There were a number of limitations associated with my research and they have been outlined below. All of these limitations would have had an influence on the biological significance of my work and future research will require a larger number of animals to verify portions of my work.

1) Small tendon sample size

One of the biggest limitations of my thesis was the low numbers of horse tendons used in my experimental work. As tendon injury is common in Thoroughbred racehorses between the ages of 2-7, it was my aim to obtain horse tendons within this target population. However, it was very difficult to find horse tendons that fitted these criteria because of location (few Thoroughbred horses were available in Scotland) and the specificity of the target population. At the start of my PhD, I obtained horse tendons of varying breeds and ages from Weiper's Equine Clinic at the University of Glasgow which allowed me to practice on the methodology of extracting fibroblasts from SDFT tendons. I was lucky to obtain a couple of tendon samples from two TB racehorses that fitted the correct criteria. However, very small numbers of TB horses were available from the University of Glasgow and as a result of this, I had to look further afield.

2) Long transport time prior to processing of samples

I was able to obtain another couple of TB racehorse tendons that fitted the above criteria from an abattoir in Cheshire. As there were no laboratory facilities nearby, the horse tendons had to be transported back to Glasgow in an ice box to help minimise tissue breakdown post mortem. The ice box helped to preserve the tendon tissues, however it is possible that the effects of the long journey between Cheshire and Glasgow (approx. 5 hours) may have had an underlying influence on the cells in situ (although the cells were processed immediately upon arrival). There is some evidence to suggest this may be the case as subsequent research work completed by the University of Glasgow horse tendon research group demonstrated that there was a higher percentage of large γ H2AX puncta (associated with DNA damage) in fibroblasts sourced from the

abattoir in comparison with cells that had been processed from the post mortem room straight away (Rich et al., 2013).

3) Lack of history associated with TB horses sourced from the abattoir

Another limitation of the use of tendon fibroblasts sourced from the abattoir was the lack of history associated with each animal. It was unknown whether the TB horses had ever experienced racing, and if they had, what that history involved (such as distance, intensity of the racing and their standing in the races) or furthermore, whether they had had any prior forelimb tendon injuries.

4) Lack of tendon archive containing tendon lesions with differing severity

Only small numbers of horse tendons could be processed at one time, leading to difficulty in obtaining an archive of tendon lesions with a range of disease severity. Being able to stain tendon lesions with differing severity by immunohistochemistry would have been useful for certain components of this work such as the distribution and intensity of p62 in vivo.

5) Low statistical significance of my research due to small sample size

Low numbers of tendon samples, control samples and replicates in my research will have had a negative impact on the statistical significance of portions of my work. A larger sample size would have increased the significance of my results as it would have been more likely to accurately reflect the biological response from a bigger population of animals (Kalla, 2009). A higher number of samples in my work would have also reduced the likelihood of Type I and Type II errors where you are more likely to obtain a false positive or a false negative result respectively (Shuttleworth, 2008). A much larger number of animals will therefore have to be used in future experiments to investigate the

significance of my research for example; Does the culture of SDFT fibroblasts on fibronectin consistently lead to high levels of DNA damage in ambient oxygen?

6) Sourcing the correct heating apparatus suitable for my work

Another big limitation of my research was the amount of time spent on finding the most appropriate heat shock apparatus for my research. Investigation of the literature revealed there was no set method for the calibration and heating of the media in which the cells are bathed in. As a result of this, it took more than a year to find a heating rig that was not costly, easy to use, accurate and most of all, reproducible. This valuable time could have been spent in the acquisition of more data for my experimental research, however the work looking into heating apparatuses proved useful as it opened up the pitfalls of the lack of temperature calibration in research in general. In an ideal world, I would have formed a collaboration with a structural engineer to help me design a good heating rig suitable for my research at an early stage of my thesis.

5) Ideal scenario for completing my research

If the work could have been completed in an ideal fashion, a group of age matched live horses would have been purchased (e.g. 10 control animals and 10 experimental animals) and housed in stables at the University of Glasgow. The group of experimental horses would then be subjected to a set exercise regime using treadmills over a period of time. All the horses would then be humanely sacrificed (following the most appropriate welfare protocols) to obtain tendon samples for both in vitro and in vivo work. This method has a number of advantages including, a large sample number of both control and experimental animals, the history of each animal would be known (e.g. its exercise history as instituted by the treadmill regime) and better sample preservation post mortem. The disadvantages of this method would be the cost as it is expensive to buy horses and then house them for long periods of time. The time constraints of following this method would be far beyond the scope of a PhD.

Chapter 7) Conclusions and Future work

The SDFT is the most frequently injured tendon in racing Thoroughbred horses. Repetitive loading of the SDFT together with other exercise associated factors including hyperthermia are believed to overwhelm the tenocytes' reparative abilities, lead to dysfunction of the tenocytes' metabolic activities or contribute to cell death (Patterson-Kane et al., 2012). One of the main aims of this thesis was to investigate the sensitivity of SDFT derived fibroblasts to heat stress and to compare this with another tendon, the DDFT which is biologically and mechanically distinct. From this, we aimed to establish whether both heat and cold shock could be used to induce thermotolerance (a phenomenon associated with the induction of HSPs) in these cells. Additionally, another important aim was to find the most appropriate protein markers participating in the heat shock response in SDFT fibroblasts. Thus, from the latter two aims, the evolution of a number of preventative strategies to minimise cell death in vivo could be possible.

In Chapter 3, prior to the start of my heat shock investigations in SDFT and DDFT fibroblasts, the basal levels of DNA damage in these cells were quantified as the cell culture environment is known to be stressful to cells often leading to phenotypic drift and premature senescence (Yao et al., 2006a), (Burova et al., 2013), (Wright and Shay, 2002). My studies showed that the cell culture environment led to replication induced DNA damage in both SDFT and DDFT fibroblasts. The SDFT in particular was most susceptible to DNA damage when cultured on fibronectin in ambient oxygen conditions. This indicates the SDFT may be more susceptible to injury on a fibronectin matrix or alternatively, fibronectin has been suggested to potentiate the DNA damage response signalling in cells as it has been shown to increase stimulation of the phosphatidylinositol 3-kinase pathway which leads to phosphorylation of H2AX at the double strand break (De Wever et al., 2011).

One of the reasons for the high levels of DNA damage in SDFT fibroblasts was believed to be due to defective repair of DSB lesions. My data showed the SDFT showed comparable reparative abilities with the DDFT in response to genotoxic DNA damage. However, this does not equate to the repair of matrix

damage which may be sub-optimal especially in a tendon known to have low turnover of the ECM.

My findings indicate that the cell culture environment may need to be modified to lessen the effects of cell culture related DNA damage. The use of collagen matrices, low serum and/or confluency was introduced for all cellular experiments after chapter 3 in SDFT and DDFT fibroblasts to minimise replication induced DNA damage in these cells. My data was also based on the results from one horse and future work will require larger numbers of horses to determine the significance of my findings.

In Chapter 4, the Cell MicroControls heating rig was used for heating SDFT and DDFT fibroblasts in my research. This apparatus was found to be the most suitable for my work as it indirectly measured cell culture media temperature of the test dishes to 0.5°C accuracy. Most of the work reported in the literature does not describe any measurement or calibration of media temperature which raises the possibility that some published heat shock data may be inaccurate.

After exploratory work to determine a “lethal temperature” for tendon fibroblasts (52°C), my heat shock research showed that both SDFT and DDFT fibroblasts were able to survive a lethal heat shock when the cells were preconditioned with a sub-lethal heat shock. My data suggests the SDFT may be more susceptible to heat shock in comparison with the DDFT as cell loss was greater, however more work would be required to verify this finding. The SDFT is notoriously injury-prone in vivo and it would not be surprising to find these cells are more susceptible to heat shock related cell death in comparison with a non-injury-prone tendon.

The increased sensitivity of SDFT fibroblasts to heat stress related cell death may be caused by saturation of the lysosomes (which target damaged proteins for degradation) in response to protein damage caused by heat shock. In Chapter 3, it was shown that unheated SDFT cells had higher levels of lysosomal activity in vitro (as measured by the senescence associated beta galactosidase stain) in comparison with DDFT cells and foal SDFT fibroblasts. The reasons for these high levels of activity in unheated adult SDFT fibroblasts are unknown, however it is possible cell culture related stress may increase protein damage in

these cells and thus increasing the workload of the lysosomes. The accumulation of protein damage as a result of the cell culture related stress and heat shock may lead to saturation of the lysosomes.

The preconditioned cold shock SDFT and DDFT fibroblast (carried out prior to a lethal heat shock) experiments were completed separately from the respective unconditioned experiments. My data indicates that cold shock may have induced thermotolerance for up to 24 hours post heating in SDFT fibroblasts as the cell loss was not as great compared with the unconditioned cells. In contrast, no thermotolerance was induced in DDFT fibroblasts as the percentage of cell loss was similar for both the preconditioned cold shocked cells and the unconditioned cells. Future work is required to verify these findings. The reason for the induction of thermotolerance in SDFT fibroblasts was believed to be due to its ability to rapidly mobilise Hsp-72 protein in the early recovery period post cooling as shown in Figure 4-7, leading to a time associated accumulation of this protein in cells. It is possible that the use of colder temperatures (below 26°C) could be used to induce higher levels of Hsp-72 protein in these cells thus allowing the thermotolerance effect to last for longer than 24hrs. Severe cold shock temperatures were avoided in these experiments as studies in mouse organotypic hippocampal slice cultures have shown that temperatures as low as 17°C had detrimental effects in cells including cell death (Tong et al., 2013).

In Chapter 5, we investigated the distribution of protein markers involved in the heat shock response. In my studies, DAXX, a useful protein marker, was visualised in equine SDFT fibroblasts. DAXX was shown to disperse from nuclear puncta into the nucleoplasm during heat shock and this was reversible in the recovery period post heating. The re-localisation of this protein during heat shock was a useful marker of a mild heat shock response in equine tendon fibroblasts. The dispersal of DAXX was thought to be part of the constitutive heat shock response in equine tendon fibroblasts as re-shocking the cells a second time led to the same response i.e. re-localisation of DAXX into the nucleoplasm at the same time points. When the SDFT fibroblasts were cold shocked, the size of the DAXX puncta increased rather than decreased (due to heat shock related dispersal into the nucleoplasm) and the reasons for this were unknown. However it was thought to be associated with the recruitment of DAXX to the PML NBs to fulfil some function linked with the cold shock response.

Finally, in this chapter, up-regulation of p62 was shown in chronic SDFT lesions of a couple of Thoroughbred horses mostly in the tendon matrix and the endotendon of the tendon. The reason for the up-regulation of p62 was thought to be associated with the cytokine healing response of a healing tendon lesion, however future work will be required to investigate this further.

Future work could focus on:

Chapter 3

1) More research is required to investigate the ways of reducing replication induced DNA damage in equine tendon fibroblasts. One of the ways this could be achieved may be to seed cells on a “natural” matrix, on tendon slices taken from the tissue.

2) One of the limitations of this research was that the use of 2% oxygen would ideally have been introduced for all of the experiments (as 20% oxygen is non-physiological in vivo) but the expense of the appropriate oxygen tanks was too great. Finding another experimental set-up where low oxygen could be used relatively inexpensively would be useful.

Chapter 4

1) Improve the accuracy of temperature measurement by directly measuring media temperature in the dish where the cells are located. A possible design arrangement could involve the incorporation of a very thin thermistor onto the inner surface of the cell culture dish.

2) Find the most appropriate cold shock equipment where media temperature could be measured and calibrated easily.

3) Determine the cold shock temperatures which SDFT fibroblasts are able to withstand without inducing adverse effects on the cells as there may be greater expression of Hsp-72 protein at a colder temperature.

4) Examine whether cold shock has beneficial effects when applied post heating as studies in human stroke patients have shown that infarct size is smaller when cold shock is given after an ischaemic event (Shintani et al., 2011)

5) Compare markers of lysosomal activity and cell death in unheated and heated adult SDFT and foal SDFT fibroblasts (which had very little lysosomal activity) to see if there are differences in lysosomal activity between the two groups of cells and whether this could determine cell fate following heat shock. A lysosomal marker that could be used is the MagicRed™ cathepsin kit (AbD Serotec) which detects active lysosomal cathepsins, a protease enzyme (Pryor, 2012).

Chapter 5

1) Determine whether DAXX returns to the PML NBs following the application of a lethal heat shock. This protein marker may then be used to determine cell fate depending on its localisation in the cell at certain time points post heating.

2) Examine the interaction partners of DAXX during heat and cold shock and this will allow a fuller understanding of its function during this stress response.

3) Source a larger number of equine tendons with varying severity of lesions in the SDFT. One of the limitations of my work was the small sample size, especially for the immunohistochemistry work with p62 staining. Most of the early onset lesions in horses are asymptomatic and typically when lesions are found, they tend to be chronic in nature (often several weeks to months after the injury). Specimens from a tissue bank containing equine tendon lesions (of varying severity) are available from a tendon group at the RVC (The Royal Veterinary College) in London. If time had allowed, I would like to have examined some of these tendon sections of varying degrees of severity and stain them for p62 and other markers including cytokines.

In summary, my thesis has highlighted that SDFT fibroblasts are particularly susceptible to heat shock related stress in vitro. Further study of the

mechanisms of the heat shock response in these cells, such as with DAXX as a marker, could be used to devise and evaluate future treatments to prevent cell death in these cells as a result of heat shock. The induction of thermotolerance for 24 hours by a preconditioning cold shock was an interesting finding and could be of biological significance, however further work with a larger sample size are required to determine this.

Chapter 8) References

- ABRAMOFF, M. D., MAGALHAES, P. J. & RAM, S. J. 2004. Image processing with ImageJ. *Biophotonics International*, 11, 36-42.
- AHN, S.-G. & THIELE, D. J. 2003. Redox regulation of mammalian heat shock factor 1 is essential for Hsp gene activation and protection from stress. *Genes & Development*, 17, 516-528.
- AIELLO, S. E. 2012. The Merck Veterinary Manual for Veterinary Professionals. In: AIELLO, S. E. & MOSES, M. A. (eds.) *Reference Guides: Serum Biochemical Reference Ranges*. Whitehouse, NJ, USA: Merck Sharpe and Dohme Corp.
- ÅKERFELT, M., MORIMOTO, R. I. & SISTONEN, L. 2010. Heat shock factors: integrators of cell stress, development and lifespan. *Nat Rev Mol Cell Biol*, 11, 545-555.
- AL-FAGEEH, M. B. & SMALES, C. M. 2006. Control and regulation of the cellular responses to cold shock: the responses in yeast and mammalian systems. *Biochem J*, 397, 247-259.
- ALEXANDER, R. M. 2002. Tendon elasticity and muscle function. *Comparative Biochemistry and Physiology - Part A: Molecular & Integrative Physiology*, 133, 1001-1011.
- ALLEN, C. B., SCHNEIDER, B. K. & WHITE, C. W. 2001. Limitations to oxygen diffusion and equilibration in in vitro cell exposure systems in hyperoxia and hypoxia. *American Journal of Physiology - Lung Cellular and Molecular Physiology*, 281, L1021-L1027.
- ANANTHAN, J., GOLDBERG, A. & VOELLMY, R. 1986. Abnormal proteins serve as eukaryotic stress signals and trigger the activation of heat shock genes. *Science*, 232, 522-524.
- AONO, J., YANAGAWA, T., ITOH, K., LI, B., YOSHIDA, H., KUMAGAI, Y., YAMAMOTO, M. & ISHII, T. 2003. Activation of Nrf2 and accumulation of ubiquitinated A170 by arsenic in osteoblasts. *Biochemical and Biophysical Research Communications*, 305, 271-277.
- ARGÜELLES, D., CARMONA, J. U., CLIMENT, F., MUÑOZ, E. & PRADES, M. 2008. Autologous platelet concentrates as a treatment for musculoskeletal lesions in five horses. *Veterinary Record*, 162, 208-211.
- ARMSTRONG, S. J., FRANKLIN, F. C. H. & JONES, G. H. 2001. Nucleolus-associated telomere clustering and pairing precede meiotic chromosome synapsis in *Arabidopsis thaliana*. *Journal of Cell Science*, 114, 4207-4217.
- BAJT, M. L., LAWSON, J. A., VONDERFECHT, S. L., GUJRAL, J. S. & JAESCHKE, H. 2000. Protection against Fas Receptor-Mediated Apoptosis in Hepatocytes and Nonparenchymal Cells by a Caspase-8 Inhibitor in Vivo: Evidence for a Postmitochondrial Processing of Caspase-8. *Toxicological Sciences*, 58, 109-117.
- BALER, R., DAHL, G. & VOELLMY, R. 1993. Activation of human heat shock genes is accompanied by oligomerization, modification, and rapid translocation of heat shock transcription factor HSF1. *Molecular and Cellular Biology*, 13, 2486-2496.
- BALER, R., WELCH, W. & VOELLMY, R. 1992. Heat shock gene regulation by nascent polypeptides and denatured proteins: hsp70 as a potential autoregulatory factor. *The Journal of Cell Biology*, 117, 1151-1159.
- BALOGH, G., HORVÁTH, I., NAGY, E., HOYK, Z., BENKÓ, S., BENSAUDE, O. & VÍGH, L. 2005. The hyperfluidization of mammalian cell membranes acts as a signal to initiate the heat shock protein response. *FEBS Journal*, 272, 6077-6086.

- BANES, A. J., WEINHOLD, P. W., YANG, X., TZUZAKI, M., BYNUM, D., BOTTLANG, M. & BROWN, T. 1999. Gap junctions regulate responses of tendon cells ex vivo to mechanical loading. *Clinical Orthopaedics and Related Research*, 367, S356-S370.
- BARTLETT, B. J., ISAKSON, P., LEWERENZ, J., SANCHEZ, H., KOTZEBUE, R. W., CUMMING, R. C., HARRIS, G. L., NEZIS, I. P., SCHUBERT, D. R., SIMONSEN, A. & FINLEY, K. D. 2011. p62, Ref(2)P and ubiquitinated proteins are conserved markers of neuronal aging, aggregate formation and progressive autophagic defects. *Autophagy*, 7, 572-583.
- BATSON, E. L., PARAMOUR, R. J., SMITH, T. J., BIRCH, H. L., PATTERSON-KANE, J. C. & GOODSHIP, A. E. 2003. Are the material properties and matrix composition of equine flexor and extensor tendons determined by their functions? *Equine Veterinary Journal*, 35, 314-318.
- BAUMEISTER, P., HUEBNER, T., REITER, M., SCHWENK-ZEIGER, S. & HARREUS, U. 2009. Reduction of Oxidative DNA Fragmentation by Ascorbic Acid, Zinc and N-Acetylcysteine in Nasal Mucosa Tissue Cultures. *Anticancer Research*, 29, 4571-4574.
- BEERE, H. M., WOLF, B. B., CAIN, K., MOSSER, D. D., MAHBOUBI, A., KUWANA, T., TAILOR, P., MORIMOTO, R. I., COHEN, G. M. & GREEN, D. R. 2000. Heat-shock protein 70 inhibits apoptosis by preventing recruitment of procaspase-9 to the Apaf-1 apoptosome. *Nat Cell Biol*, 2, 469-475.
- BELLAMY, G. & BORNSTEIN, P. 1971. Evidence for Procollagen, a Biosynthetic Precursor of Collagen. *Proceedings of the National Academy of Sciences*, 68, 1138-1142.
- BELLMANN, K., CHARETTE, S., NADEAU, P., POIRIER, D., LORANGER, A. & LANDRY, J. 2010. The mechanism whereby heat shock induces apoptosis depends on the innate sensitivity of cells to stress. *Cell Stress and Chaperones*, 15, 101-113.
- BEREDJIKLIAN, P., FAVATA, M., CARTMELL, J., FLANAGAN, C., CROMBLEHOLME, T. & SOSLOWSKY, L. 2003. Regenerative versus reparative healing in tendon: a study of biomechanical and histological properties in fetal sheep. *Ann Biomed Eng*, 31, 1143 - 1152.
- BI, Y., EHIRCHIOU, D., KILTS, T. M., INKSON, C. A., EMBREE, M. C., SONOYAMA, W., LI, L., LEET, A. I., SEO, B.-M., ZHANG, L., SHI, S. & YOUNG, M. F. 2007. Identification of tendon stem/progenitor cells and the role of the extracellular matrix in their niche. *Nat Med*, 13, 1219-1227.
- BIEWENER, A. A. 1998. Muscle-tendon stresses and elastic energy storage during locomotion in the horse. *Comparative Biochemistry and Physiology Part B: Biochemistry and Molecular Biology*, 120, 73-87.
- BIRCH, H., WILSON, A. & GOODSHIP, A. 1997a. The effect of exercise-induced localised hyperthermia on tendon cell survival. *J Exp Biol*, 200, 1703-1708.
- BIRCH, H. L. 2007. Tendon matrix composition and turnover in relation to functional requirements. *International Journal of Experimental Pathology*, 88, 241-248.
- BIRCH, H. L., BAILEY, J. V. B., BAILEY, A. J. & GOODSHIP, A. E. 1999. Age-related changes to the molecular and cellular components of equine flexor tendons. *Equine Veterinary Journal*, 31, 391-396.
- BIRCH, H. L., RUTTER, G. A. & GOODSHIP, A. E. 1997b. Oxidative energy metabolism in equine tendon cells. *Research in Veterinary Science*, 62, 93-97.

- BIRCH, H. L., WILSON, A. M. & GOODSHIP, A. E. 2008a. Physical activity: does long-term, high-intensity exercise in horses result in tendon degeneration? *Journal of Applied Physiology*, 105, 1927-1933.
- BIRCH, H. L., WORBOYS, S., EISSA, S., JACKSON, B., STRASSBURG, S. & CLEGG, P. D. 2008b. Matrix metabolism rate differs in functionally distinct tendons. *Matrix Biology*, 27, 182-189.
- BIRK, D. E. & MAYNE, R. 1997. Localisation of collagen types I, III and V during tendon development. Changes in collagen types I and III are correlated with changes in fibril diameter. *European Journal of Cell Biology*, 189, 352-361.
- BJØRKØY, G., LAMARK, T., BRECH, A., OUTZEN, H., PERANDER, M., ØVERVATN, A., STENMARK, H. & JOHANSEN, T. 2005. p62/SQSTM1 forms protein aggregates degraded by autophagy and has a protective effect on huntingtin-induced cell death. *The Journal of Cell Biology*, 171, 603-614.
- BOATRRIGHT, K. M., RENATUS, M., SCOTT, F. L., SPERANDIO, S., SHIN, H., PEDERSEN, I. M., RICCI, J.-E., EDRIS, W. A., SUTHERLIN, D. P., GREEN, D. R. & SALVESEN, G. S. 2003. A Unified Model for Apical Caspase Activation. *Molecular Cell*, 11, 529-541.
- BOELLMANN, F., GUETTOUCHE, T., GUO, Y., FENNA, M., MNAYER, L. & VOELLMY, R. 2004. DAXX interacts with heat shock factor 1 during stress activation and enhances its transcriptional activity. *Proceedings of the National Academy of Sciences*, 101, 4100-4105.
- BONFANTI, L., MIRONOV JR, A. A., MARTÍNEZ-MENÁRGUEZ, J. A., MARTELLA, O., FUSELLA, A., BALDASSARRE, M., BUCCIONE, R., GEUZE, H. J. & LUINI, A. 1998. Procollagen Traverses the Golgi Stack without Leaving the Lumen of Cisternae: Evidence for Cisternal Maturation. *Cell*, 95, 993-1003.
- BONNER, W. M., REDON, C. E., DICKEY, J. S., NAKAMURA, A. J., SEDELNIKOVA, O. A., SOLIER, S. & POMMIER, Y. 2008. [gamma]H2AX and cancer. *Nat Rev Cancer*, 8, 957-967.
- BOOT-HANDFORD, R. & BRIGGS, M. 2010. The unfolded protein response and its relevance to connective tissue diseases. *Cell and Tissue Research*, 339, 197-211.
- BOSCH, G., VAN SCHIE, H. T. M., DE GROOT, M. W., CADBY, J. A., VAN DE LEST, C. H. A., BARNEVELD, A. & VAN WEEREN, P. R. 2010. Effects of platelet-rich plasma on the quality of repair of mechanically induced core lesions in equine superficial digital flexor tendons: A placebo-controlled experimental study. *Journal of Orthopaedic Research*, 28, 211-217.
- BOUCHIER-HAYES, L., OBERST, A., MCSTAY, G. P., CONNELL, S., TAIT, S. W. G., DILLON, C. P., FLANAGAN, J. M., BEERE, H. M. & GREEN, D. R. 2009. Characterization of Cytoplasmic Caspase-2 Activation by Induced Proximity. *Molecular Cell*, 35, 830-840.
- BRATTON, D. L., FADOK, V. A., RICHTER, D. A., KAILEY, J. M., GUTHRIE, L. A. & HENSON, P. M. 1997. Appearance of Phosphatidylserine on Apoptotic Cells Requires Calcium-mediated Nonspecific Flip-Flop and Is Enhanced by Loss of the Aminophospholipid Translocase. *Journal of Biological Chemistry*, 272, 26159-26165.
- BRATTON, S. B., WALKER, G., SRINIVASULA, S. M., SUN, X.-M., BUTTERWORTH, M., ALNEMRI, E. S. & COHEN, G. M. 2001. Recruitment, activation and retention of caspases-9 and -3 by Apaf-1 apoptosome and associated XIAP complexes. *EMBO J*, 20, 998-1009.
- BUCCIANTINI, M., GIANNONI, E., CHITI, F., BARONI, F., FORMIGLI, F., ZURDO, J., TADDEI, N., RAMPONI, G., DOBSON, C. M. & STEFANI, M. 2002. Inherent

- toxicity of aggregates implies a common mechanism for protein misfolding diseases. *Nature*, 416, 507-511.
- BUCKLEY, M. R., EVANS, E. B., MATUSZEWSKI, P. E., CHEN, Y.-L., SATCHEL, L. N., ELLIOTT, D. M., SOSLOWSKY, L. J. & DODGE, G. R. 2013. Distributions of types I, II and III collagen by region in the human supraspinatus tendon. *Connective Tissue Research*, 54, 374-379.
- BURHANS, W. C. & HEINTZ, N. H. 2009. The cell cycle is a redox cycle: Linking phase-specific targets to cell fate. *Free Radical Biology and Medicine*, 47, 1282-1293.
- BURHANS, W. C. & WEINBERGER, M. 2007. DNA replication stress, genome instability and aging. *Nucleic Acids Research*, 35, 7545-7556.
- BURMA, S., CHEN, B. P., MURPHY, M., KURIMASA, A. & CHEN, D. J. 2001. ATM Phosphorylates Histone H2AX in Response to DNA Double-strand Breaks. *Journal of Biological Chemistry*, 276, 42462-42467.
- BUROVA, E., BORODKINA, A., SHATROVA, A. & NIKOLSKY, N. 2013. Sublethal Oxidative Stress Induces the Premature Senescence of Human Mesenchymal Stem Cells Derived from Endometrium. *Oxidative Medicine and Cellular Longevity*, 2013, 12.
- BURROWS, S., BECKER, D. L., FLECK, R. A. & PATTERSON-KANE, J. C. 2009. Gap junctional propagation of apoptosis in tendon fibroblast monolayers in response to physiological hyperthermia. *Transactions of the Orthopaedic Research Society*, 34, 27.
- BURRY, R. 2010a. Antibodies. *Immunocytochemistry*. Springer New York.
- BURRY, R. W. 2010b. Immunocytochemistry: A Practical guide to Biomedical research. *Chapter 2: Antibodies*. New York: Springer.
- BUTCHER, M. T., HERMANSON, J. W., DUCHARME, N. G., MITCHELL, L. M., SODERHOLM, L. V. & BERTRAM, J. E. A. 2009. Contractile behavior of the forelimb digital flexors during steady-state locomotion in horses (*Equus caballus*): An initial test of muscle architectural hypotheses about in vivo function. *Comparative Biochemistry and Physiology Part A: Molecular & Integrative Physiology*, 152, 100-114.
- CANTY-LAIRD, E. G., LU, Y. & KADLER, K. E. 2012. Stepwise proteolytic activation of type I procollagen to collagen within the secretory pathway of tendon fibroblasts in situ. *Biochemical Journal*, 441, 707-717.
- CANTY, E. G., LU, Y., MEADOWS, R. S., SHAW, M. K., HOLMES, D. F. & KADLER, K. E. 2004. Coalignment of plasma membrane channels and protrusions (fibripositors) specifies the parallelism of tendon. *The Journal of Cell Biology*, 165, 553-563.
- CAO, M., STEFANOVIC-RACIC, M., GEORGESCU, H. I., FU, F. H. & EVANS, C. H. 2000. Does Nitric Oxide Help Explain the Differential Healing Capacity of the Anterior Cruciate, Posterior Cruciate, and Medial Collateral Ligaments? *The American Journal of Sports Medicine*, 28, 176-182.
- CAO, S. S. & KAUFMAN, R. J. 2012. Unfolded protein response. *Current Biology*, 22, R622-R626.
- CARROLL, M. & BEEK, O. 1992. Protection against hippocampal CA1 cell loss by post-ischemic hypothermia is dependent on delay of initiation and duration. *Metabolic Brain Disease*, 7, 45-50.
- CELESTE, A., PETERSEN, S., ROMANIENKO, P. J., FERNANDEZ-CAPETILLO, O., CHEN, H. T., SEDELNIKOVA, O. A., REINA-SAN-MARTIN, B., COPPOLA, V., MEFFRE, E., DIFILIPPANTONIO, M. J., REDON, C. E., PILCH, D. R., OLARU, A., ECKHAUS, M., CAMERINI-OTERO, R. D., TESSAROLLO, L., LIVAK, F., MANOVA, K., BONNER, W. M., NUSSENZWEIG, M. C. & NUSSENZWEIG, A.

2002. Genomic instability in mice lacking histone H2AX. *Science*, 296, 922-927.
- CHANG, C.-C., NAIK, MANDAR T., HUANG, Y.-S., JENG, J.-C., LIAO, P.-H., KUO, H.-Y., HO, C.-C., HSIEH, Y.-L., LIN, C.-H., HUANG, N.-J., NAIK, NANDITA M., KUNG, CAMY C. H., LIN, S.-Y., CHEN, R.-H., CHANG, K.-S., HUANG, T.-H. & SHIH, H.-M. 2011. Structural and Functional Roles of Daxx SIM Phosphorylation in SUMO Paralog-Selective Binding and Apoptosis Modulation. *Molecular Cell*, 42, 62-74.
- CHANG, H. Y., NISHITOH, H., YANG, X., ICHIJO, H. & BALTIMORE, D. 1998. Activation of apoptosis signal-regulating kinase 1 (ASK1) by the adapter protein Daxx. *Science*, 281, 1860-1863.
- CHAPPELL, S. A., OWENS, G. C. & MAURO, V. P. 2001. A 5' Leader of Rbm3, a Cold Stress-induced mRNA, Mediates Internal Initiation of Translation with Increased Efficiency under Conditions of Mild Hypothermia. *Journal of Biological Chemistry*, 276, 36917-36922.
- CHEN, H., CHOPP, M., JIANG, Q. & GARCIA, J. H. 1992. Neuronal damage, glial response and cerebral metabolism after hypothermic forebrain ischemia in the rat. *Acta Neuropathologica*, 84, 184-189.
- CHENG, L., SMITH, D. J., ANDERSON, R. L. & NAGLEY, P. 2011. Modulation of Cellular Hsp72 Levels in Undifferentiated and Neuron-Like SH-SY5Y Cells Determines Resistance to Staurosporine-Induced Apoptosis. *PLoS ONE*, 6, e24473.
- CHESEN, A. B., DABAREINER, R. M., CHAFFIN, M. K. & CARTER, G. K. 2009. Tendinitis of the proximal aspect of the superficial digital flexor tendon in horses: 12 cases (2000-2006). *Journal of the American Veterinary Medical Association*, 234, 1432-1436.
- CHOW, A., STEEL, R. & ANDERSON, R. 2009. Hsp72 chaperone function is dispensable for protection against stress-induced apoptosis. *Cell Stress and Chaperones*, 14, 253-263.
- CHUEN, F. S., CHUK, C. Y., PING, W. Y., NAR, W. W., KIM, H. L. & MING, C. K. 2004. Immunohistochemical Characterization of Cells in Adult Human Patellar Tendons. *J. Histochem. Cytochem.*, 52, 1151-1157.
- CLARK, D., PENNER, M., ORELLANA-JORDAN, I. & COLBOURNE, F. 2008. Comparison of 12, 24 and 48h of systemic hypothermia on outcome after permanent focal ischemia in rat. *Exp Neurol*, 212, 386 - 392.
- COHEN, I., RIDER, P., CARMİ, Y., BRAİMAN, A., DOTAN, S., WHITE, M. R., VORONOV, E., MARTIN, M. U., DINARELLO, C. A. & APTE, R. N. 2010. Differential release of chromatin-bound IL-1 α discriminates between necrotic and apoptotic cell death by the ability to induce sterile inflammation. *Proceedings of the National Academy of Sciences*, 107, 2574-2579.
- COLBOURNE, F., CORBETT, D., ZHAO, Z., YANG, J. & BUCHAN, A. 2000. Prolonged but delayed postischemic hypothermia: a long-term outcome study in the rat middle cerebral artery occlusion model. *J Cereb Blood Flow Metab*, 20, 1702 - 1708.
- COLIGE, A., LI, S.-W., SIERON, A. L., NUSGENS, B. V., PROCKOP, D. J. & LAPIÈRE, C. M. 1997. cDNA cloning and expression of bovine procollagen I N-proteinase: A new member of the superfamily of zinc-metalloproteinases with binding sites for cells and other matrix components. *Proceedings of the National Academy of Sciences*, 94, 2374-2379.

- COLIGE, A., RUGGIERO, F., VANDENBERGHE, I., DUBAIL, J., KESTELOOT, F., VAN BEEUMEN, J., BESCHIN, A., BRYNS, L., LAPIÈRE, C. M. & NUSGENS, B. 2005. Domains and Maturation Processes That Regulate the Activity of ADAMTS-2, a Metalloproteinase Cleaving the Aminopropeptide of Fibrillar Procollagens Types I-III and V. *Journal of Biological Chemistry*, 280, 34397-34408.
- COLLIER, N. C. & SCHLESINGER, M. J. 1986. The dynamic state of heat shock proteins in chicken embryo fibroblasts. *The Journal of Cell Biology*, 103, 1495-1507.
- COLLINS, A. 2004. The comet assay for DNA damage and repair. *Molecular Biotechnology*, 26, 249-261.
- COOK, J. L. & PURDAM, C. R. 2009. Is tendon pathology a continuum? A pathology model to explain the clinical presentation of load-induced tendinopathy. *British Journal of Sports Medicine*, 43, 409-416.
- CORDES, N., SEIDLER, J., DURZOK, R., GEINITZ, H. & BRAKEBUSCH, C. 2005. [beta]1-integrin-mediated signaling essentially contributes to cell survival after radiation-induced genotoxic injury. *Oncogene*, 25, 1378-1390.
- COSS, R. A., ALDEN, M. E., WACHSBERGER, P. R. & SMITH, N. N. 1996. Response of the microtubular cytoskeleton following hyperthermia as a prognostic indicator of survival of Chinese hamster ovary cells. *International Journal of Radiation Oncology*Biophysics*, 34, 403-410.
- COSS, R. A., DEWEY, W. C. & BAMBURG, J. R. 1982. Effects of Hyperthermia on Dividing Chinese Hamster Ovary Cells and on Microtubules in Vitro. *Cancer Research*, 42, 1059-1071.
- COUTINHO, P., QIU, C., FRANK, S., WANG, C. M., BROWN, T., GREEN, C. R. & BECKER, D. L. 2005. Limiting burn extension by transient inhibition of Connexin43 expression at the site of injury. *British Journal of Plastic Surgery*, 58, 658-667.
- CRATA, K., GANEM, N. J., DAGHER, R., LANTERMANN, A. B., IVANOVA, E. V., PAN, Y., NEZI, L., PROTOPOPOV, A., CHOWDHURY, D. & PELLMAN, D. 2012. DNA breaks and chromosome pulverization from errors in mitosis. *Nature*, 482, 53-58.
- CREVIER-DENOIX, N., COLLOBERT, C., POURCELOT, P., DENOIX, J. M., SANAA, M., GEIGER, D., BERNARD, N., RIBOT, X., BORTOLUSSI, C. & BOUSSEAU, B. 1997. Mechanical properties of pathological equine superficial digital flexor tendons. *Equine Veterinary Journal*, 29, 23-26.
- CRISTOFALO, V. J. 2005. SA B Gal staining: Biomarker or delusion. *Experimental Gerontology*, 40, 836-838.
- CRUZ, H. J., DIAS, E. M., MOREIRA, J. L. & CARRONDO, M. J. T. 1997. Cell-dislodging methods under serum-free conditions. *Applied Microbiology and Biotechnology*, 47, 482-488.
- CULLEN, K. E. & SARGE, K. D. 1997. Characterization of Hypothermia-induced Cellular Stress Response in Mouse Tissues. *Journal of Biological Chemistry*, 272, 1742-1746.
- DAHLGREN, L., BROWER-TOLAND, B. & NIXON, A. 2005a. Cloning and expression of type III collagen in normal and injured tendons of horses. *Am J Vet Res*, 66, 266 - 270.
- DAHLGREN, L. A., MOHAMMED, H. O. & NIXON, A. J. 2005b. Temporal expression of growth factors and matrix molecules in healing tendon lesions. *Journal of Orthopaedic Research*, 23, 84-92.
- DAKIN, S. G., WERLING, D., HIBBERT, A., ABAYASEKARA, D. R. E., YOUNG, N. J., SMITH, R. K. W. & DUDHIA, J. 2012. Macrophage Sub-Populations and the

- Lipoxin A₄ Receptor Implicate Active Inflammation during Equine Tendon Repair. *PLoS ONE*, 7, e32333.
- DANNO, S., ITOH, K., MATSUDA, T. & FUJITA, J. 2000. Decreased Expression of Mouse Rbm3, a Cold-Shock Protein, in Sertoli Cells of Cryptorchid Testis. *The American Journal of Pathology*, 156, 1685-1692.
- DANNO, S., NISHIYAMA, H., HIGASHITSUJI, H., YOKOI, H., XUE, J.-H., ITOH, K., MATSUDA, T. & FUJITA, J. 1997. Increased Transcript Level of RBM3, a Member of the Glycine-Rich RNA-Binding Protein Family, in Human Cells in Response to Cold Stress. *Biochemical and Biophysical Research Communications*, 236, 804-807.
- DE FERAUDY, S., REVET, I., BEZROOKOVE, V., FEENEY, L. & CLEAVER, J. E. 2010. A minority of foci or pan-nuclear apoptotic staining of γ H2AX in the S phase after UV damage contain DNA double-strand breaks. *Proceedings of the National Academy of Sciences*, 107, 6870-6875.
- DE WEVER, O., SOBCZAK-THEPOT, J., VERCOUTTER-EDOUART, A.-S., MICHALSKI, J.-C., OUELAA-BENSLAMA, R., STUPACK, D. G., BRACKE, M., WANG, J. Y. J., GESPACH, C. & EMANI, S. 2011. Priming and potentiation of DNA damage response by fibronectin in human colon cancer cells and tumor-derived myofibroblasts. *International Journal of Oncology*, 39, 393-400.
- DENOIX, J. M. 1994. Functional anatomy of tendons and ligaments in the distal limb (manus and pes). *Veterinary Clinics of North America: Equine Practice*, 10, 273-322.
- DESAGHER, S., OSEN-SAND, A., NICHOLS, A., ESKES, R., MONTESSUIT, S., LAUPER, S., MAUNDRELL, K., ANTONSSON, B. & MARTINOU, J.-C. 1999. Bid-induced Conformational Change of Bax Is Responsible for Mitochondrial Cytochrome c Release during Apoptosis. *The Journal of Cell Biology*, 144, 891-901.
- DICKENS, LAURA S., BOYD, ROBERT S., JUKES-JONES, R., HUGHES, MICHELLE A., ROBINSON, GEMMA L., FAIRALL, L., SCHWABE, JOHN W. R., CAIN, K. & MACFARLANE, M. 2012. A Death Effector Domain Chain DISC Model Reveals a Crucial Role for Caspase-8 Chain Assembly in Mediating Apoptotic Cell Death. *Molecular Cell*, 47, 291-305.
- DIMRI, G. P., LEE, X., BASILE, G., ACOSTA, M., SCOTT, G., ROSKELLEY, C., MEDRANO, E. E., LINSKENS, M., RUBELJ, I. & PEREIRA-SMITH, O. 1995. A biomarker that identifies senescent human cells in culture and in aging skin in vivo. *Proceedings of the National Academy of Sciences of the United States of America*, 92, 9363-9367.
- DOWLING, B. A., DART, A. J., HODGSON, D. R., ROSE, R. J. & WALSH, W. R. 2002. The Effect of Recombinant Equine Growth Hormone on the Biomechanical Properties of Healing Superficial Digital Flexor Tendons in Horses. *Veterinary Surgery*, 31, 320-324.
- DRESIOS, J., ASCHRAFI, A., OWENS, G. C., VANDERKLISH, P. W., EDELMAN, G. M. & MAURO, V. P. 2005. Cold stress-induced protein Rbm3 binds 60S ribosomal subunits, alters microRNA levels, and enhances global protein synthesis. *Proceedings of the National Academy of Sciences of the United States of America*, 102, 1865-1870.
- DRIESSENS, N., VERSTEYHE, S., GHADDHAB, C., BURNIAT, A., DE DEKEN, X., VAN SANDE, J., DUMONT, J.-E., MIOT, F. & CORVILAIN, B. 2009. Hydrogen peroxide induces DNA single- and double-strand breaks in thyroid cells and is therefore a potential mutagen for this organ. *Endocrine-Related Cancer*, 16, 845-856.

- DU, Y., WOOTEN, M. C., GEARING, M. & WOOTEN, M. W. 2009a. Age-associated oxidative damage to the p62 promoter: implications for Alzheimer disease. *Free Radical Biology and Medicine*, 46, 492-501.
- DU, Y., WOOTEN, M. C. & WOOTEN, M. W. 2009b. Oxidative damage to the promoter region of SQSTM1/p62 is common to neurodegenerative disease. *Neurobiology of Disease*, 35, 302-310.
- DURGAM, S. S., STEWART, A. A., PONDENIS, H. C., YATES, A. C., EVANS, R. B. & STEWART, M. C. 2011. Responses of equine tendon- and bone marrow-derived cells to monolayer expansion with fibroblast growth factor-2 and sequential culture with pulverized tendon and insulin-like growth factor-I. *American Journal of Veterinary Research*, 73, 162-170.
- DYSON, S. J. 2004. Medical management of superficial digital flexor tendonitis: a comparative study in 219 horses (1992-2000). *Equine Veterinary Journal*, 36, 415-419.
- EGERBACHER, M., ARNOCKY, S., CABALLERO, O., LAVAGNINO, M. & GARDNER, K. 2008. Loss of Homeostatic Tension Induces Apoptosis in Tendon Cells: An In Vitro Study. *Clinical Orthopaedics and Related Research*, 466, 1562-1568.
- ELMORE, S. 2007. Apoptosis: A Review of Programmed Cell Death. *Toxicologic Pathology*, 35, 495-516.
- ELY, E. R., AVELLA, C. S., PRICE, J. S., SMITH, R. K. W., WOOD, J. L. N. & VERHEYEN, K. L. P. 2009. Descriptive epidemiology of fracture, tendon and suspensory ligament injuries in National Hunt racehorses in training. *Equine Veterinary Journal*, 41, 372-378.
- ENDEMANN, M., BERGMEISTER, H., BIDMON, B., BOEHM, M., CSAICSICH, D., MALAGA-DIEGUEZ, L., ARBEITER, K., REGELE, H., HERKNER, K. & AUFRICHT, C. 2007. Evidence for HSP-mediated cytoskeletal stabilization in mesothelial cells during acute experimental peritoneal dialysis. *American Journal of Physiology - Renal Physiology*, 292, F47-F56.
- FAREWELL, A. & NEIDHARDT, F. C. 1998. Effect of Temperature on In Vivo Protein Synthetic Capacity in Escherichia coli. *Journal of Bacteriology*, 180, 4704-4710.
- FARRIS, D. J., TREWARTHA, G. & POLLY MCGUIGAN, M. 2011. Could intra-tendinous hyperthermia during running explain chronic injury of the human Achilles tendon? *Journal of Biomechanics*, 44, 822-826.
- FERRY, A. L., VANDERKLISH, P. W. & DUPONT-VERSTEEGDEN, E. E. 2011. Enhanced survival of skeletal muscle myoblasts in response to overexpression of cold shock protein RBM3. *American Journal of Physiology - Cell Physiology*, 301, C392-C402.
- FLICK, J., DEVKOTA, A., TSUZAKI, M., ALMEKINDERS, L. & WEINHOLD, P. 2006. Cyclic loading alters biomechanical properties and secretion of PGE2 and NO from tendon explants. *Clinical Biomechanics*, 21, 99-106.
- FRACKENPOHL, J., ARVIDSSON, P. I., SCHREIBER, J. V. & SEEBACH, D. 2001. The Outstanding Biological Stability of β - and γ -Peptides toward Proteolytic Enzymes: An In Vitro Investigation with Fifteen Peptidases. *ChemBioChem*, 2, 445-455.
- FRISCH, S. M. & FRANCIS, H. 1994. Disruption of Epithelial Cell-Matrix Interactions Induces Apoptosis. *The Journal of Cell Biology*, 124, 619-626.
- FRY, T., EVANS, J. H. & SANDERSON, M. J. 2001. Propagation of intercellular calcium waves in C6 glioma cells transfected with connexins 43 or 32. *Microscopy Research and Technique*, 52, 289-300.

- FULDA, S., GORMAN, A. M., HORI, O. & SAMALI, A. 2010. Cellular Stress Responses: Cell Survival and Cell Death. *International Journal of Cell Biology*, 2010.
- FULTON, I. C., MACLEAN, A. A., O'RIELLY, J. L. & CHURCH, S. 1994. Superior check ligament desmotomy for treatment of superficial digital flexor tendonitis in Thoroughbred and Standardbred horses. *Australian Veterinary Journal*, 71, 233-235.
- GABAI, V. L., MERIIN, A. B., MOSSER, D. D., CARON, A. W., RITS, S., SHIFRIN, V. I. & SHERMAN, M. Y. 1997. Hsp70 Prevents Activation of Stress Kinases. *Journal of Biological Chemistry*, 272, 18033-18037.
- GABAI, V. L., YAGLOM, J. A., VOLLOCH, V., MERIIN, A. B., FORCE, T., KOUTROUMANIS, M., MASSIE, B., MOSSER, D. D. & SHERMAN, M. Y. 2000. Hsp72-Mediated Suppression of c-Jun N-Terminal Kinase Is Implicated in Development of Tolerance to Caspase-Independent Cell Death. *Molecular and Cellular Biology*, 20, 6826-6836.
- GENTILE, M., LATONEN, L. & LAIHO, M. 2003. Cell cycle arrest and apoptosis provoked by UV radiation - induced DNA damage are transcriptionally highly divergent responses. *Nucleic Acids Research*, 31, 4779-4790.
- GIANCOTTI, F. G. 1997. Integrin signaling: specificity and control of cell survival and cell cycle progression. *Current Opinion in Cell Biology*, 9, 691-700.
- GIBSON, K. T., BURBIDGE, H. M. & ANDERSON, B. H. 1997. Tendonitis of the branches of insertion of the superficial digital flexor tendon in horses. *Australian Veterinary Journal*, 75, 253-256.
- GIUSTINIANI, J., DAIRE, V., CANTALOUBE, I., DURAND, G., POÛS, C., PERDIZ, D. & BAILLET, A. 2009. Tubulin acetylation favors Hsp90 recruitment to microtubules and stimulates the signaling function of the Hsp90 clients Akt/PKB and p53. *Cellular Signalling*, 21, 529-539.
- GLASS, J. R., DEWITT, R. G. & CRESS, A. E. 1985. Rapid Loss of Stress Fibers in Chinese Hamster Ovary Cells after Hyperthermia. *Cancer Research*, 45, 258-262.
- GLICK, D., BARTH, S. & MACLEOD, K. F. 2010. Autophagy: cellular and molecular mechanisms. *The Journal of Pathology*, 221, 3-12.
- GOFF, L. & STUBBS, N. 2007. Animal Physiotherapy: Assessment, Treatment and Rehabilitation of Animals. In: MCGOWAN, C., GOFF, L. AND STUBBS, N. (ed.) *Biomechanics of Locomotion: the horse*. Singapore: Blackwell Publishing Ltd.
- GOLDBERG, G. S., MORENO, A. P. & LAMPE, P. D. 2002. Gap Junctions between Cells Expressing Connexin 43 or 32 Show Inverse Permselectivity to Adenosine and ATP. *Journal of Biological Chemistry*, 277, 36725-36730.
- GOODMAN, S. A., MAY, S. A., HEINEGÅRD, D. & SMITH, R. K. W. 2004. Tenocyte response to cyclical strain and transforming growth factor beta is dependent upon age and site of origin. *Biorheology*, 41, 613-628.
- GOODSHIP, A. E. 1993. The pathophysiology of flexor tendon injury in the horse. *Equine Veterinary Education*, 5, 23-29.
- GOODSHIP, A. E., BIRCH, H. L. & WILSON, A. M. 1994. The pathobiology and repair of tendon and ligament injury. *Veterinary Clinics of North America: Equine Practice*, 10, 323-349.
- GREENBAUM, D., COLANGELO, C., WILLIAMS, K. & GERSTEIN, M. 2003. Comparing protein abundance and mRNA expression levels on a genomic scale. *Genome biology*, 4, 117.

- GRUNERT, M., GOTTSCHALK, K., KAPAHNKE, J., GUNDISCH, S., KIESER, A. & JEREMIAS, I. 2012. The adaptor protein FADD and the initiator caspase-8 mediate activation of NF- κ B by TRAIL. *Cell Death Dis*, 3, e414.
- GUEST, D. J., SMITH, M. R. W. & ALLEN, W. R. 2010. Equine embryonic stem-like cells and mesenchymal stromal cells have different survival rates and migration patterns following their injection into damaged superficial digital flexor tendon. *Equine Veterinary Journal*, 42, 636-642.
- GUO, F.-J., XIONG, Z., LU, X., YE, M., HAN, X. & JIANG, R. 2014. ATF6 upregulates XBP1S and inhibits ER stress-mediated apoptosis in osteoarthritis cartilage. *Cellular Signalling*, 26, 332-342.
- GUO, Y., GUETTOUCHE, T., FENNA, M., BOELLMANN, F., PRATT, W. B., TOFT, D. O., SMITH, D. F. & VOELLMY, R. 2001. Evidence for a Mechanism of Repression of Heat Shock Factor 1 Transcriptional Activity by a Multichaperone Complex. *Journal of Biological Chemistry*, 276, 45791-45799.
- HADJIPANAYI, E., MUDERA, V. & BROWN, R. A. 2009. Close dependence of fibroblast proliferation on collagen scaffold matrix stiffness. *Journal of Tissue Engineering and Regenerative Medicine*, 3, 77-84.
- HALLIWELL, B. 2003. Oxidative stress in cell culture: an under-appreciated problem? *FEBS Letters*, 540, 3-6.
- HAN, W., WU, L., CHEN, S., BAO, L., ZHANG, L., JIANG, E., ZHAO, Y., XU, A., HEI, T. K. & YU, Z. 2006. Constitutive nitric oxide acting as a possible intercellular signaling molecule in the initiation of radiation-induced DNA double strand breaks in non-irradiated bystander cells. *Oncogene*, 26, 2330-2339.
- HANUS, J., ZHANG, H., WANG, Z., LIU, Q., ZHOU, Q. & WANG, S. 2013. Induction of necrotic cell death by oxidative stress in retinal pigment epithelial cells. *Cell Death and Disease*, 4, e965.
- HARIHARAN, N., ZHAI, P. & SADOSHIMA, J. 2011. Oxidative stress stimulates autophagic flux during ischaemia/reperfusion. *Antioxidants and Redox Signalling*, 14, 2179-2190.
- HARPER, E. 1980. Collagenases. *Annual Review of Biochemistry*, 49, 1063-1078.
- HERBIG, U., JOBLING, W. A., CHEN, B. P. C., CHEN, D. J. & SEDIVY, J. M. 2004. Telomere Shortening Triggers Senescence of Human Cells through a Pathway Involving ATM, p53, and p21CIP1, but Not p16INK4a. *Molecular Cell*, 14, 501-513.
- HOSAKA, Y., KIRISAWA, R., YAMAMOTO, E., UEDA, H., IWAI, H. & TAKEHANA, K. 2002. Localization of Cytokines in Tendinocytes of the Superficial Digital Flexor Tendon in the Horse. *Journal of Veterinary Medical Science*, 64, 945-947.
- HOSAKA, Y., OZOE, S., KIRISAWA, R., UEDA, H., TAKEHANA, K. & YAMAGUCHI, M. 2006. Effect of heat on synthesis of gelatinases and pro-inflammatory cytokines in equine tendinocytes. *Biomedical Research*, 27, 233-241.
- HOSAKA, Y., TERAOKA, H., YAMAMOTO, E., UEDA, H. & TAKEHANA, K. 2005. Mechanism of Cell Death in Inflamed Superficial Digital Flexor Tendon in the Horse. *Journal of Comparative Pathology*, 132, 51-58.
- HOTCHIN, N. A. & HALL, A. 1995. The assembly of integrin adhesion complexes requires both extracellular matrix and intracellular rho/rac GTPases. *The Journal of Cell Biology*, 131, 1857-1865.
- HSU, H., XIONG, J. & GOEDEL, D. V. 1995. The TNF receptor 1-associated protein TRADD signals cell death and NF- κ B activation. *Cell*, 81, 495-504.
- HUNT, C. R., PANDITA, R. K., LASZLO, A., HIGASHIKUBO, R., AGARWAL, M., KITAMURA, T., GUPTA, A., RIEF, N., HORIKOSHI, N., BASKARAN, R., LEE,

- J.-H., LÖBRICH, M., PAULL, T. T., ROTI ROTI, J. L. & PANDITA, T. K. 2007. Hyperthermia Activates a Subset of Ataxia-Telangiectasia Mutated Effectors Independent of DNA Strand Breaks and Heat Shock Protein 70 Status. *Cancer Research*, 67, 3010-3017.
- ICHIJIMA, Y., SAKASAI, R., OKITA, N., ASAHINA, K., MIZUTANI, S. & TERAOKA, H. 2005. Phosphorylation of histone H2AX at M phase in human cells without DNA damage response. *Biochemical and Biophysical Research Communications*, 336, 807-812.
- ICHIJIMA, Y., YOSHIOKA, K.-I., YOSHIOKA, Y., SHINOHE, K., FUJIMORI, H., UNNO, J., TAKAGI, M., GOTO, H., INAGAKI, M., MIZUTANI, S. & TERAOKA, H. 2010. DNA Lesions Induced by Replication Stress Trigger Mitotic Aberration and Tetraploidy Development. *PLoS ONE*, 5, e8821.
- ISHII, T., YANAGAWA, T., YUKI, K., KAWANE, T., YOSHIDA, H. & BANNAI, S. 1997. Low Micromolar Levels of Hydrogen Peroxide and Proteasome Inhibitors Induce the 60-kDa A170 Stress Protein in Murine Peritoneal Macrophages. *Biochemical and Biophysical Research Communications*, 232, 33-37.
- ITAKURA, E. & MIZUSHIMA, N. 2011. p62 targeting to the autophagosome formation site requires self-oligomerization but not LC3 binding. *The Journal of Cell Biology*, 192, 17-27.
- JAATTELA, M., WISSING, D., KOKHOLM, K., KALLUNKI, T. & EGEBLAD, M. 1998. Hsp70 exerts its anti-apoptotic function downstream of caspase-3-like proteases. *EMBO J*, 17, 6124-6134.
- JAIN, A., LAMARK, T., SJØTTEM, E., BOWITZ LARSEN, K., ATESOH AWUH, J., ØVERVATN, A., MCMAHON, M., HAYES, J. D. & JOHANSEN, T. 2010. p62/SQSTM1 Is a Target Gene for Transcription Factor NRF2 and Creates a Positive Feedback Loop by Inducing Antioxidant Response Element-driven Gene Transcription. *Journal of Biological Chemistry*, 285, 22576-22591.
- JANG, J.-H. & CHUNG, C.-P. 2005. Fibronectin-mediated adhesion rescues cell cycle arrest induced by fibroblast growth factor-1 by decreased expression of P21cip/waf in human chondrocytes. *In Vitro Cellular & Developmental Biology - Animal*, 41, 126-129.
- JÄRVINEN, M., JÓZSA, L., KANNUS, P., JÄRVINEN, T. L. N., KVIST, M. & LEADBETTER, W. 1997. Histopathological findings in chronic tendon disorders. *Scandinavian Journal of Medicine & Science in Sports*, 7, 86-95.
- JIA, L., GOPINATHAN, G., SUKUMAR, J. T. & GRIBBEN, J. G. 2012. Blocking Autophagy Prevents Bortezomib-Induced NF- κ B Activation by Reducing I- κ B α Degradation in Lymphoma Cells. *PLoS ONE*, 7, e32584.
- JONES, G. C., CORPS, A. N., PENNINGTON, C. J., CLARK, I. M., EDWARDS, D. R., BRADLEY, M. M., HAZLEMAN, B. L. & RILEY, G. P. 2006. Expression profiling of metalloproteinases and tissue inhibitors of metalloproteinases in normal and degenerate human achilles tendon. *Arthritis & Rheumatism*, 54, 832-842.
- JOZSA, L., KANNUS, P., BALINT, B. J. & REFFY, A. 1991. Three-dimensional ultrastructure of human tendons. *Acta Anatomica (Basel)*, 142, 306-312.
- JUDY, M. E., NAKAMURA, A., HUANG, A., GRANT, H., MCCURDY, H., WEIBERTH, K. F., GAO, F., COPPOLA, G., KENYON, C. & KAO, A. W. 2013. A Shift to Organismal Stress Resistance in Programmed Cell Death Mutants. *PLoS Genet*, 9, e1003714.
- KALLA, S. 2009. *Statistical significance and Sample Size* [Online]. Available: <https://explorable.com/statistical-significance-sample-size> [Accessed August 24 2014].
- KANNUS, P. 2000. Structure of the tendon connective tissue. *Scandinavian Journal of Medicine & Science in Sports*, 10, 312-320.

- KASASHIMA, Y., TAKAHASHI, T., SMITH, R. K. W., GOODSHIP, A. E., KUWANO, A., UENO, T. & HIRANO, S. 2004. Prevalence of superficial digital flexor tendonitis and suspensory desmitis in Japanese Thoroughbred flat racehorses in 1999. *Equine Veterinary Journal*, 36, 346-350.
- KASTELIC, J., GALESKI, A. & BAER, E. 1978. The Multicomposite Structure of Tendon. *Connective Tissue Research*, 6, 11-23.
- KAUFMAN, R. J. 2002. Orchestrating the unfolded protein response in health and disease. *The Journal of Clinical Investigation*, 110, 1389-1398.
- KERR, J. F. R., WYLLIE, A. H. & CURRIE, A. R. 1972. Apoptosis: A basic biological phenomenon with wideranging implications in tissue kinetics. *British Journal of Cancer*, 26, 239-257.
- KHELIFI, A. F., D'ALCONTRES, M. S. & SALOMONI, P. 2005. Daxx is required for stress-induced cell death and JNK activation. *Cell Death Differ*, 12, 724-733.
- KIM, E. J., PARK, J. S. & UM, S. J. 2003. Identification of Daxx interacting with p73, one of the p53 family, and its regulation of p53 activity by competitive interaction with PML. *Nucleic Acids Research*, 31, 5356-5367.
- KIM, H. J., KANG, B. S. & PARK, J.-W. 2005. Cellular defense against heat shock-induced oxidative damage by mitochondrial NADP⁺-dependent isocitrate dehydrogenase. *Free Radical Research*, 39, 441-448.
- KINNER, A., WU, W., STAUDT, C. & ILIAKIS, G. 2008. γ -H2AX in recognition and signaling of DNA double-strand breaks in the context of chromatin. *Nucleic Acids Research*, 36, 5678-5694.
- KLUCK, R. M., BOSSY-WETZEL, E., GREEN, D. R. & NEWMAYER, D. D. 1997. The Release of Cytochrome c from Mitochondria: A Primary Site for Bcl-2 Regulation of Apoptosis. *Science*, 275, 1132-1136.
- KO, K. S. & MCCULLOCH, C. A. G. 2001. Intercellular Mechanotransduction: Cellular Circuits That Coordinate Tissue Responses to Mechanical Loading. *Biochemical and Biophysical Research Communications*, 285, 1077-1083.
- KO, Y.-G., KANG, Y.-S., PARK, H., SEOL, W., KIM, J., KIM, T., PARK, H.-S., CHOI, E.-J. & KIM, S. 2001. Apoptosis Signal-regulating Kinase 1 Controls the Proapoptotic Function of Death-associated Protein (Daxx) in the Cytoplasm. *Journal of Biological Chemistry*, 276, 39103-39106.
- KOMAROVA, E. Y., AFANASYEVA, E. A., BULATOVA, M. M., CHEETHAM, M. E., MARGULIS, B. A. & GUZHOVA, I. V. 2004. Downstream Caspases Are Novel Targets for the Antiapoptotic Activity of the Molecular Chaperone Hsp70. *Cell Stress & Chaperones*, 9, 265-275.
- KRAUS-HANSEN, A. E., FACKELMAN, G. E., BECKER, C., WILLIAMS, R. M. & PIPERS, F. S. 1992. Preliminary studies on the vascular anatomy of the equine superficial digital flexor tendon. *Equine Veterinary Journal*, 24, 46-51.
- KRYSKO, D. V., LEYBAERT, L., VANDENABEELE, P. & D'HERDE, K. 2005. Gap junctions and the propagation of cell survival and cell death signals. *Apoptosis*, 10, 459-469.
- KRYSKO, D. V., MUSSCHE, S., LEYBAERT, L. & D'HERDE, K. 2004. Gap Junctional Communication and Connexin43 Expression in Relation to Apoptotic Cell Death and Survival of Granulosa Cells. *Journal of Histochemistry & Cytochemistry*, 52, 1199-1207.
- KUBO, K., KANEHISA, H. & FUKUNAGA, T. 2005. Effects of cold and hot water immersion on the mechanical properties of human muscle and tendon in vivo. *Clinical Biomechanics*, 20, 291-300.
- KURIEN, B. T. & SCOFIELD, R. H. 2006. Western blotting. *Methods*, 38, 283-293.

- KURZ, D., DECARY, S., HONG, Y. & ERUSALIMSKY, J. 2000. Senescence-associated (beta)-galactosidase reflects an increase in lysosomal mass during replicative ageing of human endothelial cells. *J Cell Sci*, 113, 3613-3622.
- KURZ, E. U., DOUGLAS, P. & LEES-MILLER, S. P. 2004. Doxorubicin Activates ATM-dependent Phosphorylation of Multiple Downstream Targets in Part through the Generation of Reactive Oxygen Species. *Journal of Biological Chemistry*, 279, 53272-53281.
- KUUSISTO, E., SALMINEN, A. & ALAFUZOFF, I. 2002. Early accumulation of p62 in neurofibrillary tangles in Alzheimer's disease: possible role in tangle formation. *Neuropathology and Applied Neurobiology*, 28, 228-237.
- LA COUR, T., KIEMER, L., MØLGAARD, A., GUPTA, R., SKRIVER, K. & BRUNAK, S. 2004. Analysis and prediction of leucine-rich nuclear export signals. *Protein Engineering Design and Selection*, 17, 527-536.
- LAIOS, E., REBEYKA, I. & PRODY, C. 1997. Characterization of cold-induced heat shock protein expression in neonatal rat cardiomyocytes. *Molecular and Cellular Biochemistry*, 173, 153-159.
- LALLEMAND-BREITENBACH, V. & DE THE, H. 2010. PML Nuclear Bodies. *Cold Spring Harbor Perspectives in Biology*, 2, a000661.
- LANDRY, J., BERNIER, D., CHRÉTIEN, P., NICOLE, L. M., TANGUAY, R. M. & MARCEAU, N. 1982. Synthesis and Degradation of Heat Shock Proteins during Development and Decay of Thermotolerance. *Cancer Research*, 42, 2457-2461.
- LAVAGNINO, M., ARNOCZKY, S. P., EGERBACHER, M., GARDNER, K. L. & BURNS, M. E. 2006. Isolated fibrillar damage in tendons stimulates local collagenase mRNA expression and protein synthesis. *Journal of Biomechanics*, 39, 2355-2362.
- LEADBETTER, W. B. 1992. Cell-matrix response in tendon injury. *Clinics in Sports Medicine*, 11, 533-578.
- LEATHERBARROW, E. L., HARPER, J. V., CUCINOTTA, F. A. & O'NEILL, P. 2006. Induction and quantification of γ -H2AX foci following low and high LET-irradiation. *International Journal of Radiation Biology*, 82, 111-118.
- LEE, B. Y., HAN, J. A., IM, J. S., MORRONE, A., JOHUNG, K., GOODWIN, E. C., KLEIJER, W. J., DIMAIO, D. & HWANG, E. S. 2006. Senescence-associated β -galactosidase is lysosomal β -galactosidase. *Ageing Cell*, 5, 187-195.
- LEE, H.-M., SHIN, D.-M., YUK, J.-M., SHI, G., CHOI, D.-K., LEE, S.-H., HUANG, S. M., KIM, J.-M., KIM, C. D., LEE, J.-H. & JO, E.-K. 2011. Autophagy Negatively Regulates Keratinocyte Inflammatory Responses via Scaffolding Protein p62/SQSTM1. *The Journal of Immunology*, 186, 1248-1258.
- LEE, H. S., MILLWARD-SADLER, S. J., WRIGHT, M. O., NUKI, G., AL-JAMAL, R. & SALTER, D. M. 2002. Activation of Integrin-RACK1/PKC α signalling in human articular chondrocyte mechanotransduction. *Osteoarthritis and Cartilage*, 10, 890-897.
- LEE, J.-M., CALKINS, M. J., CHAN, K., KAN, Y. W. & JOHNSON, J. A. 2003. Identification of the NF-E2-related Factor-2-dependent Genes Conferring Protection against Oxidative Stress in Primary Cortical Astrocytes Using Oligonucleotide Microarray Analysis. *Journal of Biological Chemistry*, 278, 12029-12038.
- LEPOCK, J. R. 2003. Cellular effects of hyperthermia: relevance to the minimum dose for thermal damage. *International Journal of Hyperthermia*, 19, 252.
- LI, N., ALAM, J., VENKATESAN, M. I., EIGUREN-FERNANDEZ, A., SCHMITZ, D., DI STEFANO, E., SLAUGHTER, N., KILLEEN, E., WANG, X., HUANG, A., WANG,

- M., MIGUEL, A. H., CHO, A., SIOUTAS, C. & NEL, A. E. 2004. Nrf2 Is a Key Transcription Factor That Regulates Antioxidant Defense in Macrophages and Epithelial Cells: Protecting against the Proinflammatory and Oxidizing Effects of Diesel Exhaust Chemicals. *The Journal of Immunology*, 173, 3467-3481.
- LIANG, M., CORNELL, H. R., ZARGAR BABOLDASHTI, N., THOMPSON, M. S., CARR, A. J. & HULLEY, P. A. 2012. Regulation of Hypoxia-Induced Cell Death in Human Tenocytes. *Advances in Orthopedics*, 2012, 12.
- LIN, D.-Y., HUANG, Y.-S., JENG, J.-C., KUO, H.-Y., CHANG, C.-C., CHAO, T.-T., HO, C.-C., CHEN, Y.-C., LIN, T.-P., FANG, H.-I., HUNG, C.-C., SUEN, C.-S., HWANG, M.-J., CHANG, K.-S., MAUL, G. G. & SHIH, H.-M. 2006. Role of SUMO-Interacting Motif in Daxx SUMO Modification, Subnuclear Localization, and Repression of Sumoylated Transcription Factors. *Molecular Cell*, 24, 341-354.
- LIN, J. H. C., WEIGEL, H., COTRINA, M. L., LIU, S., BUENO, E., HANSEN, A. J., HANSEN, T. W., GOLDMAN, S. & NEDERGAARD, M. 1998. Gap-junction-mediated propagation and amplification of cell injury. *Nat Neurosci*, 1, 494-500.
- LIN, Y. L., BRAMA, P. A. J., KIERS, G. H., VAN WEEREN, P. R. & DEGROOT, J. 2005. Extracellular Matrix Composition of the Equine Superficial Digital Flexor Tendon: Relationship with Age and Anatomical Site. *Journal of Veterinary Medicine Series A*, 52, 333-338.
- LIU, A. Y., BIAN, H., HUANG, L. E. & LEE, Y. K. 1994. Transient cold shock induces the heat shock response upon recovery at 37 degrees C in human cells. *Journal of Biological Chemistry*, 269, 14768-14775.
- LIU, T.-T., HU, C.-H., TSAI, C.-D., LI, C.-W., LIN, Y. F. & WANG, J.-Y. 2010. Heat stroke induces autophagy as a protection mechanism against neurodegeneration in the brain. *Shock*, 34, 643-648.
- LÖBRICH, M., SHIBATA, A., BEUCHER, A., FISHER, A., ENSMINGER, M., GOODARZI, A. A., BARTON, O. & JEGGO, P. A. 2010. γ H2AX foci analysis for monitoring DNA double-strand break repair: Strengths, limitations and optimization. *Cell Cycle*, 9, 662-669.
- LOCKSLEY, R. M., KILLEEN, N. & LENARDO, M. J. 2001. The TNF and TNF Receptor Superfamilies: Integrating Mammalian Biology. *Cell*, 104, 487-501.
- LONGO, U. G., OLIVIA, F., DENARO, V. & MAFFULLI, N. 2008. Oxygen species and overuse tendinopathy in athletes. *Disability & Rehabilitation*, 30, 1563-1571.
- LOUGHERY, J., COX, M., SMITH, L. M. & MEEK, D. W. 2014. Critical role for p53-serine 15 phosphorylation in stimulating transactivation at p53-responsive promoters. *Nucleic Acids Research*, 42, 7666-7680.
- LUCHETTI, F., CANONICO, B., DELLA FELICE, M., BURATTINI, S., BATTISTELLI, M., PAPA, S. & FALCIERI, E. 2003. Hyperthermia triggers apoptosis and affects cell adhesiveness in human neuroblastoma cells. *Histology and Histopathology*, 18, 1041-1052.
- LUCHETTI, F., MANNELLO, F., CANONICO, B., BATTISTELLI, M., BURATTINI, S., FALCIERI, E. & PAPA, S. 2004. Integrin and cytoskeleton behaviour in human neuroblastoma cells during hyperthermia-related apoptosis. *Apoptosis*, 9, 635-648.
- LUI, P. P. Y. 2013. Identity of tendon stem cells - how much do we know? *Journal of Cellular and Molecular Medicine*, 17, 55-64.

- MADDEN, L., SANDSTRÖM, M., LOVELL, R. & MCNAUGHTON, L. 2008. Inducible heat shock protein 70 and its role in preconditioning and exercise. *Amino Acids*, 34, 511-516.
- MAEHARA, K., TAKAHASHI, K. & SAITOH, S. 2010. CENP-A Reduction Induces a p53-Dependent Cellular Senescence Response To Protect Cells from Executing Defective Mitoses. *Molecular and Cellular Biology*, 30, 2090-2104.
- MAFFULLI, N., EWEN, S. W. B., WATERSTON, S. W., REAPER, J. & BARRASS, V. 2000. Tenocytes from Ruptured and Tendinopathic Achilles Tendons Produce Greater Quantities of Type III Collagen than Tenocytes from Normal Achilles Tendons. *The American Journal of Sports Medicine*, 28, 499-505.
- MAGNUSSON, S. P., HANSEN, P. & KJÆR, M. 2003. Tendon properties in relation to muscular activity and physical training. *Scandinavian Journal of Medicine & Science in Sports*, 13, 211-223.
- MAH, L. J., EL-OSTA, A. & KARAGIANNIS, T. C. 2010. [gamma]H2AX: a sensitive molecular marker of DNA damage and repair. *Leukemia*, 24, 679-686.
- MAIER, C., SUN, G., KUNIS, D., YENARI, M. & STEINBERG, G. 2001. Delayed induction and long-term effects of mild hypothermia in a focal model of transient cerebral ischemia: neurological outcome and infarct size. *J Neurosurg*, 94, 90 - 96.
- MAIURI, M. C., ZALCKVAR, E., KIMCHI, A. & KROEMER, G. 2007. Self-eating and self-killing: crosstalk between autophagy and apoptosis. *Nat Rev Mol Cell Biol*, 8, 741-752.
- MAJNO, G. & JORIS, I. 1995. Apoptosis, Oncosis and Necrosis: An overview of cell death. *American Journal of Pathology*, 146, 3-15.
- MANTOVANI, A., SOZZANI, S., LOCATI, M., ALLAVENA, P. & SICA, A. 2002. Macrophage polarization: tumor-associated macrophages as a paradigm for polarized M2 mononuclear phagocytes. *Trends in Immunology*, 23, 549-555.
- MARFE, G., ROTTA, G., DE MARTINO, L., TAFANI, M., FIORITO, F., DI STEFANO, C., POLETTINI, M., RANALLI, M., RUSSO, M. A. & GAMBACURTA, A. 2012. A new clinical approach: Use of blood-derived stem cells (BDSCs) for superficial digital flexor tendon injuries in horses. *Life Sciences*, 90, 825-830.
- MAROU, M. A., KHEDDACHE-ATMANE, S., EL ASMI, F., DIANOUX, L., AUBRY, M. & CHELBI-ALIX, M. K. 2012. Requirement of PML SUMO Interacting Motif for RNF4- or Arsenic Trioxide-Induced Degradation of Nuclear PML Isoforms. *PLoS ONE*, 7, e44949.
- MARR, C., LOVE, S., BOYD, J. & MCKELLAR, Q. 1993. Factors affecting the clinical outcome of injuries to the superficial digital flexor tendon in National Hunt and point-to-point racehorses. *Vet Rec.*, 132, 476-479.
- MARUSYK, A., WHEELER, L. J., MATHEWS, C. K. & DEGREGORI, J. 2007. p53 Mediates Senescence-Like Arrest Induced by Chronic Replicational Stress. *Molecular and Cellular Biology*, 27, 5336-5351.
- MASTERSON, J. C. & O'DEA, S. 2007. 5-Bromo-2-deoxyuridine activates DNA damage signalling responses and induces a senescence-like phenotype in p16-null lung cancer cells. *Anti-Cancer Drugs*, 18, 1053-1068.
- MATHEW, R., KARP, C. M., BEAUDOIN, B., VUONG, N., CHEN, G., CHEN, H.-Y., BRAY, K., REDDY, A., BHANOT, G., GELINAS, C., DIPOLA, R. S., KARANTZA-WADSWORTH, V. & WHITE, E. 2009. Autophagy Suppresses Tumorigenesis through Elimination of p62. *Cell*, 137, 1062-1075.

- MAUL, G. G., GULDNER, H. H. & SPIVACK, J. G. 1993. Modification of discrete nuclear domains induced by herpes simplex virus type 1 immediate early gene 1 product (ICP0). *Journal of General Virology*, 74, 2679-2690.
- MAUL, G. G., YU, E., ISHOV, A. M. & EPSTEIN, A. L. 1995. Nuclear domain 10 (ND10) associated proteins are also present in nuclear bodies and redistribute to hundreds of nuclear sites after stress. *Journal of Cellular Biochemistry*, 59, 498-513.
- MAYTIN, E. V., WIMBERLY, J. M. & ANDERSON, R. R. 1990. Thermotolerance and the Heat Shock Response in Normal Human Keratinocytes in Culture. *J Investig Dermatol*, 95, 635-642.
- MCDONOUGH, H., CHARLES, P. C., HILLIARD, E. G., QIAN, S.-B., MIN, J.-N., PORTBURY, A., CYR, D. M. & PATTERSON, C. 2009. Stress-dependent Daxx-CHIP Interaction Suppresses the p53 Apoptotic Program. *Journal of Biological Chemistry*, 284, 20649-20659.
- MCMILLAN, D. R., XIAO, X., SHAO, L., GRAVES, K. & BENJAMIN, I. J. 1998. Targeted Disruption of Heat Shock Transcription Factor 1 Abolishes Thermotolerance and Protection against Heat-inducible Apoptosis. *Journal of Biological Chemistry*, 273, 7523-7528.
- MCNEILLY, C. M., BANES, A. J., BENJAMIN, M. & RALPHS, J. R. 1996. Tendon cells in vivo form a three dimensional network of cell processes linked by gap junctions. *Journal of Anatomy*, 189, 593-600.
- MCNICOL & RICHMOND 1998. Optimizing immunohistochemistry: antigen retrieval and signal amplification. *Histopathology*, 32, 97-103.
- MEERSHOEK, L. S., SCHAMHARDT, H. C., ROEPSTORFF, L. & JOHNSTON, C. 2001. Forelimb tendon loading during jump landings and the influence of fence height. *Equine Veterinary Journal*, 33, 6-10.
- MILLAR, N. L., HUEBER, A. J., REILLY, J. H., XU, Y., FAZZI, U. G., MURRELL, G. A. C. & MCINNES, I. B. 2010. Inflammation Is Present in Early Human Tendinopathy. *The American Journal of Sports Medicine*, 38, 2085-2091.
- MILLAR, N. L., REILLY, J. H., KERR, S. C., CAMPBELL, A. L., LITTLE, K. J., LEACH, W. J., ROONEY, B. P., MURRELL, G. A. C. & MCINNES, I. B. 2012. Hypoxia: a critical regulator of early human tendinopathy. *Annals of the Rheumatic Diseases*, 71, 302-310.
- MIZUSHIMA, N., YAMAMOTO, A., MATSUI, M., YOSHIMORI, T. & OHSUMI, Y. 2004. In Vivo Analysis of Autophagy in Response to Nutrient Starvation Using Transgenic Mice Expressing a Fluorescent Autophagosome Marker. *Molecular Biology of the Cell*, 15, 1101-1111.
- MORAN, L., MIRAULT, M.-E., ARRIGO, A. P., GOLDSCHMIDT-CLERMONT, M. & TISSIERES, A. 1978. Heat Shock of *Drosophila melanogaster* Induces the Synthesis of New Messenger RNAs and Proteins. *Philosophical Transactions of the Royal Society of London. B, Biological Sciences*, 283, 391-406.
- MOSSER, D. D., CARON, A. W., BOURGET, L., DENIS-LAROSE, C. & MASSIE, B. 1997. Role of the human heat shock protein hsp70 in protection against stress-induced apoptosis. *Molecular and Cellular Biology*, 17, 5317-27.
- MOSSER, D. D. & MARTIN, L. H. 1992. Induced thermotolerance to apoptosis in a human T lymphocyte cell line. *Journal of Cellular Physiology*, 151, 561-570.
- MUSLIMOVIĆ, A., NYSTRÖM, S., GAO, Y. & HAMMARSTEN, O. 2009. Numerical Analysis of Etoposide Induced DNA Breaks. *PLoS ONE*, 4, e5859.
- MUSTAFI, S. B., CHAKRABORTY, P. K., DEY, R. S. & RAHA, S. 2009. Heat Stress Upregulates Chaperone Heat Shock Protein 70 and Antioxidant Manganese Superoxide Dismutase through Reactive Oxygen Species (ROS), p38MAPK, and Akt. *Cell Stress & Chaperones*, 14, 579-589.

- NEFKENS, I., NEGOREV, D. G., ISHOV, A. M., MICHAELSON, J. S., YEH, E. T. H., TANGUAY, R. M., MULLER, W. E. G. & MAUL, G. G. 2003. Heat shock and Cd²⁺ exposure regulate PML and Daxx release from ND10 by independent mechanisms that modify the induction of heat-shock proteins 70 and 25 differently. *J Cell Sci*, 116, 513-524.
- NEUTELINGS, T., LAMBERT, C. A., NUSGENS, B. V. & COLIGE, A. C. 2013. Effects of Mild Cold Shock (25°C) Followed by Warming Up at 37°C on the Cellular Stress Response. *PLoS ONE*, 8, e69687.
- NICHOLSON, D. W., ALI, A., THORNBERRY, N. A., VAILLANCOURT, J. P., DING, C. K., GALLANT, M., GAREAU, Y., GRIFFIN, P. R., LABELLE, M., LAZEBNIK, Y. A., MUNDAY, N. A., RAJU, S. M., SMULSON, M. E., YAMIN, T.-T., YU, V. L. & MILLER, D. K. 1995. Identification and inhibition of the ICE/CED-3 protease necessary for mammalian apoptosis. *Nature*, 376, 37-43.
- NIVON, M., ABOU-SAMRA, M., RICHEL, E., GUYOT, B., ARRIGO, A.-P. & KRETZ-REMY, C. 2012. NF-κB regulates protein quality control after heat stress through modulation of the BAG3-HspB8 complex. *Journal of Cell Science*, 125, 1141-1151.
- NIVON, M., RICHEL, E., CODOGNO, P., ARRIGO, A.-P. & KRETZ-REMY, C. 2009. Autophagy activation by NFκB is essential for cell survival after heat shock. *Autophagy*, 5, 766-783.
- O'BRIEN, M. 2005. Anatomy of the tendons. In: MAFFULLI, N., RENSTROM, P. & LEADBETTER, W. B. (eds.) *Tendon Injuries: Basic Science and Clinical Medicine*. London: Springer.
- O'MEARA, B., BLADON, B., PARKIN, T. D. H., FRASER, B. & LISCHER, C. J. 2010. An investigation of the relationship between race performance and superficial digital flexor tendonitis in the Thoroughbred racehorse. *Equine Veterinary Journal*, 42, 322-326.
- ODA, K., ARAKAWA, H., TANAKA, T., MATSUDA, K., TANIKAWA, C., MORI, T., NISHIMORI, H., TAMAI, K., TOKINO, T., NAKAMURA, Y. & TAYA, Y. 2000. p53AIP1, a Potential Mediator of p53-Dependent Apoptosis, and Its Regulation by Ser-46-Phosphorylated p53. *Cell*, 102, 849-862.
- ORYAN, A., MOSHIRI, A. & MEIMANDI-PARIZI, A.-H. 2012. Short and long term healing of the experimentally transverse sectioned in rabbits. *Sports Medicine, Arthroscopy, Rehabilitation, Therapy and Technology*, 4, 14.
- PANKIV, S., CLAUSEN, T. H., LAMARK, T., BRECH, A., BRUUN, J.-A., OUTZEN, H., ØVERVATN, A., BJØRKØY, G. & JOHANSEN, T. 2007. p62/SQSTM1 Binds Directly to Atg8/LC3 to Facilitate Degradation of Ubiquitinated Protein Aggregates by Autophagy. *Journal of Biological Chemistry*, 282, 24131-24145.
- PANKIV, S., LAMARK, T., BRUUN, J.-A., ØVERVATN, A., BJØRKØY, G. & JOHANSEN, T. 2010. Nucleocytoplasmic Shuttling of p62/SQSTM1 and Its Role in Recruitment of Nuclear Polyubiquitinated Proteins to Promyelocytic Leukemia Bodies. *Journal of Biological Chemistry*, 285, 5941-5953.
- PARKIN, T. D. H. 2008. Epidemiology of Racetrack Injuries in Racehorses. *Veterinary Clinics of North America: Equine Practice*, 24, 1-19.
- PARRINELLO, S., SAMPER, E., KRTOLICA, A., GOLDSTEIN, J., MELOV, S. & CAMPISI, J. 2003. Oxygen sensitivity severely limits the replicative lifespan of murine fibroblasts. *Nat Cell Biol*, 5, 741-747.
- PARRY, D. A. D., BARNES, G. R. G. & CRAIG, A. S. 1978a. A Comparison of the Size Distribution of Collagen Fibrils in Connective Tissues as a Function of Age and a Possible Relation between Fibril Size Distribution and

- Mechanical Properties. *Proceedings of the Royal Society of London. Series B. Biological Sciences*, 203, 305-321.
- PARRY, D. A. D., CRAIG, A. S. & BARNES, G. R. G. 1978b. Tendon and Ligament from the Horse: An Ultrastructural Study of Collagen Fibrils and Elastic Fibres as a Function of Age. *Proceedings of the Royal Society of London. Series B. Biological Sciences*, 203, 293-303.
- PATTERSON-KANE, J. C., BECKER, D. L. & RICH, T. 2012. The Pathogenesis of Tendon Microdamage in Athletes: the Horse as a Natural Model for Basic Cellular Research. *Journal of Comparative Pathology*, 147, 227-247.
- PATTERSON-KANE, J. C., PARRY, D. A. D., GOODSHIP, A. E. & FIRTH, E. C. 1997a. Exercise modifies the age-related change in crimp pattern in the core region of the equine superficial digital flexor tendon. *New Zealand Veterinary Journal*, 45, 135-139.
- PATTERSON-KANE, J. C., WILSON, A. M., FIRTH, E. C., PARRY, D. A. D. & GOODSHIP, A. E. 1997b. Comparison of collagen fibril populations in the superficial digital flexor tendons of exercised and nonexercised Thoroughbreds. *Equine Veterinary Journal*, 29, 121-125.
- PAULL, T. T., ROGAKOU, E. P., YAMAZAKI, V., KIRCHGESSNER, C. U., GELLERT, M. & BONNER, W. M. 2000. A critical role for histone H2AX in recruitment of repair factors to nuclear foci after DNA damage. *Current biology : CB*, 10, 886-895.
- PEARCE, C. J., ISMAIL, M. & CALDER, J. D. 2009. Is Apoptosis the Cause of Noninsertional Achilles Tendinopathy? *The American Journal of Sports Medicine*, 37, 2440-2444.
- PERKINS, N. R., REID, S. W. J. & MORRIS, R. S. 2005. Risk factors for injury to the superficial digital flexor tendon and suspensory apparatus in Thoroughbred racehorses in New Zealand. *New Zealand Veterinary Journal*, 53, 184-192.
- PETROV, R., MACDONALD, M. H., TESCH, A. M. & HOOGMOED, L. M. V. 2003. Influence of topically applied cold treatment on core temperature and cell viability in equine superficial digital flexor tendons. *American Journal of Veterinary Research*, 64, 835-844.
- PILOTTE, J., DUPONT-VERSTEEGDEN, E. E. & VANDERKLISH, P. W. 2011. Widespread Regulation of miRNA Biogenesis at the Dicer Step by the Cold-Inducible RNA-Binding Protein, RBM3. *PLoS ONE*, 6, e28446.
- PINCHBECK, G. L., CLEGG, P. D., PROUDMAN, C. J., STIRK, A., MORGAN, K. L. & FRENCH, N. P. 2004. Horse injuries and racing practices in National Hunt racehorses in the UK: the results of a prospective cohort study. *The Veterinary Journal*, 167, 45-52.
- PIPERNO, G., LEDIZET, M. & CHANG, X.-J. 1987. Microtubules containing acetylated Alpha Tubulin in mammalian cells in culture. *The Journal of Cell Biology*, 104, 289-302.
- PLATT, D., WILSON, A. M., TIMBS, A., WRIGHT, I. M. & GOODSHIP, A. E. 1994. Novel force transducer for the measurement of tendon force in vivo. *Journal of Biomechanics*, 27, 1489-1493.
- POSO, A. R., EKLUND-UUSITALO, S., HYYPPÄ, S. & PIRILA, E. 2002. Induction of heat shock protein 72 mRNA in skeletal muscle by exercise and training. *Equine Veterinary Journal*, 34, 214-218.
- PRADE, L., ENGH, R. A., GIROD, A., KINZEL, V., HUBER, R. & BOSSEMAYER, D. 1997. Staurosporine-induced conformational changes of cAMP-dependent protein kinase catalytic subunit explain inhibitory potential. *Structure (London, England : 1993)*, 5, 1627-1637.

- PRYOR, P. R. 2012. Chapter eight - Analyzing Lysosomes in Live Cells. *In*: CONN, P. M. (ed.) *Methods in Enzymology*. Academic Press.
- RALPHS, J. R., WAGGETT, A. D. & BENJAMIN, M. 2002. Actin stress fibres and cell-cell adhesion molecules in tendons: organisation in vivo and response to mechanical loading of tendon cells in vitro. *Matrix Biology*, 21, 67-74.
- RANCOURT, R. C., HAYES, D. D., CHESS, P. R., KENG, P. C. & O'REILLY, M. A. 2002. Growth arrest in G1 protects against oxygen-induced DNA damage and cell death. *Journal of Cellular Physiology*, 193, 26-36.
- RAVAGNAN, L., GURBUXANI, S., SUSIN, S. A., MAISSE, C., DAUGAS, E., ZAMZAMI, N., MAK, T., JAATTELA, M., PENNINGER, J. M., GARRIDO, C. & KROEMER, G. 2001. Heat-shock protein 70 antagonizes apoptosis-inducing factor. *Nat Cell Biol*, 3, 839-843.
- RELLO, S., STOCKERT, J. C., MORENO, V., GÁMEZ, A., PACHECO, M., JUARRANZ, A., CAÑETE, M. & VILLANUEVA, A. 2005. Morphological criteria to distinguish cell death induced by apoptotic and necrotic treatments. *Apoptosis*, 10, 201-208.
- RENATUS, M., STENNICKE, H. R., SCOTT, F. L., LIDDINGTON, R. C. & SALVESEN, G. S. 2001. Dimer formation drives the activation of the cell death protease caspase 9. *Proceedings of the National Academy of Sciences*, 98, 14250-14255.
- RHUDY, R. W. & MCPHERSON, J. M. 1988. Influence of the extracellular matrix on the proliferative response of human skin fibroblasts to serum and purified platelet-derived growth factor. *Journal of Cellular Physiology*, 137, 185-191.
- RICH, T., HENDERSON, L. B., BECKER, D. L., CORNELL, H. & PATTERSON-KANE, J. C. 2013. Indicators of replicative damage in equine tendon fibroblast monolayers. *BMC Veterinary Research*, 9, 1-16.
- RICHARDSON, L., DUDHIA, J., CLEGG, P. & SMITH, R. 2007. Stem cells in veterinary medicine - attempts at regenerating equine tendon after injury. *Trends in biotechnology*, 25, 409 - 416.
- RIEMERSMA, D. J. & SCHAMHARDT, H. C. 1985. In vitro mechanical properties of equine tendons in relation to cross-sectional area and collagen content. *Research in Veterinary Science*, 39, 263-270.
- RILEY, G. P. 2005. Gene expression and matrix turnover in overused and damaged tendons. *Scandinavian Journal of Medicine & Science in Sports*, 15, 241-251.
- RITOSSA, F. 1962. A new puffing pattern induced by temperature shock and DNP in drosophila. *Experientia*, 18, 571-573.
- RITTY, T. M., ROTH, R. & HEUSER, J. E. 2003. Tendon Cell Array Isolation Reveals a Previously Unknown Fibrillin-2-Containing Macromolecular Assembly. *Structure (London, England : 1993)*, 11, 1179-1188.
- RODIER, F., COPPE, J.-P., PATIL, C. K., HOEIJMAKERS, W. A. M., MUNOZ, D. P., RAZA, S. R., FREUND, A., CAMPEAU, E., DAVALOS, A. R. & CAMPISI, J. 2009. Persistent DNA damage signalling triggers senescence-associated inflammatory cytokine secretion. *Nat Cell Biol*, 11, 973-979.
- ROGAKOU, E. P., BOON, C., REDON, C. & BONNER, W. M. 1999. Megabase Chromatin Domains Involved in DNA Double-Strand Breaks in Vivo. *The Journal of Cell Biology*, 146, 905-916.
- ROGAKOU, E. P., PILCH, D. R., ORR, A. H., IVANOVA, V. S. & BONNER, W. M. 1998. DNA Double-stranded Breaks Induce Histone H2AX Phosphorylation on Serine 139. *Journal of Biological Chemistry*, 273, 5858-5868.

- ROOBOL, A., CARDEN, M. J., NEWSAM, R. J. & SMALES, C. M. 2009. Biochemical insights into the mechanisms central to the response of mammalian cells to cold stress and subsequent rewarming. *FEBS Journal*, 276, 286-302.
- ROY, J., TRAN, P. K., RELIGA, P., KAZI, M., HENDERSON, B., LUNDMARK, K. & HEDIN, U. 2002. Fibronectin Promotes Cell Cycle Entry in Smooth Muscle Cells in Primary Culture. *Experimental Cell Research*, 273, 169-177.
- RUBIN, H. 1997. Cell aging in vivo and in vitro. *Mechanisms of Ageing and Development*, 98, 1-35.
- RUDOLPH, P., KNUCHEL, R., ENDL, E., HEIDEBRECHT, H. J., HOFSTADER, F. & PARWARESCH, R. 1998. The immunohistochemical marker Ki-S2: cell cycle kinetics and tissue distribution of a novel proliferation-specific antigen. *Modern Pathology*, 11.
- SAKAHIRA, H., ENARI, M. & NAGATA, S. 1998. Cleavage of CAD inhibitor in CAD activation and DNA degradation during apoptosis. *Nature*, 391, 96-99.
- SALEH, A., SRINIVASULA, S. M., BALKIR, L., ROBBINS, P. D. & ALNEMRI, E. S. 2000. Negative regulation of the Apaf-1 apoptosome by Hsp70. *Nat Cell Biol*, 2, 476-483.
- SALMINEN, A., KAARNIRANTA, K., HAAPASALO, A., HILTUNEN, M., SOININEN, H. & ALAFUZOFF, I. 2012. Emerging role of p62/sequestosome-1 in the pathogenesis of Alzheimer's disease. *Progress in Neurobiology*, 96, 87-95.
- SAMALI, A. & COTTER, T. G. 1996. Heat Shock Proteins Increase Resistance to Apoptosis. *Experimental Cell Research*, 223, 163-170.
- SAMALI, A. & ORRENIUS, S. 1998. Heat Shock Proteins: Regulators of Stress Response and Apoptosis. *Cell Stress & Chaperones*, 3, 228-236.
- SANZ, L., DIAZ-MECO, M. T., NAKANO, H. & MOSCAT, J. 2000. The atypical PKC-interacting protein p62 channels NF- κ B activation by the IL-1-TRAF6 pathway. *EMBO J*, 19, 1576-1586.
- SCAFFIDI, P., MISTELI, T. & BIANCHI, M. E. 2002. Release of chromatin protein HMGB1 by necrotic cells triggers inflammation. *Nature*, 418, 191-195.
- SCHAEFFER, V., LAVENIR, I., OZCELIK, S., TOLNAY, M., WINKLER, D. T. & GOEDERT, M. 2012. Stimulation of autophagy reduces neurodegeneration in a mouse model of human tauopathy. *Brain*, 135, 2169-2177.
- SCOTT, A., KHAN, K. M., HEER, J., COOK, J. L., LIAN, O. & DURONIO, V. 2005. High strain mechanical loading rapidly induces tendon apoptosis: an ex vivo rat tibialis anterior model. *British Journal of Sports Medicine*, 39, e25.
- SCOTT, I. C., BLITZ, I. L., PAPPANO, W. N., IMAMURA, Y., CLARK, T. G., STEIGLITZ, B. M., THOMAS, C. L., MAAS, S. A., TAKAHARA, K., CHO, K. W. Y. & GREENSPAN, D. S. 1999. Mammalian BMP-1/Tolloid-Related Metalloproteinases, Including Novel Family Member Mammalian Tolloid-Like 2, Have Differential Enzymatic Activities and Distributions of Expression Relevant to Patterning and Skeletogenesis. *Developmental Biology*, 213, 283-300.
- SEDELNIKOVA, O. A., ROGAKOU, E. P., PANYUTIN, I. G. & BONNER, W. M. 2002. Quantitative Detection of DNA Double-Strand Breaks with γ -H2AX Antibody. *Radiation Research*, 158, 486-492.
- SEIBENHENER, M. L., BABU, J. R., GEETHA, T., WONG, H. C., KRISHNA, N. R. & WOOTEN, M. W. 2004. Sequestosome 1/p62 Is a Polyubiquitin Chain Binding Protein Involved in Ubiquitin Proteasome Degradation. *Molecular and Cellular Biology*, 24, 8055-8068.
- SEKHAR, K. R., YAN, X. X. & FREEMAN, M. L. 2002. Nrf2 degradation by the ubiquitin proteasome pathway is inhibited by KIAA0132, the human homolog to INrf2. *Oncogene*, 21, 6829-6834.

- SHEA, K. P., MCCARTHY, M. B., LEDGARD, F., ARCIERO, C., CHOWANIEC, D. & MAZZOCCA, A. D. 2010. Human Tendon Cell Response to 7 Commercially Available Extracellular Matrix Materials: An In Vitro Study. *Arthroscopy: The Journal of Arthroscopic & Related Surgery*, 26, 1181-1188.
- SHI, Y., MOSSER, D. D. & MORIMOTO, R. I. 1998. Molecular chaperones as HSF1-specific transcriptional repressors. *Genes & Development*, 12, 654-666.
- SHINTANI, Y., TERAO, Y. & OHTA, H. 2011. Molecular Mechanisms Underlying Hypothermia-Induced Neuroprotection. *Stroke Research and Treatment*, 2011.
- SHUTTLEWORTH, M. 2008. *Type I Error-Type II Error* [Online]. Available: <https://explorable.com/type-i-error> [Accessed Aug 24 2014].
- SIMPSON, R. J. 2006. SDS-PAGE of Proteins. *Cold Spring Harbor Protocols*, 2006, pdb.prot4313.
- SIRBU, B. M., COUCH, F. B., FEIGERLE, J. T., BHASKARA, S., HIEBERT, S. W. & CORTEZ, D. 2011. Analysis of protein dynamics at active, stalled, and collapsed replication forks. *Genes & Development*, 25, 1320-1327.
- SMITH, N. N., HARVEY, W. F., BEDFORD, J. S. & COSS, R. A. 1993. Thermal response of synchronous CHO cells with different shapes. *International Journal of Hyperthermia*, 9, 799-802.
- SMITH, R. 2008. Mesenchymal stem cell therapy for equine tendinopathy. *Disabil Rehabil*, 30, 1752 - 1758.
- SMITH, R. K. W. 2003. Pathophysiology of Tendon Injury. In: ROSS, M. D. A. D., S.J. (ed.) *Diganosis and Management of Lameness in the Horse*. St. Louis, Missouri: Saunders, Elsevier Inc.
- SMITH, R. K. W., BIRCH, H. L., GOODMAN, S., HEINEGÅRD, D. & GOODSHIP, A. E. 2002. The influence of ageing and exercise on tendon growth and degeneration-hypotheses for the initiation and prevention of strain-induced tendinopathies. *Comparative Biochemistry and Physiology - Part A: Molecular & Integrative Physiology*, 133, 1039-1050.
- SMITH, R. K. W. & WEBBON, P. M. The physiology of normal tendon and ligament. In: RANTANEN, N. W. & HAUSER, M. L., eds. Proceedings of the Dubai International Equine Symposium 'The Equine Athlete: Tendon, ligament and soft tissue injuries', 1996 Dubai. Veterinary Data.
- SMITH, R. K. W., WERLING, N. J., DAKIN, S. G., ALAM, R., GOODSHIP, A. E. & DUDHIA, J. 2013. Beneficial Effects of Autologous Bone Marrow-Derived Mesenchymal Stem Cells in Naturally Occurring Tendinopathy. *PLoS ONE*, 8, e75697.
- SOLDATENKOV, V. A. & DRITSCHILO, A. 1997. Apoptosis of Ewing's Sarcoma Cells Is Accompanied by Accumulation of Ubiquitinated Proteins. *Cancer Research*, 57, 3881-3885.
- SONG, J. J. & LEE, Y. J. 2003. Role of the ASK1-SEK1-JNK1-HIPK1 Signal in Daxx Trafficking and ASK1 Oligomerization. *Journal of Biological Chemistry*, 278, 47245-47252.
- SPEER, K. P., WARREN, R. F. & HOROWITZ, L. 1996. The efficacy of cryotherapy in the postoperative shoulder. *Journal of Shoulder and Elbow Surgery*, 5, 62-68.
- SRINIVAS, P. R. 2012. Protein Electrophoresis: Methods and Protocols. In: KURIEN, B. T. & SCOFIELD, R. H. (eds.) *Introduction to Protein Electrophoresis*. New York, USA: Humana Press.
- STANLEY, R. L., EDWARDS, L. J., GOODSHIP, A. E., FIRTH, E. C. & PATTERSON-KANE, J. C. 2008. Effects of exercise on tenocyte cellularity and tenocyte nuclear morphology in immature and mature equine digital tendons. *Equine Veterinary Journal*, 40, 141-146.

- STANLEY, R. L., FLECK, R. A., BECKER, D. L., GOODSHIP, A. E., RALPHS, J. R. & PATTERSON-KANE, J. C. 2007. Gap junction protein expression and cellularity: comparison of immature and adult equine digital tendons. *Journal of Anatomy*, 211, 325-334.
- STENNICKE, H. R. & SALVESEN, G. S. 1998. Properties of the caspases. *Biochimica et Biophysica Acta (BBA) - Protein Structure and Molecular Enzymology*, 1387, 17-31.
- STEPHEN, M. J., POINDEXTER, B. J., MOOLMAN, J. A., SHEIKH-HAMAD, D. & BICK, R. J. 2009. Do binucleate cardiomyocytes have a role in myocardial repair? Insights using isolated rodent myocytes and cell culture. *Open Cardiovascular Medicine Journal*, 3, 1-7.
- STEPHENS, P. R., NUNAMAKER, D. M. & BUTTERWECK, D. M. 1989. Application of a Hall-effect transducer for measurement of tendon strains in horses. *American Journal of Veterinary Research*, 50, 1089-1095.
- STROBER, W. 2001. Trypan Blue Exclusion Test of Cell Viability. *Current Protocols in Immunology*, Appendix 3B.
- STROMBERG, B. 1973. Morphologic, Thermographic and ¹³³Xe Clearance Studies on Normal and Diseased Superficial Digital Flexor Tendons in Race Horses. *Equine Veterinary Journal*, 5, 156-161.
- STUKENBERG, P. 2004. Triggering p53 after cytokinesis failure. *J Cell Biol*, 165, 607 - 608.
- SUN, G., XU, X., WANG, Y., SHEN, X., CHEN, Z. & YANG, J. 2008. Mycoplasma pneumoniae Infection Induces Reactive Oxygen Species and DNA Damage in A549 Human Lung Carcinoma Cells. *Infect. Immun.*, 76, 4405-4413.
- SUZUKI, K., BOSE, P., LEONG-QUONG, R., FUJITA, D. & RIABOWOL, K. 2010. REAP: A two minute cell fractionation method. *BMC Research Notes*, 3, 294.
- SYRBU, S. & COHEN, M. 2011. An Enhanced Antigen-Retrieval Protocol for Immunohistochemical Staining of Formalin-Fixed, Paraffin-Embedded Tissues. In: KALYUZHNY, A. E. (ed.) *Signal Transduction Immunohistochemistry*. Humana Press.
- TAATJES, D., SOBEL, B. & BUDD, R. 2008. Morphological and cytochemical determination of cell death by apoptosis. *Histochemistry and Cell Biology*, 129, 33-43.
- TAK, P. P. & FIRESTEIN, G. S. 2001. NF- κ B: a key role in inflammatory diseases. *The Journal of Clinical Investigation*, 107, 7-11.
- TAKADA, K., HIROSE, J., SENBA, K., YAMABE, S., OIKE, Y., GOTOH, T. & MIZUTA, H. 2011. Enhanced apoptotic and reduced protective response in chondrocytes following endoplasmic reticulum stress in osteoarthritic cartilage. *International Journal of Experimental Pathology*, 92, 232-242.
- TAKAHASHI, M., LI, T.-S., SUZUKI, R., KOBAYASHI, T., ITO, H., IKEDA, Y., MATSUZAKI, M. & HAMANO, K. 2006. Cytokines produced by bone marrow cells can contribute to functional improvement of the infarcted heart by protecting cardiomyocytes from ischemic injury. *American Journal of Physiology - Heart and Circulatory Physiology*, 291, H886-H893.
- TAN, Q., LUI, P. P. Y. & LEE, Y. W. 2013. In vivo identity of tendon stem cells and the roles of stem cells in tendon healing. *Stem Cells and Development*, 22, 3128-3140.
- TANAKA, H., OKADA, T., KONISHI, H. & TSUJI, T. 1993. The effect of reactive oxygen species on the biosynthesis of collagen and glycosaminoglycans in cultured human dermal fibroblasts. *Archives of Dermatological Research*, 285, 352-355.

- TANG, J., AGRAWAL, T., CHENG, Q., QU, L., BREWER, M. D., CHEN, J. & YANG, X. 2013. Phosphorylation of Daxx by ATM Contributes to DNA Damage-Induced p53 Activation. *PLoS ONE*, 8, e55813.
- TANG, J., XIE, W. & YANG, X. 2005. Association of caspase-2 with the promyelocytic leukemia protein nuclear bodies. *Cancer Biology & Therapy*, 4, 645-649.
- TAYLOR, S., VAUGHAN-THOMAS, A., CLEMENTS, D., PINCHBECK, G., MACRORY, L., SMITH, R. & CLEGG, P. 2009. Gene expression markers of tendon fibroblasts in normal and diseased tissue compared to monolayer and three dimensional culture systems. *BMC Musculoskeletal Disorders*, 10, 27.
- TERASAKI, M., CHEN, L. B. & FUJIWARA, K. 1986. Microtubules and the endoplasmic reticulum are highly interdependent structures. *The Journal of Cell Biology*, 103, 1557-1568.
- THEODORE, M., KAWAI, Y., YANG, J., KLESHCHENKO, Y., REDDY, S. P., VILLALTA, F. & ARINZE, I. J. 2008. Multiple Nuclear Localization Signals Function in the Nuclear Import of the Transcription Factor Nrf2. *Journal of Biological Chemistry*, 283, 8984-8994.
- THORPE, C. T., STREETER, I., PINCHBECK, G. L., GOODSHIP, A. E., CLEGG, P. D. & BIRCH, H. L. 2010. Aspartic Acid Racemization and Collagen Degradation Markers Reveal an Accumulation of Damage in Tendon Collagen That Is Enhanced with Aging. *Journal of Biological Chemistry*, 285, 15674-15681.
- THORPE, C. T., UDEZE, C. P., BIRCH, H. L., CLEGG, P. D. & SCREEN, H. R. C. 2012. Specialization of tendon mechanical properties results from interfascicular differences. *Journal of The Royal Society Interface*, 9, 3108-3117.
- TIAN, T., LAVAGNINO, M., GARDNER, K. & ARNOCKY, S. 2004. Hyperthermia increases the magnitude of caspase-3 activation and DNA fragmentation in tendon cells undergoing cyclic strain: a potential intrinsic factor in the etiology of tendon overuse injuries. *Transactions of the Orthopaedic Research Society*, 29, 881.
- TONG, G., ENDERSFELDER, S., ROSENTHAL, L.-M., WOLLERSHEIM, S., SAUER, I. M., BÜHRER, C., BERGER, F. & SCHMITT, K. R. L. 2013. Effects of moderate and deep hypothermia on RNA-binding proteins RBM3 and CIRP expressions in murine hippocampal brain slices. *Brain Research*, 1504, 74-84.
- TSAI, W.-C., CHANG, H.-N., YU, T.-Y., CHIEN, C.-H., FU, L.-F., LIANG, F.-C. & PANG, J.-H. S. 2011. Decreased proliferation of aging tenocytes is associated with down-regulation of cellular senescence-inhibited gene and up-regulation of p27. *Journal of Orthopaedic Research*, 29, 1598-1603.
- TSAI, W.-C., LIANG, F.-C., CHENG, J.-W., LIN, L.-P., CHANG, S.-C., CHEN, H.-H. & PANG, J.-W. S. 2013. High glucose concentration up-regulates the expression of matrix metalloproteinase-9 and -13 in tendon cells. *BMC Musculoskeletal Disorders*, 14 1-7.
- TU, S., MCSTAY, G. P., BOUCHER, L.-M., MAK, T., BEERE, H. M. & GREEN, D. R. 2006. In situ trapping of activated initiator caspases reveals a role for caspase-2 in heat shock-induced apoptosis. *Nat Cell Biol*, 8, 72-77.
- TULAPURKAR, M., ASIEGBU, B., SINGH, I. & HASDAY, J. 2009. Hyperthermia in the febrile range induces HSP72 expression proportional to exposure temperature but not to HSF-1 DNA-binding activity in human lung epithelial A549 cells. *Cell Stress and Chaperones*, 14, 499-508.

- TVEITA, A. A., DIETRICH, E. S. & TVEITA, T. 2012. Myocardial gene expression profiling of rewarming shock in a rodent model of accidental hypothermia. *Cryobiology*, 64, 201-210.
- TYEDMERS, J., MOGK, A. & BUKAU, B. 2010. Cellular strategies for controlling protein aggregation. *Nat Rev Mol Cell Biol*, 11, 777-788.
- UETAKE, Y. & SLUDER, G. 2004. Cell cycle progression after cleavage failure. *The Journal of Cell Biology*, 165, 609-615.
- VADLAMUDI, R. K., JOUNG, I., STROMINGER, J. L. & SHIN, J. 1996. p62, a Phosphotyrosine-independent Ligand of the SH2 Domain of p56lck, Belongs to a New Class of Ubiquitin-binding Proteins. *Journal of Biological Chemistry*, 271, 20235-20237.
- VAN EPS, A. W., LEISE, B. S., WATTS, M., POLLITT, C. C. & BELKNAP, J. K. 2012. Digital hypothermia inhibits early lamellar inflammatory signalling in the oligofructose laminitis model. *Equine Veterinary Journal*, 44, 230-237.
- VAN EPS, A. W. & POLLITT, C. C. 2009. Equine laminitis model: Cryotherapy reduces the severity of lesions evaluated seven days after induction with oligofructose. *Equine Veterinary Journal*, 41, 741-746.
- VOGEL, K. G., PAULSSON, M. & HEINEGÅRD, D. 1984. Specific inhibition of type I and type II collagen fibrillogenesis by the small proteoglycan of tendon. *Biochem. J.*, 223, 587-597.
- WAGGETT, A. D., BENJAMIN, M. & RALPHS, J. R. 1999. Gap junction inhibitors abolish strain response in tendon cells in vitro. *Transactions of the Orthopaedic Research Society*, 24, 630.
- WAGGETT, A. D., BENJAMIN, M. & RALPHS, J. R. 2006. Connexin 32 and 43 gap junctions differentially modulate tenocyte response to cyclic mechanical load. *European Journal of Cell Biology*, 85, 1145-1154.
- WALKER, J. 1996. The Bicinchoninic Acid (BCA) Assay for Protein Quantitation. In: WALKER, J. (ed.) *The Protein Protocols Handbook*. Humana Press.
- WANG, J. H. C., LI, Z., YANG, G. & KHAN, M. 2004. Repetitively stretched fibroblasts produce inflammatory mediators. *Clinical Orthopaedics and Related Research*, 422, 243-250.
- WARD, I. M. & CHEN, J. 2001. Histone H2AX Is Phosphorylated in an ATR-dependent Manner in Response to Replicational Stress. *Journal of Biological Chemistry*, 276, 47759-47762.
- WATAI, Y., KOBAYASHI, A., NAGASE, H., MIZUKAMI, M., MCEVOY, J., SINGER, J. D., ITOH, K. & YAMAMOTO, M. 2007. Subcellular localization and cytoplasmic complex status of endogenous Keap1. *Genes to Cells*, 12, 1163-1178.
- WATTS, A., YEAGER, A., KOPYOV, O. & NIXON, A. 2011. Fetal derived embryonic-like stem cells improve healing in a large animal flexor tendonitis model. *Stem Cell Research & Therapy*, 2, 4.
- WELLMANN, S., BÜHRER, C., MODEREGGER, E., ZELMER, A., KIRSCHNER, R., KOEHNE, P., FUJITA, J. & SEEGER, K. 2004. Oxygen-regulated expression of the RNA-binding proteins RBM3 and CIRP by a HIF-1-independent mechanism. *Journal of Cell Science*, 117, 1785-1794.
- WELLMANN, S., TRUSS, M., BRUDER, E., TORNILLO, L., ZELMER, A., SEEGER, K. & BUHRER, C. 2010. The RNA-Binding Protein RBM3 Is Required for Cell Proliferation and Protects Against Serum Deprivation-Induced Cell Death. *Pediatric Research*, 67, 35-41 10.1203/PDR.0b013e3181c13326.
- WILLIAMS, I. F., MCCULLAGH, K. G. & SILVER, I. A. 1984. The Distribution of Types I and III Collagen and Fibronectin in the Healing Equine Tendon. *Connective Tissue Research*, 12, 211-227.

- WILLIAMS, R. B., HARKINS, L. S., HAMMOND, C. J. & WOOD, J. L. N. 2001. Racehorse injuries, clinical problems and fatalities recorded on British racecourses from flat racing and National Hunt racing during 1996, 1997 and 1998. *Equine Veterinary Journal*, 33, 478-486.
- WILMINK, J., WILSON, A. M. & GOODSHIP, A. E. 1992. Functional significance of the morphology and micromechanics of collagen fibres in relation to partial rupture of the superficial digital flexor tendon in racehorses. *Research in Veterinary Science*, 53, 354-359.
- WILSON, A. & LICHTWARK, G. 2011. The anatomical arrangement of muscle and tendon enhances limb versatility and locomotor performance. *Philosophical Transactions of the Royal Society B: Biological Sciences*, 366, 1540-1553.
- WILSON, A. M. & GOODSHIP, A. E. Mechanical properties of the equine superficial digital flexor tendon. Seventh Meeting of the European Society of Biomechanics 1991. Aarhus, Denmark, B15.
- WILSON, A. M. & GOODSHIP, A. E. 1994. Exercise-induced hyperthermia as a possible mechanism for tendon degeneration. *Journal of Biomechanics*, 27, 899-905.
- WONG, C. & STEARNS, T. 2005. Mammalian cells lack checkpoints for tetraploidy, aberrant centrosome number, and cytokinesis failure. *BMC Cell Biology*, 6, 6.
- WRIGHT, W. E. & SHAY, J. W. 2002. Historical claims and current interpretations of replicative aging. *Nat Biotech*, 20, 682-688.
- WRIGHT, W. E. & SHAY, J. W. 2006. Inexpensive low-oxygen incubators. *Nat. Protocols*, 1, 2088-2090.
- WU, W., ZHANG, C., CHEN, Z., ZHANG, G. & YANG, J. 2009. Differences in heating methods may account for variation in reported effects on γ H2AX focus formation. *Mutation Research/Genetic Toxicology and Environmental Mutagenesis*, 676, 48-53.
- XIA, H., NHO, R., KLEIDON, J., KAHM, J. & HENKE, C. A. 2008. Polymerized Collagen Inhibits Fibroblast Proliferation via a Mechanism Involving the Formation of a β 1 Integrin-Protein Phosphatase 2A-Tuberous Sclerosis Complex 2 Complex That Suppresses S6K1 Activity. *Journal of Biological Chemistry*, 283, 20350-20360.
- XIAO, X., ZUO, X., DAVIS, A. A., MCMILLAN, D. R., CURRY, B. B., RICHARDSON, J. A. & BENJAMIN, I. J. 1999. HSF1 is required for extra-embryonic development, postnatal growth and protection during inflammatory responses in mice. *EMBO J*, 18, 5943-5952.
- YAMAGUCHI, Y., MANN, D. M. & RUOSLAHTI, E. 1990. Negative regulation of transforming growth factor -beta by the small proteoglycan of tendon. *Nature*, 346, 281-284.
- YANAMOTO, H., NAGATA, I., NIITSU, Y., ZHANG, Z., XUE, J.-H., SAKAI, N. & KIKUCHI, H. 2001. Prolonged Mild Hypothermia Therapy Protects the Brain Against Permanent Focal Ischemia. *Stroke*, 32, 232-239.
- YANG, J., LIU, X., BHALLA, K., KIM, C. N., IBRADO, A. M., CAI, J., PENG, T.-I., JONES, D. P. & WANG, X. 1997a. Prevention of Apoptosis by Bcl-2: Release of Cytochrome c from Mitochondria Blocked. *Science*, 275, 1129-1132.
- YANG, N.-C. & HU, M.-L. 2005. The limitations and validities of senescence associated- β -galactosidase activity as an aging marker for human foreskin fibroblast Hs68 cells. *Experimental Gerontology*, 40, 813-819.
- YANG, X., KHOSRAVI-FAR, R., CHANG, H. Y. & BALTIMORE, D. 1997b. Daxx, a Novel Fas-Binding Protein That Activates JNK and Apoptosis. *Cell*, 89, 1067-1076.

- YAO, L., BESTWICK, C., BESTWICK, L., MAFFULLI, N. & ASPDEN, R. 2006a. Phenotypic drift in human tenocyte culture. *Tissue Eng*, 12, 1843 - 1849.
- YAO, L., BESTWICK, C. S., BESTWICK, L. A., MAFFULLI, N. & ASPDEN, R. M. 2006b. Phenotypic drift in human tenocyte culture. *Tissue Engineering*, 12, 1843-1849.
- YASUI, K., KADA, K., HOJO, M., LEE, J.-K., KAMIYA, K., TOYAMA, J., OPTHOF, T. & KODAMA, I. 2000. Cell-to-cell interaction prevents cell death in cultured neonatal rat ventricular myocytes. *Cardiovascular Research*, 48, 68-76.
- YE, X., ZERLANKO, B., ZHANG, R., SOMAIAH, N., LIPINSKI, M., SALOMONI, P. & ADAMS, P. D. 2007. Definition of pRB- and p53-Dependent and -Independent Steps in HIRA/ASF1a-Mediated Formation of Senescence-Associated Heterochromatin Foci. *Molecular and Cellular Biology*, 27, 2452-2465.
- YEDJOU, C. G., TCHOUNWOU, C. K., HAILE, S., EDWARDS, F. & TCHOUNWOU, P. B. 2010. N-Acetyl-Cysteine protects against DNA damage associated with lead toxicity in HepG2 cells. *Ethnicity & Disease* 20, S1-101-3.
- YOUNG, N. J., BECKER, D. L., FLECK, R. A., GOODSHIP, A. E. & PATTERSON-KANE, J. C. 2009. Maturation alterations in gap junction expression and associated collagen synthesis in response to tendon function. *Matrix Biology*, 28, 311-323.
- YUAN, J., MURRELL, G. A. C., WEI, A.-Q. & WANG, M.-X. 2002. Apoptosis in rotator cuff tendonopathy. *Journal of Orthopaedic Research*, 20, 1372-1379.
- ZANTOP, T., TILLMANN, B. & PETERSEN, W. 2003. Quantitative assessment of blood vessels of the human Achilles tendon: an immunohistochemical cadaver study. *Archives of Orthopaedic and Trauma Surgery*, 123, 501-504.
- ZHANG, J., PAN, T. & WANG, J. H. C. 2014. Cryotherapy suppresses tendon inflammation in an animal model. *Journal of Orthopaedic Translation*, Article in Press.
- ZHANG, J. & WANG, J. 2010. Characterization of differential properties of rabbit tendon stem cells and tenocytes. *BMC Musculoskeletal Disorders*, 11, 10.
- ZHANG, J. & WANG, J. H. C. 2013. Human Tendon Stem Cells Better Maintain Their Stemness in Hypoxic Culture Conditions. *PLoS ONE*, 8, e61424.
- ZHANG, S., MCCARTER, J. D., OKAMURA, O., Y., YAGHI, F., HINEK, A., WITHERS, S. & CALLAHAN, J. W. 1994. Kinetic mechanism and characterisation of human B-galactosidase precursor secreted by permanently transfected Chinese hamster ovary cells. *Biochemical Journal*, 304, 281-288.
- ZHANG, Y., LI, T.-S., LEE, S.-T., WAWROWSKY, K. A., CHENG, K., GALANG, G., MALLIARAS, K., ABRAHAM, M. R., WANG, C. & MARBÁN, E. 2010a. Dedifferentiation and Proliferation of Mammalian Cardiomyocytes. *PLoS ONE*, 5, e12559.
- ZHANG, Y., WANG, B., ZHANG, W., ZHOU, G., CAO, Y. & LIU, W. 2010b. Enhanced proliferation capacity of porcine tenocytes in low O₂ tension culture. *Biotechnology Letters*, 32, 181-187.
- ZHENG, L., DAI, H., ZHOU, M., LI, X., LIU, C., GUO, Z., WU, X., WU, J., WANG, C., ZHONG, J., HUANG, Q., GARCIA-AGUILAR, J., PFEIFER, G. P. & SHEN, B. 2012. Polyploid cells rewire DNA damage response networks to overcome replication stress-induced barriers for tumour progression. *Nat Commun*, 3, 815.
- ZHENG, Q., SU, H., RANEK, M. J. & WANG, X. 2011. Autophagy and p62 in Cardiac Proteinopathy. *Circulation Research*, 109, 296-308.

- ZHONG, S., SALOMONI, P. & PANDOLFI, P. P. 2000a. The transcriptional role of PML and the nuclear body. *Nat Cell Biol*, 2, E85-E90.
- ZHONG, S., SALOMONI, P., RONCHETTI, S., GUO, A., RUGGERO, D. & PANDOLFI, P. P. 2000b. Promyelocytic Leukemia Protein (Pml) and Daxx Participate in a Novel Nuclear Pathway for Apoptosis. *The Journal of Experimental Medicine*, 191, 631-640.
- ZÖLZER, F. & STREFFER, C. 1995. Cell Cycle-Dependent Expression of Ki-67 Antigen in Human Melanoma Cells Subjected to Irradiation and/or Hyperthermia. *Radiation Research*, 143, 98-101.
- ZOU, H., HENZEL, W. J., LIU, X., LUTSCHG, A. & WANG, X. 1997. Apaf-1, a Human Protein Homologous to *C. elegans* CED-4, Participates in Cytochrome c-Dependent Activation of Caspase-3. *Cell*, 90, 405-413.
- ZOU, J., GUO, Y., GUETTOUCHE, T., SMITH, D. F. & VOELLMY, R. 1998. Repression of Heat Shock Transcription Factor HSF1 Activation by HSP90 (HSP90 Complex) that Forms a Stress-Sensitive Complex with HSF1. *Cell*, 94, 471-480.